Derivation of a direct abundance index for tropical tunas based on their associative behavior with floating objects

Yannick Diby Armel Baidai

THÈSE POUR OBTENIR LE GRADE DE DOCTEUR DE L'UNIVERSITÉ DE MONTPELLIER

En Sciences de la Mer

École doctorale GAIA

Unité de recherche : Centre pour la Biodiversité Marine, l'Exploitation et la Conservation (MARBEC)

Derivation of a direct abundance index for tropical tunas based on their associative behavior with floating objects

Présentée par Yannick Diby Armel BAIDAI
Le 17 Décembre 2020

Sous la direction de Laurent DAGORN
Et Daniel GAERTNER

Devant le jury composé de

Roger PRADEL, Directeur de Recherche, CNRS, CEFE	Président
Ray HILBORN, Professeur, University of Washington	Rapporteur
Victor RESTREPO, Vice-President Science, ISSF	Rapporteur
Allassane OUATTARA, Professeur, Université Nangui Abrogoua	Examinateur
Carolina MINTE-VERA, Senior scientist, IATTC	Examinateur
Laurent DAGORN, Directeur de Recherche, IRD, UMR MARBEC	Directeur de thèse
Daniel GAERTNER, Chargé de Recherche, IRD, UMR MARBEC	Co-directeur de thèse
Manuela CAPELLO, Chargé de Recherche, IRD, UMR MARBEC	Co-encadrante de thèse
Monin Justin AMANDE, Chargé de Recherche, African Marine Expertises	Invité

UNIVERSITÉ DE MONTPELLIER

"*Amat Victoria Curam*"

To my parents who gave me the courage to undertake this adventure.

Acknowledgements

It is with a smile that I remember today that even as a child, my answer to the question “What do you want to be when you grow up?” was almost invariably: “Scientist, Sir”! Disdaining comments and quibbles from other kids shouting that it was not a “real job”. The funny thing is that at that time, I actually had no idea of the true meaning of the word “Scientist”. I was just sublimated and obsessed by the “exploits” of my unusual heroes of the time. Rather than Tintin, I was more interested in crazy inventions of Professor Calculus. Faced with the power of Wolverine, I shuddered at Professor X's exhilarating knowledge. Do not even ask me who was my favorite ninja turtle (the nerd genius Donatello, of course). During these three years of thesis, I have been able to get a little closer to the deep meaning of this word and its real implications. Of the two hundred or so pages of this manuscript, these few lines were among the most difficult to write, as they will never be able to faithfully express the extent of my gratitude to all those people who in one way or another contribute to the achievement of this old childhood dream.

First, I would like to express my sincere gratitude to my quartet of supervisors who gave me the exciting opportunity to undertake this thesis work (in order of appearance in this adventure). I would like to address a special gratitude to Monin Justin Amandé (Doc). From “Bigeye” to today, what a long way and thrilling adventures. I still remember that endless job interview, the hours of work coding and rewriting procedures over and over again, the “Miami Law” decreed with our observers. At every stage, I have always been able to count on your support, your unfailingly and pertinent advices as a mentor and role model. The first time I met Manuela Capello was on skype. She was trying to explain to the layman that I was, a thorny story about models. At the time, the only models I knew were doing fashion shows for clothing brands. I never would have suspected that they could also be used to count such turbulent and mysterious animals as tuna. I would like to thank her for her availability and patience in answering my countless questions, and for guiding me through this thesis. I understand better now: “ABBI can also count tunas”. During this skype meeting, Laurent Dagorn was also present. I personally met him a few weeks later in this room of the IRD representation in Abidjan, where he pushed the science of tuna to the point of experiencing the famous Ivorian “Garba”. His spirit and scientific curiosity have captivated me since that day. I would like to thank him for his continuous support, ideas, and the opportunity he gave me to develop new skills, extend my expertise, and expand my collaborative network. One of my first experiences with the French

culture was the use of the coffee break as a means of socialization and exchange with other scientists. It was during my very first discovery of these coffee breaks that I met Daniel Gartner, my second main supervisor, who have spared no effort for the success of this thesis. He has always been able to bring a fresh look to this thesis and each of our discussions have been rich as much in lessons as in pertinent advices. I would like to express my particular gratitude to him.

Secondly, I would like to thank Ray Hilborn, Allassane Ouattara, Victor Restrepo, Roger Pradel and Carolina Minte-Vera for contributing their knowledge as part of my PhD committee. Likewise, I would also like to express my gratitude to all those people who gave me their intellectual support throughout this process; these include Jean-Louis Denebourg, David Kaplan, Francis Marsac, Antoine Duparc, Laurent Floch, Norbert Billet, Laura Mannoci, Fabien Forget. My special thanks to Geraldine Perez with whom I found myself embarked on this tuna story, and who has never stopped helping me in these endless administrative issues, which I still, do not understand at all. Thank you also for all our fascinating discussions, which made me understand, to me who only swore by earthworms, that the trophic level above them was also full of mysteries to elucidate.

My gratitude also goes to the organizations that funded this thesis project, namely the “Institut de Recherche pour le Développement” (IRD) and the “Agence Nationale pour la Recherche” (ANR), who granted me a bursary and gave me an invaluable support during the difficult context of the COVID-19.

Last but not least, this thesis would have not been possible without the support of my family. Thank you all for being there for me.

Publications arising during this candidature

This thesis is submitted as a series of manuscripts, which are to be submitted, or published in peer-reviewed journal.

Peer-reviewed articles included in this thesis

Published or accepted articles:

Baidai, Y., Dagorn, L., Amande, M.J., Gaertner, D., and Capello, M. 2020. Machine learning for characterizing tropical tuna aggregations under Drifting Fish Aggregating Devices (DFADs) from commercial echosounder buoys data. *Fisheries Research*: 105613. https://doi:10.1016/j.fishres.2020.105613 (**Chapter 2**).

Baidai, Y., Dagorn, L., Amande, M.J., Gaertner, D., and Capello, M. 2020. Tuna aggregation dynamics at Drifting Fish Aggregating Devices: A view through the eyes of commercial echosounder buoys. *ICES Journal of Marine Science* (*In press*): https://doi:10.1093/icesjms/fsaa178 (**Chapter 3**).

Articles in preparation:

Processing data from satellite-linked buoys used in tropical tuna fisheries for scientific purposes: A standard protocol. In preparation for *Deep-Sea Research Part II: Topical Studies in Oceanography*. (**Chapter 1**).

Direct assessment of skipjack tuna abundance in Indian Ocean based on its associative behaviour with floating objects. In preparation for *Proceedings of the National Academy of Sciences*. (**Chapter 4**).

Peer-reviewed articles not included in this thesis

Mannocci, L., **Baidai, Y.,** Forget, F., Tolotti, M.T., Dagorn L., and Capello M. 2020. Using machine learning to detect bycatch risk. In preparation for *Biological Conservation.*

Technical and working papers during this candidature

Baidai, Y., Capello, M., Billet, N., Floch, L., Simier, M., Sabarros, P., and Dagorn, L. 2017. Towards the derivation of fisheries-independent abundance indices for tropical tunas: Progress in the echosounders buoys data analysis. IOTC-2017-WPTT19-22.

Baidai, Y., Capello, M., Amande, J., Gaertner, D., and Dagorn, L. 2018. Supervised learning approach for detecting presence-absence of tuna under FADs from echosounder buoys data. ICCAT-SCRS/2018/125.

Baidai, Y., Amande, M.J., Gaertner, D., Dagorn, L., and Capello, M. 2018. Recent advances on the use of supervised learning algorithms for detecting tuna aggregations under FADs from echosounder buoys data. IOTC-2018-WPTT20-25.

Baidai, Y., Dagorn, L., Amande, M. J., Gaertner, D., and Capello, M. 2019. Aggregation processes of tuna under Drifting Fish Aggregating Devices (DFADs) assessed through fisher's echosounder buoy in the Indian Ocean. IOTC-2019-WPTT21-55_Rev1.

Baidai, Y., Dagorn, L., Amande, M.J., Gaertner, D., and Capello, M. 2019. Mapping tuna occurrence under Drifting Fish Aggregating Devices from fisher's echosounder buoys in Indian Ocean. IOTC-2019-WPTT21-56_Rev1.

A. Diallo, **Baidai Y.**, Manocci L., Capello, M. 2019. Towards the derivation of fisheries-independent abundance indices for tropical tuna: Report on biomass estimates obtained from a multi-frequency echosounder buoy model (M3I+). IOTC-2019-WPTT21-54_Rev1.

Zudaire, I., Tolotti, M., Murua, J., Capello, M., Andrés, M., Cabezas, O., Krug, I., Grande, M., Arregui, I., Uranga, J., Goñi, N., Ferarios, J.M., Ruiz, J., **Baidai, Y.,** Ramos, M.L., Báez, J.C., Abascal, F., Moreno, G., Santiago, J., Dagorn, L., and Murua, H. 2019. Preliminary results of the BIOFAD project : testing designs and identify options to mitigate impacts of drifting Fish Aggregating Devices on the ecosystem. WCPFC-SC15-2019/EB-WP-11 (Rev.01).

Zudaire, I., Mariana Tolotti, M., Murua, J., Capello, M., Andrés, M., Cabezas, O., Krug, I., Grande, M., Arregui, I., Uranga, J., Goñi, N., Sabarros, P.S., Ferarios, M.J., Jon, R., **Baidai, Y.**, Ramos, M.L., Báez, J.C., Abascal, F., Moreno, G., Santiago, J., Dagorn, L.,

Arrizabalaga, H. and Murua, H. 2019. Results of BIOFAD project: testing designs and identify options to mitigate impacts of drifting fish aggregating devices on the ecosystem. IOTC-2019-WPTT21-52.

Baidai, Y., Dagorn, L., Amande, M. J., Gaertner, D., and Capello, M. 2020. Aggregation processes of tuna under Drifting Fish Aggregating Devices (DFADs) assessed through fisher's echosounder buoy in the Atlantic Ocean. *Collected Volume of Scientific Papers ICCAT* 76(6): 762–776.

Baidai, Y., Dagorn, L., Amande, M.J., Gaertner, D., and Capello, M. 2020. Mapping tuna occurrence under Drifting Fish Aggregating Devices from fisher's echosounder buoys in Atlantic Ocean. *Collected Volume of Scientific Papers ICCAT* 76(6): 777–784.

Grande, M., Capello, M., **Baidai, Y.**, Uranga, J., Boyra, G., Quincoces, I., Orue, B., Ruiz, J., Zudaire, I., and Murua, H. 2020. From fishermen to scientific tools: progress on the recovery and standardized processing of instrumented buoys data. *Collected Volume of Scientific Papers ICCAT* 76(6): 881–891.

Abstract

Representing the majority of the world's tuna catches, tropical tuna species are of critical importance due to their essential role as food and economic resource. The sustainable management of this valuable resource depends on an accurate estimate of the abundance of the exploited populations and the impact of fishing pressure on them. The present thesis provides a new direct abundance index for tropical tuna populations that account for their free-swimming and associated components. Indeed, tropical tuna species are characterized by a singular behavioural trait that causes them to associate with floating objects drifting at sea. This characteristic has led to the development of a specific fishing mode widely used in tuna purse seine fishery, consisting in the capture of schools associated to floating objects. Recent decades have thus seen the massive deployment of thousands of floating objects known as fish aggregating devices (FADs), specifically designed to attract and concentrate tuna schools. The drifting FADs are equipped with satellite-linked echosounder buoys, which ensure their continuous monitoring, providing fishers with near-real time information on their location and associated tuna biomasses. This thesis presents a standard methodological framework for processing the information from echosounder buoys for scientific use, including a new approach based on supervised learning for processing the acoustic data they provide. The analysis of these data has allowed improving the general knowledge on the associative dynamics of tuna aggregations. Ocean-specific differences were evidenced, with notably longer periods of absence of tuna under FADs in the Indian Ocean than in the Atlantic Ocean. The novel index for estimating tuna abundance proposed by this thesis also exploit this associative behaviour. It relies on a modelling approach combining data on the dynamics of the occupancy of floating objects from echosounder buoys with data on the associative dynamics of tuna individuals. An initial application to the western Indian skipjack tuna population has made it possible to provide time series of absolute and relative abundances, used for stock assessments of this species. This new abundance index addresses the current critical need for complementary methods for estimating tropical tuna stocks expressed by all regional fisheries management organizations.

Keywords: Direct abundance index, Associative behaviour, Tropical tunas, Echosounder buoys, Fish Aggregating Devices.

Résumé substantiel (French extended abstract)

Introduction

Les thons, animaux emblématiques de nos océans, font partie des espèces de poissons les plus lucratives au monde. D'une importance socio-économique cruciale à la fois pour les pays développés et en développement, les thons fournissent une grande variété de services écosystémiques directs, notamment à travers leur rôle en tant que ressource alimentaire et économique. Ces superprédateurs occupent en outre, une place fondamentale dans les réseaux trophiques marins; et une déplétion de leurs populations pourrait se traduire par de dramatiques effets délétères sur le fonctionnement et la stabilité des écosystèmes (Sund *et al.*, 1981; Baum and Worm, 2009; Young *et al.*, 2010; Duffy *et al.*, 2017). Parmi les 7 principales espèces de thon exploitées, trois espèces tropicales, à savoir le thon à nageoire jaune ou albacore (*Thunnus albacares*), le thon obèse ou patudo (*T. obesus*) et la bonite à ventre rayé ou listao (*Katsuwonus pelamis*), représentent à elles seules, la majorité des captures mondiales, principalement pêchées par les flottilles industrielles de thoniers senneurs. On estime que plus de la moitié des prises de thons de ces engins de pêches, proviennent de captures associées à des dispositifs de concentration de poissons ou DCP (Fonteneau *et al.*, 2013). Les DCP sont des objets flottants spécifiquement conçus et déployés par les pêcheurs pour faciliter leurs prises de thons tropicaux, en exploitant leur comportement associatif avec les objets flottants en mer (Fréon and Dagorn, 2000; Castro *et al.*, 2002). Les DCP sont généralement équipés de bouées-satellite échosondeurs qui fournissent en continu aux pêcheurs diverses informations, notamment sur leur géolocalisation et les biomasses de poissons qui leurs sont associées (Lopez *et al.*, 2014; Moreno *et al.*, 2019). L'essor massif de la pêche sous DCP au cours de ces dernières décennies, suscite toutefois des préoccupations majeures quant à leurs impacts, tant d'un point de vue écologique que sur la durabilité des pêcheries thonières elles-mêmes (Dagorn *et al*., 2013).

En vertu de leurs caractéristiques hautement migratoires et de leurs vastes répartitions, la gestion des ressources thonières est sous la responsabilité d'organisations régionales de gestion de la pêche (ORGP) qui sont des organismes intergouvernementaux composés de pays possédant des intérêts en matière de pêche thonière dans une zone géographique spécifique. De manière générale, la gestion des ressources thonières repose sur un ensemble de processus regroupés sous le nom « d'évaluation de stocks », qui vise en substance à définir les niveaux d'exploitation optimale des thons, notamment à partir de l'évaluation de l'abondance de leurs

populations et de l'impact de la pression de pêche sur celles-ci. La performance d'un tel mécanisme de gestion est intimement lié à la disponibilité d'indicateurs d'abondances robustes capable de décrire fidèlement les changements survenant au sein de ces populations. Cependant, la plupart des méthodes d'évaluation d'abondance développées pour les populations de poissons reste relativement difficile à mettre en œuvre pour les espèces tropicales de thons en raison de leurs caractéristiques migratoires et de leur vaste distribution spatiale. En conséquence, actuellement les estimations de l'abondance de leurs populations reposent presque essentiellement sur les données de capture et d'effort associées à la pêche commerciale.

Objectifs de la thèse

Le présent travail a pour principal objet de développer une nouvelle méthodologie pour l'estimation des populations d'espèces de thon tropical, en exploitant leur comportement associatif autour d'objets flottants. Cet objectif implique une nécessaire amélioration des connaissances sur le comportement des thons et plus particulièrement une meilleure compréhension de leur dynamique associative. À cet égard, les informations sur les agrégations de poissons sous DCP, collectées par les bouées échosondeurs utilisées par les thoniers senneurs, constituent un atout majeur. La réalisation de l'objectif de cette thèse a ainsi été définie selon une stratégie de recherche articulée autour de trois axes majeurs :

(i). développer un cadre méthodologique pour l'exploitation scientifique des données enregistrées par les bouées échosondeurs équipant les DCP;
(ii). analyser les dynamiques associatives des agrégations de thons autour des DCP à partir de ces nouvelles sources de données ;
(iii). dériver un nouvel indice d'abondance des thons tropicaux sur la base de leur comportement associatif avec les objets flottants et des données des bouées échosondeurs.

Résumés des chapitres

Chapitre 1 : *Développement d'un protocole standard de traitement pour l'exploitation scientifique des données des bouées satellites utilisées par les thoniers senneurs tropicaux.*

Ce chapitre est lié au premier des objectifs spécifiques définis. Il propose un protocole standard de collecte de données dédié aux bouées satellites utilisées dans les pêcheries thonières tropicales. Ces bouées qui équipent les dispositifs de concentration de poissons à la dérive (DCP), fournissent aux pêcheurs un flux continu d'informations tant sur certaines caractéristiques de l'océan (e.g. température de surface, vitesse des courants), que sur les communautés pélagiques de poissons associées aux DCP. Cette quantité sans précédent de données se caractérise par une large distribution à l'échelle de l'océan, une haute résolution spatiale et temporelle, mais aussi par une très forte hétérogénéité entre les natures et formats de données collectées par les différents modèles et marques de bouées. L'exploitation de ces données dans un but scientifique reste donc résolument tributaire de la disponibilité de méthodes de traitement permettant leur contrôle, leur validation et leur standardisation. Ce premier chapitre décrit les données fournies par les principaux modèles de bouées utilisés par la flotte européenne de thoniers senneurs, et propose un protocole standard de traitement visant à en améliorer leur cohérence, leur fiabilité et leur valeur. Ce protocole aborde les trois points majeurs affectant ces données : (*i*) les erreurs structurelles, (*ii*) les données collectées à terre (*iii*) et à bord des navires. Il fournit cinq critères de filtrage spécifiques dont trois dédiés à la résolution des erreurs structurelles, et compare différentes procédures de filtrage pour les données enregistrées sur le continent et à bord des navires.

Ces comparaisons ont révélé que l'utilisation de cartes à haute résolution de traits de côtes pour la détection des données de bouées émises sur le continent se traduisait par des performances de filtrage relativement similaires à celles à basse résolution de traits de côtes. Ce qui présente un intérêt notable en terme de coûts de calcul compte tenu des très grands volumes que représentent ces données. Deux algorithmes ont également été comparés pour la discrimination des positions enregistrées par des bouées dérivant en mer et celles émettant à bord de navires. Le premier était basé sur un moteur de règles établies à partir de l'analyse du comportement des thoniers senneurs et des patterns généraux de vitesses associés aux objets dérivant en mer. Le second reposait sur une classification automatique utilisant l'apprentissage supervisée par

forêts aléatoires. Les deux approches se sont révélées de performances très similaires, avec toutefois des spécificités liées à la résolution temporelle des données traitées.

Le protocole proposé par ce premier chapitre n'offre cependant, pas de méthodologie standard pour le traitement des données acoustiques collectées par les différentes marques de bouées échosondeurs. En effet, la grande variabilité au sein des formats des données acoustiques, et des caractéristiques matérielles et techniques des échosondeurs intégrés aux bouées constitue une limite majeure au développement d'un cadre général permettant le traitement des données acoustiques collectées en mesure d'abondance. Néanmoins, du fait de la grande quantité de données concernées, la contribution des techniques d'apprentissage automatique pourrait s'avérer être une option valable à envisager pour la mise au point d'un tel cadre méthodologique, visant à la caractérisation des agrégations de poissons sous objets flottants et la fourniture d'estimations fiables de leur abondance à partir des bouées échosondeurs

***Chapitre 2** : Caractérisation des agrégations de thons tropicaux sous dispositifs de concentration de poissons par classification automatique des données des bouées échosondeurs.*

Découlant également de l'objectif spécifique liminaire de ce travail de thèse, ce second chapitre présente une nouvelle méthodologie reposant sur l'utilisation de techniques d'apprentissage automatique pour traduire les données acoustiques collectées par les bouées échosondeurs en mesures de présence et d'abondance des thons.

L'approche couple des procédures d'agrégation spatiale et temporelle des données acoustiques collectées, à une classification supervisée utilisant l'algorithme des forêts aléatoires. Elle vise à caractériser les agrégations associées aux DCP en y déterminant la présence ou l'absence de thons, ainsi que les classes de tailles d'agrégation auxquelles elles correspondent. L'entrainement des modèles de classification s'est appuyé sur un jeu de données d'apprentissage construit par croisement des données acoustiques avec les données d'activités sur DCP issues des journaux de bord et des rapports des observateurs embarqués à bord des thoniers senneurs français dans les océans Atlantique et Indien, de 2013 à 2018. Les données acoustiques collectées la veille d'opérations de pêches sous DCP, ainsi que les captures

réalisées ont respectivement été associées à la présence de thons et aux classes de taille d'agrégation; tandis que l'absence de thons a été reliée aux données de visites sans pêche et de déploiement de DCP.

L'analyse des performances des classifications réalisées a montré des précisions satisfaisantes de l'ordre de 75 % et 85 % pour la discrimination de la présence ou de l'absence d'agrégations de thons sous DCP, respectivement dans les océans Atlantique et Indien. A l'inverse, la classification des données acoustiques en catégories de taille des agrégations de thon (à savoir, inférieure à 10 tonnes, entre 10 et 25 tonnes et supérieure à 25 tonnes) s'est traduite par une précision globale plus faible de l'ordre de 50 %, dans les deux océans. Par ailleurs, les données acoustiques enregistrées à des profondeurs (6 à 45 m dans l'Atlantique et 30 à 150 m dans l'océan Indien) et à des périodes spécifiques à l'océan (de 4 h à 16 h généralement) ont été identifiées par l'algorithme comme les variables explicatives les plus importantes dans les différentes classifications effectuées.

En fournissant, un nouvel outil permettant d'exploiter les données acoustiques des bouées échosondeurs pour la caractérisation des agrégations de thons associées aux DCP, ce travail a constitué l'une des étapes cruciales vers l'utilisation de ces nouvelles sources de données pour l'étude de l'écologie et du comportement des thons tropicaux, et le développement de nouveaux indices d'abondance pour leurs populations.

***Chapitre 3** : Analyse de la dynamique associative des agrégations de thons tropicaux autour des dispositifs de concentration des poissons à partir des bouées échosondeurs.*

L'amélioration des connaissances sur le comportement associatif des thons tropicaux avec les objets flottants est une priorité de recherche essentielle pour assurer l'exploitation durable de leurs populations. En lien avec le second objectif spécifique défini pour ce travail de thèse, le second chapitre a abordé de nouvelles questions relatives à la dynamique associative des agrégations de thons associées aux objets flottants, à partir des données collectées par les bouées échosondeurs le long de plus de 9000 trajectoires de DCP nouvellement déployés dans les océan Atlantique et Indien, entre 2016 et 2018.

Des séries chronologiques de présence/absence d'agrégations de thons obtenues grâce à la procédure de classification supervisée des données acoustiques présentée au chapitre précédent, ont servi à l'évaluation de métriques clés permettant de décrire ces dynamiques associatives. Les résultats ont montré qu'en moyenne les durées de séjour à l'eau des DCP ne différaient pas significativement entre océans (de l'ordre de 60 jours). Toutefois, comparativement à l'océan Atlantique, une proportion plus élevée de DCP dans l'océan Indien n'a montré aucun signe de colonisation par les thons tout au long de leurs trajectoires (respectivement 22 et 34%).

Le temps moyen de colonisation d'un DCP nouvellement déployé par une agrégation de thons a été estimé à partir d'une nouvelle approche permettant d'éviter les biais découlant de la grande variabilité des temps de séjour à l'eau des DCP dans le jeu de données. On a ainsi déterminé qu'en moyenne la colonisation d'un DCP par une agrégation de thons survenait en moyenne au bout de 16 jours dans l'océan Atlantique, contre 40 jours dans l'océan Indien.

En moyenne, les DCP colonisés sont restés continuellement occupés par des agrégations de thon pendant 6 et 9 jours, respectivement dans les océans Indien et Atlantique. La durée moyenne entre deux agrégations consécutives autour d'un même DCP (temps d'absence d'agrégation autour du DCP) variait entre 9 jours dans l'océan Indien et 5 jours dans l'océan Atlantique. Globalement, tout au long de leur période de séjour à l'eau, les DCP colonisés sont restés occupés par les thons pendant une plus large proportion de temps dans l'océan Atlantique (63%) que dans l'océan Indien (45%).

En outre, des analyses basées sur les approches de courbes de survie ont permis de montrer que l'occupation des DCP par les agrégations de thons était déterminée par un processus indépendant du temps avec des modes de résidence à long terme de l'ordre de 2 à 3 semaines respectivement dans les océans Atlantique et Indien, et à court terme (de 4 à 5 jours), relativement proches en durée des temps continus de présence estimés au niveau des individus de thons (CRT). Cela suggère que la composition des espèces et/ou les conditions locales (par exemple les proies, les congénères ou la densité des objets flottants) pourraient jouer un rôle clé dans la dynamique d'agrégation. Des analyses évaluant ces mesures comportementales à des échelles spatio-temporelles plus restreintes pourraient aider à comprendre la dynamique des agrégations à une échelle locale, ainsi que le rôle joué par ces divers facteurs environnementaux.

Ces résultats illustrent la contribution notable que les données issues des bouées échosondeurs peuvent apporter à l'amélioration des connaissances sur le comportement et l'écologie des

thons. Ils revêtent également une importance particulière pour le développement de nouvelles méthodes d'estimations des populations. En effet, la taille des populations et les densités de DCP entre les deux océans sont présumées représenter les principaux facteurs causatifs à la base de la variabilité des périodes d'absence de thons sous DCP. De fait, l'intégration de ces nouvelles métriques au sein de modèles d'évaluation des populations pourrait se révéler être une voie prometteuse vers le développement de nouveaux indices d'abondance pour les thonidés tropicaux.

Chapitre 4 : *Indice d'abondance basés sur le comportement associatif : une nouvelle méthode d'estimation directe des populations de thons tropicaux.*

Le quatrième chapitre de cette thèse décrit une approche de modélisation permettant de fournir des estimations directes de l'abondance des populations de thons tropicaux à partir de leur comportement associatif avec les objets flottants. Cette approche utilise cinq variables principales en entrée correspondant aux métriques reliées aux dynamiques d'occupation des objets flottants par les agrégations de thons (i.e. la proportion d'objets flottants occupés, l'abondance locale sous les objets flottants et le nombre total d'objets flottants), et à celles décrivant les dynamiques associatives individuelles des thons, à savoir les temps continus de résidence (CRT) et d'absence (CAT).

L'étude du cas du listao (*Katsuwonnus pelamis*) dans l'océan Indien occidental a permis de fournir des séries temporelles d'abondance absolues et relatives de la population de cette espèce pour la période 2013-2018. Cette méthode a adoptée par la Commission des Thons de l'Océan Indien (CTOI), pour les évaluations de stocks de cette espèce pour l'année 2020. L'étude s'est principalement appuyée sur les données issues des bouées échosondeurs équipant les DCP de la flottille française de thoniers senneurs. Ces données ont servi de base pour l'estimation de la densité d'objets flottants dans la zone d'étude et l'évaluation de la proportion de ceux occupés par les thons. L'abondance locale associée aux objets flottants a été déterminée à partir de la moyenne des captures de listao réalisées sous objets flottants par les thoniers senneurs. La valeur de CRT des listaos dans la zone d'étude était basée sur les travaux antérieurs de marquage électronique réalisés dans la zone par Govinden *et al.*, (2010). L'absence de mesure

expérimentale des CAT dans la région a été contournée en estimant cette valeur à partir d'une conjecture établie sur la relation de proportionnalité inverse entre cette métrique et le nombre total d'objets flottants dans la zone d'étude. La sensibilité des estimations d'abondance à différentes valeurs de coefficient de proportionnalité a ensuite été évaluée. Puis, les gammes plausibles de valeurs de ce coefficient ont été empiriquement déterminées par la comparaison des valeurs absolues d'abondance estimées avec les biomasses totales de listao pêchées dans la zone.

Les résultats montrent que les tendances d'abondance fournies demeurent peu sensibles aux variations des valeurs plausibles du coefficient de proportionnalité. Ils suggèrent en outre un net déclin de la population totale de listao dans l'océan Indien occidental au cours des années 2013 à 2015, parallèle à l'augmentation soutenue du nombre de DCP observée au cours de la même période ; suivie d'une relative stabilisation de l'abondance des populations à partir de l'année 2016. L'adoption à partir de l'année 2015 de mesures limitant le nombre de DCP par les senneurs dans l'océan Indien, couplée aux conditions environnementales et aux caractéristiques biologiques propres à cette espèce (productivité forte et variable), pourraient constituer des possibles facteurs causatifs de cette stabilisation.

Ce chapitre a ainsi montré qu'à partir d'un nombre limité d'observables décrivant les dynamiques associatives aux échelles individuelles et collectives des agrégations, il était possible de produire des estimations relativement fiables des populations de thons, capables de soutenir les évaluations de stocks. Il souligne aussi la nécessité d'une disponibilité accrue des données des bouées échosondeurs, ainsi que le développement à grande échelle de programmes de collectes de données visant à améliorer les actuelles connaissances sur les CRT et CAT des espèces thonières tropicales.

Discussion générale

Ce travail de thèse fournit un cadre méthodologique permettant d'utiliser les données issues des bouées échosondeurs dans une approche de modélisation permettant l'estimation directe de l'abondance des populations de thons tropicaux à partir de leurs dynamiques associatives avec les objets flottants. Malgré des incertitudes liées à l'absence de certaines données expérimentales (i.e. CAT) ou à leur disponibilité relativement limitée (i.e. nombre total de DCP utilisés), les estimations d'abondance réalisées au cours de cette étude se sont révélées

cohérentes avec celles traditionnellement utilisées pour les évaluations de stocks du listao dans l'océan Indien.

L'importance des données des bouées échosondeurs pour une gestion opérationnelle des pêcheries a constitué l'un des points de discussion abordé par ce travail de thèse. En effet, les bouées offrent une source inédite d'information permettant d'évaluer en temps réel la distribution spatio-temporelle des espèces de thon tropical, et ouvrent un vaste champ d'applications possibles. Ces informations pourraient par exemple être intégrées dans une gestion opérationnelle des pêcheries et fournir des arguments scientifiques susceptibles d'appuyer en temps-réel, les prises de mesures de gestion et de conservation par les ORGP (e.g. identification des périodes et zones appropriées de fermeture spatio-temporelle de la pêche, nombre limite de DCP, etc.). Des modèles de distribution d'espèces (SDM) reliant ces nouvelles données aux conditions océaniques, pourraient offrir une compréhension accrue de l'influence de l'environnement sur la répartition des thons, aussi bien que la possibilité de prévoir les réactions des populations de thons, à divers facteurs de changement. Par ailleurs, cette nouvelle source d'informations est susceptible d'apporter un soutien intéressant à la pêche artisanale et de petite échelle. L'intégration dans les accords de pêche de mécanismes de partage des informations sur la distribution des thons et autres espèces associées, collectées par les bouées des thoniers senneurs industriels, dans les ZEE des états côtiers, pourrait très certainement contribuer à une meilleure structuration de l'accès aux ressources côtières pélagiques entre les acteurs industriels et artisanaux. En outre, le suivi quasi-constant de la circulation océanique réalisé par les bouées échosondeurs pourrait servir de base au développement ou à l'amélioration de systèmes de surveillance et d'alerte visant à réduire les impacts liés aux échouages des DCP (notamment sur les écosystèmes côtiers et récifaux), et à plus grande échelle de contrôler les mouvements des débris marins qui constituent actuellement une préoccupation environnementale majeure. Ces nouvelles données sont également susceptibles d'apporter de nouvelles connaissances sur l'écologie et le comportement des thons tropicaux. Par exemple, les estimations de populations issus de cette étude semblent être de nature à indiquer une atténuation du phénomène de fragmentation des bancs, se manifestant à travers une réduction globale du nombre de bancs dans l'océan Indien, parallèle à une augmentation de leur taille, et de celle des agrégations associées aux objets flottants.

Toutefois, les données des bouées revêtent un caractère commercial et hautement stratégique pour les compagnies de pêches qui en sont propriétaires. En conséquence, malgré l'amélioration constante de la collaboration entre le secteur industriel de la pêche thonière et les scientifiques ;

leur accessibilité reste encore soumise à des processus longs et complexes limitant leur disponibilité à une communauté plus large de chercheurs. Le développement d'études soulignant leur importance et la pertinence de l'amélioration de leur accessibilité est susceptible de donner l'impulsion décisive aux ORGP et leurs parties prenantes vers un accès plus ouvert et une gestion opérationnelle et en temps réel des pêches intégrant ces nouvelles sources de données.

Conclusion

La conclusion de ce travail de thèse s'articule autour des nouvelles potentialités offertes par la nouvelle méthodologie proposée pour l'estimation des abondances des populations de thons. Elle insiste sur la pertinence de ce nouvel indice d'abondance, pour répondre aux besoins des Organismes Régionaux de Gestion de la Pêche au thon (ORGP), en matière de méthodologies complémentaires aux données de captures et d'effort pour l'estimation des stocks des thons tropicaux. Elle relève aussi que bien qu'initialement destinés aux espèces thonières tropicales, cette méthodologie pourrait potentiellement être appliquée à toute population d'espèce animale présentant un comportement associatif autour de points d'agrégation, qu'il s'agisse d'objets ou d'autres animaux vivants. La nécessité d'études complémentaires évaluant ce potentiel et permettant d'ouvrir de nouvelles perspectives pour leur application à un plus large éventail d'espèces animale, est également soulignée.

Tables of contents

List of figures

List of tables

Introduction

"*Vous arrivez devant la nature avec des théories, la nature flanque tout par terre.*

You come to the nature with theories, the nature blows them away".

Pierre-Auguste Renoir

1. Introduction

It is said that the word “calculus” (from the Latin word for “stone”) comes from an ancient pastoral practice of counting sheep leaving the pens, using stones placed in a basket whose count was later checked when the animals returned from the meadows. For these ancient shepherds, as for any wildlife manager nowadays, knowing the precise size of populations is a crucial issue for the optimal control, conservation or exploitation of resources. Unfortunately, estimating the size of a natural population is much more complex than the ancient shepherd method of counting stones. Exhaustive census is rarely possible for natural populations, since very often, there is no practical way to access all individuals or the entire distribution area of the population. As a result, mathematical models supported by a set of assumptions are rather used to link the population size with indicative metrics of its status, called indices of abundance. The core underlying assumption is based on the expected relationship between the overall population and measurements made on samples of that population. The whole art of population assessment therefore lies in identifying the nature of the relationships between abundance indices (A) measured on given spatial and temporal units, and the overall population (N). Fundamentally, these two quantities can be related by a proportionality parameter (p), according to the following equation:

$$N = pA \tag{I. 1}$$

In practice, numerous models going from a simple constant parameter to much more complex formulas can be used to describe this proportionality relationship. Similarly, abundance indices can be expressed in different forms, depending on the characteristics of the species (Skalski *et al.*, 2005). For species that are easily accessible (e.g. noisy, visible or not very mobile), the abundance estimates can be made by direct observation and census of the number of individuals (e.g. large mammal herbivores: (Varman and Sukumar, 1995; Jachmann, 2002); birds: (Gregory *et al.*, 1992); insects: (Yoo *et al.*, 2003); etc.). A review of direct wildlife census methods can be found in Lewis (1970). Abundance may also be assessed indirectly by means of signs or evidences left by the animals, which provide relative indices whose variations over a defined period, reflect changes in the same direction in the overall population (Schwarz and Seber, 1999; Wilson and Delahay, 2001). When the species are difficult to observe directly because they are fast-moving, highly migratory, or distributed over large areas, an accurate measurement of their population size is difficult to implement. Providing reliable indices of

abundance can quickly become more difficult, and very often the latter alternative (relative indices) may turn out to be the privileged or sometimes the only one available.

With their extensive oceanic distribution and their highly migratory behaviour, tuna species are particularly illustrative of this situation. However, the health and sustainability of these iconic species strongly depend on the availability of reliable methods to estimate the status of their populations and their vulnerability to overfishing. Tuna are among the world's most lucrative fish species, with an estimated global market value of more than $42 billion per year (Galland *et al.*, 2016); and belong to species of crucial socio-economic importance to both developed and developing countries. They provide a wide variety of direct ecosystem services by supporting food security for many countries, generating employment in tuna fisheries and creating vital coastal livelihoods and economies (Bell *et al.*, 2009, 2015; Gilman *et al.*, 2014). As apex predators, tunas also have an ecological role recognized as key in the health and functioning of the ecosystem; and their depletion could lead to dramatic cascading ecological effects (Sund *et al.*, 1981; Baum and Worm, 2009; Young *et al.*, 2010; Duffy *et al.*, 2017). Of the 15 species of tuna, seven species commonly referred to as "principal market tunas", occupy a major economic importance in the global market (Majkowski, 2007). These principal market tunas include albacore (*Thunnus alalunga*), Atlantic bluefin tuna (*T. thynnus*), bigeye tuna (*T. obesus*), Pacific bluefin tuna (*T. orientalis*), southern bluefin tuna (*T. maccoyii*), yellowfin tuna (*T. albacares*), and skipjack tuna (*Katsuwonus pelamis*). They represented an estimated catch volume of 4.9 million tonnes in 2017, heavily dominated by catches of the three tropical tuna species (i.e. skipjack, yellowfin and bigeye tuna, representing 56%, 30%, and 8% of the total tuna catches respectively) (ISSF, 2019). Industrial tuna fishing began in the 1940s and 1950s due to a growing demand for canned tuna, with longline and pole and line as the main fishing gears (Figure I.1). Currently, purse seine represents the major gear capturing tropical tunas worldwide (65 % of the global tuna catches), followed by longline (11%), pole-and-line (8%), gillnets (4%) and miscellaneous gears (12%). This shift occurred during the 1980s as a result of the rapid development and global expansion of the tropical tuna purse seine fishery.

Management of tuna species and other large species such as swordfish and marlin is under the responsibility of intergovernmental arrangements known as Regional Fishery Management Organizations (RFMOs). The five main tuna RFMOs in the world, from the oldest to the most recent, are: (1) the Inter-American Tropical Tuna Commission (IATTC) for the Pacific Ocean, (2) the International Commission for the Conservation of Atlantic Tunas (ICCAT) for the Atlantic Ocean, (3) the Indian Ocean Tuna Commission (IOTC) for the Indian Ocean, (4) the

Commission for the Conservation of Southern Bluefin Tuna (CCSBT) and the Western and Central Pacific Fisheries Commission (WCPFC).

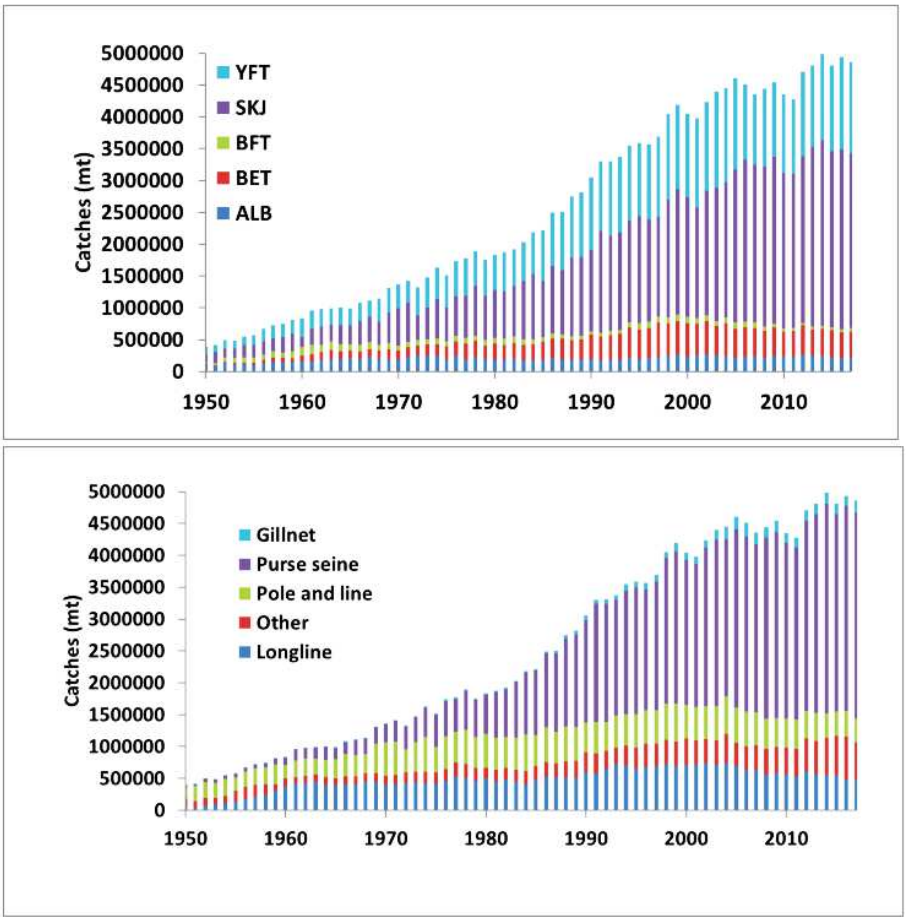

Figure I.1 Global trends in catch (tonnes) of major commercial tunas, by species (top) and gear (bottom), 1950-2017. Source: ISSF, (2019).

These organizations face the ongoing challenge of sustainable management of tuna resources through specific processes called "stock assessment". A fish stock is defined as a unit of a fish population considered in fisheries management. It may be all or a part of the population defined on the basis of spatial distribution or other biological or ecological coherences. Stock assessment is the part of fisheries science that aims to provide support for decision making by (1) evaluating the abundance of the stock and the impact of fishing on it, (2) identifying the potential effects of alternative harvest scenarios, and (3) defining the level of exploitation that would ensure an optimal exploitation of the fish stock (Sparre and Venema, 1998; Hilborn, 2003). Fishery stock assessment primarily relies on data relating to total removal, age and length structure, and abundance indices of the population (Hilborn, 2012). However, a critical issue in

tuna fisheries management lies in the availability of abundance indices capable of reliably depict changes in tuna populations. Indeed, in spite of the significant progress made throughout history of marine fisheries science, a wide range of methods developed for assessing abundance of fish populations remain unfortunately difficult to implement for tuna species, or limited to a few species, or certain stages of development (early life stages or spawning stages with a more limited spatial distribution). The following paragraphs review the main population assessment techniques and abundance indices used in tuna management, and discuss their relevance, strengths and limitations particularly in relation to the three major tropical tuna species (namely skipjack tuna (*Katsuwonnus pelamis*), bigeye tuna (*Thunnus obsesus*) and yellowfin tuna (*Thunnus albacares*) as they account for most of the world's commercial tuna catches (ISSF, 2019).

2. Abundance indices in tuna fisheries management

Abundance indices used for the assessment of fish populations, including tunas, are mainly based on two types of data sources: fisheries-dependent and fisheries-independent data. Fisheries-dependent data are related to the fishing process itself, and mainly consist of usually mandatory information on catches and fishing activities (e.g. fishing effort) provided by the fishers themselves. On the other hand, fishery-independent data are mostly based on scientific surveys and involve a wide variety of techniques whose relevance for collecting data on the abundance and composition of fish stocks is largely dependent on species characteristics (e.g. acoustic or aerial surveys, etc.).

2.1. Fisheries-independent indices

Fishery-independent indices are constructed from data collected during periodic or episodic surveys conducted by scientists or fisheries management agencies. Although high quality data can be obtained through scientifically designed and standardized sampling and data collection carried out in independent surveys (National Research Council, 2000); fisheries-independent data may be affected by deficiencies related to their expensive cost and limited spatial and temporal coverage (Hilborn and Walters, 1992).

Fishery-independent assessments of tuna population are typically based on direct observations through visual or acoustic surveys, or indirectly through larval censuses. Mark and recapture methods are also commonly used in tuna population assessments. However, they deserve a special status as "semi-independent" surveys, since in the case of tuna population studies they are partly dependent on fishing activities, especially for information retrieval. These different survey techniques and the derived abundance indices are presented in the following sections.

2.1.1. Aerial surveys

The very first series of scientific aerial surveys to assess tuna populations were conducted from the 1990s onwards in the North-Western Atlantic (Lutcavage, 1995; Lutcavage *et al.*, 1997), and along the Southern Australian coasts (Cowling and O'Reilly, 1999; Eveson *et al.*, 2016). Before, spotting tuna schools from aircrafts was primarily used by the commercial tuna fishery as a fishing-assistance operation with the aim to improve their efficiency although some surveys were conducted for scientific purposes (Stéquert and Marsac, 1989; Petit, 1991; Basson and Farley, 2014). Aerial surveys consist of transects carried out in an aircraft at a constant speed and altitude, during which schools or aggregations of tuna (several schools) are visually detected, geolocated and roughly estimated in size by human observers (Figure I.2). Detection is made possible by the surface activity of tunas (jumping, fast swimming) related to their feeding or foraging activity (Bauer *et al.*, 2020). The estimation of an abundance index from aerial surveys data is typically based on the distance sampling theory (Buckland *et al.*, 2015). The transect is defined in a given area within which the estimate of the density of tuna schools (D) is usually calculated using the following formula:

$$D = \left(\frac{1}{2wL}\right) n \qquad \text{(I. 2)}$$

where n denotes the number of detected tuna schools, L the transect length and w the width of the detection from the line of the transect. Aerial survey data also offer substantial information on the spatial distribution of the species concerned, and their ecology, especially when related to environmental data (Royer *et al.*, 2004).

Despite the relative simplicity of its methodological framework, the use of aerial surveys for tuna population assessment has limitations in terms of the spatial coverage that can be achieved by the method. Indeed, aerial surveys on the scale of large oceanic regions remain hardly

conceivable, both technically and economically. The method is therefore suitable for tuna species with a geographically limited distribution at one or another life stage. Nearly all its applications have been carried out on juvenile bluefin tuna, a temperate species known to assemble during this life stage at specific locations and periods (Eveson *et al.*, 2016, 2018a; Bauer *et al.*, 2020; Rouyer *et al.*, 2020).

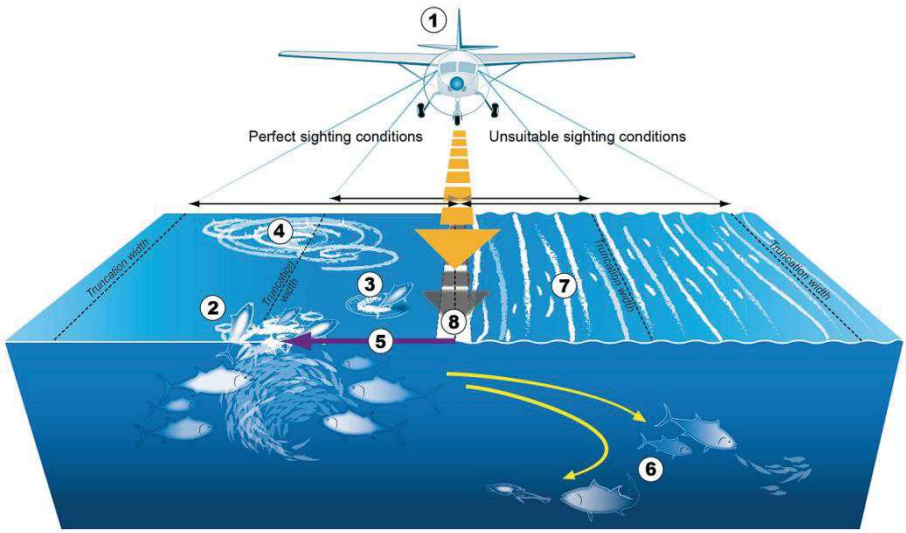

Figure I.2: Schematic drawing illustrating Atlantic bluefin tuna (*Thunnus thynnus*) aerial surveys under perfect (left side) and impaired (right side) survey conditions. (1) aircraft on transect line; (2) tuna school feeding with multiple jumpers; (3) small tuna school feeding with single tuna jumping; (4) large tuna school aggregation zones extending over several miles; (5) perpendicular distance; (6) tuna schools chasing in deeper waters; (7) waves with whitecaps; (8) blind spot for lateral detection. Source: Bauer *et al.*, (2015).

The reliability of abundance indices constructed from aerial surveys is related to a good knowledge of the surface and vertical behaviour of the species of interest. Variability over time in the vertical behaviour of the species in response to the prevailing environmental conditions, is likely to induce significant biases in the interpretation of the aerial survey time-series (Bauer *et al.*, 2015, 2020). The detectability of animals can also be strongly impeded by both environmental conditions and the sighting prowess of human observers (Eveson *et al.*, 2018b). In practice, aerial surveys are generally limited to favourable weather conditions. For instance, aerial surveys of juvenile bluefin tuna in the Western Mediterranean Sea are conducted only during the summer season (Fromentin *et al.*, 2003; Rouyer *et al.*, 2020). On the other hand, observer rotation and assistance with video camera or unmanned aerial vehicles (UAVs) could

potentially help to reduce the perception bias in tuna spotting (Colefax *et al.*, 2018; Žydelis *et al.*, 2019; Jech *et al.*, 2020).

Finally, despite attempts to infer the number of fish from the size of the detected school (Bauer *et al.*, 2015), aerial surveys still only provide a qualitative or semi-quantitative index of abundance, since they only give information on the density of schools and not on the biomass or density of individuals. The contribution of remote sensing techniques with LIDAR (Light Detection and Ranging) systems for the detection of tuna (Oliver *et al.*, 1994; Churnside *et al.*, 1998; Larese, 2005), as well as acoustic surveys coupled with underwater observations are seen as promising prospects for improving this approach (Weber *et al.*, 2013; Rouyer *et al.*, 2018).

2.1.2. Acoustic surveys

The Allied fleet's need for a detection system against German submarines during the First World War constituted the first significant impetus to the progress in underwater acoustics, resulting in the development and first effective use of passive acoustic detection systems. Since then, there have been substantial advances in underwater acoustics techniques that have greatly benefited fisheries research. The use of acoustic techniques for observing fish and estimating fish abundance, described in detail by many authors (e.g. Maclennan, 1990; Simmonds and MacLennan, 2005), has become increasingly important over time.

Estimating abundance of marine species through acoustic techniques relies on the use of active acoustic detection systems, specifically scientific echosounders that emit a sound pulse and measure the backscattered echoes from targets. Acoustic abundance estimation is then carried out following two approaches depending on whether the targets are dense schools or scattered individuals (Fernandes *et al.*, 2002). When targets are sufficiently dispersed to allow their individual detection, absolute estimates of their abundance can then be made simply by counting their individual echoes (e.g. marine mammals: (Barlow and Taylor, 2005; Lewis *et al.*, 2007)). For fish schools or shoals, the so-called “echo-integration” approach is used (Foote, 1983). It consists of a quantitative estimation of the biomass based on the linearity relationship between the specific acoustic energy backscattered by a single fish and the total acoustic backscatter of the group of fish. Echo-integration thus implies an appropriate knowledge on the acoustic characteristic of fish species studied, namely their target strength value (acoustic reflection coefficient of the fish).

Currently, the use of acoustics to assess the abundance of marine species is a common method applied to a wide range of fish such as small pelagic species (e.g. Brandt, 1991; Hampton, 1992, 1996; Porteiro et al., 1996; Gjøsæter et al., 1998; Toresen et al., 1998). However, the spatial distribution of tuna, particularly tropical species, represents a significant limitation to the application of this method given the size of the areas to be sampled. In addition, the relative paucity of data on the acoustic properties of tropical tuna species strongly compromises the processing of the acoustic signal into biomass estimates. As a result, there are still few applications of acoustics to assess their population abundance (Bertrand, 2000; Moreno *et al.*, 2019; Uranga *et al.*, 2020), with nevertheless, the exception of Atlantic bluefin tuna for which a relative index based on the counting of echoes from single targets outside schools, is used since 2016 in stock assessments (Melvin *et al.*, 2018; Minch, 2020).

2.1.3. Larval surveys

Abundance indices based on larval surveys have been widely used to infer information on the spawning biomass of bluefin tuna (Ingram *et al.*, 2007, 2010, 2013, 2015; Lamkin *et al*., 2015). Scott *et al*. (1993) were the first to derive an abundance index for the Western bluefin tuna stock using larval abundances from annual ichthyoplankton surveys conducted since 1977 by the NOAA Fisheries in the Gulf of Mexico (for details on the sampling procedures refer to Richards and Potthoff, 1980 and McGowan and Richards, 1986).

Being the species with the most extreme spatiotemporally restricted spawning behaviour with relatively well-identified spawning grounds (Richards, 1976; Scott *et al.*, 1993; García *et al.*, 2005; Alemany *et al.*, 2010; Muhling *et al.*, 2010), bluefin tuna represents the most suitable candidate among tuna species for the use of larval surveys to study the abundance of its populations. This is mainly linked to the fact that unlike bluefin tuna, tropical tunas species have generally a significant overlap between spawning and feeding grounds, and longer spawning seasons of several months (Muhling *et al.*, 2017). In addition, the visual identification of tropical tuna species in their larval stage is particularly challenging and may require the contribution of genetic analyses (Viñas and Tudela, 2009).

2.1.4. Mark-recapture techniques

Mark-recapture is a common technique used to estimate the size of animal populations, to study movements and migration of individuals, to provide information on death and growth rates of wild species, as well as on fishing pressure (Katsanevakis *et al.*, 2012). Widely used in terrestrial ecology for population assessment, mark-recapture techniques have been thoroughly addressed and reviewed by numerous authors (e.g. Seber 1986, 1992; Krebs 1999; Schwarz and Seber 1999; Seber and Schwarz 2002; Southwood and Henderson 2009; Katsanevakis *et al.* 2012). Mark-recapture methods basically consist of capturing, marking (tagging) and releasing a number of individuals from a population and then re-sampling the same population to assess the number of marked individuals within the recaptures. The ratio of marked recaptures (R) to initially marked individuals (M) provides a detection probability (comparable to the proportionality parameter used in Equation I.1) which thus makes it possible to estimate the size of the entire population (N). For single episodes of capture and recapture, the simplest way to estimate abundance is given by the Lincoln-Peterson estimator for a closed population (Schwarz and Seber, 1999):

$$\widehat{N} = \left(\frac{M}{R}\right) C \qquad \text{(I. 3)}$$

where C is the total number of recaptures. Mark-recapture experiments also provide valuable data on species biology, such as growth rates (Lehodey *et al.*, 1999; Hearn and Polacheck, 2003) and migration patterns (Sibert *et al.*, 1999; Shiham and Sibert, 2002; Ichinokawa *et al.*, 2008). Nevertheless, the validity of the mark-recapture approach for abundance estimates depends on certain restrictive assumptions:

- no effect of marking on individual fitness;
- a constant ratio of marked to unmarked animals during the sampling interval;
- a uniform probability of individuals being captured (or recaptured);
- and a homogeneous distribution of individuals in the population after capture and tagging.

In large-scale tuna-tagging projects, data may be significantly affected by the post-release mortality associated with tagging (potentially as a result of an increased predation on released fish due to stress, physiological impairment or injuries resulting from the tagging operation), and by tag shedding (Hoyle *et al.*, 2015; Katara *et al.*, 2017; Gaertner *et al.*, 2019).

In addition, in tuna tagging programs, recaptures of tuna are primarily provided by the commercial fishery. As a consequence, conventional tagging techniques cannot be considered

fully independent of the fishery and rather deserve a status of "partially" or "semi-independent". Depending on the nature of the fisheries, recapture rates can be substantially biased by a poor tagging reporting (Fromentin, 2010). Problems may also arise from the way in which tagged tunas disperse within the population to be estimated (Langley and Million, 2012; Kolody and Hoyle, 2015). On the other hand, the implementation of large-scale tuna tagging programs is expensive, logistically difficult and requires considerable effort and planning (Leroy *et al.*, 2015). Tuna tagging data are therefore provided on an episodic basis.

Finally, although data from mark-recapture experiments have been an integral part of monitoring tuna stocks since the late 1970s (Leroy *et al.*, 2015), they are rarely used alone to estimate tuna abundance, but are rather generally combined with annually collected fishery-dependent data in integrated assessment models to obtain abundance estimates (e.g. ICCAT, 2014, 2018, 2019; IOTC, 2020).

2.1.5. Close-Kin Mark Recapture

Traditionally, individual fish censuses represented the most obvious form of fish population assessment, but recent advances in molecular genetics now offer promising tools for measuring a wide range of population characteristics and monitoring their evolution over time (Pope *et al.*, 2010). Bravington *et al.*, (2016a) presented an original alternative for estimating the absolute abundance of tuna populations based on a modified mark-recapture framework where "recaptures" are parents rather than individuals: the Close-Kin Mark Recapture (CKMR). The CKMR provides a fishery independent approach to estimate the spawning stock biomass based on the likelihood of detecting parent-offspring pairs (POPs) in a sample of fisheries landings. It relies on the kinship relationships between randomly sampled numbers of adults (m_a) and juveniles (m_j) to estimate the total abundance of adults in the population (N_{adult}), according to a relatively simple concept: each juvenile represents a genetically tagged "recapture" of its two parents (Figure I.3). Thus, the probability of a given juvenile being the offspring of an adult in the total population is $2/N_{adult}$. Pairwise comparisons of genotypes of the sampled adults and juveniles, then makes possible to estimate N_{adult}, from an equation analogous to the Equation I.3, the Lincoln–Petersen abundance estimator in standard mark-release recapture (Bravington *et al.*, 2016b):

$$\widehat{N}_{adult} = \frac{2m_a m_j}{P} \qquad \text{(I. 4)}$$

where *P* denotes the actual number of parent-offspring pairs (POPs) found experimentally. The successful application of this approach for the assessment of the absolute abundance of southern bluefin tuna (*Thunnus macoyii*) by Bravington *et al.* (2016b) has highlighted its interesting potential for monitoring and assessing stocks of other tuna species (Kolody and Bravington, 2019). Currently, the Indian Ocean Tuna Commission (IOTC) has prioritized in its 2019 Work Plan, new research surveys based on CKMR for yellowfin tuna.

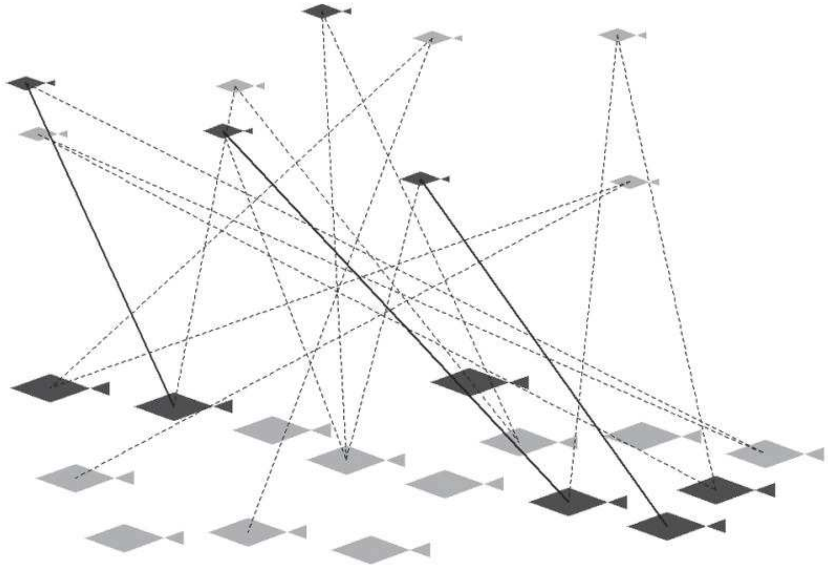

Figure I.3: Schematic of parent-offspring pairs (POPs) relationships. Juveniles are the small fish at the top, and lines to larger fish represent parent-offspring connections; dark and light shades correspond to sampled and non-sampled individuals respectively. Solid lines represent the number of matches between adults and juveniles. Source: Bravington *et al.,* (2016b).

2.2. Fishery-dependent index: the Catch Per Unit of Effort

In the management of tropical tuna fisheries, the wide distribution and highly migratory nature of tropical tuna species make the implementation and generalisation of fishery-independent data collection methods particularly challenging. As a consequence, stock assessments for these species rely almost exclusively on indirect abundance estimators calculated from input data associated with commercial catches (Maunder and Punt, 2004). Catch data, when related to the corresponding effort deployed by fishermen, are used to provide information on relative trends in the evolution of stocks in a given area and period, following the conceptual relationship described above (Equation I.1), by relating the catch rate or Catch-Per-Unit-Effort (CPUE) to the abundance (N), through the catchability of tuna (q).

$$CPUE = qN \quad (\text{I. } 5)$$

However, the interpretation of CPUE as an abundance index is notoriously problematic in fisheries science. Indeed, several factors likely to influence catchability can be misinterpreted as changes in abundance (National Research Council, 2000; Harley *et al.*, 2001; Maunder and Punt, 2004; Maunder *et al.*, 2006; Ye and Dennis, 2009). The typical situation of non-proportionality between CPUE and abundance is known as "hyperstability" and corresponds to CPUE that remains high while abundance declines (Hilborn and Walters, 1992; Harley *et al.*, 2001). A hyperstable CPUE can lead to an overestimation of abundance and underestimation of fish mortality. The opposite, referred to as "hyperdepletion" (CPUE declining faster than abundance), can result in an overestimation of mortality while stocks remain weakly exploited. Addressing the inappropriateness of using CPUE data to assess the status of communities, Maunder *et al.*, (2006) noted that the most common causes of this non-proportionality were related to:

(i) changes of efficiency of fleets leading to increased catchability as a result of improved fishing techniques and operations, and accumulation of knowledge and information on the distribution and behaviour of fish;

(ii) changes in species targeting which result in decreased catchability of one species to the benefit of another, and which may be incorrectly interpreted as a decrease in the abundance of the first species;

(iii) environmental variations that may differently affect the species catchability from one area (or period) to another;

(iv) and time-varying spatial dynamics of fish and fishing fleet: since commercial fishing activities are obviously focused on areas with high population density, they may therefore give a biased picture of abundance.

To allow undistorted comparisons over time, CPUE data are usually standardized using statistical models, to account for these various factors unrelated to changes in population abundance (Maunder and Punt, 2004; Bishop, 2006).

In tropical purse seine fisheries, the continuous evolution of fishing power and strategies has considerably increased the catchability of tropical tuna species over the past three decades (Fonteneau *et al.*, 1999; Lopez *et al.*, 2014; Scott and Lopez, 2014; Torres-Irineo *et al.*, 2014a; Dai *et al.*, 2020). The increasing use of drifting fish aggregating devices (FADs) by purse seine fleets is one of the most important factors contributing to the increase in their fishing efficiency

(Fonteneau *et al.*, 2000, 2013). FADs are man-made floating objects deployed by fishermen to facilitate their catches, by exploiting a peculiar behavioural trait of tropical tunas that lead them to gather around objects floating at sea (Fréon and Dagorn, 2000; Castro *et al.*, 2002). Throughout the history of the tuna purse seine fishery, FADs have been equipped with increasingly technologically advanced instruments, providing fishers with various information, especially on the geolocation of FADs and the fish biomass associated with them (Lopez *et al.*, 2014; Moreno *et al.*, 2019). In the early days of tropical tuna purse-seine fishing, the purse-seiner activities mainly consisted of active periods of searching for free-swimming schools of tunas and fishing, although fishing on randomly encountered natural objects (e.g. logs) occurred since the start of the fishery. This search time for free-swimming schools constituted a relatively relevant metric for measuring the fishing effort associated with a catch in a given area and period (Fonteneau *et al.*, 1999). The non-random nature of FAD-based fishery (due to remote information on fish presence and location) has quickly made inconsistent the traditional purse-seiner nominal effort, based on this metric. As a result, although purse seine fleets alone account for the majority of the total global tropical tuna catches (ISSF, 2019), serious concerns have been raised about the use of time series of CPUE from this fishery in tropical tuna stock assessment models.

2.3. Towards the derivation of novel abundance indices for tropical tunas

For important and heavily exploited species such as tunas, the appropriateness of management policy decisions is generally closely linked to robust estimates of the status of populations in order to monitor their evolution over time and to interpret the magnitude of catches. Time series of abundances estimates (from fishery-independent or dependent sources) constitute, with information on mortality (natural and fishing mortalities) and population structure (compositional age, size, or sex ratios), the three main types of data commonly used in fisheries stock assessments (Hilborn, 2012). In the case of tropical tuna species, although a few independent methods for estimating abundance may be appropriate (notably the CMKR), in most cases they remain practical for only part of the stock, are logistically difficult to maintain in the long term or are simply too costly. As a result, abundance estimates of tropical tunas are primarily based on input data associated with catches, namely standardized CPUE data from longline fisheries for yellowfin and bigeye tuna. Regarding skipjack tuna, it is considered by most tuna RFMOs as a notoriously difficult species to assess. Catches of skipjack tuna by longline fisheries are so low that their catch rates are not considered to be particularly reflective

of the abundance of skipjack, or to exert a significant fishing mortality on this species. Skipjack tuna, which accounts for more than half of the global tuna catches, is mainly caught by purse-seiners under drifting FADs (Dagorn *et al.*, 2013a; ISSF, 2019). The purse-seine CPUE with its inherent uncertainties discussed in previous sections (particularly those related to the development of the FAD-based fishery), is therefore used as abundance index this species. These issues have in recent years led to a growing interest among scientists and fisheries managers in alternative methods for assessing the abundance of tropical tunas, which could help to reduce uncertainty in stock assessment results.

Since the late 2000s, FADs deployed by purse-seine fisheries have been progressively equipped with satellite-linked echosounder buoys that continuously collect a range of data around them, including their geolocation and acoustic information on their associated biomass (Lopez *et al.*, 2014; Moreno *et al.*, 2019). In some ways, these devices have turned drifting FADs into unprecedented observers of the open ocean (Imzilen *et al.*, 2019) and have thus offered new opportunities to study different aspects of the ecology and behaviour of pelagic communities that associate with floating objects, including tunas (Moreno *et al.*, 2016; Brehmer *et al.*, 2019). Taking advantage of these new opportunities, Santiago *et al.*, (2016, 2019), have developed the Buoy-derived Abundance Index (BAI): a catch-independent index of abundance for tropical tuna species based on data collected by satellite-linked echosounder buoys. The BAI is a relative index, which relies on an assumed proportionality relationship between the FAD-associated biomass (estimated from acoustic data provided by echosounder buoys) and the total abundance of tuna. This index has been incorporated as a complementary abundance index into the last stock assessment of Atlantic yellowfin tuna conducted in 2019.

In addition, recent decades have seen the increasing development of passive acoustics with the use of acoustic tags attached to fish that allow the monitoring of their movements (e.g. Ohta and Kakuma, 2005; Dagorn *et al.*, 2007a; Schaefer and Fuller, 2013; Rodriguez-Tress *et al.*, 2017; Tolotti *et al.*, 2020). However, until the findings of Capello *et al.*, (2016), this technology was primarily dedicated to improving knowledge of the biology and behaviour of fish species and did not appear to have much application in fish abundance assessments (Nielsen *et al.*, 2009). Capello *et al.*, (2016) have evidenced that for species that exhibit associative behaviour around aggregating points, absolute abundance of total populations could be derived from a model based on specific metrics that describe this behavioural characteristic, and from data on the local population around the aggregating points.

These two approaches open up interesting prospects in which FADs long exploited by fishers across the oceans to improve their catches, could be diverted to improve the assessment of tropical tuna populations through the development of novel abundance indices. Such indices could be based on the associative behaviour of these species with floating objects and the unprecedented data sources offered by echosounder buoys.

3. Thesis objective

The general objective of the thesis is **to derive a novel abundance index for tropical tuna species based on their associative behaviour around floating objects**. This objective implies a necessary improvement of knowledge about tuna behaviour and especially a better understanding of their associative dynamics with floating objects. Its implementation has therefore been defined according to a research strategy built around a consecution of three specific objectives:

(i) To develop a methodological framework to extract reliable scientific information from data recorded by commercial echosounder buoys that equip FADs;

(ii) To describe the dynamics of tuna aggregations around FADs from these new data sources;

(iii) To provide a new abundance index for tropical tunas based on their associative behaviour with floating objects and echosounder data.

4. Thesis structure

The present thesis is structured in four main chapters. The first two address the preliminary specific objective related to the processing of data from echosounder buoys. Indeed, echosounder buoys data come from devices primarily intended to provide fishers with information on their target tuna species. Their use in a scientific framework therefore requires the development of adequate and standardized procedures for their collection, processing and validation. **The first chapter** is related to this prerequisite, and proposes a data collection protocol specifically designed for satellite-linked buoys used in the tropical purse seine fishery.

The **second chapter** presents a new processing approach for acoustic data collected by echosounder buoys, which breaks with the traditional echo-integration approach, and allows the characterization of fish aggregations under floating objects from the implementation of machine learning techniques.

Based on the methodological framework provided in the previous sections, **the third chapter** addresses new questions on the dynamics of tuna aggregations with floating objects, at the scale of the Atlantic and Indian Oceans. Through the analysis of occupancy of floating objects by tunas, obtained from echosounder buoys, this chapter measures some key parameters characterizing the aggregations dynamics of these species.

Chapter 4 describes the modelling approach underlying the new abundance index proposed for tropical tuna species, which relate their individual behavioural traits to the dynamics of floating object occupancy by their aggregations determined from echosounder buoys. An application of the model to the case study of the abundance of the skipjack tuna (*Katsuwonus pelamis*) in Western Indian Ocean is presented.

Finally, the general conclusions and perspectives arising from this thesis dissertation are discussed.

Chapter 1

Processing data from satellite-linked buoys used in tropical tuna fisheries for scientific purposes: A standard protocol

"*Le savant doit ordonner ; on fait la Science avec des faits comme une maison avec des pierres; mais une accumulation de faits n'est pas plus une science qu'un tas de pierres n'est une maison.*

The Scientist must set in order. Science is built up with facts, as a house is with stones. But a collection of facts is no more a science than a heap of stones is a house."

Henri Poincaré

Abstract

Satellite-linked buoys used by tropical tuna purse seiners on drifting fish aggregating devices (DFADs) provide a continuous stream of information on both the ocean characteristics and the pelagic communities associated with DFADs. This unprecedented amount of data is characterized by an ocean-scale distribution with high spatial and temporal resolution, but also by different data formats and specifications depending on buoy models and brands. Their use for scientific studies is therefore critically dependent on the algorithms used for their processing and standardization. This paper describes the data provided by the main buoy models used by the European purse seine fleet and presents a standardized processing protocol for their use in scientific studies. Three major issues that need to be addressed prior to the scientific exploitation of these industry-based data are identified (structural errors, data collected on land and onboard vessels) and five specific filtering criteria are proposed to improve their quality. Different filtering procedures are also compared for some of the criteria, and their advantages and limitations are discussed.

Keywords: Instrumented DFADs; Satellite-linked buoys; Purse seiners; Tropical tunas; Data processing.

1.1. Introduction

Defined as man-made floating objects specifically designed to attract tunas and improve catches, Drifting Fish Aggregating Devices (DFADs) constitute one of the major fishing tools used in the tropical tuna purse seine fisheries (Fonteneau *et al.*, 2013). It has been estimated that around 65% of the global tropical tuna purse seine landings originate from catches under DFADs (Scott and Lopez, 2014a). The DFAD-based fishery relies on a behavioural trait of several pelagic marine species including tropical tunas leading them to gather in mass around objects floating at sea. Since their introduction in tropical tuna purse seine fisheries, DFAD technology has been subject to a rapid evolution beginning with various designs of rafts and fishers attaching different instruments to locate them, from reflectors to radio buoys and later satellite-linked GPS systems (Dagorn *et al.*, 2013a; Lopez *et al.*, 2014). Currently, most deployed DFADs are equipped with satellite-linked echosounder buoys that provide near real-time and remote information on the presence and the size of the fish aggregation associated to the DFADs (Lopez *et al.*, 2014; Moreno *et al.*, 2019b). This remote information results in significant increase in the fishing efficiency of purse seiners (Fonteneau *et al.*, 2000).

The positive effect of DFADs on purse seine fishing efficiency and their intensive use have raised several questions related to their impacts on tuna stocks and ecology, as well as on marine ecosystems (Dagorn *et al.*, 2013a). The major changes in fishing strategies induced by the use of DFADs have also introduced significant biases and limitations in the traditional methods used to assess tuna populations from purse-seiner commercial data (Fonteneau *et al.*, 2013; Torres-Irineo *et al.*, 2014a). As a result, one of the key concerns of Tuna Regional Management Organisations (TRFMOs) currently lies in the need for complementary data and methods to reduce the uncertainties associated with DFADs in stock assessment models and to assess their actual influence on the sustainability of fisheries. In such context, the huge amount of data collected by the instrumented buoys equipping DFADs could constitute an important asset. Because of their number, wide spatial distribution and constant maintenance by fishers, satellite-linked echosounder buoys allow effortless and cost-effective collection of various types of data likely to provide valuable insights on the ocean dynamics (Imzilen *et al.*, 2019), as well as on the distribution and behaviour of fish (Lopez *et al.*, 2017; Orue *et al.*, 2019c). Due to these characteristics, instrumented DFADs appear to be privileged observatories of marine pelagic communities (Moreno *et al.*, 2016a; Brehmer *et al.*, 2019). At present, three major

manufacturers dominate the DFAD buoy industry[1], and offer different models varying in terms of hardware and software (Moreno *et al.*, 2019b). Data collected on DFADs therefore consist of complex datasets that greatly vary in nature and format depending on buoy models. Although some processing protocols have already been proposed (Maufroy *et al.*, 2015; Orue *et al.*, 2019c), they remain relatively brand specific. In parallel, growing concerns about the impacts of DFAD use have led to the development of a number of specific plans for their management by TRFMOs, incorporating, inter alia, the strengthening of reporting requirements on DFAD activities (e.g. IOTC: Res. 19/08; ICCAT: Rec 19-02; IATTC: C-19-01; WCPFC: CMM 2018-01).

As a key priority in their use for scientific or regulatory purposes, the typical heterogeneity in DFAD-related data therefore requires the design of a standard framework to process this huge amount of industry-based data into exploitable scientific data, notably through appropriate standards and procedures for their collection and processing. To this end, through an extensive exploratory analysis and comparison of performance of different processing algorithms applied to data from different manufacturers and models of buoys, we present a standard protocol including cleaning, control and validation procedures for the processing of raw data collected by satellite-linked buoys used in tropical tuna purse seine fisheries.

1.2. Material and Methods

1.2.1. *Data collection*

Buoys data has been gathered in the Atlantic and Indian Oceans, under specific data-exchange agreements signed between different research organisms (i.e. AZTI and IRD) and EU tuna purse seiner associations (i.e. ORTHONGEL[2] for French fleet of purse-seiners, Echebastar and Atunsa companies in ANABAC[3] and OPAGAC[4] for Spanish fleets), under the frame of EU project RECOLAPE[5].

[1] Marine Instruments (www.marineinstruments.es), Satlink (www.satlink.es) and Zunibal (www.zunibal.com)
[2] Organisation française des producteurs de thons congelés et surgelés
[3] Asociación Nacional de Armadores de Buques Atuneros Congeladores
[4] Organización de Productores Asociados de Grandes Atuneros Congeladores
[5] MARE/2016/22 "Strengthening regional cooperation in the area of fisheries data collection"

For each ocean and fleet, a dataset was created. It consisted in information collected by a sample of 1,000 buoys from the three main buoy manufacturers, during a random month of the year 2016. According to their hardware and software, a wide range of information can be provided by the different buoy models (see Moreno *et al.*, 2019). Common information provided included the buoy identification code, hour, date, position (latitude and longitude) and buoy speed. The Table 1.1 provides a list of the different buoy models present in the different datasets, as well as a description of the raw data received by the research organisms.

Since the objective of this work was not to compare the characteristics of the databases between fleets or organizations, but rather to define a common processing protocol adapted to their potential specificities, the datasets examined for each fleet (also corresponding to specific data exchange-agreements) will herein be referred to as D1 and D2. Following the same principle, the different buoy models included in this study were also anonymized. The D1 datasets consisted of 62,902 and 61,194 rows for the Atlantic and Indian oceans respectively, whereas the D2 datasets were composed of 25,304 rows for the Atlantic Ocean, and 22,461 rows for the Indian Ocean.

1.2.2. *Data processing protocol*

The data processing protocol consists in the definition of five specific filtering criteria, structured into three main processing steps (see Figure 1.1).

1.2.2.1. Stage 1: Structural errors filtering

Structural errors are here defined as duplicate or irrelevant rows in the dataset resulting from failures in data collection or transfer. Three types of structural errors mainly related to failures during satellite-communication have been identified.

(i) Filter F1: Duplicate rows

Duplicate data refer to rows with identical buoy codes, timestamps and positions. Generally, all other information in the duplicate rows remain strictly identical, however in rare cases, missing values may occur for some lines. Duplicates were identified based on their identical buoy codes, timestamps and locations. In the cases of missing data, the row considered as the original was the one with the most complete information.

Table 1.1: Description of the raw acoustic data received depending on buoy manufacturers and the different data-exchange agreements (DEA1 and DEA2).

		Marine Instruments		Satlink	Zunibal
		DEA1	DEA2		
Buoy Operation Data	Buoy identification code	☒	☒	☒	☒
	Owner vessel(s)	☒	☐	☒	☐
	Buoy activation date	☒	☐	☐	☐
	Buoy deactivation date	☒	☐	☐	☐
	Flash (notification on activation of the buoy flash)	☒	☐	☐	☐
	Buoy operating mode)	☒	☒	☐	☐
	Buoy battery level	☒	☒	☐	☐
Location data and other data	Timestamp of GPS position data	☒	☒	☒	☒
	GPS position data	☒	☒	☒	☒
	Buoy speed	☒	☒	☒	☒
	Buoy drift angle	☒	☐	☐	☐
	Sea water temperature	☒	☒	☐	☐
Acoustic sampling data	Timestamp of acoustic data collection	☒	☒	☒	☐
	Sampling frequencies	☒	☐	☐	☐
	Echosounder detection range	☒	☒	☐	☐
	Gain of acoustic samplings	☒	☒	☐	☐
	Resolution (number of bits used in each layer)	☒	☒	☐	☐
	Number of depth layers	☒	☒	☐	☐
	Total biomass index (estimated tonnage from the echosounder)	☒	☐	☒	☐
	Maximum biomass estimated at any layer	☐	☐	☒	☐
Acoustic data format		Integers (from 0-7 or 0-15) representing the intensity of the acoustic signal detected		Biomass (t) estimated per layer of 11.2 m over 115 m depth (10 layers), based on a buoy-integrated algorithm	Biomass in tons (dB for each layer)
Buoys models in the dataset		M3+, M4I, M3I, MSI		DL+, DSL+, ISD+, ISL+	T7+

(ii) Filter F2: Ubiquitous rows

Ubiquitous rows correspond to cases where two rows have identical buoy codes and timestamps, but are associated with different locations. Rows with the above characteristics were identified and the distance between locations was calculated. When the two positions were separated by less than 1 km, a randomly selected row was retained while the other was considered "ubiquitous". Otherwise, the two rows were assigned as "ubiquitous".

(iii) Filter F3: Isolated positions

Positions separated from their nearest neighbours on a buoy track, by more than 48 hours or having an inconsistent speed (considering a threshold of 35 knots, a value far above speeds of tuna purse seiners currently operating), were referred to as isolated positions. By addressing the buoy track (ensemble of positions belonging to a single GPS buoy), this filtering step allows to identify distinct series of consecutive positions (segments) separated by potential GPS failures, buoy relocations or buoy deactivation/reactivation events on a given buoy track.

1.2.2.2. Stage 2: Filtering of land positions (Filter F4)

Buoys located on land (due to beaching events or active buoys brought back to port) were detected using shoreline data from the GSHHG database (Global Self-consistent, Hierarchical, High-resolution Geography; Wessel and Smith, 1996). The influence of different shoreline resolutions on the filtering procedure was assessed through the comparisons of results from low and high-resolution shorelines buffered with 0.05°.

1.2.2.3. Stage 3: Filtering of water/board buoys (Filter F5)

Echosounder buoys can be activated on board ships prior to their deployment. Similarly, buoys retrieved from water may also continue to collect data on board vessels for variable durations. This leads to a buoy track composed of on-board and water segments. In order to discriminate on-board from water positions, two different approaches were compared. The former consists in a rule-based algorithm using buoy speed and its variation as main variables for classifying buoys data referred to as "kinetic classification algorithm". The second relies on a random forest model (Breiman, 2001) trained from a learning dataset built from information provided by the Zunibal buoys. The two algorithms allow the classification of buoys data into three classes: "water" (for buoys actually at water), "board" (for buoys emitting on board a vessel) and

"undetermined" (subset of positions that remained unclassified). Finally, comparisons of the classification results of the two algorithms were carried out through the calculation of simple matching coefficient estimated from confusion matrices derived from the outputs of the two approaches (Sokal, 1958). For this purpose, unclassified buoy positions were considered as emitting as water.

(i) Kinetic classification algorithm (KiC)

The kinetic classification algorithm uses deterministic rules encoded in the form of if-then-else statements as a representation of knowledge. The different rules derive from the knowledge of surface currents in tropical oceans and the behaviour of tuna purse seiners. The algorithm consisted of two iterative classification steps based on three main parameters (see Figure 1.2A): (*i*) the *buoy speed* (calculated between consecutive buoy positions separated by less than 24 hours) (*ii*) the *buoy speed history* (maximum value of the speed recorded over a time window of 3 days before the current buoy position), (*iii*) and the *change in buoy speed* (absolute value of the speed difference between two consecutive points). The three rules governing the first classification step were stated as follows:

1) A position with a *buoy speed* higher or equal to 6 knots correspond to an on-board position;
2) A position with a *buoy speed history* of less than 6 knots corresponds to a buoy emitting at water;
3) A position that does not meet either of the two rules has an undetermined status.

The selected cut-off value of 6 knots is largely higher than the theoretical maximum drift speed in the Atlantic and Indian Oceans. Since the average speed of tuna seiners is well above this value (from 9 to more than 12 knots), buoys whose speed exceeds this threshold are very likely to be on board a vessel. The second rule is related to the fact that active purse seine vessels rarely maintain speeds below 6 knots for a long duration, therefore buoys that display low speeds for a continuous period can be considered as actually emitting at water. A number of segments (series of consecutive positions along a buoy track) can be classified from this set of rules. From those segments, (1) "constant sequences" defined as consecutive positions with the same predicted status (on-board – on-board, or water – water), and (2) "transition sequences", where the buoy shifts from one status to another, were defined.

The second classification step relied on the significant differences in the *change of buoy speed* observed between constant and transition sequences (Figure 1.2B). Remaining positions were classified from neighbour to neighbour by comparing their *change of buoy speed* with the

corresponding distributions found respectively for constant or transition sequences (using a Student *t*-test at confidence level of 95%). This procedure was carried out in both directions (forward and backward) on each buoy segment.

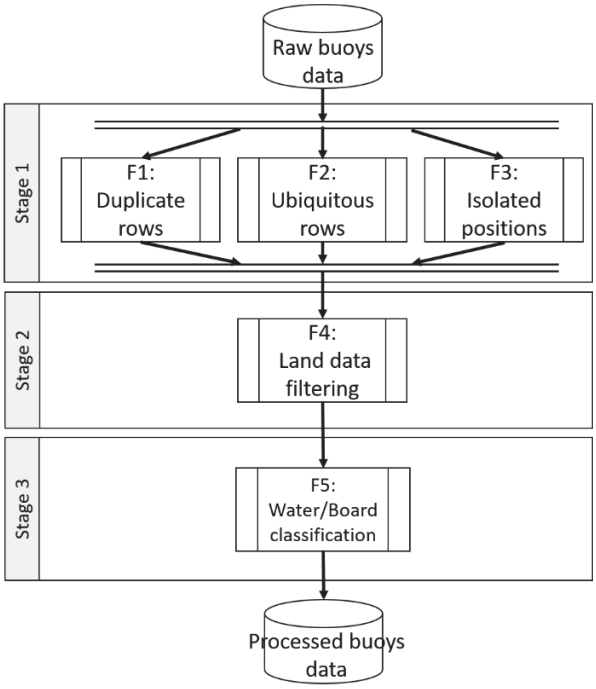

Figure 1.1: Workflow of the standard processing protocol for satellite-linked echosounder buoys used in tropical purse seine fisheries.

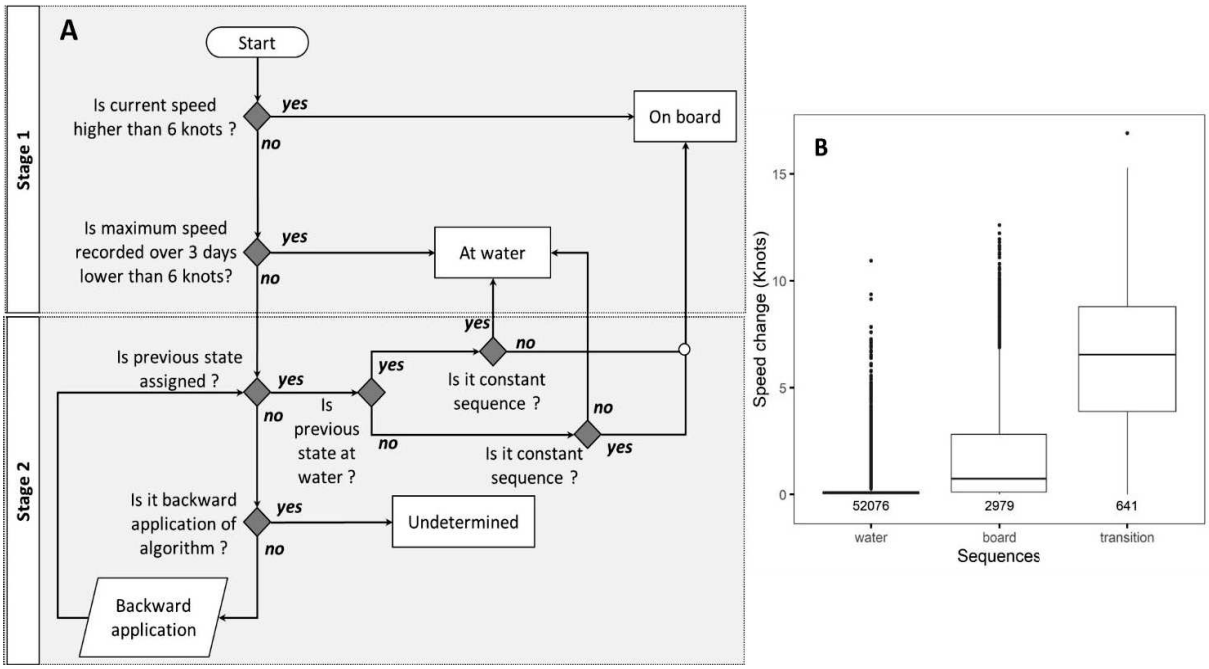

Figure 1.2: Description of the kinetic classification algorithm (panel A), and speed changes in constant (board: board-board, water: water-water), and transition state (board-sea, sea-board) from the D1 dataset in Atlantic Ocean (panel B), Values represent the number of data in each sequences.

(ii) Random forest approach (RF)

The RF approach derives from the procedure proposed by Orue *et al.*, (2019). The learning dataset was built from data provided by the buoys from model 9, which have the capability to detect the buoy immersion in seawater, thanks to an algorithm fed with data from an inbuilt conductivity sensor. The RF classification model was constructed using (*i*) distance between two consecutive points, (*ii*) buoy speed; (*iii*) change in speed; (*iv*) acceleration, (*v*) azimuth (degree), (*vi*) change in azimuth (degree) and (*vii*) time since the first and last observation of the corresponding buoy trajectory (days), as predictors variables. This RF model has previously shown good performance in discriminating water/board positions from a buoy model, (*kappa* = 0.87, further details on model construction and evaluation can be found in Orue *et al.*, 2019)

1.3. Results

1.3.1. *Dataset structure*

In each of the two oceans, large differences between the composition in buoy models available in the two datasets (D1 and D2) were observed (Figure 1.3). The D1 datasets consisted of two to four model buoys depending on the oceans, and were mostly dominated by the buoy from the "Model 3". The D2 datasets were composed of about twice as many, with a majority proportion of "Model 6" and "Model 8" buoys in the Atlantic and Indian Oceans respectively.

The temporal resolution of the data provided was also characterized by a significant variability depending on the fleet (or data exchange agreement) or buoy model. The D2 datasets were limited to a single data provided per day and per buoy, regardless of the ocean or buoy model. In contrast, the data resolution was higher in the D1 dataset, with about 3 to 9 data per day depending on the buoy model for both oceans (Figure 1.4).

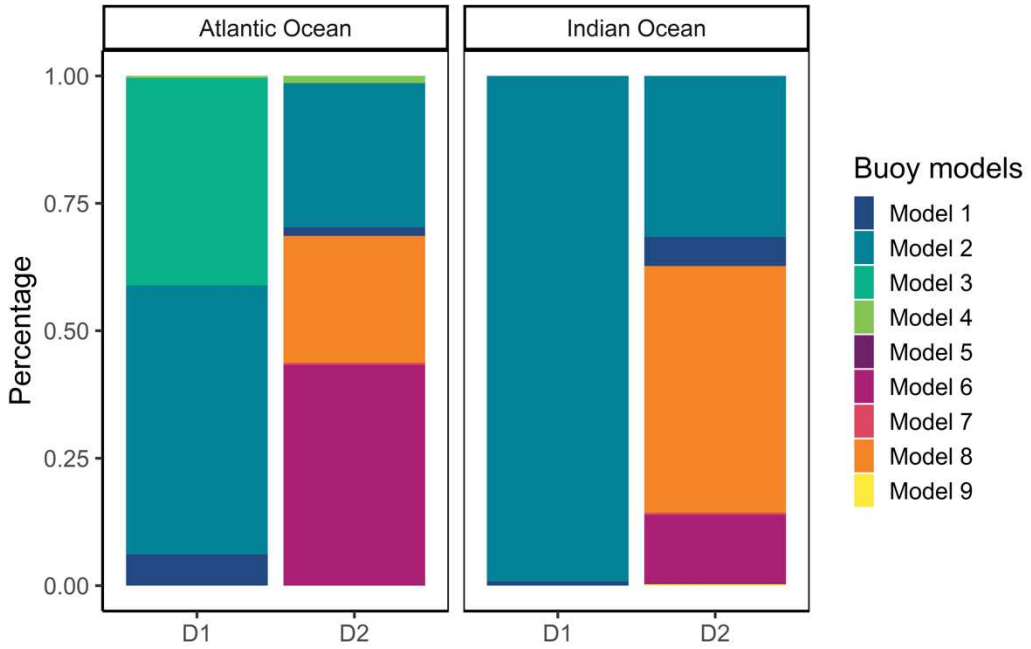

Figure 1.3: Percentage of buoy model constituting the datasets in the Atlantic and Indian Oceans.

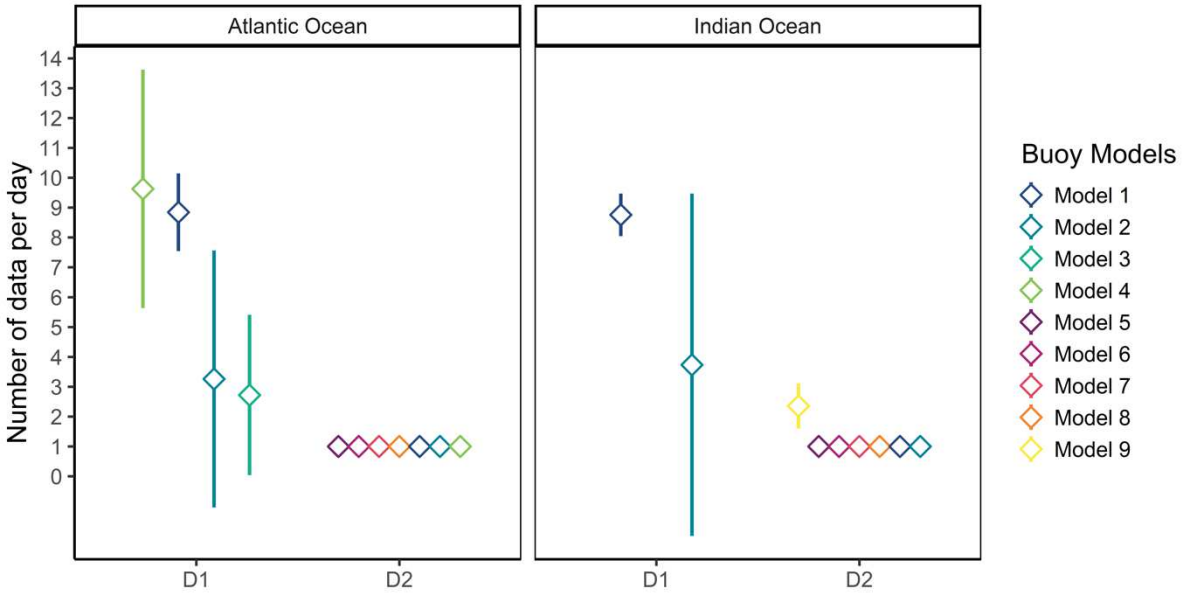

Figure 1.4: Average and standard deviation of the temporal resolution of the data provided by the different buoy models in the Atlantic and Indian Ocean datasets.

1.3.2. *Structural errors filtering outputs*

For all oceans and datasets, structural errors represented less than 1.5% of the entire data (Table 1.2). Duplicate rows occur only in the D1 datasets, while the largest amount of isolated and ubiquitous rows was reported for D2 dataset in the Indian Ocean.

Table 1.2: Number and percentage (in brackets) of structural errors for the different datasets in the Atlantic Ocean (AO) and the Indian Ocean (IO).

Filters	D1		D2	
	AO	IO	AO	IO
F1. Duplicated	47 (0.07%)	94 (0.15%)	0 (0%)	0 (0%)
F2. Ubiquitous	11 (0.02%)	11 (0.02%)	0 (0%)	149 (0.66%)
F3. Isolated	38 (0.06%)	46 (0.07%)	91 (0.36%)	174 (0.77%)
Total	96 (0,15%)	151 (0,24%)	91 (0,36%)	323 (1,43%)

1.3.3. *Land filtering outputs*

The amounts of data filtered from the use of low and high-resolution shoreline data were roughly similar, although with slight differences in the Indian Ocean (Table 1.3). The percentage of land positions ranged between 1% and 8%.

Table 1.3: Number and percentage (in brackets) of data recorded on land for the different datasets in the Atlantic Ocean (AO) and Indian Ocean (IO).

F4. Land	D1		D2	
	AO	IO	AO	IO
Low Res.	5,099 (8.1%)	1,708 (2.8%)	317 (1.3%)	205 (0.9%)
High Res.	4,915 (7.8%)	2,352 (3.8 %)	325 (1.3%)	333 (1.5%)

1.3.4. *F5 outputs: water/board classifications*

Cross-comparisons of classifications performed by random forest and kinetic algorithms resulted in high matching coefficients for the four datasets. The two approaches showed very strong agreements for D2 dataset in the Indian Ocean (99%), and D1 datasets in both oceans (more than 96%). The weakest agreement (94%) was observed for the D2 dataset collected in the Indian Ocean (Table 1.4).

Less than 0.5% of positions from the D1 dataset remained not classified by the kinetic algorithm. This value was considerably higher for the D2 dataset, which showed increases from 10 to more than 30 times the number of unclassified data compared to D1 dataset, in Indian and Atlantic oceans, respectively (Table 1.5). More than 87 % of the positions were classified as "water" by the both approaches, while "on-board" positions varied from 0.1 to 5.5% depending on the algorithm, ocean and dataset.

Table 1.4: Simple matching coefficients (percentage of agreement) between the random forest and the kinetic algorithm classifications for the different datasets in Atlantic and Indian Oceans.

	Atlantic Ocean	Indian Ocean
D1	96%	97%
D2	99%	94%

Table 1.5: Number and percentage (in brackets) of water, board and unclassified positions from kinetic classification (KiC) and random forest (RF) algorithm in the different datasets for Atlantic (AO) and Indian (IO) Oceans.

F5. Water/Board		D1		D2	
		AO	IO	AO	IO
Board	RF	2,746 (4.4%)	595 (1.0%)	122 (0.5%)	971 (4.3%)
	KiC	3,469 (5.5%)	492 (0.8%)	22 (0.1%)	170 (0.7%)
Water	RF	55,135 (84.5%)	56,020 (91.5%)	22,853 (90.3%)	18,976 (84.5%)
	KiC	54,136 (86.1%)	58,679 (95.9%)	22,897 (90.5%)	21,307 (94.9%)
Unclassified	RF	2,010 (3.2%)	2,076 (3.4%)	1,924 (7.6%)	1,941 (8.7%)
	KiC	102 (0.2%)	164 (0.3%)	1,977 (7.8%)	726 (3.2%)

1.4. Discussion

This paper presents a standardized processing method and an exhaustive description of data from satellite-linked buoy models used by the European purse seiners. To date, there is still a significant lack of information on DFADs worldwide, although this information could be crucial to address current issues raised by their massive use in tropical tuna fisheries. As outlined by Dagorn *et al.*, (2013), the route towards a sustainable use of DFADs requires an attentive assessment of their impacts on tuna stocks and non-target species, as well as on habitats and ecosystem. In such context, information provided by satellite-linked buoys, could be a valuable tool to ensure an adequate monitoring of the DFAD use, and thus to support the various DFAD management plans adopted by the TRFMOs in recent years. They could also play an important role in improving the catch per-unit-effort standardization (CPUE), notably through the development of common indicators of the number of operational buoys at sea (Fonteneau *et al.*, 1999; Katara *et al.*, 2016, 2017). Similarly, characterization of fish aggregations underneath DFADs based on the acoustic data collected is likely to help in the development of new approaches to mitigate purse seine bycatch (L. Manocci, 2020, pers. comm.), or the derivation of alternative abundance indices for tropical tuna species (Capello *et al.*, 2016; Santiago *et al.*, 2016). Finally, the near real-time assessment of the spatio-temporal dynamics of DFAD trajectories based on buoy data, undeniably constitutes a promising tool to address the growing concerns related to DFAD beaching events and their impacts on sensitive habitats (Maufroy *et al.*, 2015; Davies *et al.*, 2017; Escalle *et al.*, 2019a).

The first step towards the achievement of each of these objectives is to ensure an adequate level of quality of the data provided, through an appropriate protocol to process these industry-based data primarily intended for use at vessel or fleet scale into standardized data that can be used at a more global scale. In this work, the proposed protocol relies on a set of filters defined and validated on different datasets greatly varying in structure and characteristic depending on the data-exchange agreements between national research institutes and fleets, as well as the buoy specificities. Mainly focused on position data and other related information provided by the buoys, the protocol aims to provide the basic level of quality required for the use of these data for scientific purposes.

However, it does not include a standard framework for the processing of acoustic data collected from the different echosounder buoy brands. Although, those data may be important for ecological and behavior investigations based on echosondeur buoys, developing a standard

protocol for their processing constitutes a challenging task. Indeed, the types and formats of acoustic data provided are highly variable between brands and within models of the same brand. Due to their specific hardware and software characteristics, buoys operate over a wide range of frequencies, sampling rates, detection range, or resolution (depth and thickness of water column layers sampled). They generally provide biomass indices computed from proprietary algorithms, which can be associated or not with the raw acoustic backscatter values for some models, or with categorical scores representing the backscatter signal in each of the sampled layers for others (Moreno *et al.*, 2019b). Addressing this issue, some authors have designed specific processing approaches in order to process the acoustic measurement from one of the buoy models, into tuna abundance data (Lopez *et al.*, 2016). As an alternative, given the large amount of data involved, the contribution of data-driven supervised learning techniques could prove to be a valid option to be explored in order to develop a general methodological framework for characterizing fish aggregations under floating objects and providing reliable estimates of their abundance from echosounder buoys (Baidai *et al.*, 2020c). The aim of the present protocol is to achieve standardization of the preliminary operations prior to the implementation of this type of studies and their subsequent application to the data collected.

One of the major issues associated to buoys data is related to the identification of buoys actually at water from those emitting on-board a vessel. Although, some models have integrated sensors allowing the detection of buoy soaking, this information is not available for a wide majority of models. Maufroy *et al.* (2015) in their analysis of spatio-temporal patterns associated with the use of DFADs, were the first authors to describe a processing protocol for buoy data. They proposed an automatic classification of "water" and "on-board" positions, based on a random forest approach trained with a subset of manually pre-classified data, and followed by a post-processing step to improve classification performance. The random forest approach from Orue *et al.*, (2019), on the other hand, benefited from ground truth information provided by sensors embedded in some buoy models, indicating whether the buoy is in the water or not. The comparisons of its results with the kinetic algorithm classification proposed in this work, revealed very high agreement rates for the classified positions. This is not surprising, since the analysis of the importance of the predictors in the random forest model revealed that the most relevant variables to discriminate on-board from water positions (i.e. buoy speed and its variation, see Orue *et al.*, 2019), are also the main parameters on which the KiC algorithm is based. Nevertheless, the random forest algorithm produces a higher number of unclassified positions than the KiC algorithm, as the first and last positions of the analysed buoy segments

are systematically unclassified due to the impossibility of calculating the predictive parameters associated with them. Unclassified positions from KiC algorithm are rather due to both the presence of very short trajectories and the low temporal resolution of data. Indeed, this algorithm uses rules that require the availability of a sufficient amount of data, measured with a high temporal resolution (at least 2 positions per day), to provide a correct analysis of the speed history along the buoy's track. Its performances are thus, significantly affected by the time-resolution of the datasets, as evidenced by the differences between the outputs for the D1 and D2 datasets (resulting from the one position per day in the D2 datasets relative to the higher temporal resolution in the D1 datasets). As precautionary principle, it could be proposed to consider the unclassified positions as actual positions at water. Nevertheless, in order to minimize misclassification, the use of high-resolution data (all the positions recorded in a day) is recommended if available. A more attentive assessment should however be given to this high-resolution datasets, as the study revealed their higher probability of containing structural errors.

High-resolution shoreline data should also be privileged for land filtering procedures. Lower resolutions could potentially lead to an underestimation of echosounder data collected on land, due to the possible removal of small reefs and islands. However, due to the huge amount of data to handle (e.g. the “Marine Instruments” buoys operated by the French purse seine fleet, represents over the period 2010-2018, a raw data volume of around 150 million entries), and the subsequent computational costs required by their processing, the use of low-resolution data should not be excluded, especially since the study showed that the results from the both resolutions are roughly similar.

1.5. Conclusion

Scientists have long interacted productively with fishermen to benefit from their knowledge, or to gain access to the sea for sampling (Armstrong *et al.*, 2008). Opportunistic data from fishing activities, such as those provided by satellite-linked echosounder buoys, could be regarded as a continuous industry-based survey that can provide valuable information to refine the understanding of the open-sea and its pelagic communities. However, not originally intended for scientific exploitation, these industry-based data must be subject to a careful assessment of their validity. In this paper, from an exhaustive analysis of the heterogeneous set of data provided by the main satellite-linked buoys used by the tropical tuna purse seine fleets, we described the preliminary operations to be applied in order to use these data in scientific

applications. Despite the lack of appropriate procedures for acoustic data strictly speaking, this approach offers a standardized framework for the necessary processing of satellite-linked buoy data for scientific research.

Acknowledgments

This project was funded by the RECOLAPE project (MARE/2016/22 “Strengthening regional cooperation in the area of fisheries data collection” Annex III “Biological data collection for fisheries on highly migratory species”). IRD scientists were also supported by the BLUEMED project ANR project BLUEMED (ANR-14-ACHN-0002). We would like to thank the fishing companies (ORTHONGEL, Echebastar and Atunsa companies in ANABAC and OPAGAC) that shared the buoy data and buoy providers (Satlink, Marine Instruments and Zunibal) for the useful exchanges on the buoys technical characteristics.

Chapter 2

Machine learning for characterizing tropical tuna aggregations under Drifting Fish Aggregating Devices (DFADs) from commercial echosounder buoys data

---

"*J'essaie toujours de faire ce que je ne sais pas faire, c'est ainsi que j'espère apprendre à le faire.*

I'm always trying to do what I can't do, that's how I hope to learn to do it."

Pablo Ruiz Picasso

This chapter is published as:

Baidai, Y., Dagorn, L., Amande, M.J., Gaertner, D., and Capello, M. 2020. Machine learning for characterizing tropical tuna aggregations under Drifting Fish Aggregating Devices (DFADs) from commercial echosounder buoys data. *Fisheries Research*, 229:105613. https://doi.org/10.1016/j.fishres.2020.105613

Machine learning for characterizing tropical tuna aggregations under Drifting Fish Aggregating Devices (DFADs) from commercial echosounder buoys data.

Y. Baidai[12], L. Dagorn[1], M.J. Amande[2], D. Gaertner[1], M. Capello[1]

[1]MARBEC, Univ Montpellier, CNRS, Ifremer, IRD, Sète, France

[2]Centre de Recherches Océanologiques (CRO), Abidjan, Cote d'Ivoire

Abstract

The use of echosounder buoys deployed in conjunction with Drifting Fish Aggregating Devices (DFADs) has progressively increased in the tropical tuna purse seine fishery since 2010 as a means of improving fishing efficiency. Given the large spatial coverage of DFADs, the acoustic signal provided by echosounder buoys can provide an alternate source of information to the conventional CPUE index for deriving trends on tropical tuna stocks. This work aims to derive reliable indices of presence of tunas (and abundance) using echosounder buoy data. A novel methodology is presented which utilizes random forest classification to translate the acoustic data from the buoys into metrics of tuna presence and abundance. The training datasets were constructed by cross-referencing acoustic data with logbook and observer data which reported activities on DFADs (tuna catches, new deployments and visits of DFADs) in the Atlantic and Indian Oceans from 2013 to 2018. The analysis showed accuracies of 75 and 85 % for the recognition of the presence/absence of tuna aggregations under DFADs in the Atlantic and Indian Oceans, respectively. The acoustic data recorded at ocean-specific depths (6 – 45 m in the Atlantic and 30 – 150 m in the Indian Ocean) and periods (4 am – 4 pm) were identified by the algorithm as the most important explanatory variables for detecting the presence of tuna. The classification of size categories of tuna aggregations showed a global accuracy of nearly 50% for both oceans. This study constitutes a milestone towards the use of echosounder buoys data for scientific purposes, including the development of promising fisheries-independent indices of abundance for tropical tunas.

Keywords: Tropical tunas; Direct abundance indicator; Echosounder buoys; Fish Aggregating Devices; Purse seiner.

2.1. Introduction

Many marine species are known to naturally aggregate under floating objects. Although still poorly understood, this behaviour is widely exploited by fishermen, who deploy man-made floating objects (hereafter referred to as Fish Aggregating Devices or FADs) worldwide to improve their catches (Kakuma, 2001; Fonteneau *et al.*, 2013; Albert *et al*., 2014). The use of drifting FADs (DFADs) in tropical tuna fisheries was first introduced in the late 1980s in the Eastern Pacific Ocean by the US purse seine fleet (Lennert-Cody and Hall, 2001) and was later extended to all oceans and fleets from the 1990s. The instrumentation of DFADs with GPS beacons and echosounder buoys, in the mid and late 2000s respectively (Lopez *et al.*, 2014), led to major changes in fishing strategies and behaviour of purse-seine fleets (Torres-Irineo *et al.*, 2014a). By providing skippers with almost real-time remote information on the precise location of DFADs, and on the potential presence and size of the tuna aggregation, echosounder buoys reduced the search time between two successful DFAD sets (Lopez *et al.,* 2014). As a result, modern DFADs have significantly increase fishing efficiency (Fonteneau *et al.*, 2013). Consequently, their use has increased considerably in the past few decades. Recent studies indicate that in less than a decade, the number of DFADs deployed in the Atlantic and Indian Oceans have increased at least fourfold (Fonteneau *et al.*, 2015; Maufroy *et al.*, 2017). It is estimated that over half of the annual tropical tuna purse seine catch originate from fishing sets on DFADs (Dagorn *et al.*, 2013; Fonteneau *et al*., 2013).

Aside from being highly efficient fishing tools, the large number and vast spatial distribution of DFADs, coupled with their constantly evolving technology (Lopez *et al.*, 2014), mean that they can also potentially provide unprecedented scientific insights into pelagic communities (Moreno *et al*., 2016; Brehmer *et al*., 2018). The echosounder buoys attached to DFADs regularly produce and transmit biomass estimation data. This dataset potentially holds a major opportunity for improving the management of tropical tuna stocks through the development of fishery-independent abundance indices (Capello *et al*., 2016; Santiago *et al*., 2016). Currently, the main abundance indicators used in stock assessment for tropical tunas are derived through the standardization of Catch per Unit of Effort (CPUE) from commercial data (Fonteneau *et al.*, 1998; Maunder *et al.*, 2006). However, owing to the constant technological advances occurring in the purse seine fishery, it is extremely difficult to accurately standardize the CPUE time-series (Fonteneau *et al.*, 1999). Traditionally, search time was used to quantify normal fishing effort in this fishery, however, owing to its non-random nature, the DFAD-based fishery has

made this metric inconsistent, thus introducing major biases and uncertainties in the relationship between tuna catches and abundance (Fonteneau *et al.*, 1999; Gaertner *et al.*, 2015).

The need for the consideration of non-traditional data sources to provide alternate abundance indices for stock assessment of tunas is becoming increasingly apparent. In this regard, the large amount of acoustic data autonomously collected by commercial echosounder buoys on DFADs is of undeniable value. However, the direct exploitation of this data remains challenging. The biomass estimate that a buoy produces is limited by the reliability and variability of the information provided, which depends on the hardware and software characteristics of the buoy, and varies between manufacturers (Lopez *et al*., 2014; Santiago *et al*., 2016). As a result, the data provided by echosounder buoys are heterogeneous in types and formats, with limited studies having provided an assessment of their accuracy for use in scientific investigations. (Lopez *et al*., 2016; Baidai *et al*., 2017; Orue *et al*., 2019a).

In recent years, fisheries scientists have shown a growing interest in machine learning methods for the processing of both passive acoustic data (Roch *et al.*, 2008; Zaugg *et al*., 2010; Noda *et al*., 2016; Malfante *et a*l., 2018) and acoustic data collected by scientific echosounders (Fernandes, 2009; Robotham *et al*., 2010; Bosch *et al*., 2013). Despite this trend, very few studies have been conducted on the implementation of automated classification methods for analysing the extensive datasets collected by commercial vessels (Uranga *et al*., 2017).

This paper presents a new methodology, based on machine learning, for processing the echosounder data collected from one of the main models of echosounder buoy used to equip DFADs worldwide (Moreno *et al.*, 2019).

2.2. Material and Methods

2.2.1. *Database description*

2.1.1.1. Echosounder buoy data

We used data from the Marine Instruments M3I buoy (https://www.marineinstruments.es), collected on DFADs deployed by the French purse seine vessels operating in the Western Indian and Eastern Atlantic oceans from 2013 to 2018. The dataset consists of more than 60 million data points collected by approximately 35 000 M3I buoys (see Supplementary information S1).

This model of buoy includes a solar powered echosounder operating at a frequency of 50 kHz, with a power output of 500 W, a beam angle of 36°, and a sampling frequency of 5 minutes (Figure 2.1A). The acoustic data are processed by an internal module that automatically converts the acoustic energy into two acoustic indices; (i) a total biomass index and (ii) 50 integer acoustic scores (ranging from 0 to 7) indicating the acoustic energy recorded within 3 m depth layers, over a total detection range of 150 meters (Figure 2.1B). In the default-operating mode, the internal module stores the 50 acoustic scores that correspond to the highest total biomass index recorded every 2 hours. From here on these 50 acoustic scores will be referred to as an "acoustic sample". The assessment of the accuracy of the total biomass index calculated directly by the buoy's internal module can be found in Supplementary information S1. The set of acoustic scores which constitute the acoustic sample is transmitted via satellite to the purse seine vessel every 12 hours under default settings. During the satellite communication, the GPS position of the buoy is also recorded and transmitted.

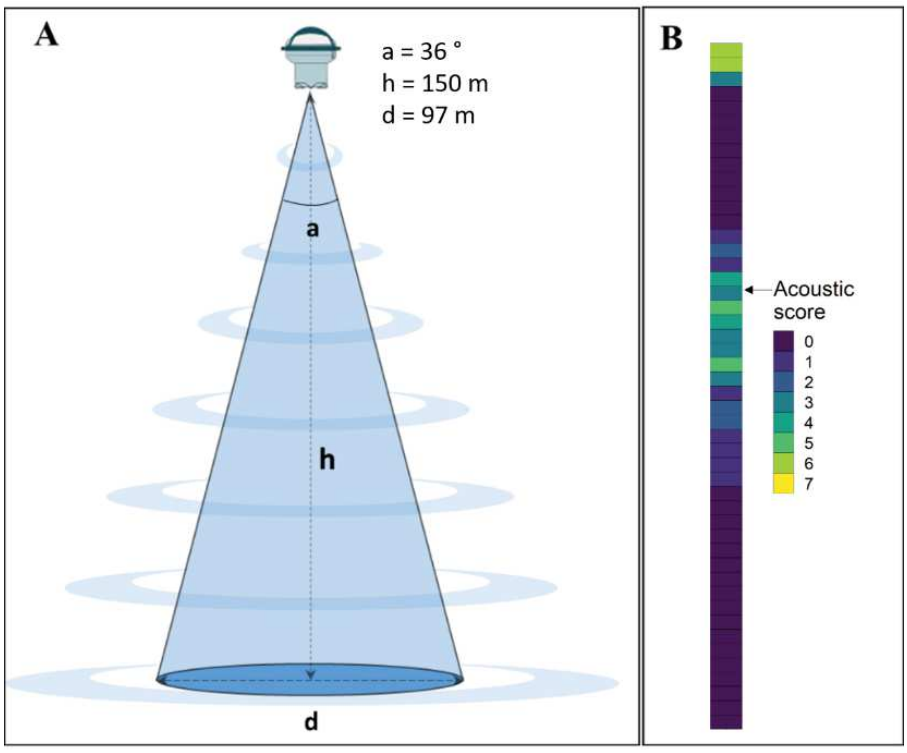

Figure 2.1: Technical specifications of the Marine Instruments M3I echosounder buoy. (A): beam width or cover angle (a), depth range (h), and diameter (D) at 150 m, (B): example of an acoustic sample.

2.1.1.2. Activity data on DFADs

To ground truth the echosounder buoy dataset, catch and fishing activities were obtained from fishing logbooks of purse seine vessels and from on-board observers from 2013 to 2018 in the western Indian and eastern Atlantic oceans (further information can be found in the Supplementary information S1: 1. Database description). Observer data were collected under the EU Data Collection Framework (DCF) and the French OCUP program (Observateur Commun Unique et Permanent), which reached a coverage rate of 100% in the Atlantic Ocean in 2015 (Goujon *et al*., 2018), and over 80% since 2016, in the Indian Ocean (Goujon *et al*., 2017). The aim of merging these two datasets was to obtain the best information available through different data sources (i.e. correcting potentially misreported operations on DFADs). From this joint dataset, the date, time, GPS location and buoy identification code associated with (i) fishing sets, (ii) newly deployed DFADs and (iii) visits to DFADs equipped with buoys owned by the vessel and which did not result in a fishing operation, were selected. For successful fishing sets on DFADs, catch data for the three primary target species; yellowfin (*Thunnus albacares*), bigeye (*Thunnus obesus*) and skipjack tuna (*Katsuwonus pelamis*) were also considered. These catch data were used to ground truth the buoy's ability to detect the presence and size of tuna aggregations, assuming that the entire fish aggregation is encircled and captured by the fishing vessel. Conversely, newly deployed DFADs and visits to DFADs that did not result in any catch were used to ground truth the buoy's ability of detecting the absence of a tuna aggregation. For this assessment, DFAD deployments and visits where fishing sets were reported within the following week, were omitted, to ensure that the data truly represented the absence of tuna at the DFADs. Similarly, only the deployments of new DFADs were considered and all other deployment operations were discarded (e.g., reinforcement of an existing DFAD, deployment of a buoy on a natural log).

Skunk fishing sets (sets where the tuna school totally or partially escaped) and activities, for which the reported set position was inconsistent with the position reported by the buoy, were removed. Only data for which the buoy identification code corresponded to a buoy code present in the echosounder buoy database were retained in the analysis. The final database used for each activity and ocean is described in Table 2.1.

Table 2.1: Number of fishing sets (with catch ≥ 1 ton), visit and deployment data collected from 2013-2018 and used in the presence-absence classification for the Atlantic and Indian Oceans.

	Atlantic Ocean			Indian Ocean		
	Catch	Visit	Deployment	Catch	Visit	Deployment
Logbook	817	255	405	2918	1031	6722
Observers	151	0	228	513	0	2487
Total	968	255	633	3431	1031	9209

2.1.2. *Acoustic data pre-processing*

Daily acoustic data provided by an individual buoy consists of a 50 × N matrix ***S***, where 50 represents the number of depth layers and N corresponds to the number of acoustic samples provided for that day according to the operating mode of the buoy (in the default operating mode, the acoustic scores are stored every 2 hours, thus N=12). Elements of the matrix ***S*** correspond to the daily acoustic scores S_{ij} (i.e., integers ranging between 0 and 7) recorded at different depth layers i (i=1, 50) and different times of the day j (j=1, N). In a pre-processing step, the temporal and spatial information was aggregated to standardize the data and achieve a reduction in dimensions as follows:

(1) the acoustic scores of the two shallowest layers (0 – 6 m depth), representing the transducer blanking zone, were removed, leading to a 48 × N matrix;

(2) then, for each layer i, the daily acoustic scores S_{ij} were averaged over 4-hours periods, resulting in a reduced matrix ***S'*** of 48 × 6 (Figure 2.2);

(3) a clustering method was applied on ***S'*** along the dimension i, to identify homogeneous groups of depth layers. The clustering method was based on a dissimilarity matrix computed from Euclidean distance and Ward's method (Murtagh and Legendre, 2014). The acoustic scores in each identified group were compared through a Kruskal-Wallis test[6];

[6] Clustering analyses were conducted using the R function "*hclust*" (R Core Team, 2019), and the Kruskal-Wallis test with the R function "*kruskal.test*"

(4) for each homogeneous group *G*, the acoustic scores recorded previously for each of the *i* depth layers constituting the group were summed and rescaled to obtain a unique score (S''_{Gj}) per group *G* and time period *j*, according to Equation (2.1).

$$S''_{Gj} = \frac{\sum_{i=1}^{n_G} S'_{ij}}{maxs \times n_G} \tag{2.1}$$

where *j* denotes the 4-hours time period, n_G the number of depth layers belonging to group G and *maxs* is a constant denoting the maximum score (7 in the case of M3I buoys). The result of the pre-processing step leads to a $N_G \times 6$ matrix ***S''*** (i.e., N_G groups of layers × 6 four-hour periods recorded during a day), summarizing the acoustic information collected on a daily scale, and referred to hereafter as a "daily acoustic matrix" (Figure 2.2).

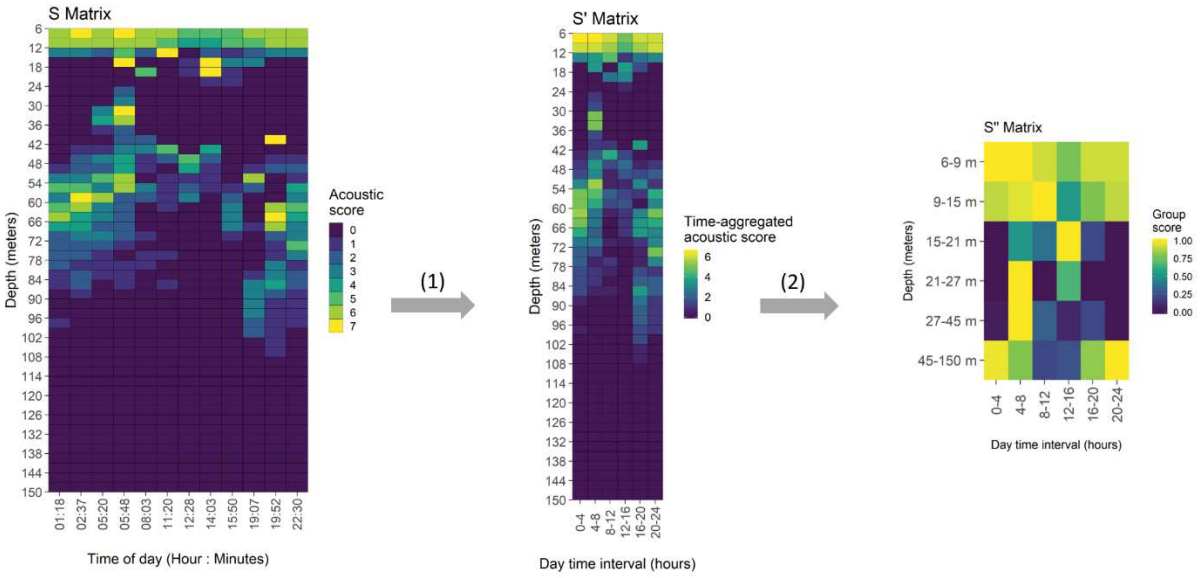

Figure 2.2: Schematic view of the acoustic data pre-processing. (1) Temporal resolution reduction, averaging acoustic samples over a 4-hour period. (2) Layer aggregation combining the 48 vertical layers into 6 layers based on cluster analysis. The final output is a 6×6 matrix summarizing the acoustic signal recorded over 24 hours between 6 and 150 m. Acoustic scores are integer values (ranging from 0 to 7), representing the intensity of the acoustic backscattered signal per 3 m depth layer. Time-aggregated acoustic scores represent the average value of the acoustic scores over the 4-hour interval. Group scores represent the sum of layer scores (scaled between 0 and 1) per homogeneous group of layers identified from the clustering analysis.

2.1.3. *Supervised learning classification*

2.1.3.1. Training dataset

The training datasets were constructed by cross-matching activity data (catch, deployments, visits without fishing sets) with the daily acoustic matrices, using buoy identification codes, dates and times for each ocean. A first binary training dataset was constructed for describing the presence or absence of tuna, in which catch events corresponded to tuna presence and deployment and visits without catch, to the absence of tuna (see Table 2.2). A second multiclass training dataset was created for describing the size of the tuna aggregation. The catch data were divided into three classes: < 10 tons, 10 – 25 tons, >25 tons, based on the total catch of the set (i.e., the sum of the catch of the three target tuna species: yellowfin tuna, bigeye tuna and skipjack tuna). The number and limits of the size classes were selected in order to retain a sufficient and balanced number of data points in each class for the learning process, while also maintaining consistency with the catch data. Class limits were based on the first quantile (10 tons) and the average (25 tons) of catches under DFADs in the dataset (see Table 2.3).

Table 2.2: Structure of the training dataset used in the presence-absence and multiclass classification for the Atlantic and Indian Oceans (over the period 2013-2018).

Ocean	No tuna	Tuna		
		< 10 tons	[10, 25 tons]	> 25 tons
Atlantic	888	397	303	268
Indian	10240	904	1288	1239

Table 2.3: Summary statistics of major tuna catches (in tons) from DFAD fishing operations collected from observer and logbook databases from 2013 to 2018, in the Atlantic and Indian Oceans. (Min. and Max. denote for minimum and maximum catch values, respectively. SD represents standard deviation and Qu. stands for quantile)

Ocean	Min.	1st Qu.	Median	Mean	3rd Qu.	Max.	SD
Atlantic	1	6	15	22.61	30	177.70	25.59
Indian	1	10	20	26.73	34	300	26.77

The daily acoustic matrices of tuna presence were constructed using the acoustic data recorded the day before catch events. Similarly, the daily acoustic matrices corresponding to tuna absence were selected from the daily acoustic matrices obtained the day prior to DFAD visits without fishing sets, and those obtained on the fifth day after new DFAD deployments. The rationale for considering these 5-day periods after deployment was to account for the acoustic signal produced by the non-tuna species. Prior studies (Deudero *et al*., 1999; Castro *et al*., 2002; Nelson, 2003; Moreno *et al*., 2007; Macusi *et al*., 2017) have indicated that the colonization of DFADs by non-tuna species takes place during the first days after deployment. Furthermore, preliminary analyses conducted on 528 and 5868 newly deployed DFADs, in the Eastern Atlantic and Western Indian oceans respectively, indicated a rapid increase in the acoustic signal recorded by the buoys during the first five days following deployment (Supplementary information S3: Fig. S3.1 and S3.2). After considering all of these reasons, we assumed that acoustic data recorded at this post deployment time-scale are more likely to represent the presence of non-tuna species under DFADs.

2.1.3.2. Random forest algorithm

The random forest classification algorithm[7] (Breiman, 2001) was applied on an ocean-specific basis. Predictors were represented by daily acoustic matrix values. Three thousand trees were grown for each classification. This high value does not negatively impact the model's performance (Breiman, 2001), and helps to stabilize the importance of the variables more effectively (Liaw and Wiener, 2002; Probst *et al.*, 2019). For each classification model, the number of variables randomly sampled as candidates at each split was assessed through a grid-search strategy implemented with the R package "caret" (Kuhn, 2008). In order to deal with the imbalanced number of observations in the different size categories a stratified down-sampling procedure, which consisted of resampling the dominant size categories to make their frequencies closer to the least common size category, was also applied (Kuhn and Johnson, 2013).

[7] The random forest classification was performed by using the R package "randomForest" (Liaw and Wiener, 2002)

2.1.3.3. Model evaluation

The overall accuracy (i.e., the proportion of correct predictions) and the kappa coefficient (Cohen, 1968) were used to assess the overall performance of both binary and multi-size category classifications. Kappa coefficient is a reliability index estimated according to Equation (2.2):

$$kappa = \frac{\Pr(a) - \Pr(e)}{1 - \Pr(e)} \tag{2.2}$$

where *Pr(a)* is the total proportion of agreement between the two classifications and *Pr(e)* is the theoretical proportion of agreement expected by chance. The closer this ratio is to 1, the better the classification performed. In each classification, the conventional statistical measures of the performance of a binary classification test: sensitivity, specificity, and precision were evaluated from confusion matrices, using Equations (2.3) to (2.5):

$$Sensitivity = \frac{TP}{TP + FN} \tag{2.3}$$

$$Specificity = \frac{TN}{FP + TN} \tag{2.4}$$

$$Precision = \frac{TP}{TP + FP} \tag{2.5}$$

where for presence/absence classification, *TP* (true positive) and *TN* (true negative) are the proportions of presence (or absence) correctly classified; *FN* (false negative) and *FP* (false positive) are the proportions of absence (or presence) incorrectly predicted. For multiclass classification, positive cases correspond to the aggregation size category considered during the evaluation, while all other categories correspond to negative cases. Sensitivity (also known as recall or true positive rate) measures the efficiency of the algorithm in correctly classifying positive cases, and specificity (or true negative rate) measures the efficiency of the algorithm in correctly classifying negative cases. Precision (or positive predictive value) is the fraction of correctly predicted presence among all tuna presence prediction.

The importance of the predictors in the classification process for each ocean was assessed through the analysis of the mean decrease in accuracy of the random forest model (i.e., the increase of prediction error after permuting each variable while all others remained unchanged during the tree construction; Breiman, 2001). Model training and evaluation were performed through a hold-out validation method which was repeated ten times. In each of the ten replicates,

the original dataset was divided into two subsets: the training set and the validation dataset (representing 75% and 25% of the initial data, respectively).

2.3. Results

2.3.1. *Pre-processing of sampled depth layers*

The clustering analysis carried out on the 3 m depth layers led to the formation of six groups of layers whose composition was relatively similar between the two oceans (Figure 2.3). In both oceans, the comparison of the acoustic scores between the identified groups showed highly significant differences (*p-value* at Kruskal-Wallis test < 0.001 for both Indian and Atlantic Oceans). Scores declined strongly with depth. The deepest group of layers (which also aggregated the greatest number of layers), exhibited the lowest acoustic values, with averages close to zero (Figure 2.4).

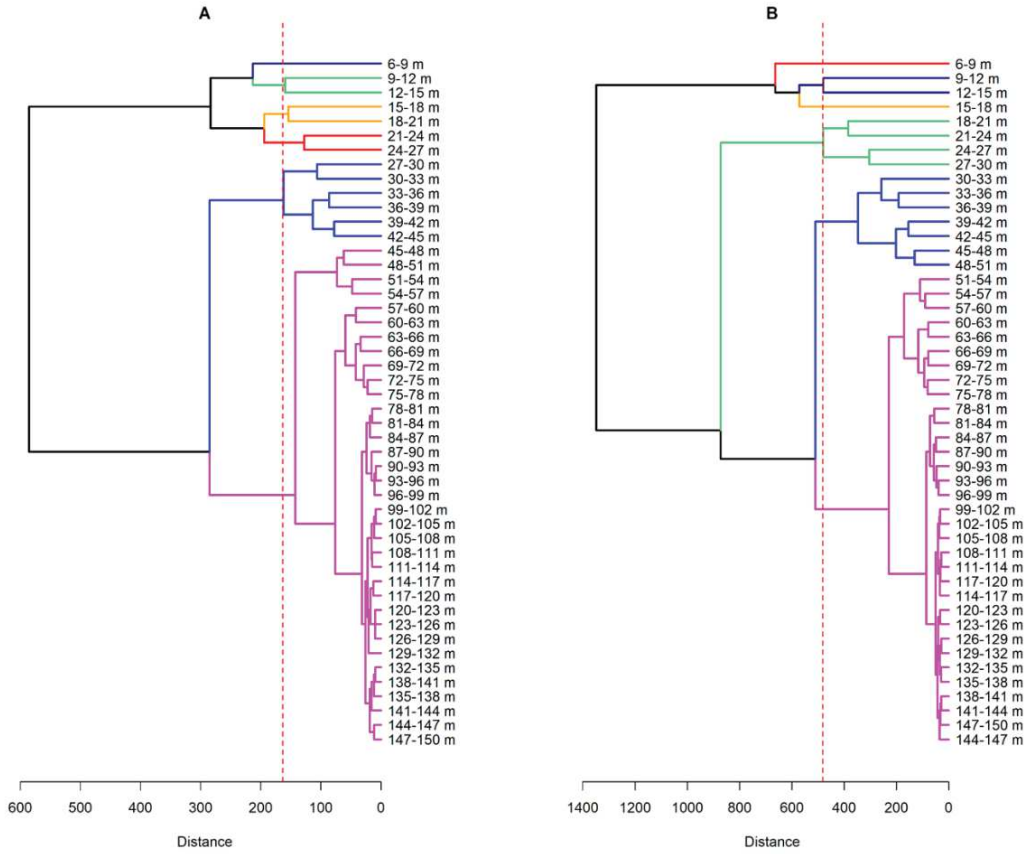

Figure 2.3: Dendrogram from the cluster analysis of raw acoustic data for the Atlantic (A) and Indian (B) Oceans. The red horizontal line indicates the height at which the dendrogram was sliced to create the 6 groups of layers. Colors identify the different groups of depth layers used to pre-process the acoustic data.

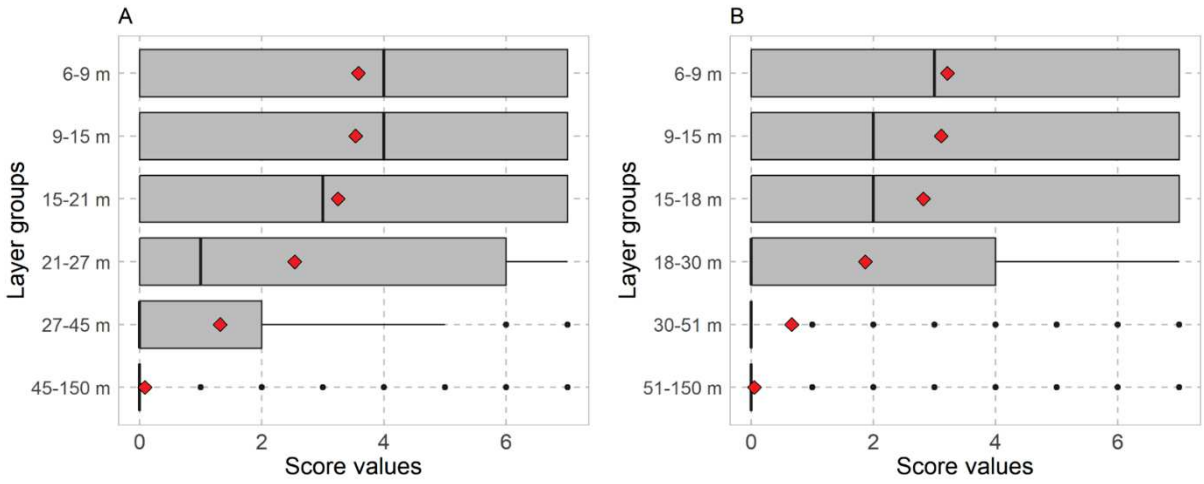

Figure 2.4: Boxplot of acoustic score values in the aggregated-layer groups identified by the cluster analysis, for the Atlantic (A), and Indian (B) Oceans. Red diamonds represent mean value of scores in each layer group.

2.3.2. *Presence/absence classification*

The random forest algorithm performed well in discriminating between the presence and absence of tuna, with an overall accuracy of 75 and 85% in the Atlantic and Indian oceans, respectively (Table 2.4). In the Atlantic Ocean, the classification model was effective in detecting DFAD aggregations with tuna (sensitivity of 0.83), but exhibited a notable level of false positives (specificity of 0.67). In the Indian Ocean the opposite trend was observed with the classification of tuna presence performing well (sensitivity of 0.81) and the detection of their absence also producing reliable results (specificity of 0.90).

Table 2.4: Summary of tuna presence/absence classification performances for the Atlantic and Indian Oceans: mean and standard deviation values (in brackets) of evaluation metrics.

Evaluation Metrics	Atlantic	Indian
Accuracy	0.75 (0.02)	0.85 (0.01)
Kappa	0.51 (0.04)	0.70 (0.02)
Sensitivity	0.83 (0.02)	0.81 (0.01)
Specificity	0.67 (0.03)	0.90 (0.01)
Precision	0.73 (0.03)	0.88 (0.01)

2.3.3. *Classification of aggregation sizes*

The classification of aggregations into size classes was considerably less efficient than the presence-absence classification, with low overall accuracies (48 and 47 %) observed for the Atlantic and the Indian Oceans, respectively (Table 2.5). In the Atlantic Ocean, the highest proportion of misclassification was observed in the 10 – 25 tons category (precision of 0.22), whereas tuna schools below 10 tons and above 25 tons both performed similarly (precision of 0.32 and 0.28 respectively). In the Indian Ocean, tuna schools over 25 tons and below 10 tons were also the most reliably detected aggregation size classes (precision of 0.44 and 0.42 respectively); while intermediate aggregation sizes (10 – 25 tons) were successfully classified less regularly (precision of 0.35).

2.3.4. *Predictor importance*

For both binary and multiclass classifications, the importance of the acoustic predictors in the classification process showed strong ocean-specific patterns. In the Atlantic Ocean, the detection of tunas was principally driven by acoustic data recorded from 6 m to 45 m (Figure 2.5A and Figure 2.6A). Conversely, in the Indian Ocean, the main predictors resulted from deeper layers (30 m to 150 m, Figure 2.5B and Figure 2.6B). In these depth ranges, acoustic data recorded during daytime (4 am – 4 pm) appeared to be the most significant for both oceans and across all types of classifications. It should, however, be noted that in the Atlantic Ocean, the binary classification produced a wider time window (0 to 4 pm) than in the Indian Ocean.

Table 2.5: Summary of multiclass classification performances for the Atlantic and Indian Ocean. Mean and standard deviation (in brackets) of evaluation metrics

	Atlantic Ocean				Indian Ocean			
	No tuna	<10 tons	[10 , 25 tons]	> 25 tons	No tuna	<10 tons	[10 , 25 tons]	> 25 tons
Sensitivity	0.67 (0.03)	0.36 (0.05)	0.24 (0.08)	0.34 (0.06)	0.87 (0.03)	0.19 (0.01)	0.29 (0.02)	0.54 (0.04)
Specificity	0.82 (0.02)	0.80 (0.03)	0.84 (0.04)	0.85 (0.04)	0.80 (0.01)	0.91 (0.01)	0.82 (0.02)	0.77 (0.01)
Precision	0.77 (0.03)	0.32 (0.04)	0.22 (0.04)	0.28 (0.05)	0.59 (0.02)	0.42 (0.04)	0.35 (0.03)	0.44 (0.02)
Accuracy	0.48 (0.02)				0.47 (0.02)			
Kappa	0.26 (0.03)				0.30 (0.02)			

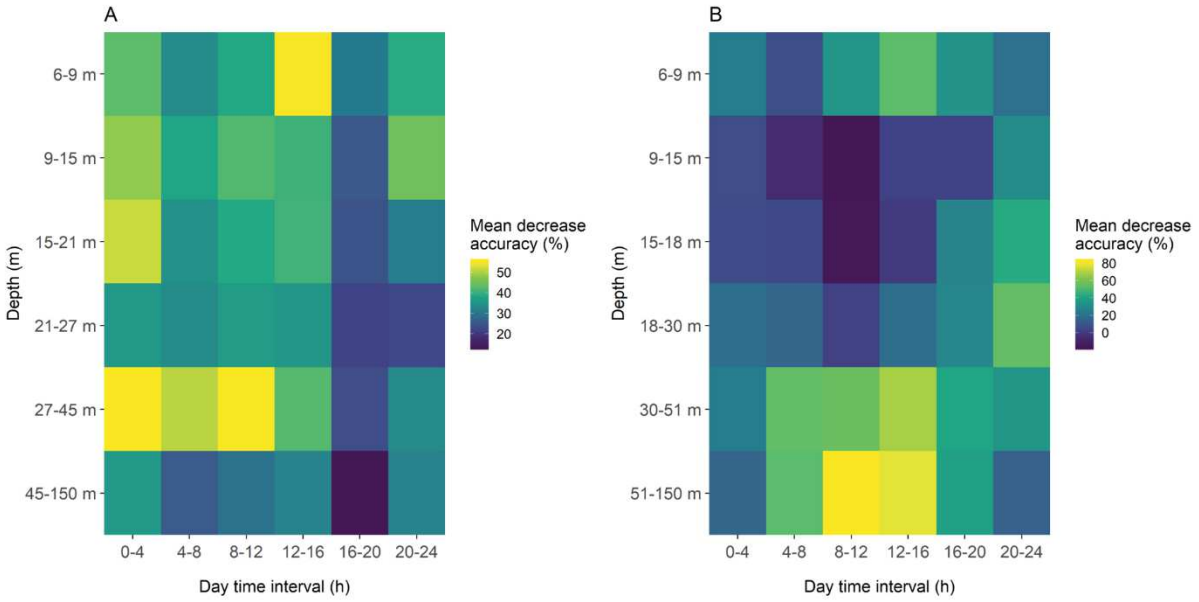

Figure 2.5: Importance of depth layers and day period in presence/absence classification for the Atlantic (A) and Indian (B) Oceans. Each cell represents a combination of depth and time period. Colours indicates the importance of the predictor in the classification.

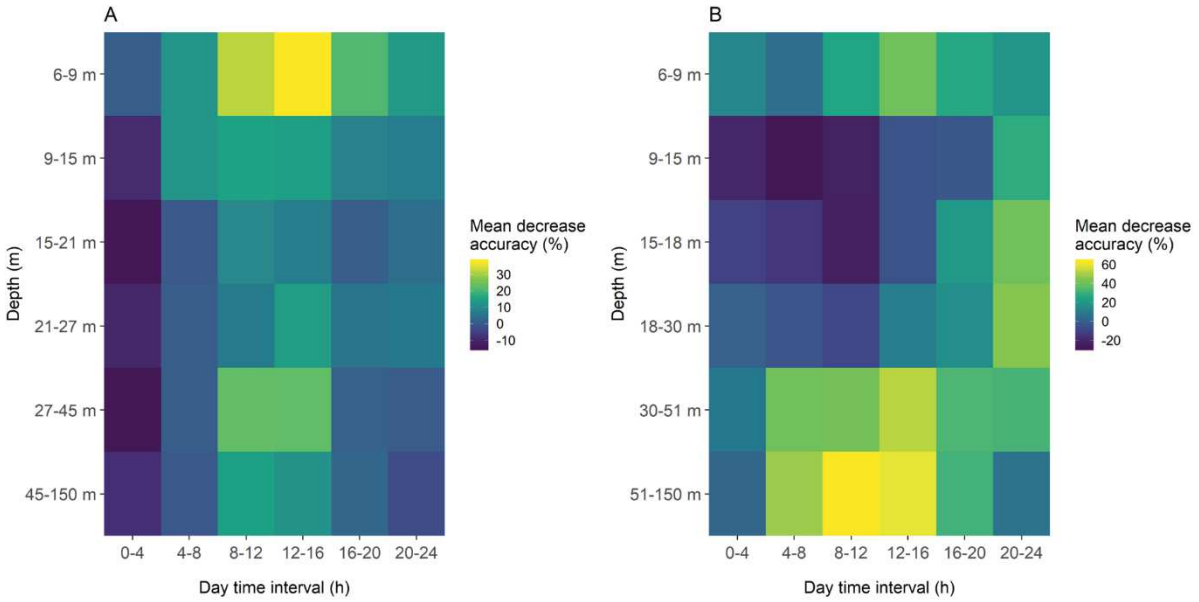

Figure 2.6: Importance of depth layers and day period in multiclass classification for the Atlantic (A) and Indian (B) Oceans. Each cell represents a combination of depth and time period. Colours indicates the importance of the predictor in the classification.

2.4. Discussion

This study describes a new methodology for processing data collected by a model of echosounder buoy commonly used in the DFAD purse seine fishery. The approach utilizes the acoustic scores recorded at different depths and times of the day and combines data pre-processing procedures and machine learning algorithms to classify tropical tuna aggregations under DFADs. Although several models of echosounder buoys process data internally and generate abundance indices for tuna, previous studies have shown that such information can be unreliable. This could explain why most purse seine skippers pay little attention to this information (Lopez *et al.*, 2014). Rather than relying solely on these processed outputs, skippers tend to combine the acoustic information recorded at specific depths and times with their empirical knowledge and the oceanographic characteristics of the region to assist their decision-making.

Working on a different brand of buoy, Lopez *et al*. (2016) developed the first approach to improve biomass estimations from data collected by echosounder buoys. These authors suggested that the acoustic signal collected during sunrise (i.e., when tuna are generally the most tightly concentrated under DFADs), should be considered for processing and assumed the structure of the aggregated biomass based on knowledge of the vertical behaviour of species under floating objects. Under this assumption, they suggested a vertical segregation between the species that make up the multispecific aggregation under DFADs (non-tuna species [3 – 25 m], small tunas [25 – 80 m] and large tunas [80 – 115 m]), and applied an echo-integration procedure to convert the acoustic signal from each depth layer into biomass estimates using specific values of target strength and individual average weight for each group. The application of this approach to a larger dataset in the Indian Ocean (287 fishing sets) by Orue *et* al (2019) was found to be less effective than expected, and potentially affected by the large spatio-temporal variability between oceanic regions which skewed the main assumptions that underlie the approach.

The methodology proposed by the present study did not make any assumptions regarding the vertical and temporal distribution of tuna at DFADs. Using a supervised learning algorithm, this methodology mimics the learning process of the fishers on how they interpret the acoustic scores based on their experience. The training dataset used for this purpose utilizes buoy data, which is considered to be ground-truthed. These ground-truthed data have three underlying assumptions. The first assumption is that the tuna caught by a purse seine vessel around a DFAD

represents all the tuna aggregated under that DFAD. This is typically the case, although it is possible that some tuna escape during the fishing procedure, such events are considered to be minor (Muir *et al.*, 2012). In exceptional situations when very large fishing sets are made (> 200 t), the skipper may decide to retain only part of the aggregation to avoid damaging the net. The second assumption is that tunas do not immediately associate with newly deployed DFADs. Although Orue *et al*. (2019b) indicated that tuna may arrive first under DFADs, previous studies (Deudero *et al*., 1999; Castro *et al*., 2002; Nelson, 2003; Macusi *et al*., 2017), including interviews with fishers (Moreno *et al*., 2007) suggested otherwise. In this study, the daily acoustic matrix recorded five days after the deployment of a new DFAD was used to represent the absence of tuna. It would be useful to develop dedicated studies that would aid in the understanding of the aggregation process of tuna and non-tuna species around DFADs. Finally, the third assumption considered that a purse seine vessel visiting its own DFAD (DFAD equipped with the vessel's buoy) without fishing also represents the absence of a tuna aggregation at the DFAD. It may be countered that a skipper could decide not to set on a DFAD when the vessel is already full, but this is an extremely rare event. External factors (e.g. strong currents) may also impede the fishing operations. However, if a vessel heads towards a DFAD that it owns, it is fair to assume that this would result in a fishing set (if tunas are present). Furthermore, in an effort to avoid any bias associated with the external factors that could influence the skipper's decision, only DFAD visits that were not followed by a fishing set within seven days were taken into consideration. Our decision to include visits without fishing operations in the training database as "absence of tuna" was taken based on numerous discussions with skippers. According to many of them, it is not uncommon that the echosounder buoys report high levels of acoustic energy even if tuna are absent from the aggregation. The objective of including these DFAD visits in the database was to improve the ability of the classification model to detect such false positives.

The results from this study highlight the effectiveness of the proposed methodology for discriminating between the presence and absence of tuna aggregations under DFADs equipped with M3I buoys in both the Indian and Atlantic oceans. To date the reliability of this model of buoy in estimating the presence and size of tuna aggregations had only been assessed anecdotally based on opinion and feedback from skippers. The development of reliable methods for processing data provided by commercial echosounder buoys represents a key step in the use of these fishing tools for scientific purposes, particularly the study of the different aspects of the ecology and behaviour of tuna associated with floating objects. The algorithm's lower

performance in the Atlantic Ocean, where a higher proportion of false positive predictions of tuna presence were generated, could well be related to the size of the training dataset. In the Atlantic Ocean, this dataset was 5.5 times smaller than that used for the Indian Ocean. However, this difference may also reflect an ocean-specific vertical distribution of fish aggregations under DFADs. In the Indian Ocean, previous studies have described a vertical segregation between tuna and non-tuna species (Forget *et al*., 2015; Macusi *et al*., 2017). Such segregation would result in the determination of an absence of tuna to be straightforward for the classification algorithm. To date no studies have investigated the vertical distribution of tuna and non-tuna species under DFADs in the Atlantic Ocean. The depth of the thermocline in the eastern Atlantic Ocean is known to be shallower than in the western Indian Ocean (Schott *et* al., 2009; Xie and Carton, 2013). This difference may result in tunas occupying shallower depths and thus mixing more regularly with non-tuna species. Such a phenomenon could provide an explanation for the higher rates of false positives generated in the Atlantic Ocean (i.e., false detection of the presence of tuna). The analysis of the relevance of the predictive factors in the random forest classifications showed that, for both oceans, daytime periods were the most relevant factor for distinguishing the presence of tuna schools from other acoustic targets. This result is likely linked to the behaviour of tuna schools and their spatial and temporal distribution around DFADs. Sonar surveys conducted on DFADs in the Indian Ocean revealed that tuna form a large number of small and dispersed schools during the night, and few and larger schools during daytime (Trygonis *et al.*, 2016). Another possible reason could be related to the influence of the diel vertical migration of the deep scattering layer (Robinson and Goómez-Gutieérrez, 1998), which may affect the acoustic signal during night-time hours.

In both oceans, the performance of the classification algorithm for discriminating between different aggregation sizes was considerably less satisfactory than the presence/absence of tunas. There are several possible explanations for these limitations. One potential source of bias may stem from the differing species composition considered in each size class. Due to skipjack tuna lacking a swim bladder, their acoustic response is very different from that of yellowfin or bigeye tuna (Josse and Bertrand 2000; Boyra *et al*. 2018), as such an aggregation of a given size would result in different acoustic signatures depending on the percentage of each species that make it up. Another source of bias could be linked to the position of the tuna aggregation in relation to the area that is sampled by the buoy (detection cone). Depending on the size of the aggregation and the behaviour of tuna around the DFAD, it is likely that the buoy's acoustic cone only detects part of the tuna aggregation. Some environmental factors could also affect

both the acoustic signal detection and fish behaviour, and could thus have an effect on the classification of the aggregation size. Water temperature, for example, is known to have an effect on both the acoustic signal (Bamber and Hill, 1979; Straube and Arthur, 1994) and the abundance of tuna (Boyce *et al.*, 2008). As such, the interpretation of buoy data, particularly concerning the accurate estimation of the aggregated biomass, may be strongly influenced by area and season-specific factors. In addition, close examination of the scores in the layer groups identified by the cluster analysis also revealed that layers deeper than 50 m were characterized by very low scores (Figure 2.4). Previous studies on the vertical distribution of fish species under DFADs found that tuna regularly occurred below this depth (Dagorn *et al*. 2007a; Dagorn *et al*. 2007b; Forget *et al*. 2015; Matsumoto *et al*. 2016; Lopez *et al*., 2017). Consequently, it appears fair to assume that the low values obtained for these depths are likely related to the limited detection capability of the device at such depths, which may also explain the poor estimates of the size of the tuna schools.

The principle findings of this work showed that machine learning offers promising pathways for processing acoustic data provided by commercial echosounder buoys. Although this work has focused on a single model of buoy, it can easily be expanded to encompass other models and brands. The only essential requirement is access to a large training database.

2.5. Conclusion

The methodology developed in this study provides accurate results for the assessment of presence/absence of tuna schools at DFADs in both the Atlantic and Indian Oceans. This approach may be applied to other models of echosounder buoy and particularly to the recent M3I+ model, a novel multi-frequency buoy that has been widely adopted in recent years. Although more extensive analyses could improve the performance of the proposed methodology, specifically regarding assessment of the aggregation size, the accurate discrimination between the presence and absence of tuna schools around DFADs is a critical step towards the exploitation of echosounder buoy data for providing novel and robust indicators of abundance for the management of FAD fisheries in years to come.

Acknowledgements

This project was co-funded by “Observatoire des Ecosystèmes Pélagiques Tropicaux exploités” (Ob7) from IRD/MARBEC and by the ANR project BLUEMED (ANR-14-ACHN-0002). The authors are grateful to ORTHONGEL and its contracting parties (CFTO, SAPMER, SAUPIQUET) for providing the echosounder buoys data. The authors also thank all the skippers who gave their time to share their experience and knowledge on the echosounder buoys. The authors sincerely thank the contribution of the staff of the Ob7 for their work on the databases of the echosounder buoys and observer data. We are also sincerely grateful to the buoy manufacturers for their useful advice and information on their echosounder buoys.

Supplementary information S1

Database description and reliability of buoy abundance index provided by the buoy

1. Database description

1.1. *Echosounder database and technical characteristics of the buoys*

At the time of this study, the echosounder database consists of data recorded by buoys from the manufacturer "Marine Instruments" (Nigràn, Spain, https://www.marineinstruments.es), equipping the French fleet in the Indian and Atlantic oceans, during the period from 2010 to the present day. The database is hosted by Ob7/IRD[8] and constitutes the totality of the Marine Instruments buoys deployed by the French fleet from 2010. The data were made available as part of an ORTHONGEL / IRD confidentiality agreement concluded in May 2016. The dataset corresponds to four different buoy models, which differ mainly in the presence or specifications of their echosounders (Table S1.1). Three of them, which represent more than 97% of all the buoy models in this database are equipped with an echosounder device (Figure S1.1).

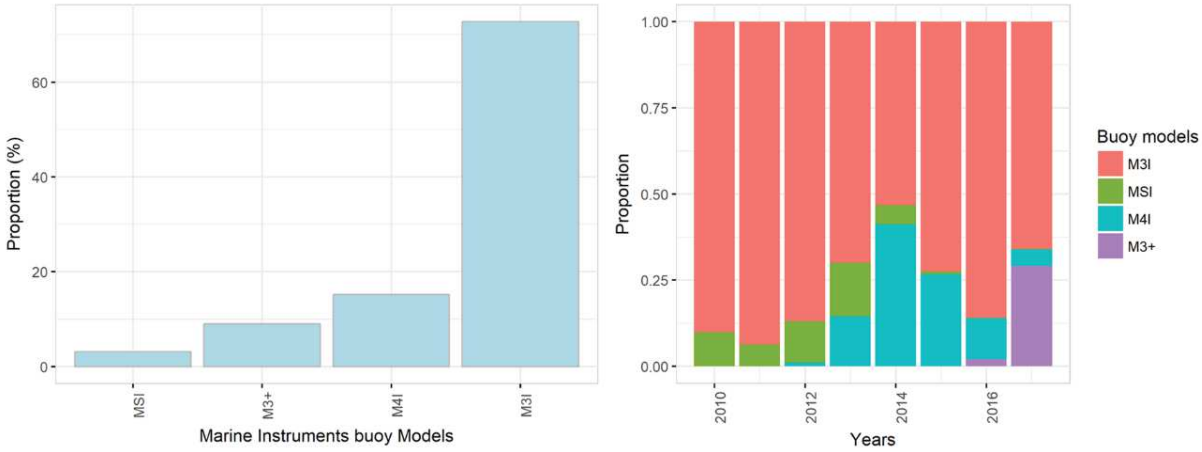

Figure S1.1 : Characteristics of the echosounder buoys database from 2010 to 2017

[8] Observatoire des Écosystèmes Pélagiques Tropicaux exploités (Institut de Recherche et de Développement)

Table S1.1: Main technical specifications of Marine Instruments buoys

	MSI	**M3I**	**M4I**	**M3I+**
Year	2010	2010	2012	2016
Satellite GPS :	Yes	Yes	Yes	Yes
Echo-sounder :	No	Yes	Yes	Yes
Frequency :	-	50 kHz	50, 120, 200 KHz	50 and 200 KHz
Power :	-	500 W	500 W	500 W
Resolution per layer :	-	3 m	3 m	3 m
Range :	-	150 m	150 m	150 m
Blind area :	-	6 m	6 m	6 m
Soundings :	-	each 5 minutes	each 5 minutes (in three frequencies)	each minute (in two frequencies)

1.2. *Operation data on DFADs : Logbook and Observers database*

Two data sources were used to gather information on activities on DFADs: fishing logbooks and observers' data, both hosted by Ob7/IRD. The logbook data covered the data collected by the French purse-seiners' skippers in fishing logbooks during the period 2013 – 2017, in both the Atlantic and Indian oceans. It was supplemented by data from observer's programs conducted in the same oceans and over the same time. Observer data were collected in the frame of the EU Data Collection Framework (DCF) and the French OCUP program, and have reached a 100% coverage rate for the French purse seine fleet since 2015 in Atlantic Ocean (Goujon *et al.*, 2018), and more than 80% after 2016, in Indian ocean (Goujon *et al.*, 2017). Catch values of the fishing sets from the combined logbook and observer database were characterised by a skewed distribution (Figure S1.2) with average values of tuna catch per set of 23 and 26 tons in the Atlantic and Indian, respectively (Table S1.2).

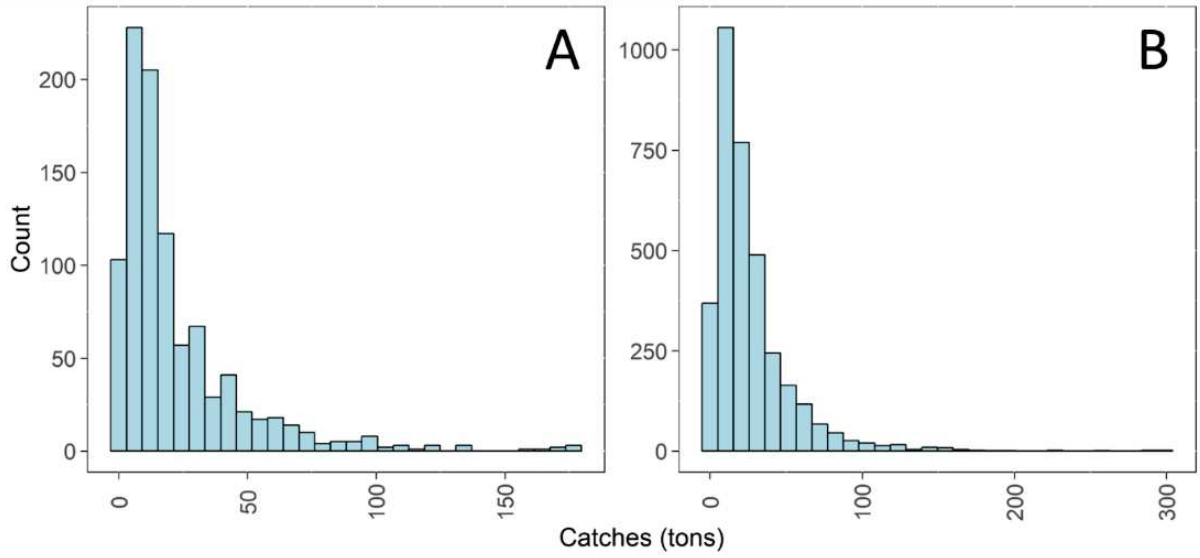

Figure S1.2 : Distribution of catches in FAD fishing operations collected from observer and logbook databases over the period 2013 to 2018, in Atlantic (panel A) and Indian oceans (panel B).

Table S1.2: .Summary statistics of major tuna catches (in tons) in FAD fishing operations collected from observer and logbook databases over the period 2013 to 2018, in Atlantic and Indian oceans. (Min. and Max. denote for minimum and maximum catch values, respectively. SD represents standard deviation)

Ocean	Min.	Median	Mean	Max.	SD
Atlantic	1	15	22.61	177.70	25.59
Indian	1	20	26.73	300	26.77

2. Reliability of M3I buoy abundance index

M3I buoys represent more than 70% of the buoy models in the database, and are equipped with echosounders. The raw acoustic values recorded at each sampling are lost after their processing by the internal modules of the buoy. Only discrete scores varying from 0 to 7, provided per 3-meter layers, which represent the percentage of the beam occupied by fish in the corresponding depth layer, are provided. For each acoustic sample, the buoy also provides a biomass index computed through a proprietary algorithm, and supposed to be proportional to the actual biomass sampled by the device. We assessed the reliability of this index by comparing its values recorded the day before the fishing set with the actual catches made on the same aggregation.

These values were used based on the assumption that aggregation under the FADs remains relatively stable over this period, and also to avoid measurement bias due to buoy handling and possible disturbances that may occur during fishing operations.

The dataset was obtained from cross-referencing catches from logbook and observers database with echosounders database, over the period from 2013 to 2017. Null fishing sets were removed from the analysis, because they represent false negative situations where buoys detect biomass that the fishing operation was not able to catch for any reason (too deep fish, strong currents, etc.). The dataset consisted in 663 and 1639 catches data respectively in Atlantic and Indian oceans. It was supplemented with buoy biomass index values recorded 5 days after deployment of a new DFAD, associated to tuna absence, to the purpose to assess the ability of index in estimating tuna absence underneath DFAD. The structure of the final dataset used for assessment of buoy biomass index can be found in the Table S1.3.

The buoy biomass index (BBI) performance was then assessed by two type of comparisons:

(i). a quantitative one, assessing the relation between Buoy Biomass Index (BBI) and actual catches;

(ii). and a qualitative one, evaluating the index performance in detection of tuna presence/absence under the DFAD.

Table S1.3 : Structure of dataset used in assessment of BBI reliability

	Atlantic	Indian
Deployments	517	5183
Fishing Sets	663	1639

2.1. *Quantitative performance of Buoy Biomass Index (BBI)*

As multiple values of BBI are provided over a full sampling day, comparisons were made by crossing actual catches with average and maximum BBI values recorded over the sampling day. Then, the relation between average or maximum values of BBI and actual biomass under DFAD, were measured through the correlation (R) and determination (R^2) coefficients.

The results indicate for both oceans and regardless of the selected BBI values (maximum or average values), a very low correlation between the abundance index estimated by the buoy and

the actual biomass under the DFAD ($R^2 < 0.1$, see Table S1.4, Figure S1.3 and Figure S1.4). This therefore highlighted the poor reliability of abundance index computed by buoy's internal modules. However, the lack of information on the manufacturer's calculation methodology did not make it possible to identify the source of these weaknesses.

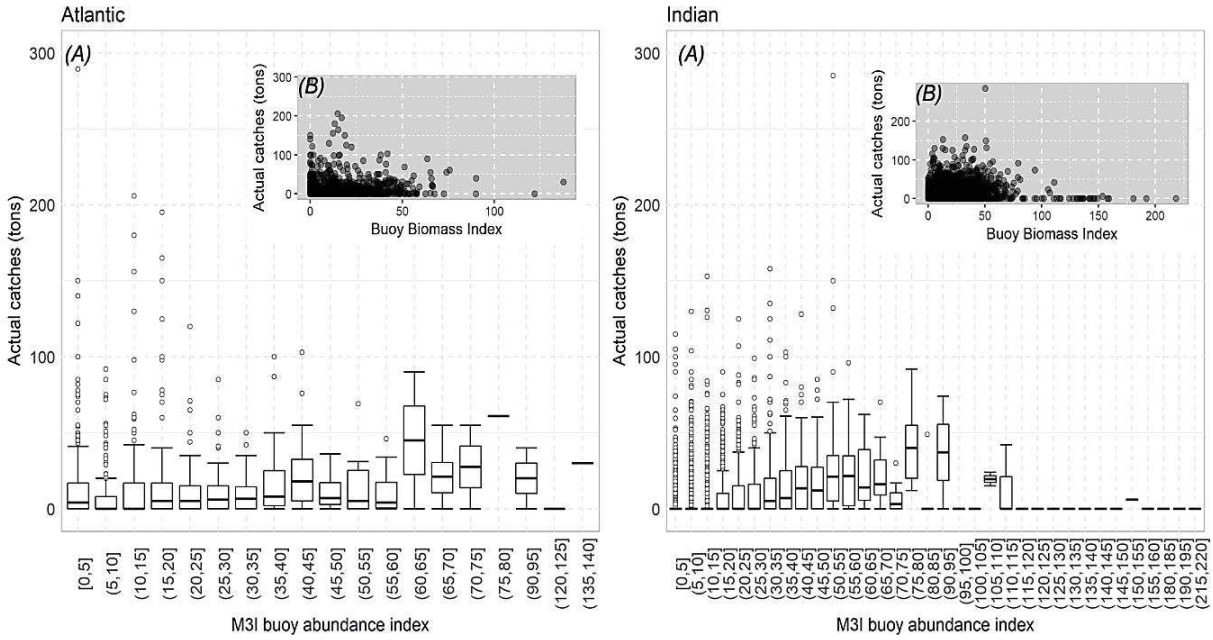

Figure S1.3: (A) Reliability boxplots and (B) scatterplots of maximum BBI values and actual catches under DFAD, in Atlantic (left) and Indian Oceans (right).

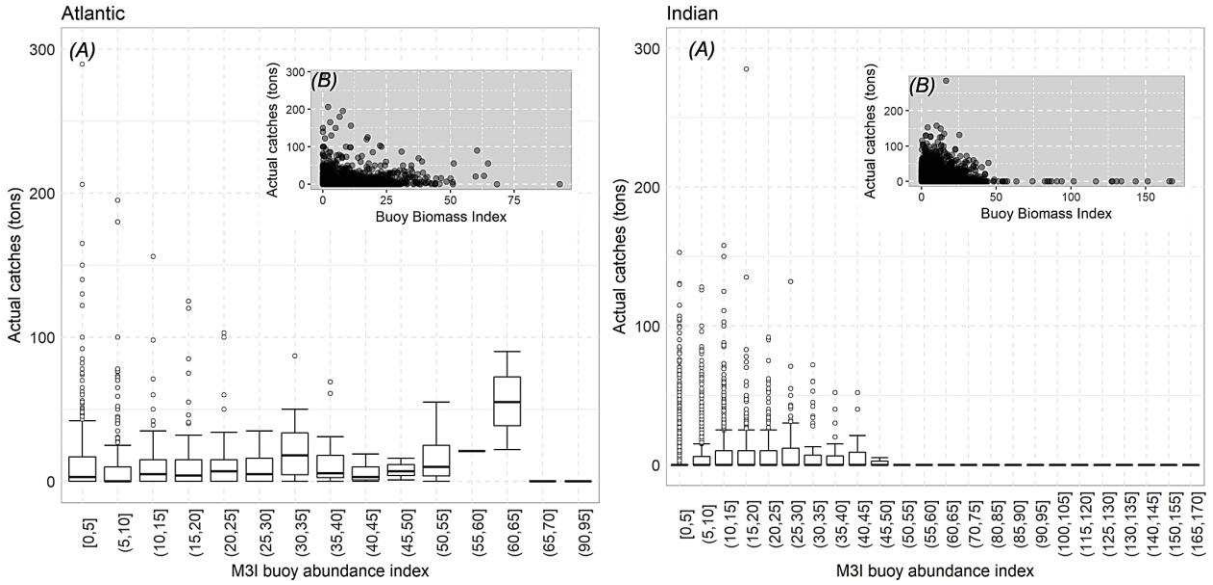

Figure S1.4: (A) Reliability boxplots and (B) scatterplots of average BBI values and actual catches under DFAD, in Atlantic (left) and Indian Oceans (right)

Table S1.4 *:* Coefficients of determination (R^2) between catch and buoy biomass index

	Atlantic	Indian
Mean BBI	5.57e-5	5.85e-3
Max BBI	1.59e-3	7.30e-2

2.2. *Qualitative performance of buoy biomass index (BBI)*

Assessment of qualitative performance of buoy biomass index aimed to determine its ability to detect tuna aggregation, under DFAD. The analysis was performed by transforming average and maximum BBI values recorded over a sampling day, into binary modalities (presence or absence), using different cut-off values (*k*). A given value of the BBI was considered as tuna presence if it was greater than *k*, and the opposite for absence. The presence threshold (*k*) can here be interpreted as a calibration value for the detection of the aggregation by the buoy. A parallel approach was also applied to the actual catch values to examine the resolution of the aggregation detection by the buoy. Catches values were transformed into presence or absence modalities, using different cut-off values (*r*), varying from 0 to 50 tons.

For all cut-off combinations, the classification in the presence or absence of aggregation, estimated from the BBI, was compared with actual presence/absence deriving from catches, using kappa coefficient (Cohen, 1968), calculated from confusion matrices. Results are summarised on Figure S1.5 and Figure S1.6, respectively for consideration of average and maximum BBI values.

They revealed that with a null cut–off value for actual catches ($r = 0$), the optimal calibration value for presence detection by the buoy was in the range of 10 and 20 tons. BBI values below this range, is more likely to be assimilated to false positive (detection of tuna presence by the buoy, when no tuna aggregation under the DFAD). Thus, even at this level, the direct estimates of tuna presence or absence by the buoy remain relatively poor. Unfortunately, in this work, the lack of information on the computation method of the buoy biomass index did not allow us to identify the potential causes of its low performance.

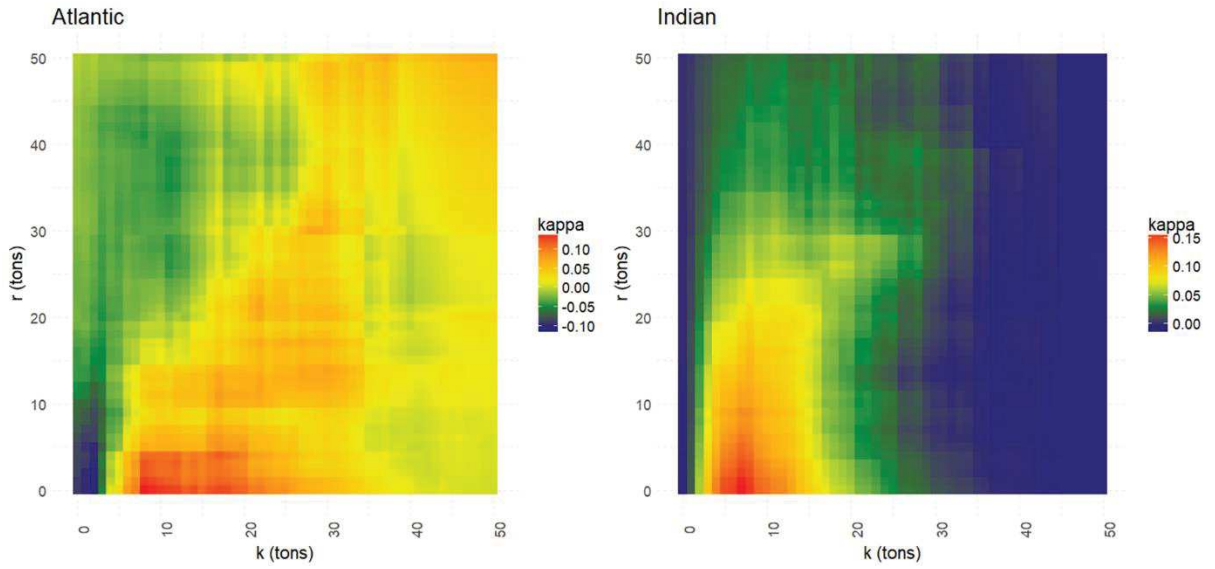

Figure S1.5: Kappa sensitivity to k (buoy calibration threshold) and r (threshold for resolution of presence detection estimated from average values of BBI

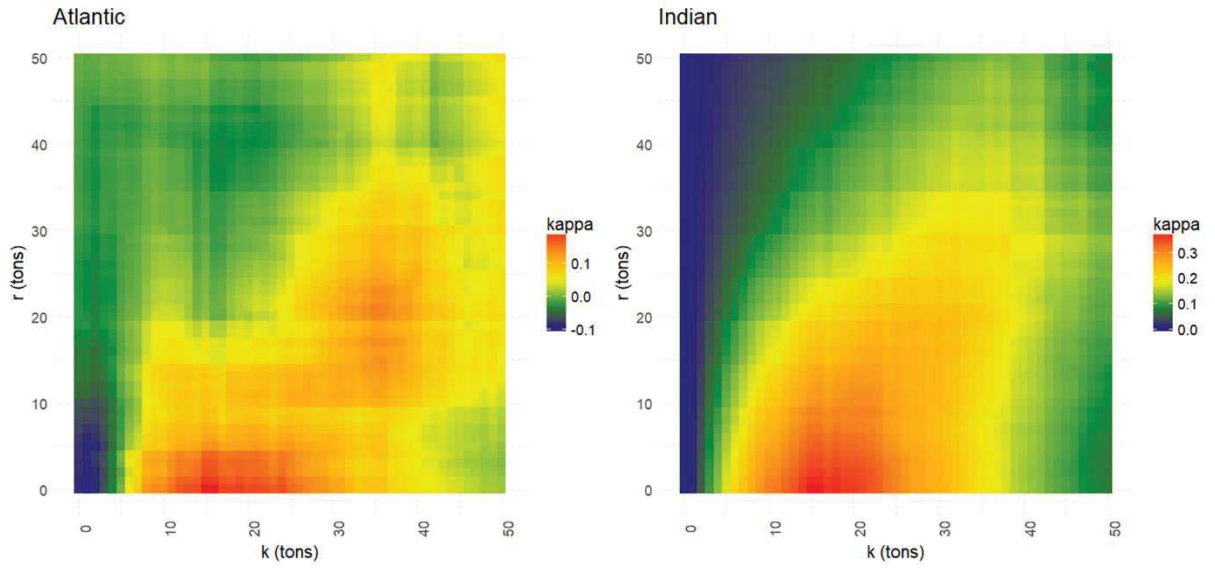

Figure S1.6: Kappa sensitivity to k (buoy calibration threshold) and r (threshold for resolution of presence detection estimated from maximum values of BBI

Supplementary information S2

The "daily acoustic matrices"

1. Introduction

Generally, echosounder buoys can be used under different operating modes, remotely switchable by fishermen. The M3I buoys have five operation modes (for more information refers to Marine Instruments[9], Nigràn, Spain: https://www.marineinstruments.es/) :

- Low Consumption Mode (default mode of the buoy): 2 positions per day (with 6 acoustic pings by position);
- Approach Mode: 4 positions for 12 hours, and 3 pings in every position;
- Recovery Mode: 1 position every 15 minutes during 2 hours (1 ping in every position);
- Flash Mode: Activates the flash and transmits one position every 15 minutes for an hour (1 ping in every position);
- Poll Mode: Transmits a position and one ping some few minutes after requesting (polling).

As a result, the amount of data collected for a full day of sampling can highly differ depending on the mode used by fishermen. The suggested methodology for processing the data provided by the buoys, into tuna occurrence or size classes of tuna aggregation, is a classification, performed on a daily scale, and based on a synthetic sample derived from acoustic information collected by the buoy over an entire day. The synthetic samples are referred to as "daily acoustic matrices". Their design relies on two distinct steps: (*1*) a sub-sampling stage, selecting the "best echo" recorded by the buoy, per slice of 4 hours on a whole day, followed by (*2*) the aggregation of acoustic scores collected by 3-meters layers into values by groups of homogeneous layers.

2. The sub sampling stage

Intuitively, the "best echo" (the single acoustic sample that reflects the best aggregation of tunas under the DFAD, over the considered 4-hour period) could have referred to the acoustic sample with the highest value of sum of layer scores. However, several interviews with fishermen,

[9] Mention of trade names or commercial companies is for identification purpose only and does not imply endorsement by the authors.

conducted prior to this work, indicated that the definition of this "best echo" varies according to different considerations. The main features stated by fishermen for the characterization of "this echo" are related to the depth, vertical distribution and the relative intensity of the acoustic signal.

We tested here the incidence of five selection methods of the "best echo", on the tuna presence/absence classification performance. These methods derive an index (*I*), from the scores of the fifty layers (S_i) of a single acoustic sample. The sample with the highest value of index is then, selected to build the acoustic matrix. Index calculation methods are detailed in the sections below.

2.1. Method 1 (sum)

The selection index results simply from the sum of layer scores of the acoustic sample.

$$I = \sum_{i=1}^{50} S_i \qquad (S2.1)$$

2.2. Method 2 (depth_weighted_sum)

The selection index is the sum of the layer scores weighted with a depth index (Equation S2.2). This approach aimed to integrate the depth significance into echo interpretation, and possible loss of backscattering signal with depth.

$$I = \sum_{i=1}^{50} i^2 \, S_i \qquad (S2.2)$$

2.3. Method 3 (layers_weigthed_sum)

The selection index derived from the sum of layer scores, multiplied by the number of active layers (*N*) in the acoustic sample (namely the layers with non-null score). It aimed to integrate the vertical distribution of echoes, empirically considered by fishermen as an important factor in echosounder data interpretations

$$I = N \sum_{i=1}^{50} S_i \qquad (S2.3)$$

2.4. Method 4 (depth_and_layers_weighted_sum)

This approach is a combination of the two selection methods described above (Equation S3.4).

$$I = N \sum_{i=1}^{50} i^2 . S_i \qquad (S3.4)$$

2.5. Method 5 (mean)

This approach averages the scores per layer of different acoustic samples to construct a single synthetic echo for the considered sub-sampling period.

2.6. Comparison of sub sampling method performances

The effectiveness of the 5 sub-sampling methods was assessed by comparing the performance of tuna aggregation size classification models, built from training sets that differ only in the type of sub-sampling method used to design the acoustic matrices. Models performance was evaluated by cross-validation, replicated 20 times, using at each iteration 75% of the dataset as training data and the remaining 25% as validation data. The kappa coefficients calculated for each model, on the validation sets, at each iteration, were then compared with an ANOVA. The analysis was carried out by considering the Atlantic and Indian Oceans separately.

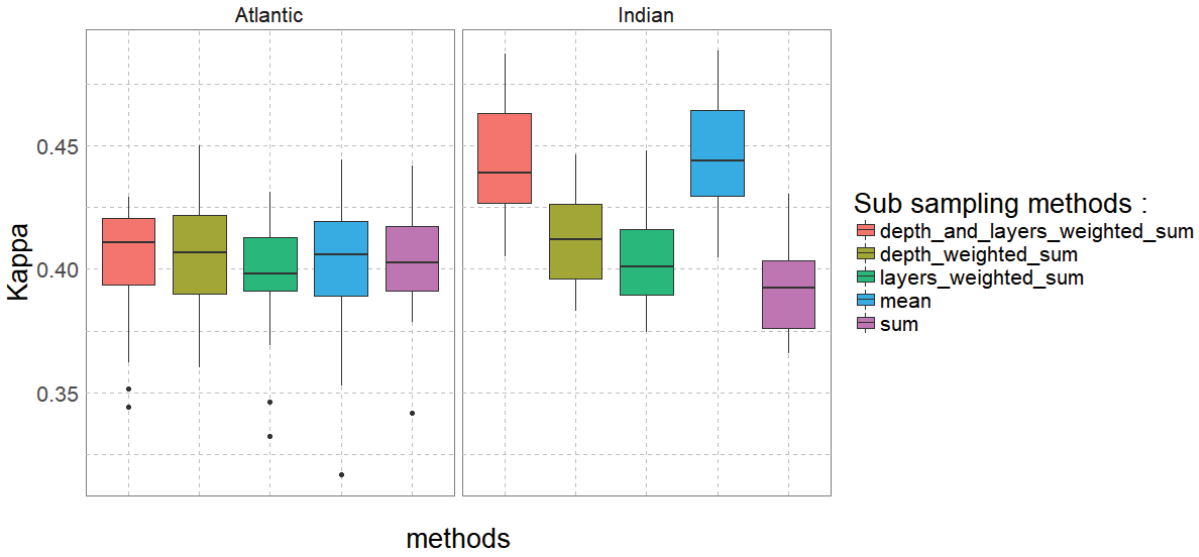

Figure S2.1: Comparison of kappa from five different sub-sampling methods in Atlantic (left panel) and Indian (right panel) Oceans

Major differences occur between oceans (Figure S2.1). In Atlantic Ocean, the type of sub-sampling methods does not significantly influence the accuracies of classification performed by the models. While in Indian, model performances significantly differ from one sub sampling approach to another ($p < 0.001$). "*mean"* and "*depth_and_layers_weighted_sum"* methods appears as the most effective sub sampling methods, with intermediate performances for "*depth_weighted"_sum* and "*layer_weighted_sum"* method. The *"sum"* method is the less effective approach in Indian Ocean.

We hypothesized that the observed differences between oceans could be due to intrinsic differences in the vertical distribution of species under DFADs, between the two oceans. Indeed, the methods integrating weights (with depth or active layers) prioritize in matrix constructions, deeper echoes or echoes with regular distribution. They are based on the hypothesis that this type of signal is more likely to come from tuna aggregations than from other acoustic reflectors (especially bycatch species). Their relative effectiveness in Indian supports this hypothesis. Indeed, the literature indicates a relative segregation between tuna species and by-catch species in this ocean (Moreno *et al.*, 2007a; Forget *et al.*, 2015; Lopez *et al.*, 2016). However, there is still a lack of information on this parameter in the Atlantic. The extremely similar performance of all sub-sampling methods tested in this ocean could possibly be linked to a more homogeneous distribution of the different acoustic reflectors, in the water column. Future research lines should focus on this point.

Finally, against expectations, the use of a synthetic sample built from the average layer values of all acoustic samples collected over the sub-sampling period appears to be an effective method. We initially thought that the variability of the biomasses sampled by the buoy (related to vertical and horizontal migration of fish under DFAD), would result in an echo that would poorly reflect the school characteristics under the DFAD. However, it is likely that biomass variations in the water layers are relatively minor, at the scale of the considered sub-sampling time window.

3. The layer aggregation stage

The second step in the building process of acoustic matrices consists in the reduction of the vertical dimension of the data (depth layers). It aims to combine the different depth layers constituting the acoustic samples into a defined number of homogeneous layer groups, using

clustering methods. The layer scores of the different groups are then aggregated into group scores. This section analyses the influence of different aggregation methods on the classification performance of algorithms.

3.1. Method 1 (agr_simple_sum)

The score in a group (S'_G) is simply the sum of the scores of its different constituent layers.

$$S'_G = \sum_{i=1}^{n_G} S_i^G \qquad (S2.5)$$

3.2. Method 2 (agr_standard)

Group scores are the standardized sum of the scores of the different constituent layers of the group.

3.3. Method 3 (agr_minmax_real)

The score of a group is the normalized sum (scale between 0 and 1) of the scores of its constituent layers, the maximum normalization value being the highest score of the same groups in the training dataset.

$$S'_G = \frac{\sum_{i=1}^{n_G} S_i^G}{\max(S^G)} \qquad (S2.6)$$

3.4. Method 4 (agr_minmax_theo)

The group scores are calculated in the same way as before, except that the maximum normalization value here is the highest theoretical value of the group scores. This corresponds to the maximum score that can be reached in a layer (*maxs*, which corresponds to 7 for M3I buoy) multiplied by the number of layers in the group (n_G).

$$S'_G = \frac{\sum_{i=1}^{n_G} S_i^G}{n_G \, maxs} \qquad (S2.7)$$

3.5. Method 5 (no_aggregation)

Clustering methods are not applied. The 50 layer scores are used for the classification purpose.

3.6. Comparison of layer aggregating method performances

The different layer aggregation methods were compared by assessing the performance of tuna aggregation size classification models, built from training sets that differ only in the type of layer scores aggregating method. Models performance was evaluated by cross-validation, replicated 20 times, (with 75% of the dataset used as training data and the remaining as validation data). Kappa coefficients calculated for each model, at each iteration, were then compared with an ANOVA. The analysis was carried out by considering the Atlantic and Indian Oceans separately.

Compared to sub-sampling methods, the performance of the different scoring methods does not vary between the two oceans (Figure S2.2). The proposed approaches offer relatively similar results, which remain significantly higher than those of classification models based on acoustic matrices on which no layer aggregation had been performed ($p < 0.001$ for both oceans).

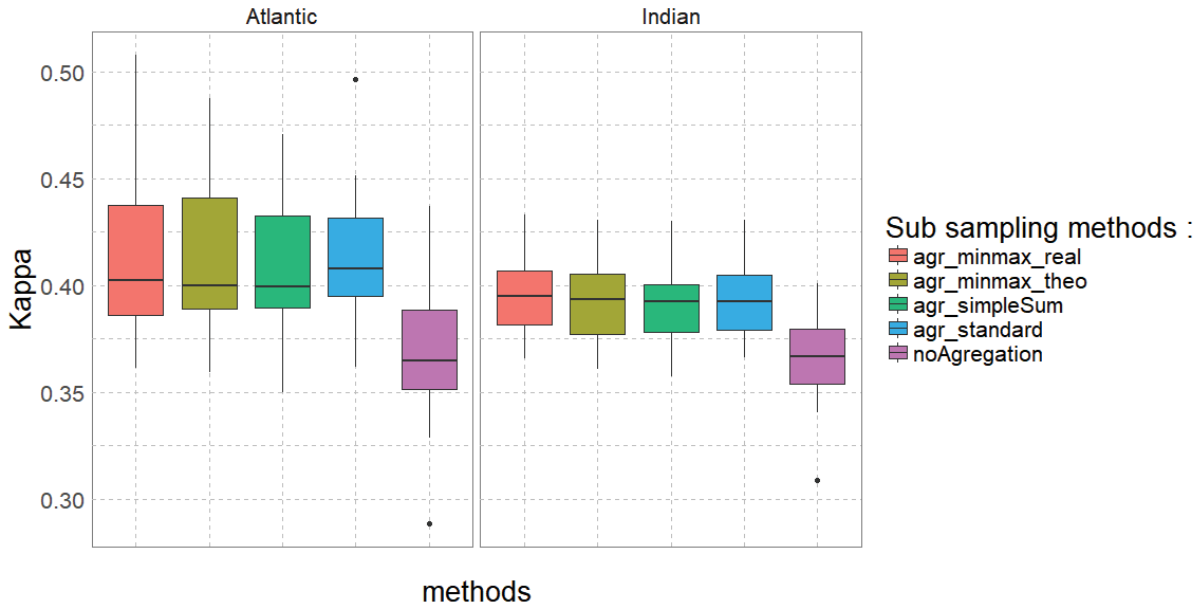

Figure S2. 2 : Comparison of kappa from five different score aggregation methods in Atlantic (left) and Indian (right) Oceans

Supplementary information S3

Constructing the training dataset: Tuna presence and absence

1. Introduction

Classification models were built from a training dataset constituted from acoustic data recorded within a defined period before or after three main type of fishing events. We considered the acoustic data recorded the day before a fishing set operation as tuna presence, under the assumption that the occurrence of the set is a confirmation of tuna presence, and that the purse-seiner catch is the best approximation of the actual biomass under the FAD.

Data collected the day before a simple DFAD visit was associated with tuna absence. Indeed, the acoustic presence of fish, ascertained by fishermen through the interpretation of buoy data, facilitates routes selection and decreases search time (Lopez *et al.*, 2014). Most of the time, the fishermen's choice to visit one of their DFADs results from the confirmation of the potential presence of tuna under the DFAD, based on the interpretation of acoustic data from the buoy. The absence of fishing set on the DFAD indicates that it is very likely that the aggregation visited is not composed of the targeted tuna species. Thus, visits without fishing sets appear like false positive situations of tuna presence, deriving from misinterpretation of buoy data (possibly skewed by environmental conditions, particular aggregation characteristics or buoy technical limitations, etc.). The explanation underlying this one-day delay before fishing sets or visits is related to the need to avoid bias related to buoy handling and/or disturbance of the aggregation under DFAD due to the fishing operation.

In a similar way, acoustic data associated to new DFAD deployments, were also associated as tuna absence. The main issue at this level was to determine the optimal range of the time window to be considered, in order to associate these data with total absence of fish or exclusive presence of bycatch species under the DFAD. The used methodology for assessed this time range is described in the following section.

2. Determining optimal time after deployment

The determination of the optimal time after deployment was based on the analysis of the time series of acoustic signals collected from the first deployment of a new DFAD to the first reported operation (fishing, recovery, etc.). Only DFADs with a minimum soaking time of 60 days were included in the analysis. The dataset consists in 528 and 5868 virgin DFAD deployments, in the Atlantic and Indian Oceans respectively.

Previous works have evidenced that generally tunas are more closely associated with FADs during the daytime period, while other species are during the night, with some specificities depending on the oceanographic regions (Forget *et al.*, 2015; Lopez *et al.*, 2017). These differences in the species association scheme led us to consider the acoustic signal, separating the daytime and night-time periods. The objective was to detect variations in the acoustic signal resulting from the process of early colonization of the DFAD by non-tuna species, according to the hypothesis supported by several studies (Deudero *et al.*, 1999; Castro *et al.*, 2002; Nelson, 2003; Moreno *et al.*, 2007b; Macusi *et al.*, 2017), that these species constitute the first in the colonization sequence of DFADs.

We were interested in the variation over time of the acoustic signal (A_t), estimated from the Equation 1, where N refers to the total number of acoustic samples collected in the period t, and $S^t_{(i,j)}$ to the score in the layer i of the j-th acoustic sample collected.

$$A_t = \frac{1}{N}\sum_{j=1}^{N}\frac{1}{50}\sum_{i=1}^{50} S^t_{(i,j)} \qquad (S3.1)$$

The results revealed that the acoustic signal exhibited, regardless of the considered period (but especially during night periods), a strong variation, immediately after the DFAD deployment, followed by a relative stabilization of the signal (Figures S3.1, S3.2 and S3.3). With slight differences in length between the two oceans, this period is most likely the minimal time interval to account for bycatch presence under DFADs.

For the purpose of building classification models that can discriminate acoustic signal from tuna aggregation, from others acoustic targets (especially bycatch species), this time after deployment has been considered in the design of training data. Although it is obvious that this value is affected by spatial and temporal variations, we have fixed its value at 5 days in both oceans, for standardization and facilitation reasons.

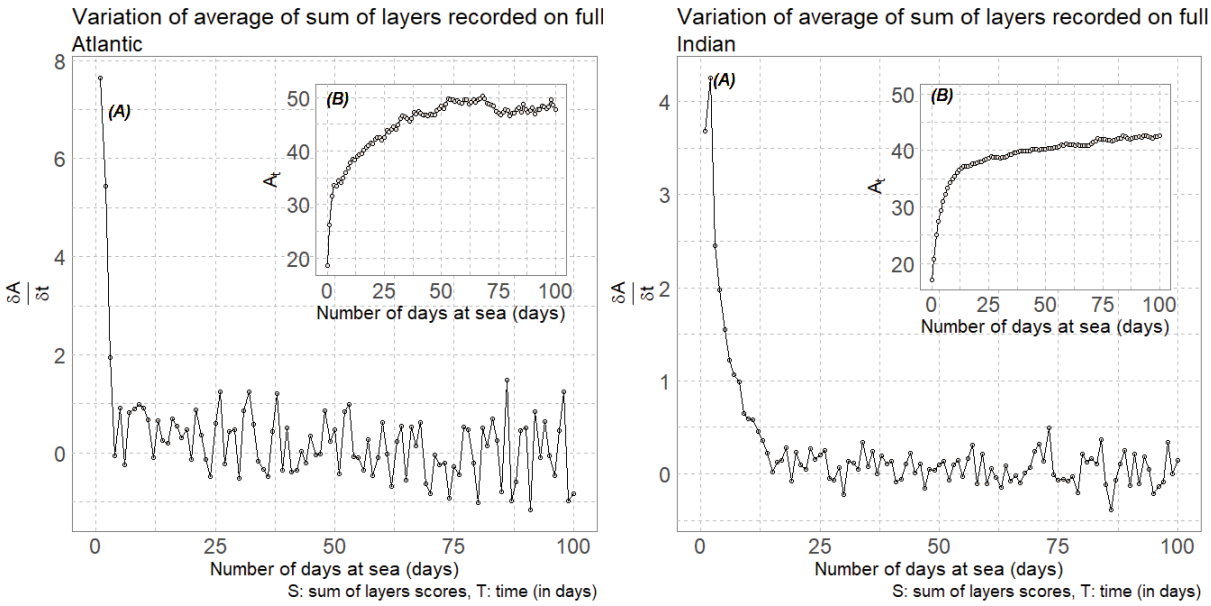

Figure S3.1: Variation over time (A), and time series (B) of daily acoustic signal recorded under virgin DFADs in Atlantic (left panel) and Indian oceans (right panel).

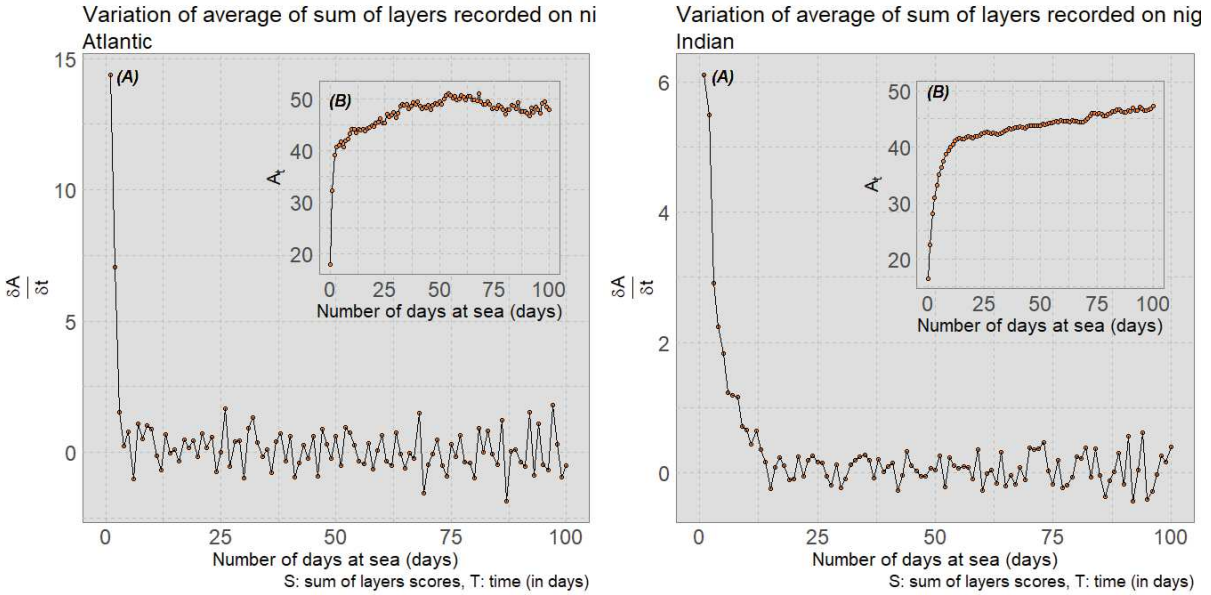

Figure S3.2: Variation over time (A), and time series (B) of daily acoustic signal recorded during night –time under virgin DFADs in Atlantic (left panel) and Indian oceans (right panel).

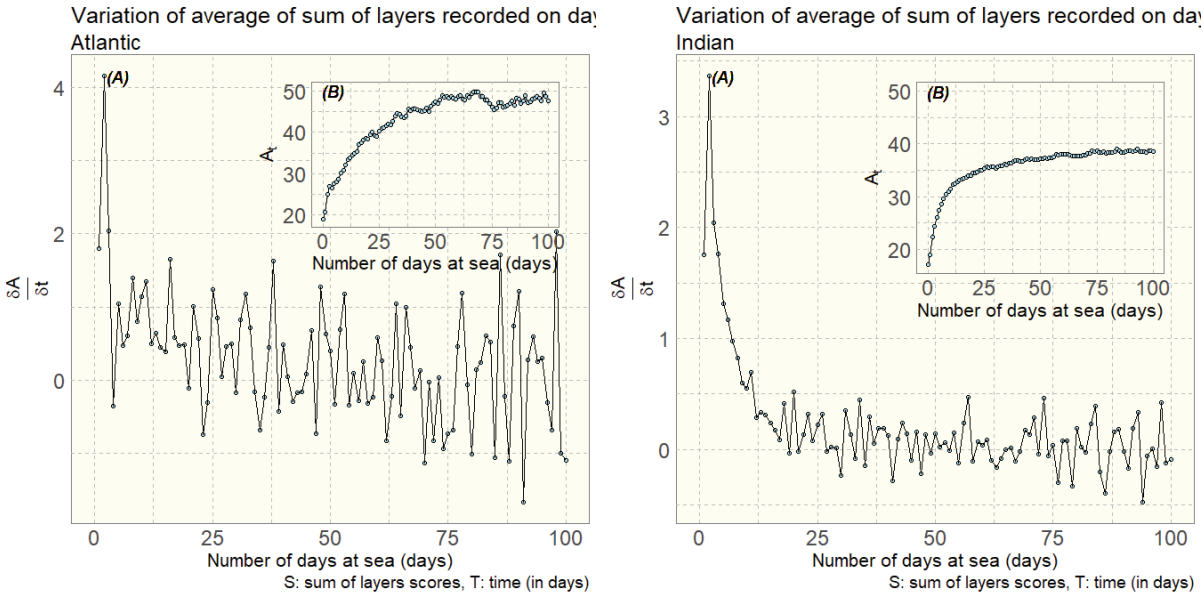

Figure S3.3: Variation over time (A), and time series (B) of daily acoustic signal recorded during daytime under virgin DFAD in Atlantic (left panel) and Indian oceans (right panel).

Chapter 3

Tuna aggregation dynamics at Drifting Fish Aggregating Devices: A view through the eyes of commercial echosounder buoys

"*Pour voir le monde à l'endroit, il faut l'observer à l'envers.*

To see the world right side up, look at it upside down."

Remy Donnadieu

This chapter has been accepted at ICES Journal of Marine Science:

Baidai, Y., Dagorn L., Amande M.J., Gaertner D., and M. Capello. 2020. Tuna aggregation dynamics at Drifting Fish Aggregating Devices: A view through the eyes of commercial echosounder buoys. *ICES Journal of Marine Science*. https://doi.org/10.1093/icesjms/fsaa178.

Tuna aggregation dynamics at Drifting Fish Aggregating Devices: A view through the eyes of commercial echosounder buoys

Y. Baidai[12], L. Dagorn[1], M.J. Amande[2], D. Gaertner[1], M. Capello[1]

[1]MARBEC, Univ Montpellier, CNRS, Ifremer, IRD, Sète, France

[2]Centre de Recherches Océanologiques (CRO), Abidjan, Cote d'Ivoire

Abstract

Improving knowledge on the associative behaviour of tropical tunas with floating objects is a key research priority for ensuring the sustainable exploitation of their populations. First introduced in the early 1990s in the tropical tuna purse seine fishery, Drifting Fish Aggregating Devices (DFADs) are man-made floating objects that are now used on a massive scale to facilitate the capture of tunas. This study addresses novel questions on the dynamics of tuna aggregations associated with floating objects, using commercial echosounder buoys data collected throughout the drifts of newly deployed DFADs in the Eastern Atlantic Ocean and Western Indian Ocean, from 2016 to 2018. Time series of presence/absence of tunas were obtained using a supervised classification process of the acoustic data. To avoid bias associated with the large variability in individual DFAD soak times, a new approach was developed to estimate the average time required for tuna aggregations to colonize new DFADs. We showed that tunas colonize DFADs after an average of 16 days in the Atlantic Ocean, and 40 days in the Indian Ocean. In addition, the analysis indicated that the time span during which tuna aggregations occupy DFADs is driven by a time-independent process with short and long-term residence modes. Our analysis indicates that DFADs were continuously occupied by tuna aggregations for an average of 6 and 9 days in the Indian and Atlantic oceans respectively. The time between two consecutive aggregations at the same DFAD averaged 9 days in the Indian Ocean and 5 days in the Atlantic Ocean. Throughout their soak time after being colonized, DFADs remained occupied by tuna for a larger proportion of time in the Atlantic Ocean (63%) than in the Indian Ocean (45%). The implications of these new findings are discussed in view of the development of new fishery-independent indices of abundance for tropical tuna populations.

Keywords: Echosounder buoys; Drifting Fish Aggregating Devices (DFADs); Tropical tunas; Associative behavior; colonization times; Residence times; Absence times.

3.1. Introduction

Substantial development in the tropical tuna purse-seine fishery has occurred over recent decades and it now accounts for the majority of the world's tropical tuna catch (ISSF, 2019). The increasing trend in catches has been accompanied by regular technological developments of vessels and fishing tools (Gaertner and Pallarés, 2002; Fonteneau *et al.*, 2000; Torres-Irineo *et al.*, 2014). Since the early 1990s, these developments have included the deployment of artificial floating objects, known as drifting Fish Aggregating Devices (DFADs) used to increase fishery efficiency. This fishing mode exploits the behavioural trait of the target tuna species, skipjack tuna (*Katsuwonus pelamis*), yellowfin tuna (*Thunnus albacares*), and bigeye tuna (*Thunnus obesus*), to naturally aggregate around floating objects (see Fréon and Dagorn, 2000 and Castro *et al.*, 2002). Thousands of DFADs specifically designed to attract tunas, are deployed by purse seine fleets in all of the world's oceans to enhance their catches. Initial estimates put the number of DFADs operated annually across the three major oceans in the range of 50,000 and 100,000 (Baske *et al.*, 2012; Scott and Lopez, 2014; Gershman *et al.*, 2015). Furthermore, the scale at which this fishing gear is used has quadrupled in less than a decade, in both the Atlantic and Indian oceans (Fonteneau *et al.*, 2015; Maufroy *et al.*, 2017). Over the past 30 years, this fishing mode has been significantly improved through the sequential introduction of new technologies (radio, GPS and echosounder buoys), with the latter now providing skippers and fleet managers with detailed information on the location and biomass associated with DFADs (Lopez *et al.*, 2014). In recent years, more than half of the world's purse seine catch of tropical tunas has come from DFAD fishing (Dagorn *et al.*, 2013; Fonteneau *et al.*, 2013).

The mechanisms underlying the associative behaviour of tropical tunas with floating objects remain poorly understood, despite the proposal of numerous hypotheses (see Fréon and Dagorn, 2000 and Castro *et al.*, 2002). As a consequence of the massive increase in the use of DFADs in the recent years, improving knowledge on the associative behaviour of tropical tunas with floating objects has become a key research priority. Primary areas of concern include the concomitant changes in catchability of tunas at floating objects as well as the understanding of the impact of DFADs on their ecology and that of other associated fauna. To date, most research efforts have focused on describing the associative dynamics of individual fish, primarily through electronic tagging studies, at both coastal anchored FADs (e.g. Holland *et al.*, 1990; Ohta and Kakuma, 2005; Dagorn *et al.*, 2007a; Mitsunaga *et al.*, 2012; Robert *et al.*, 2013; Rodriguez-Tress *et al.*, 2017), and drifting FADs (e.g. Schaefer and Fuller, 2013; Matsumoto

et al., 2014, 2016; Tolotti *et al.*, 2020). In contrast, behavioural patterns of FAD-associated aggregations (i.e. entire tuna schools under a DFAD) have received considerably less research attention. When investigated, studies were primarily focused on the spatial or temporal characterization of aggregations at fine timescales, using acoustic equipment on board research vessels (Josse and Bertrand, 2000; Doray *et al.*, 2006; Moreno *et al.*, 2007a; Trygonis *et al.*, 2016). The instrumentation of DFADs with satellite-linked echosounder buoys began in the late 2000's. Since then, their use has become widespread in many fleets. Currently, almost all deployed DFADs are equipped with these devices which provide remote and near real-time information on the DFAD location and aggregated biomass (Lopez *et al.*, 2014; Moreno *et al.*, 2019). Echosounder buoys generate a considerable stream of data that can be used to characterize DFAD aggregations (Lopez *et al.*, 2016; Orue *et al.*, 2019a; Baidai *et al.*, 2020a). The availability of such data, which is continuously being collected, represents an unprecedented opportunity to observe fish aggregations associated with floating objects over long time scales. To date, only one study has provided characteristics of tuna aggregations at DFADs over the scale of weeks and months, using data from fisher's echosounder buoys (Orue *et al.*, 2019b).

This work aims to characterize how tunas occupy DFADs, in order to improve the understanding of their aggregation dynamics around these objects. Using data from commercial echosounder buoys attached to DFADs deployed in the Western Indian Ocean and Eastern Atlantic Ocean, we assessed several parameters related to the association of tuna aggregations with DFADs. These include the elapsed time between deployment of a new DFAD and its colonization by tunas; the average duration of association of tuna aggregations with DFADs and the length of time that DFADs remains vacant between consecutive tuna aggregations.

3.2. Material and methods

3.2.1. Echosounder Data

The echosounder data used in this study were collected using M3I buoys[10] attached to DFADs from the French tropical tuna purse seiner fleet operating in the Western Indian Ocean and Eastern Atlantic Ocean, from 2016 to 2018. The M3I buoy is equipped with a GPS positioning device and an echosounder powered by solar panels, operating at a frequency of 50 kHz, with

[10] Marine Instruments, Nigrán, Spain, www.marineinstruments.es

a power of 500 W, and a beam angle of 36°. The data output of the buoy is simplified acoustic information, designed for easy visual interpretation by fishers. The M3I buoy samples the water column in 3-meter layers covering a total depth of 150 m (50 layers, with the first two corresponding to the transducer near-field). An acoustic sample consists of 50 ordered categorical scores (ranging from 0 to 7), resulting from the automatic conversion of the acoustic backscatter signal recorded per 3-meter layer, with an inbuilt algorithm. In the default-operating mode, 12 samples collected at about 2 hour intervals, are transmitted daily via satellite by the buoy.

3.2.2. Data cleaning process

The raw data provided by the echosounder buoys were cleaned using the following protocol (see Baidai *et al.,* 2017 for details on the procedure):

(1) Duplicated rows, inconsistent positions, data recorded on land, at shallow positions (depth less than 150 meter), or under low voltage conditions (poor reliability of acoustic data collected below 11.5V) were omitted from the database.

(2) A rule-based algorithm, which uses buoy speed and its variations as main classifiers, was applied to discriminate acoustic data recorded when the buoy is on board a vessel from those actually recorded when the buoy is deployed at sea.

3.2.3. Classification of tuna presence/absence

The presence or absence of tuna at a DFAD was assessed from acoustic data collected by echosounder buoys, following the methodology described in Baidai *et al.*, (2020). This approach involves preliminary processing of the acoustic data, followed by a classification using random forest algorithms applied separately to each ocean. The learning datasets were constructed by cross-referencing the acoustic data with the activities of fishers at DFADs (namely sets with associated tuna catches, DFAD deployments and DFAD visits) recorded in logbooks and by on-board observers. A detailed description of the classification procedure can be found in Supplementary Material S4. The minimum catch value representing tuna presence in the learning dataset was 1 ton. Thus, in this work, the term “tuna aggregation” refers to a fish aggregation whose tuna biomass is at least equal to this value.

An additional post-processing step was applied to improve the predictions made by the classification algorithm during the course of DFAD trajectories. Prediction results with short durations (i.e. an isolated event of presence or absence lasting a single day) were considered unlikely, attributed rather to misclassification, and corrected using the previous or following day's predicted values. This step allowed for the correction of 9 and 7% of the initial predictions made by the classification model, in the Atlantic Ocean (AO) and the Indian Ocean (IO) respectively.

3.2.4. Newly deployed DFADs

Only newly deployed DFADs (i.e. DFADs used for the very first time) equipped with echosounder buoys were considered. Natural floating objects (e.g. logs), reinforced old DFADs found at sea, relocated DFAD and buoy transfers were all excluded. Deployments of new DFADs were identified from fishing logbooks and observer data collected from 2016 to 2018 in the AO and IO. The 2016-2018 period was selected to provide a relatively homogeneous study period, while maintaining sufficient data in both oceans. Observer data were collected by the IRD-Ob7 observatory under the EU Data Collection Framework (DCF) and the French OCUP program (Observateur Commun Unique et Permanent). Trajectories and time series of tuna presence/absence associated with newly deployed DFADs were then identified by cross-referencing the logbook and observer databases with the echosounder buoy database, using the unique identification code of the buoy and the deployment date. To ensure that the subset correctly identified newly deployed DFADs (and not potentially misreported reinforcement activities), records for which fishing sets were reported during the week following the deployment were removed from the dataset. An additional cleaning step was applied to the dataset in order to omit data with inconsistent positions between the location of the DFAD deployment recorded in the logbook or observer database, and the actual position recorded by the buoy (0.3% and 0.8% of the dataset in Atlantic and Indian Oceans respectively). The cleaned dataset of newly deployed DFADs included 9118 trajectories with 498,276 presence/absence data points for the IO and 285 trajectories with 18,102 presence/absence data points for the AO (Figure 3.1).

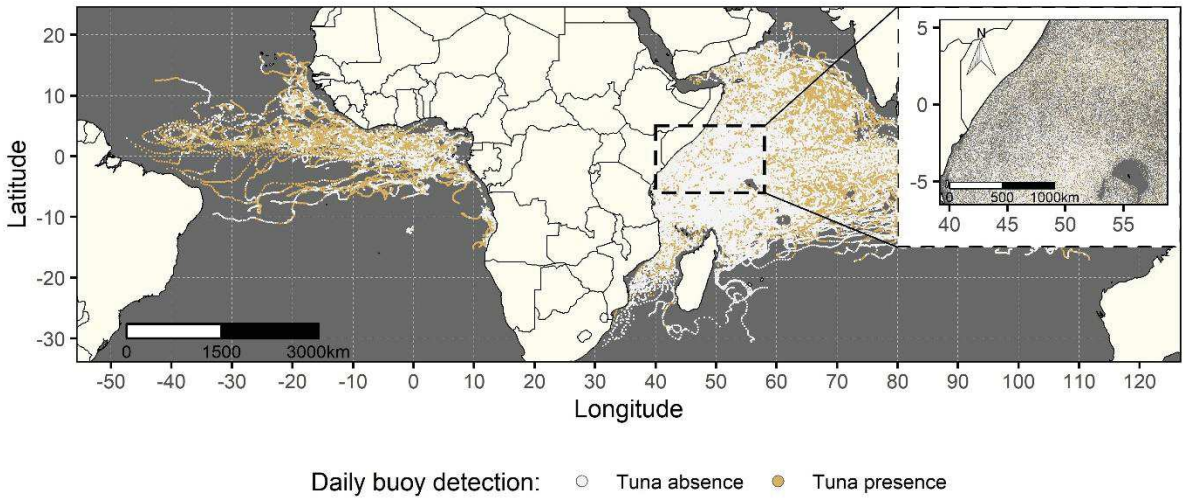

Figure 3.1: Presence/absence of tuna aggregations along the course of the trajectories of newly deployed DFADS monitored in Western Indian Ocean and Eastern Atlantic Ocean from 2016 to 2018. Orange dots indicate days when tuna aggregations were present, white dots represent days with no tuna aggregations.

3.2.5. Soak time and colonization time

Soak time was defined as the number of days between the deployment of a DFAD equipped with a buoy and the first reported operation on it (i.e., either a fishing set or the retrieval of the buoy). Tuna colonization time refers to the number of days between the deployment of a DFAD and the first day when a tuna aggregation is detected by the echosounder buoy (Figure 3.2).

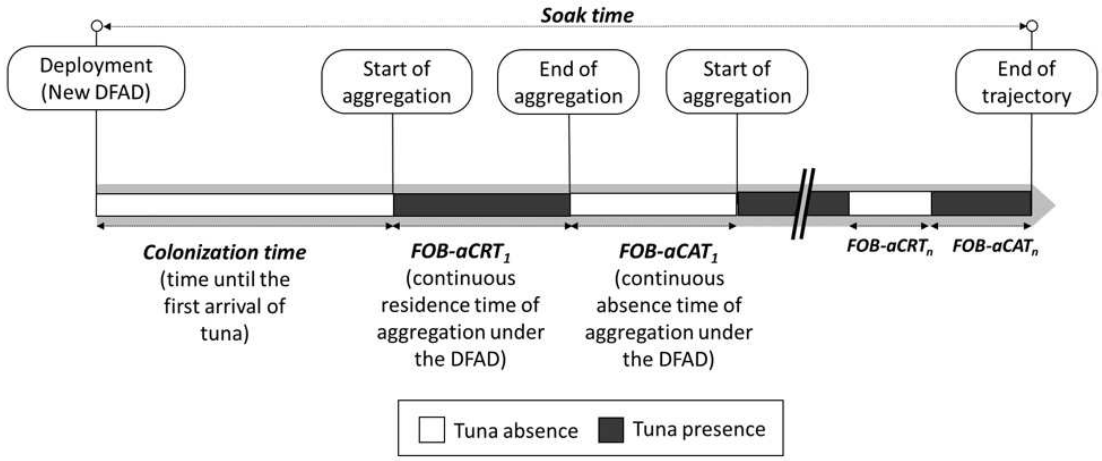

Figure 3.2: Schematic representation of the timeline of tuna aggregation dynamics at a DFAD. The term "end of trajectory" denotes here the first operation carried out on FADs likely to affect the aggregation (e.g. either a fishing set or the retrieval of the buoy).

The term "colonized DFAD" thus refers to a DFAD that has aggregated tuna at least once (for longer than one day).

Due to fishing and buoy retrievals, the number of buoys at sea available for the analysis declined for increasing soak times. This can induce bias in the estimate of tuna colonization times obtained from simple averages (Figure 3.3). Specifically, the lower the number of DFADs with long soak times, the lower the chances of observing long colonization times, which leads to an underestimate of colonization times from simple arithmetic averages. To overcome this bias, colonization times were estimated from daily colonization rates, considering the daily fraction r_i of colonized DFADs relative to the total available DFADs, for each day i after deployment, as follows:

$$r_i = \frac{N_{colonized_i}}{N_{colonized_i} + N_{uncolonized_i}} \tag{3.1}$$

Where, *Ncolonized*$_i$ indicates the number of DFADs colonized during day *i* after deployment and *Nuncolonized*$_i$ denote not-yet-colonized DFADs on day *i* after deployment. The denominator of Equation (3.1) corresponds to the total number of DFADs available for colonization on day *i*, namely, the total number of DFADs in the water that at day *i*-1 after deployment were not yet colonized.

Mann-Whitney *U* tests, were used to compare daily colonization rates between the IO and the AO. The unbiased mean colonization time (T_{col}) (in days) was then estimated as the inverse value of the average of daily colonization rates ($\bar{r}$):

$$T_{col} = \frac{1}{\bar{r}} \tag{3.2}$$

where $\bar{r}$ denotes the average daily colonization rate:

$$\bar{r} = \frac{1}{D}\sum_{i=1}^{D} r_i \tag{3.3}$$

where *D* represents the total number of days during which the daily colonization rates r_i were calculated. When numbers of available DFADs were too low (i.e., the denominator in Equation (3.1)), the daily colonization rate becomes less reliable. A preliminary sensitivity analysis, included in the Supplementary Material S4 (Figure S4.2), showed that *D* corresponds to the number of days after deployment when at least 30 DFADs remained available for colonization.

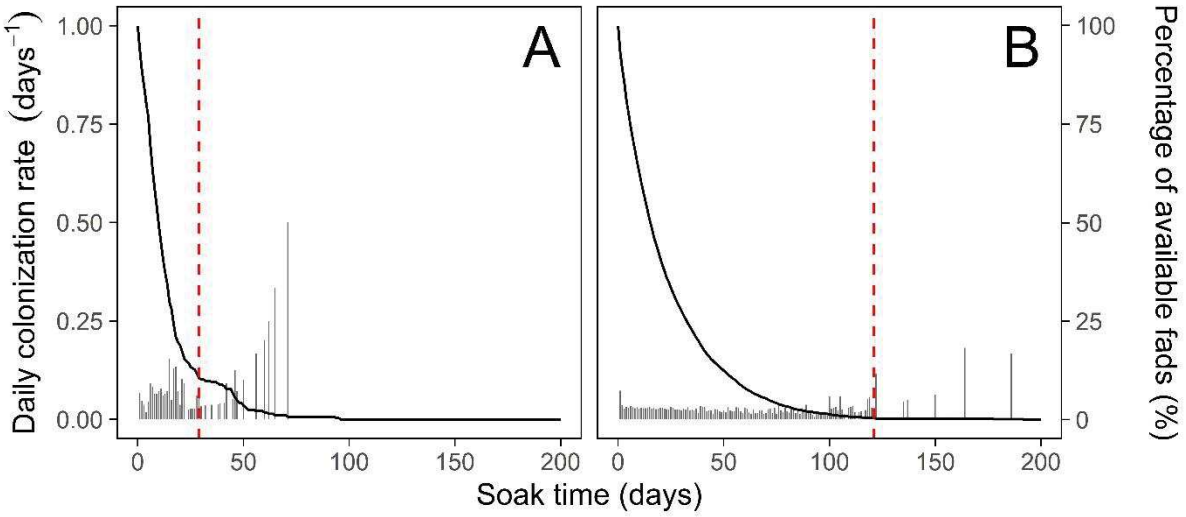

Figure 3.3: Daily colonization rates (bars) and percentage of equipped DFADs available (solid lines) over time in the Atlantic Ocean (Panel A) and the Indian Ocean (Panel B). Red dashed lines indicate the number of days after deployment at which 30 DFADs were still available.

3.2.6. Aggregation stability

The continuous residence time (CRT) is commonly used to represent the amount of time spent by acoustically-tagged individual tunas around a FAD without a day scale (>24h) absence (Ohta and Kakuma, 2005; Capello *et al.*, 2015). Alternatively, the continuous absence time (CAT) refers to the time interval between two consecutive associations for an individual tuna (Robert *et al.*, 2012; Rodriguez-Tress *et al.*, 2017). In this work, the concepts of CRT and CAT were adapted and applied to DFAD aggregations rather than to individual fish. Accordingly, the *aggregation's continuous residence time at a floating object* (FOB-aCRT) was considered as the time span within which a tuna aggregation was continuously detected at a DFAD without a day scale (>24h) absence. Similarly, the *continuous absence time of aggregation at a floating object* (FOB-aCAT) was defined as the period between two consecutive detections of tuna aggregations at the same DFAD. Values occurring directly before an operation on the DFAD (fishing event or retrieval of the buoy) were excluded from the analysis as they were artificially truncated. Finally, the overall proportion of time that a tuna aggregation remained at a colonized DFAD (named *DFAD occupancy rate*), expressed as the ratio of the sum of all FOB-aCRTs against its soak time after the colonization period, was assessed and compared between oceans using Mann-Whitney *U* tests.

3.2.7. Survival analyses of FOB-aCRT and FOB-aCAT

Survival analyses (e.g. Capello *et al.*, 2015) were used to characterize the distribution of FOB-aCATs and FOB-aCRTs. Survival curves were constructed using the fraction of FOB-aCATs and FOB-aCRTs shorter than a given time, and compared between oceans using the logrank statistical test (Harrington and Fleming, 1982), implemented in the "*survival*" package in R (Therneau, 2015).

Survival curves were also fitted using three models: (*i*) single exponential, (*ii*) double exponential and (*iii*) power law (Supplementary Material S4: Table S4.3), by adapting the methodology of Robert *et al.,* (2013) to the DFAD aggregation metrics. Exponential models assume association dynamics (presence or absence of an aggregation at a DFAD) to be independent of time. Double exponential models imply the existence of two distinct time-scales occurring within aggregation presence or absence at a DFAD. Power law models indicates a time-dependent probability of presence and absence of tuna aggregations, meaning the longer the time a DFAD is occupied or vacant, the smaller the probability that a change in state will occur. Models were discarded if one or more parameters were not significant ($p > 0.05$ based on the *t*-statistics). The best-fitting models were chosen based on the Akaike Information Criterion (AIC) and q-q plots.

3.3. Results

3.3.1. Daily colonization rates and colonization times

No significant difference was found between DFAD soak times from the AO and the IO (Mann-Whitney *U* tests, $p = 0.76$) with mean values of 63.28 days (SD 65.08 days), and 54.24 days (SD 45.52 days) respectively. Approximately 22% DFADs in the AO (62 DFADs) and 34% (3,122 DFADs) in the IO did not show any sign of colonization by tunas during their soak time. The soak time of vacant DFADs (averages of 18.66 and 28.52 days for AO and IO, respectively) was significantly lower than that of colonized DFADs (averages of 75.68 and 67.63 for AO and IO respectively), with a *p*-values (Mann-Whitney *U* tests) lower than 0.001 in both oceans (Supplementary Material S4: Figure S41.4).

For colonized DFADs, the time before the echosounder buoy detected the first aggregation of tunas averaged 13.17 days (SD 12.37 days) in the AO and 20.22 days (SD 20.83 days) in the

IO. Stable trends in daily colonization rates were observed in both oceans (see Figure 3.3). The average daily colonization rates were significantly higher (Mann-Whitney *U* test, $p < 0.001$) in the AO ($\bar{r}$ = 0.062, SD 0.037) than in the IO ($\bar{r}$ = 0.025, SD 0.011). Calculating the unbiased average colonization times following Equations (3.1 – 3.3) resulted in colonization times that were 2.5 times shorter in the AO (T_{col} = 16.10 days, SD 9.66 days – see Table 3.1) than in the IO (T_{col} = 40.46 days, SD 17.31 days – see Table 3.2).

Table 3.1: Summary of tuna aggregation metrics measured in the Atlantic Ocean

	Min.	Max.	Median	Mean	Standard deviation
DFAD Soak time (days)	1	305	44	63.28	65.08
Daily colonization rate (days^{-1})	0	0.15	0.06	0.06	0.04
Tuna colonization time (days)	-	-	-	16.10	9.66
FOB-aCAT (days)	2	86	4	5.38	6.01
FOB-aCRT (days)	2	96	4	8.96	11.52
Occupancy rate (%)	5.13	97.59	60.49	63.27	19.86

Table 3.2: Summary of tuna aggregations metrics measured in the Indian Ocean

	Min.	Max.	Median	Mean	Standard deviation
DFAD Soak time (days)	1	363	43	54.24	45.52
Daily colonization rate (days^{-1})	0	0.07	0.02	0.02	0.01
Tuna colonization time (days)	-	-	-	40.46	17.31
FOB-aCAT (days)	2	119	5	8.84	10.93
FOB-aCRT (days)	2	109	4	6.20	6.86
Occcupancy rate (%)	2.83	98.08	46.16	45.45	21.73

3.3.2. Aggregation continuous residence (FOB-aCRT) and absence times (FOB-aCAT)

A total of 15,415 FOB-aCRTs and 13,328 FOB-aCATs events were recorded during the course of the trajectories of newly deployed DFADs in the IO. In the AO, 723 FOB-aCATs and 779 FOB-aCRTs were recorded. Distributions of FOB-aCATs and FOB-aCRTs in both oceans are shown in Figure 3.4. The average duration of tuna aggregations was 8.96 days (SD 11.52) around DFADs in the AO and 6.20 days (SD 6.86) in the IO. It should be noted that very long continuous residence times of tuna aggregations under the same DFAD were also observed in both oceans (96 and 109 days, in the AO and IO respectively). The average time that DFADs remained vacant between two consecutive tuna aggregations (FOB-aCAT), was 5.38 days (SD 6.01 days), with a maximum duration of 86 days in the AO, and at 8.84 days (SD 10.93 days), with a maximum of 119 days in the IO (Table 3.1 and Table 3.2).

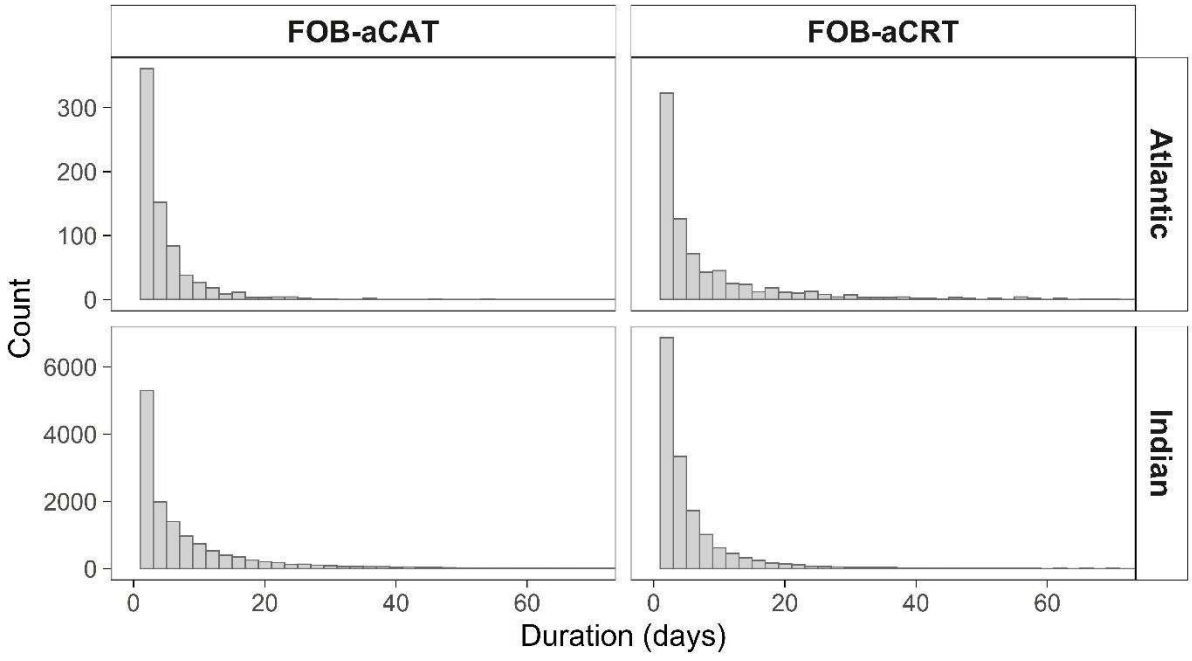

Figure 3.4 : Distribution of FOB-aCATs (left) and FOB-aCRTs (right) in the Atlantic Ocean (top) and Indian Ocean (bottom). FOB-aCRT and FOB-aCAT denote the aggregation's continuous residence time at a floating object and the continuous absence time of aggregation at a floating object, respectively.

Inter-ocean comparisons of FOB-aCAT and FOB-aCRT survival curves indicated significant differences in the associative dynamics of tuna aggregations (logrank test, $p < 0.001$ for both FOB-aCAT and FOB-aCRT ocean-comparisons – Figure 3.5).

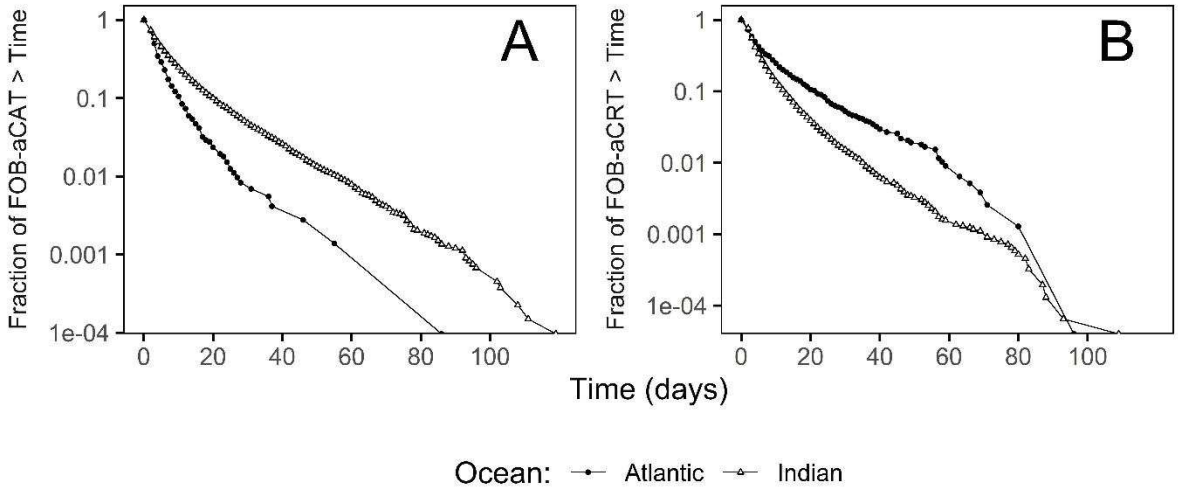

Figure 3.5: Survival curves of FOB-aCATs (Panel A) and FOB-aCRTs (Panel B) recorded on trajectories of newly deployed DFADs in Atlantic Ocean (black dots) and Indian Ocean (white dots). The y-axis is on a logarithmic scale. FOB-aCRT and FOB-aCAT denote the aggregation's continuous residence time at a floating object and the continuous absence time of aggregation at a floating object, respectively.

In the IO double exponential models were the best fitting for survival curves of both FOB-aCATs and FOB-aCRT. Short-term residences represented 94% of the FOB-aCRTs with a mean duration of 4.58 days, while long-term residences represented 6% with a mean duration of 20.18 days. Short-term absences lasted an average of 4.43 days (representing 66% of FOB-aCATs), while long-term absences had a mean duration of 15.45 days (34% of FOB-aCATs).

In the AO, a double exponential model was the best fit for the survival curve of FOB-aCRTs with averages of 3.75 days (62% of FOB-aCRTs) and 15.70 days (38% of FOB-aCRTs) for short and long-term residence times, respectively. Conversely, a single exponential model was the best fit for absence times of tuna aggregations at DFADs with a mean duration of 4.30 days (see Table 3.3 and Figure 3.6).

Table 3.3: Summary of the model fits of the survival curves of aggregation continuous residence and absence times (FOB-aCRTs and FOB-aCATs) obtained in Atlantic and Indian Oceans. , Est = parameter estimate, Std. Error = standard error, t-value = value of t-statistic, Pr(> |t|) = p-value at t-tests and AIC = Akaike Information Criterion. AIC values of the best-fitted models are highlighted in bold. Significance codes: *** = 0; ** = 0.001; * = 0.01; .= 0.05

Ocean	Metric	Fitting law	Parameter	Estimate	Std. Error	t-value	Pr(>|t|)		AIC
Atlantic Ocean	FOB-aCRT	Single exponential	a	0.14	3.61E-03	38.35	6.92E-42	***	-217.80
		Double exponential	a	0.27	8.51E-03	31.29	2.75E-36	***	**-416.09**
			b	0.06	2.13E-03	29.95	2.58E-35	***	
			p	0.62	1.89E-02	33.03	1.71E-37	***	
		Power law	a	2.29	7.19E-02	31.87	3.87E-37	***	-389.71
			b	11.73	5.11E-01	22.94	7.76E-30	***	
	FOB-aCAT	Single exponential	a	0.23	5.03E-03	46.16	7.42E-31	***	**-154.98**
		Double exponential	a	0.24	1.24E-02	19.59	1.20E-18	***	-155.22
			b	0.03	6.18E-02	0.43	6.68E-01		
			p	0.98	3.24E-02	30.26	4.86E-24	***	
		Power law	a	22.04	2.51E+01	0.88	3.87E-01		-153.74
			b	91.78	1.08E+02	0.85	4.03E-01		
Indian Ocean	FOB-aCRT	Single exponential	a	0.20	2.84E-03	69.54	3.63E-69	***	-404.29
		Double exponential	a	0.22	8.71E-03	25.04	2.85E-37	***	**-426.38**
			b	0.05	1.94E-02	2.56	1.27E-02	*	
			p	0.94	3.37E-02	27.90	2.42E-40	***	
		Power law	a	8.49	2.17E+00	3.92	2.00E-04	***	-415.36
			b	39.48	1.10E+01	3.58	6.24E-04	*	
	FOB-aCAT	Single exponential	a	0.14	2.12E-03	64.29	1.01E-80	***	-471.48
		Double exponential	a	0.23	3.10E-03	72.73	1.98E-84	***	**-875.29**
			b	0.06	1.11E-03	58.30	1.34E-75	***	
			p	0.66	1.02E-02	64.71	9.41E-80	***	
		Power law	a	3.06	5.51E-02	55.51	3.31E-74	***	-806.27
			b	17.36	4.04E-01	43.01	4,41E-64	***	

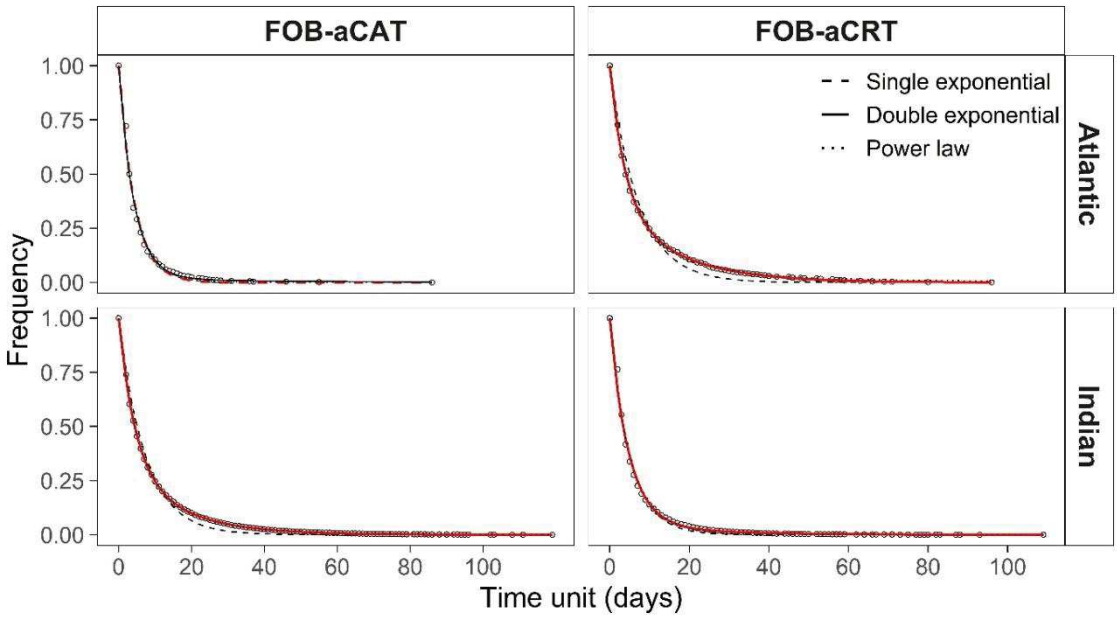

Figure 3.6: Survival curves of FOB-aCAT (left) and FOB-aCRT (right) observed in Atlantic Ocean (top) and Indian Ocean (bottom) fitted with single exponential, double exponential and power law models. The red line indicates the best fit. FOB-aCRT and FOB-aCAT denote the aggregation's continuous residence time at a floating object and the continuous absence time of aggregation at a floating object, respectively.

3.3.3. DFAD occupancy rate

Significant differences in the proportion of time that colonized DFADs were occupied by tuna were observed between the two oceans (Mann-Whitney *U* tests $p < 0.001$). After colonizing DFADs, in the AO tuna aggregations were detected for an average of 63.27% (SD 19.86%) of the soak time (Figure 3.7A), while in the IO, this figure was 45.45% (SD 21.73%) (Figure 3.7B).

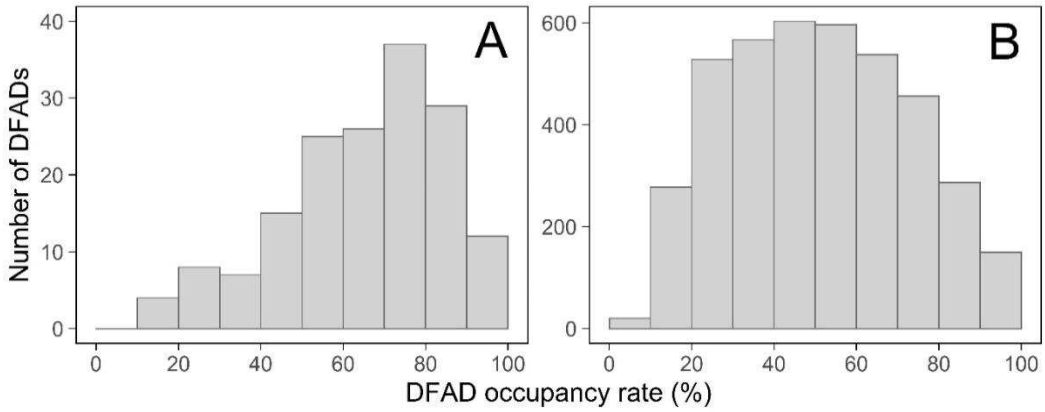

Figure 3.7: Distribution of the DFAD occupancy rates in the Atlantic Ocean (Panel A) and the Indian Ocean (Panel B).

3.4. Discussion

This work aimed at characterizing the dynamics of the tuna aggregation processes around DFADs, using acoustic data collected by commercial echosounder buoys on newly deployed DFADs in the IO and AO. To date, very few studies have designed scientific protocols to quantify the time that pelagic species take to colonize newly deployed DFADs. The only previous documented observations in the Atlantic Ocean come from Bard *et al.* (1985), who reported rapid colonization by tunas, ranging from 1 hour to 6 days, through the monitoring of a dozen newly deployed DFADs and detecting tuna presence by visual observations, on-board echosounders, or by fishing sets. Their estimates are significantly shorter than ours for the same ocean (average of 16 days); however, interpretation of these discrepancies is complicated by the large differences in methods and the time when the studies were conducted. The Bard *et al.* study was performed before the development of the FAD-fishery, when tropical tuna stocks were only moderately exploited. Furthermore, their observation protocol could not identify whether observed individuals only visited or remained associated with the DFAD. Taquet *et al.*, (2007) observed that dolphinfish (*Corypheana hippurus*) could arrive a few hours after the deployment of a new floating object, but did not necessarily associate with it. In the Indian Ocean, using Local Ecological Knowledge (LEK), Moreno *et al.*, (2007b) suggested that it typically takes one month before tunas aggregate under a newly deployed DFAD. Although aggregation dynamics at anchored FADs may differ from those at drifting FADs, it is worth noting that Macusi *et al.,* (2017) reported that fishers typically wait approximately 22 days for tuna aggregations to form at anchored FADs in the Philippines, based on interview data. In a recent study using echosounder buoys produced by a different manufacturer, Orue *et al.,* (2019b) examined acoustic data from over 900 newly deployed DFADs in the Western Indian Ocean and suggested that tunas begin to aggregate approximately 13 days after deployment. At three times longer, the findings of the current study (an average of about 40 days in the IO) appear to be more aligned with the knowledge of purse seine skippers (Moreno *et al.,* 2007b). The discrepancy between these acoustic studies may be related to (*i*) differences in methodological approaches applied in the conversion of acoustic data into indicators of presence or absence of tuna, (*ii*) the method used in the current study to estimate colonization times, which avoids possible underestimation biases linked to the large variability in DFAD soak times, or (*iii*) from the differences in the specificities of the buoy models used in each study. Since their introduction into the fishery, echosounder buoys have evolved rapidly, through continuous technological innovations in both hardware and software (Lopez *et al.*,

2014). Thus, the intrinsic performance of buoys for detecting tuna aggregations may differ by model and/or manufacturer. Hardware and software differences in the design of buoys may lead to variable thresholds for the detection of aggregations, which could ultimately result in biases in the detection of small aggregations for some models. Such disparities highlight the critical need for a detailed assessment of the reliability of outputs from the different models of buoys and the accuracy of the data processing methods they use to estimate fish abundance. This is especially important when considering the growing use of echosounder buoy data for scientific purposes (Moreno *et al.*, 2016).

Until now, most scientific knowledge on the behaviour of tunas around floating objects stems from observations of individuals, using electronic tags, with the majority of studies focused on anchored FADs (e.g. Holland *et al.*, 1990; Ohta and Kakuma, 2005; Dagorn *et al.*, 2007a; Mitsunaga *et al.*, 2012; Robert *et al.*, 2013; Rodriguez-Tress *et al.*, 2017). By exploiting the potentially massive data source that echosounder buoys on DFADs represent, this work introduces two novel metrics (FOB-aCAT and FOB-aCRT), providing descriptive elements of DFAD use by entire tuna aggregations. It is particularly interesting to note that, in both oceans, the time taken for tunas to colonize new DFADs was significantly longer than durations between consecutive tuna aggregations (average FOB-aCATs: 9 and 6 days in AO and IO respectively). This result is consistent with previous assertions regarding the role of non-tuna species in the tuna colonization process. Several authors have suggested that the colonization of FADs is a sequential process starting with the arrival of non-tuna species, which may play a key role in the attraction or retention processes of tunas (Deudero *et al.*, 1999; Castro *et al.*, 2002; Nelson, 2003; Moreno *et al.*, 2007c; Taquet *et al.*, 2007; Macusi *et al.*, 2017). The duration of the settlement stage of these pioneer communities could be one of the major factors driving the colonization time of tunas at a new DFAD. As such, colonization time may be viewed as a unique type FOB-aCAT with an extended duration due to the requisite maturation phase of the DFAD. Further studies on interspecific relationships would be of major benefit for improving our understanding of the role played by non-tuna species in the aggregative processes of tunas with DFADs.

A review of the main findings from electronic tagging studies on the associative behaviour of tunas under DFADs reveals that the continuous residence time of individual tuna (CRT) is subject to a degree of variability related to the species or the oceanic region under consideration (see Table 3.4). Off the coast of Guinea in the Atlantic Ocean, Tolotti *et al.*, (2020) estimated average CRT values of 9 and 19 days, for skipjack and yellowfin tuna respectively. For bigeye

tuna the reported CRTs were up to 25 days, which is longer than observations from other oceans. Shorter CRTs (about 1 day on average) were observed for the same three species by Dagorn *et al.*, (2007b) in the Western Indian Ocean. However, these results are likely to be underestimated due to artificial truncation of the observation experiments. Govinden *et al.*, (2010) reported residence times ranging from 4 to 10 days (median values) depending on the tuna species, at DFADs monitored in the Mozambique Channel. In Eastern Pacific Ocean, studies carried out by Matsumoto *et al.,* (2014) and Matsumoto *et al.* (2016), both indicated that individual tunas remain associated with DFADs for less than 7 days. Despite this variability, tuna CRTs reported by this limited number of tagging studies appear to be lower or equal to the average FOB-aCRTs obtained in this work (9 and 6 days in the AO and the IO, respectively), especially for skipjack tuna which is the dominant species in DFAD-associated catches (Dagorn *et al.*, 2013a).

Table 3.4: Summary of main findings from previous studies on continuous residence time of individual tunas at drifting FADs. (FL: fork length, YFT: *Thunnus albacares*, SKJ: Katsuwonus *pelamis*, BET: *Thunnus obesus*).

Study	Location	Species	FL range (cm)	CRT
Dagorn *et al.*, (2007b)	Western Indian Ocean	SKJ	*Not provided*	Average at 0.91 days (maximum: 7.03 days)
		BET		Average at 1.43 days (maximum: 3.06 days)
		YFT		Average at 1.04 days (maximum: 15.22 days)
Govinden *et al.*, (2010)	Mozambique Chanel, (Western Indian Ocean)	SKJ	47 – 57	Median at 4.47 days (maximum: 18.33 days)
		BET	54 – 56	Median at 3.89 days (maximum: 6.56 days)
		YFT	29 – 60	Median at 9.98 days (maximum: 26.72 days)
Matsumoto *et al.*, (2014)	Equatorial central Pacific Ocean	SKJ	36 – 65	Average at 2.3 days (maximum: 6.4 days)
Matsumoto *et al.*, (2016)	Equatorial central Pacific Ocean	SKJ	34.5 – 65.0	Average at 1.3 days
		BET	33.5 – 85.5	Average at 3.8 days (maximum: about 11 days)
		YFT	31.6 – 93.5	Average at 4.1 days (maximum 14.5 days)
Scutt *et al.*, (2019)	Western Central Pacific Ocean	SKJ	46 – 60	Median at 1 day (maximum: 18 days)
		BET	37 – 90	Median at 10 days (maximum: 30 days)
		YFT	36 – 98	Median at 2 days (maximum: 50 days)
Tolotti *et al.,* (2020)	Eastern Atlantic Ocean	SKJ	39 – 61	Average at 9.19 days (maximum value to 15 days)
		BET	45 – 61	Average at 25.31 days (maximum value to 55 days)
		YFT	34 – 82	Average at 19.15 days (maximum value to 55 days)

Survival analyses of the FOB-aCRTs indicated the coexistence of two distinct modes of DFAD association by tuna aggregations: a dominant mode consisting of short durations, and a longer residence mode. Nearly all of the FOB-aCRTs measured in the IO belonged to the short-term residence mode, whereas the two modes occurred in more similar proportions in the AO. There are several possible explanations for the occurrence of these different modes and their inter-ocean variation. Individually, bigeye and yellowfin tuna generally exhibit longer residence times than skipjack tuna, as indicated by the tagging studies mentioned above. Long-term residence modes may therefore reflect aggregations with a large proportion of the two former species. Furthermore, this study was conducted at a broad spatial and temporal scale. As such, it is possible that the observed differences in modes could be a result of behavioural patterns of tuna that are driven by local environmental differences (such as prey or conspecific abundance, or densities of floating objects) between seasons or oceanic regions. The long-term residence mode could also be indicative of the occurrence of turnover processes of schools at the same DFADs as reported by Weng *et al.,* (2013). Further spatially constrained analyses combined with electronic tagging studies, conducted on DFADs equipped with echosounder buoys, will be crucial to relate the individual and the collective dynamics of tuna around DFADs.

The associative behaviour of the tuna population implies that, at any given time, the overall abundance in an area is the sum of the abundance of two permanently interacting components: the associated and the free-swimming (or unassociated) populations. At present, the underlying reasons driving the association or departure of tunas from floating objects remain unclear. Nevertheless, an improved understanding of the interactions between the two population components can be achieved through the study of the relationships between the association metrics assessed at the scale of the individual (i.e. CAT and CRT) and at the scale of aggregations (FOB-aCAT and FOB-aCRT). Rodriguez-Tress *et al.,* (2017) suggested that high FAD densities tend to reduce the time that tuna spend in an un-associated state (CAT). While these findings may need to be interpreted with caution as they stem from observations at anchored FADs, this could suggest that the underlying trend may occurs irrespective of the FAD type. Logically, higher FAD densities would increase the probability of an individual encountering and associating with a FAD, hence reducing the time individual tuna spend in a free-swimming state (CAT). Similarly, FAD vacancy (FOB-aCATs) should be related to the abundance of the un-associated tuna population. Long FOB-aCATs would result when the un-associated population is small, either due to a low overall tuna population or a large density of FADs drawing them in to aggregate. Following this reasoning, the longer FOB-aCAT and

colonization time observed in the IO may thus be indicative of a smaller size of the tuna population and/or higher densities of DFADs in this ocean than in the AO. Furthermore, the double exponential curve for FOB-aCATs observed in the IO, could be a result of regions/periods where at least one of these two factors differ. Previous work by Capello *et al.*, (2016) demonstrated that indicators of abundance for tropical tuna populations could be derived from their individual associative dynamics (CRT and CAT). Combining our current understanding of the individual associative behaviour of tunas with the metrics describing tuna aggregation dynamics provided by this work could aid in developing new methods for obtaining direct abundance estimates of tuna populations. Such methods will depend upon the availability of estimates of the total number of DFADs at sea (more specifically the total number of floating objects). Currently, obtaining these statistics is a challenge in all oceans despite the recent data reporting requirements for DFAD activities by Tuna Regional Fisheries Management Organisations (t-RFMOs).

3.5. Conclusion

Using data from the echosounder buoys of French purse seiner fleets, this study characterized key parameters of tuna aggregations at DFADs: colonization times, aggregation lifetimes and time span between aggregations. In both oceans, lifespan of tuna aggregations at DFAD followed a time-independent process with two modes. This suggests that the species composition and/or the local conditions (e.g. prey, conspecifics or density of floating objects) could play key roles in aggregation dynamics. However, opposing trends also existed between the two oceans, with shorter residence time of aggregations and longer periods of DFAD vacancy in the IO than in the AO. Further spatially restricted analyses assessing these behavioural metrics at smaller spatial and temporal scales could help in understanding the dynamics of aggregations at a local scale, as well as the role played by various environmental factors. The integration of these new findings into population assessment models which account for the associative behaviour of tunas present an opportunity for the development of alternative abundance indices (independent from catch and effort data) for tropical tunas and the construction of reliable scenarios on the impacts that DFADs have on tuna populations.

Acknowledgements

This project was co-funded by the ANR project BLUEMED (ANR-14-ACHN-0002), leadered by MC and the “Observatoire des Ecosystèmes Pélagiques Tropicaux exploités” (Ob7) from IRD/MARBEC. The authors are grateful to ORTHONGEL and its contracting parties (CFTO, SAPMER, SAUPIQUET) for providing the echosounder buoys data. The authors also thank all the skippers who gave time to share their experience and knowledge on the echosounder buoys. The authors sincerely thank the contribution of the staff of the Ob7 on the databases of the echosounder buoys and observers’ data.

Supplementary information S4

1. Presence/absence classification of tuna aggregations

The classification of presence or absence of tuna aggregations under DFADs from acoustic data collected by the M3I buoy, was based on the methodology described by Baidai *et al*., (2020). The approach consists in two main steps. The first is an initial processing of acoustic data aiming to standardize them and reduce their dimensionality. Acoustic data recorded during a full day of sampling (24 hours), were clustered over six temporal 4-hour bins and six aggregated-depth layers, resulting in a synthetic sample of the daily acoustic information (a 6×6 matrix) referred to as "daily acoustic matrix". The actual classification step was then carried out using random forest models applied separately for each ocean. The training datasets were constructed by cross-matching the acoustic data with activities on DFADs (namely tuna catches, DFAD deployments and visits) recorded in logbooks and/or by observers on board the French tuna seiners, over the period 2013-2018 (Table S4.1). They consisted of daily acoustic matrices obtained from: (i) the day before a successful fishing set with the aim to represent the presence of tuna in the aggregation, (ii) the fifth day following the deployment of a new DFAD, and (iii) the day prior to DFAD visits (visit to a DFAD equipped with a vessel's own buoy which did not result in a fishing operation due to the absence of tuna) which were both assumed as tuna absence. Tunas catches values used to ground truth the presence of tuna aggregations were ranged from 1 ton to 175 tons (with an average value of 15 tons) in Atlantic Ocean, and from 1 ton to 311 tons (average value of 20 tons) in Indian Ocean (Table S4.2 and Figure S4.1).

The classification algorithm showed a good performance in successfully discriminating tuna presence and absence, in both oceans, with an overall accuracy of 74 % and 86 % in the Atlantic and Indian Oceans, respectively.

Table S4.1. Total number of DFADs operations collected from 2013 to 2018 and used as learning dataset of presence/absence classification models in the Atlantic and Indian oceans.

	Tuna absence		Tuna presence
	Deployment	Visit	Fishing set
Atlantic	695	281	989
Indian	11697	1343	4449

Table S4.1. Summary statistics of major tuna catches used in the learning dataset of tuna presence/absence classification models (by random forest algorithm) in Atlantic and Indian oceans.

Ocean	Min.	Max.	Median	Mean
Atlantic	1	175	15	21.97
Indian	1	311	20	28.13

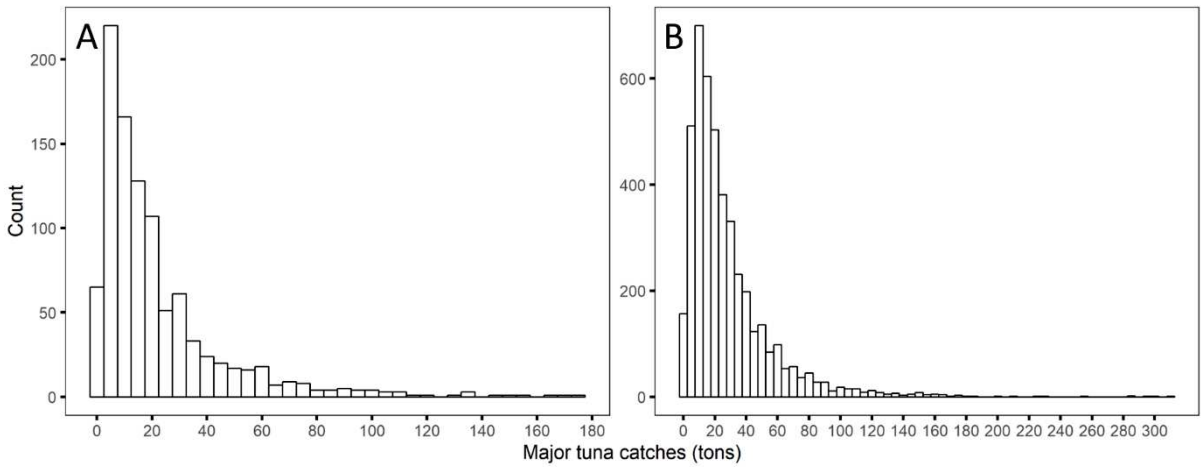

Figure S4.1. Distribution of major tuna catches in the learning dataset of tuna presence/absence classification models (by random forest algorithm) in Atlantic (Panel A) and Indian Ocean (Panel B).

2. *Sensitivity of colonization time*

The colonization time ($\bar{t}$) was assessed as the inverse value of the mean colonization rate (see Equation S4.1). Since this rate become less reliable for too low numbers of available DFADs, a sensitivity analysis was performed to determine the threshold number of DFADs from which a stable trend of the colonization time is reached.

$$\bar{t} = \frac{1}{\frac{1}{D}\sum_{i=1}^{D} r_i} \qquad \text{(Eq.S4.1)}$$

Where r_i denotes, for a given day i, the ratio of the number of colonized DFADs relative to the total number of DFADs at water on the same day; and D the number of days at which the threshold number of DFADs (as determined by the sensitivity analysis) are still available.

The analysis showed that colonization time estimates were stable for at least 30 available DFADs, corresponding to approximately 29 and 121 days of DFAD monitoring in the Atlantic and Indian Ocean datasets, respectively (Figure S4.2).

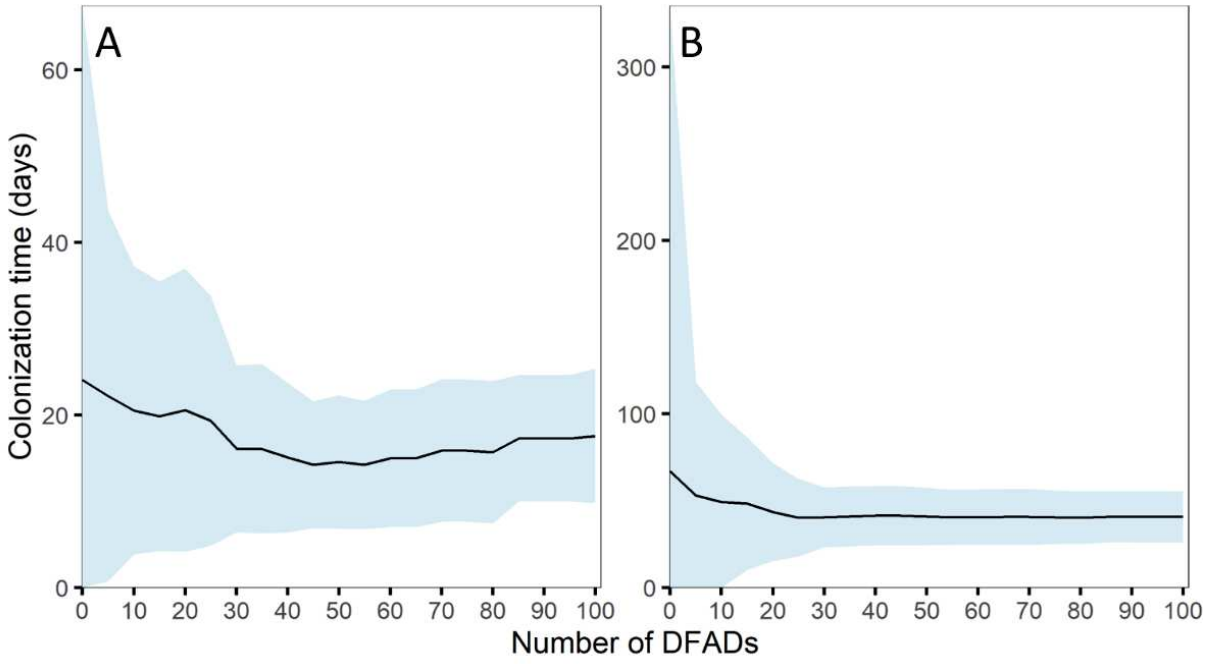

Figure S4.2. Sensitivity of colonization time to different cut-off values on the minimum number of available DFADs applied for the calculation of daily colonization rates, in the Atlantic (Panel A) and Indian Oceans (Panel B). Shaded area represents the confidence interval around the colonization time. The colonization times were estimated as the inverse of the averages of the daily colonization rates, which themselves correspond to the daily ratios of the colonized DFADs relative to the total available DFADs.

3. Soak time comparison of colonized and uncolonized DFADs

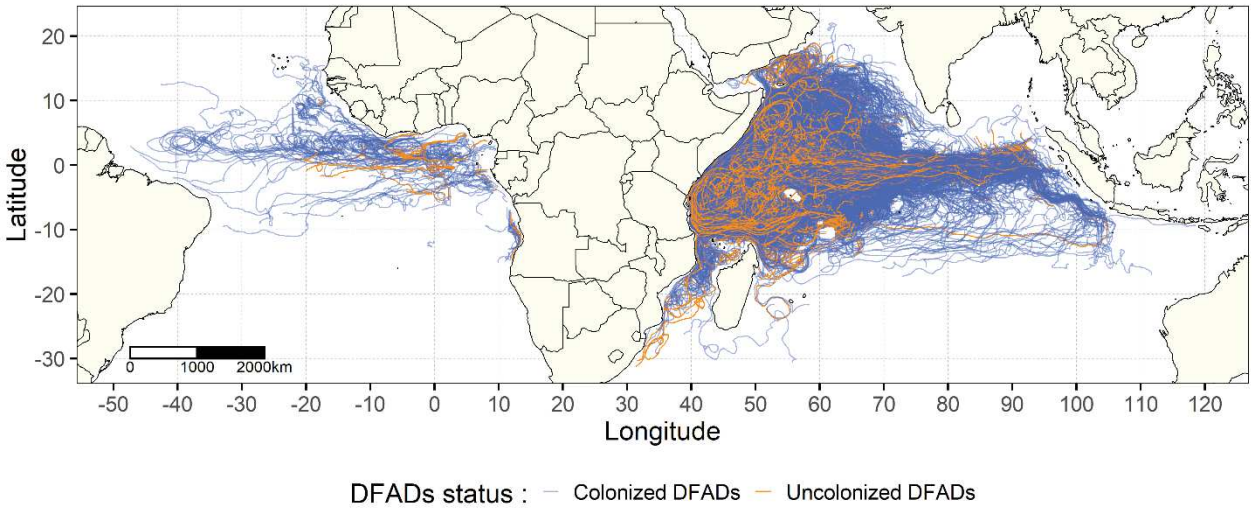

Figure S4.3. Trajectories of newly deployed DFADS monitored in Atlantic and Indian oceans. Colonized FADs (in blue) indicate trajectories where tuna presence has been detected for at least two consecutive days. Uncolonized FADs (in orange) correspond to trajectories where no tuna have been detected.

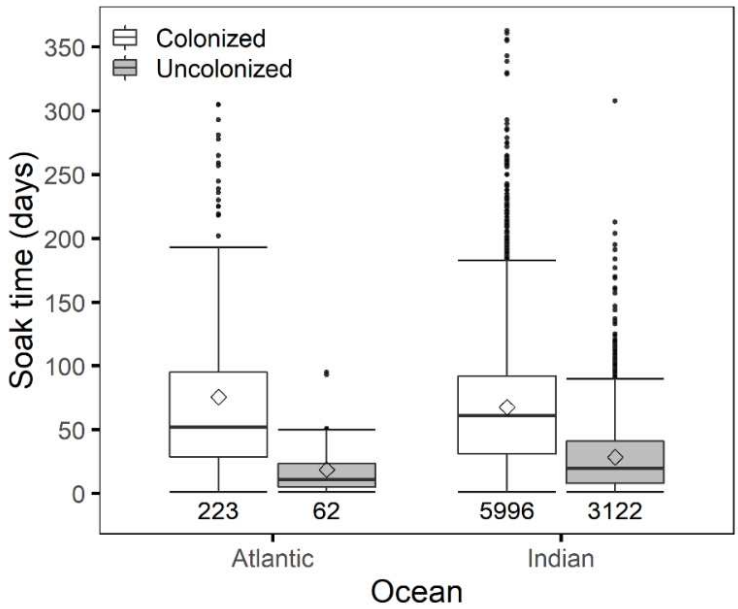

Figure S4.4. Boxplot of the soak times of colonized (white) and uncolonized (grey) DFADs in Atlantic and Indian Oceans. The numeric values and diamonds represent the number of DFADs and the average soak time in each group, respectively.

4. Survival curve fits of FOB-aCAT and Fob-aCRT

The summary of models employed to fit the survival curves of continuous residence (FOB-aCAT) absence times (FOB-aCRT) of aggregation under the floating object as a function of time, is presented in Table S4.2. For all models, the analytical formula for survival curves S(t) was constrained by the normalization condition S(0) = 1. The corresponding q-q plots are presented in Figure S4.5 and Figure S4.6, for FOB-aCAT and FOB-aCART respectively.

Table S4.2. Models used to fit the survival curves of aggregation continuous residence times (FOB-aCRTs) and aggregation continuous absence times (FOB-aCATs) as a function of time, t.

Model type	Analytic formula
Single exponential	$S(t) = e^{(-at)}$
Double exponential	$S(t) = pe^{(-at)} + (1-p)e^{(-bt)}$
Power law	$S(t) = (b/(b+t))^a$

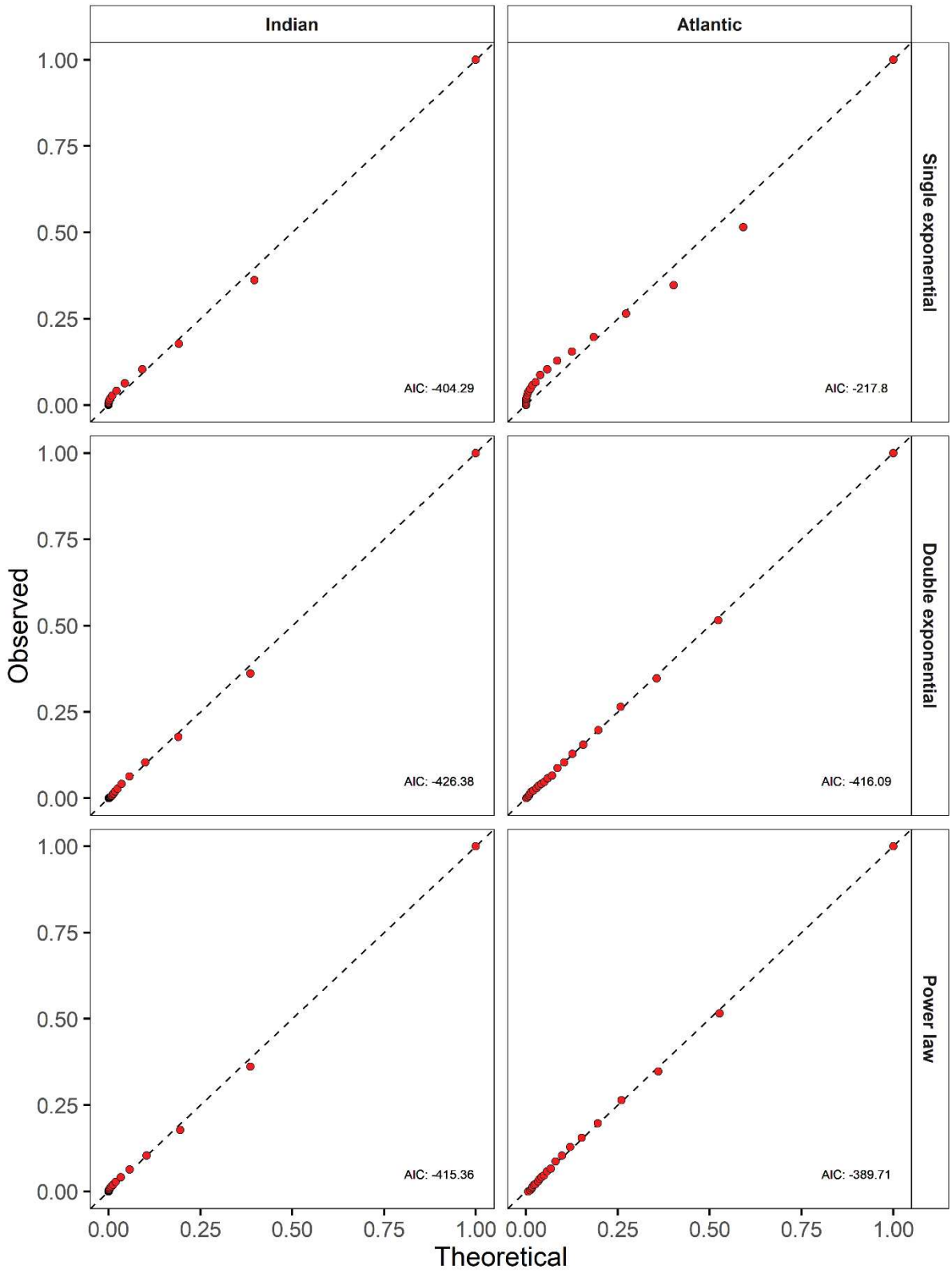

Figure S4.5. Q-Q plots of fits of single exponential, double exponential and power law models of the survival curves of continuous residence times (FOB-aCRTs) for Atlantic and Indian Oceans. AIC denotes for the values of Aikake Information Criterion.

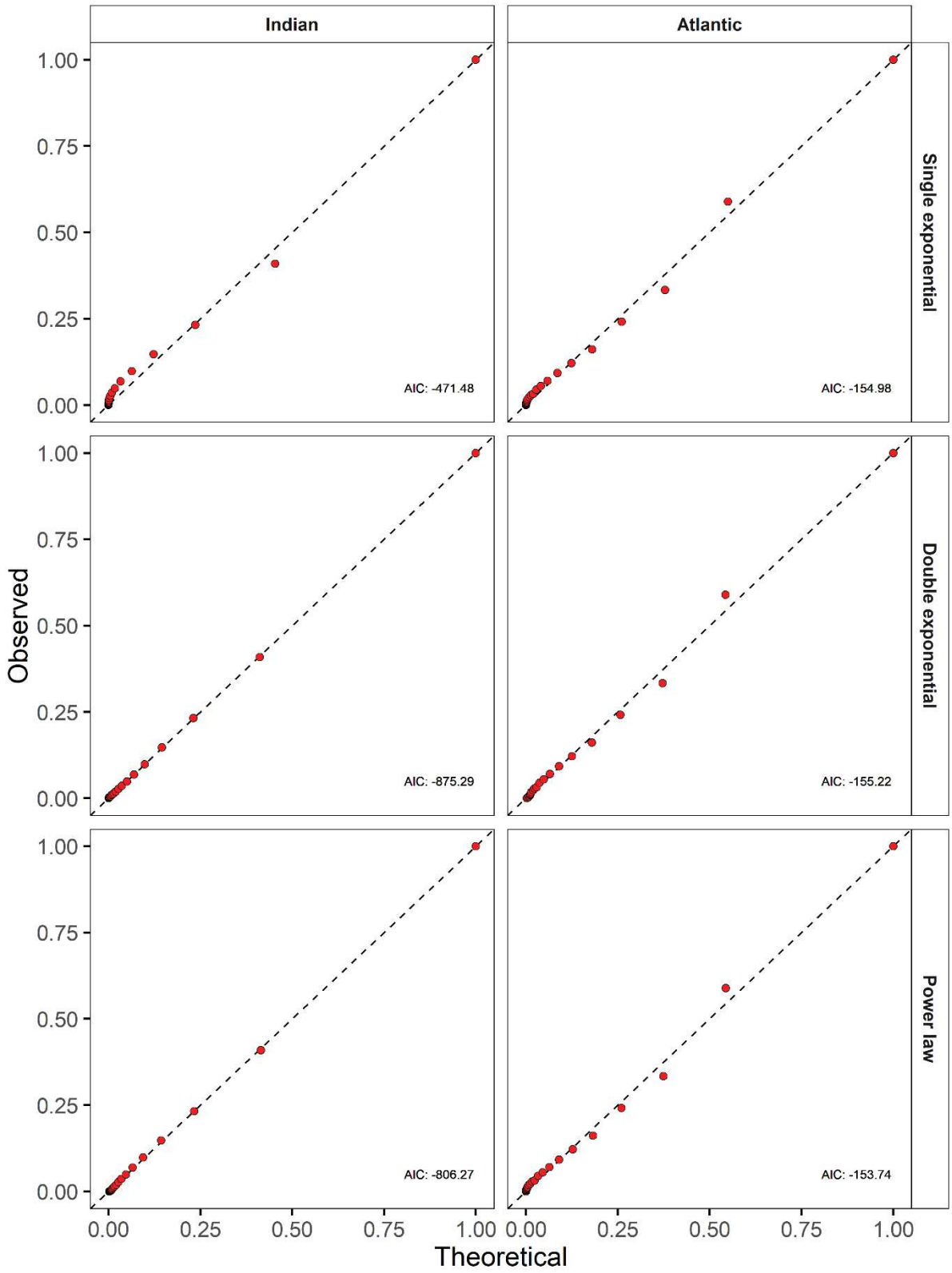

Figure S4.6. Q-Q plots of fits of single exponential, double exponential and power law models of the survival curves of continuous residence times (FOB-aCATs) for Atlantic and Indian Oceans.

5. *Summary of main variables considered by oceans*

The figure S4.7 provides a summary of the main metrics considered for the two oceans.

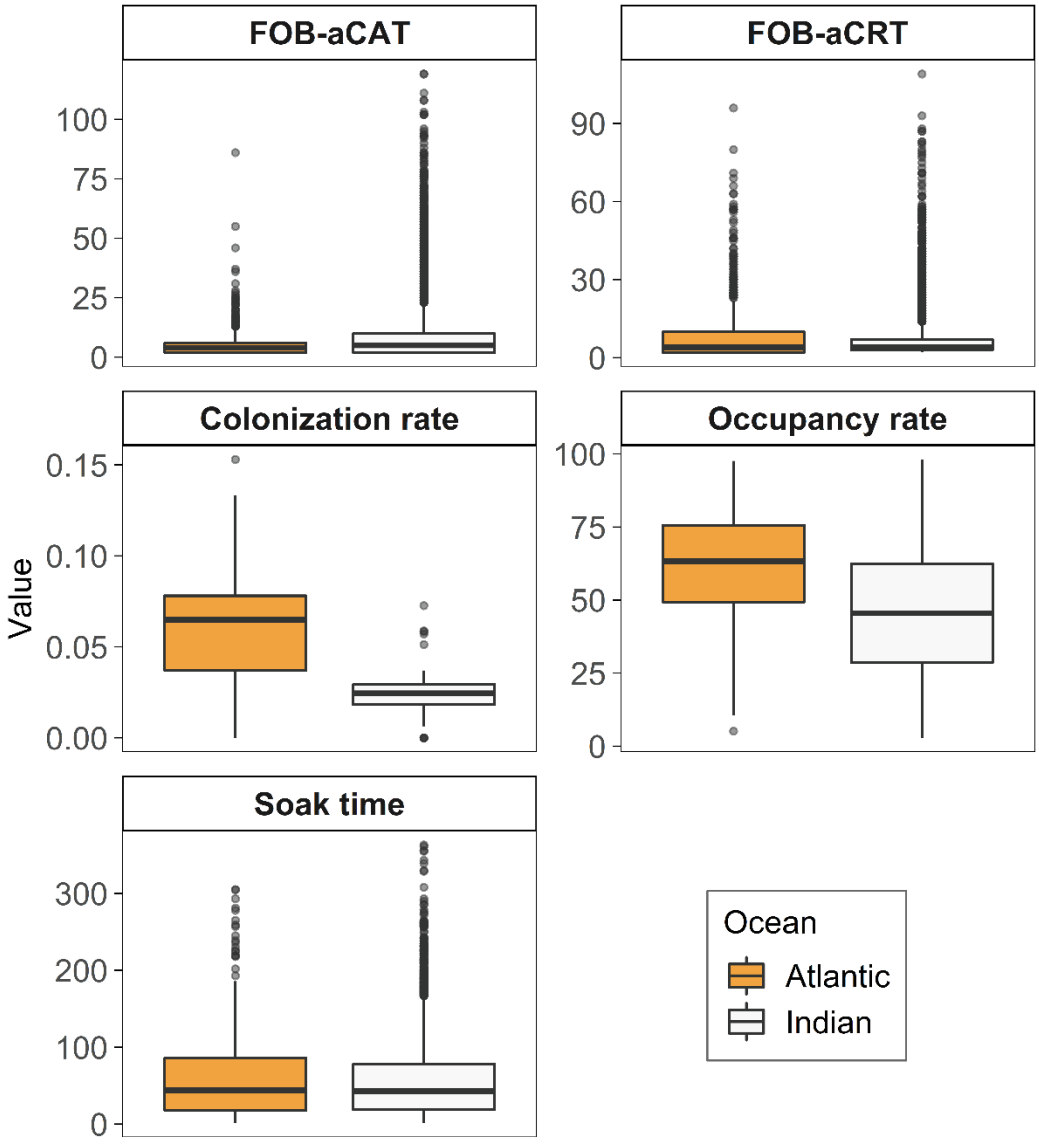

Figure S4.7: Whisker plots of the main metrics assessed between Atlantic and Indian oceans. FOB-aCRT and FOB-aCAT denote for the aggregation's continuous residence time at a floating object and the continuous absence time of aggregation at a floating object, respectively.

Chapter 4

Assessing tropical tuna populations from their associative behaviour with floating objects: A novel abundance index for skipjack tuna (*Katsuwonus pelamis*) in the Western Indian Ocean

"*La natura preferisce le crescite vertiginose o decisamente più morbide, gli esponenti e i logaritmi. La natura è per sua natura non-lineare.*

Nature prefers vertiginous growth, or resolutely softer growths, exponents and logarithms. Nature is by nature non-linear."

Paolo Giordiano

Abstract

We present a novel approach for providing direct abundance estimates of tropical tuna populations based on their associative behaviour with floating objects (FOBs) and acoustic data from fisher's echosounder buoys. This approach accounts for the associated and non-associated components of tropical tuna populations, by combining the residence and absence times of tuna at FOBs with the dynamics of FOBs occupancy by tuna aggregations. We applied this modelling approach on the western Indian Ocean skipjack tuna (*Katsuwonus pelamis*) to provide an abundance index over the period 2013 to 2018. Our results showed that the population estimates made were consistent with total catches for a range of model parameters. This suggests that this direct approach can be considered as an alternative method to the catch-per-unit-effort standardization traditionally used for stock assessment.

Keywords: Tropical tunas, Direct Abundance index, Associative behaviour, Echosounder buoys.

4.1. Introduction

Fish stock assessment is the process designed to study the status of fish stocks, which involves the use of various statistical and mathematical procedures to evaluate the impacts of fishing and to provide quantitative predictions of the potential effects of different management scenarios on fish stocks (Hilborn and Walters, 1992). A key objective of stock assessment is to provide managers with the necessary information on the changes in abundance as a response to fishing (and other factors, e.g. ecosystem and environmental effects) to take decisions to regulate the fisheries and ensure their sustainability. Stock assessment models rely on a conceptual framework consisting of models that describe the demographic processes of the exploited species, from fishery-dependent or independent data sources. One of the main approaches in stock assessment consists in modelling the dynamics of stock biomass, notably by means of abundance indices very often based on catch-per-unit-effort (CPUE) data. This indirect approach relies on a fundamental relationship in fisheries science, which relates CPUE to stock abundance by a catchability coefficient defined as the portion of the stock captured by one unit of effort. Thus, a change in CPUE trends would reflect a shift in the same direction occurring in the target stock, for a constant catchability. However, this approach may be limited by the typical factors associated with fisheries-dependent data, including the variability in catchability resulting from changes in fleet efficiency over time (Bishop, 2006). This is especially apparent in the context of tropical purse seine fishing, where the interpretation of abundance indices based on CPUE is described as notoriously problematic (Fonteneau *et al.*, 1999; Maunder *et al.*, 2006), in particular because catchability is not constant over time and requires complex standardization processes.

In their primary fishing mode, purse seiners mainly targeted free-swimming tuna schools (or associated with dolphins in Eastern Pacific Ocean). Therefore, the time devoted to the searching of tuna schools was traditionally used as a relevant metric to reflect the nominal effort. Over the last three decades, the catchability of tropical tuna species has considerably increased with the continuous implementation of new technologies on board the purse seine fleets (Gaertner and Pallares, 2001; Fonteneau *et al.*, 2013; Torres-Irineo *et al.*, 2014). The development of a purse-seine fishery based on instrumented Drifting Fish Aggregating Devices (DFADs), since the 1990s (Ariz *et al.*, 1992; Hallier and Parajua, 1992), represents one of the most important changes that have contributed to the increase in the efficiency of purse seiners. Drifting fish aggregating devices (DFADs) are man-made floating objects deployed and maintained by

industrial purse seiners to facilitate and improve their catches by taking advantage of the associative behaviour of tropical tuna species around floating objects. DFADs were immediately equipped with tracking technologies as locating these objects was key for fishers. Progressively, acoustic devices providing near-real time and remote information on tuna aggregations underneath them were incorporated to these buoys (Lopez *et al.*, 2014). Due to its non-random nature, DFAD-based fishing raises major issues for traditional purse seine effort metrics as they cannot accurately account for its effects. Indeed, the typical search time no longer reflects the true fishing effort as it does not incorporate the influence of the remote information on DFAD positions and associated biomass. This has the potential to introduce biases in the relationships between the observed catch-per-unit-effort (CPUE) and the true abundance, thus highlighting the critical need for complementary abundance indices to improve stock assessments of the main exploited tropical tuna species.

Currently, most deployed DFADs are equipped with satellite-linked echosounder buoys, which continuously collect data on the fish aggregations associated with the DFADs (Moreno *et al.*, 2019a). These instruments confer to DFADs the status of privileged observation platforms for the marine communities associated with them (Moreno *et al.*, 2016b; Brehmer *et al.*, 2019), and offer the opportunity to assess the abundance of tuna and other associated species from the huge amount of data they provide. Santiago *et al.*, (2019, 2016), proposed a catch-independent abundance index for tuna populations based on acoustic data from echosounder buoys: the Buoy-derived Abundance Index (BAI). The BAI is an indirect abundance index using an assumption similar to that of the CPUE, whereby the tuna abundance is considered proportional to the acoustic signal provided by buoys. The index uses a standardization approach to account for factors that can change the link between the abundance and the acoustic signal (hardware and software differences between buoys models, environmental variability, etc.). Alongside this approach, Capello *et al.,* (2016) have developed a new methodological framework for estimating the abundance of tropical tuna, focused on the analysis of their associative dynamics around floating objects. This approach is based on the measurement of the continuous time that tunas spend associated or not with floating objects, in order to estimate the size of the local populations from which they originate. This approach potentially allows one to estimate the total abundance from any type of data that could be used to monitor tuna behaviour around floating objects (FOB). These data usually derive from scientific experiments using archival, satellite or acoustic tagging techniques. Recent analyses demonstrated that echosounder buoys can also provide reliable information on the associative dynamics of tuna aggregations around

DFADs, likely to be used in this population assessment framework (Baidai *et al.*, 2020a, 2020b). In this work, we combine data on FOB occupancy by tunas obtained through the echosounder buoys with metrics related to the association dynamics of tropical tuna at FOBs, in order to provide a direct abundance index accounting for the associated and the free components of the population of the western Indian Ocean skipjack tuna (*Katsuwonus pelamis*), over the period 2013 – 2018.

4.2. Materials and methods

4.2.1. *Model Definition*

The associative behaviour of tropical tuna population implies that, at any given time, the overall abundance (N) in a given area (S) with p floating objects (or FOBs), results from the sum of the abundances of its free-swimming (X_u) and associated (X_a) components.

$$N(t) = X_a(t) + X_u(t) \tag{4.1}$$

with:

$$X_a(t) = \sum_{i=1}^{p} X_i(t) \tag{4.2}$$

where X_i (t) is the number of fish individuals associated to the FOB i at time t. Following the work by Sempo *et al.*, (2013), the differential equations describing the evolution of X_i through time can be written as following:

$$\frac{dX_i(t)}{dt} = \mu_i X_u(t) - \theta_i X_i(t) \tag{4.3}$$

where, the parameters μ_i and θ_i respectively denote the transition rates (probability per unit of time) from one state to another. μ_i corresponds to the probability per unit time for an unassociated fish to associate with the FOB i, hereinafter referred to as the "*association probability*". θ_i or the "*departure probability*" is the probability per unit time for an associated tuna to leave the FOB i and become unassociated. Given the schooling behaviour of tunas, these parameters can be related both to the behaviour of an individual or to that of the school to which it belongs. Capello *et al.*, (2016) demonstrated that μ_i and θ_i can be inferred from the continuous bout of times that tunas spend unassociated or associated to a FOB, respectively the continuous

absence time (CAT) and continuous residence time (CRT), and that at equilibrium, the total population can therefore be related to its associated component, according to the following equation:

$$N = \frac{CRT + CAT}{CRT} X_a \tag{4.4}$$

On the other hand, considering *m* as the local tuna abundance under an inhabited FOB (i.e., a FOB occupied by tunas), and *f* as the proportion of inhabited FOBs of the system, the associated population can be estimated as follows:

$$X_a = mfp \tag{4.5}$$

Substituting the associated population from (4) with its value from (5), the total population can be expressed as follows:

$$N = \frac{CRT + CAT}{CRT} mfp \tag{4.6}$$

Similarly, from Equation (1) the unassociated (free-swimming) population is expressed from the following relation:

$$X_u = \frac{CAT}{CRT} mfp \tag{4.7}$$

4.2.2. *Application to skipjack tuna in the Indian Ocean*

4.2.2.1. Study area and period

The study area extended between latitudes 20° S and 8° N and covered longitudes located between the African coasts and 80° E. This area concentrated all the skipjack tuna catches of the French purse seine fleet over the period from 2013 to 2018 (Figure 4.1). The study covers the years 2013-2018 where echosounder buoys data are available. Analyses were conducted on a quarterly basis.

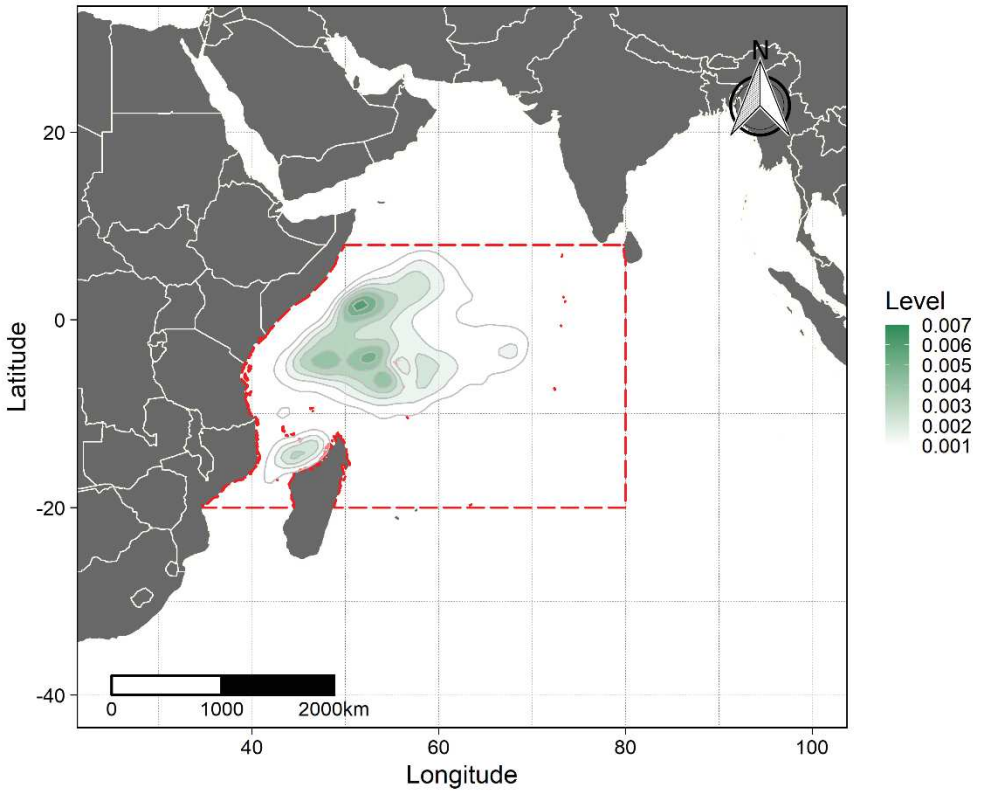

Figure 4.1: Spatial boundaries (red dashed line) of study area zone and kernel density of skipjack tuna catches operated by the French purse seiners on FOBs over the period 2013-2018.

4.2.2.2. Data collection

4.2.2.2.1. *FOB-associated average tuna biomass (m)*

Skipjack catches operated under FOBs in the study area, available from the French purse seine fishery database hosted by the Ob7/IRD ("Observatoire des Ecosystèmes Pélagiques Tropicaux exploités"), and processed using the T3 ("Traitement des Thons Tropicaux") (Duparc *et al.,* 2018), were used to estimate the average skipjack biomass associated with an inhabited FOB (*m*). Table 4.1 resumes the number of available fishing sets on a quarterly basis.

Table 4.1 : Number of fishing sets on FOB per trimester used to estimate the average biomass of skipjack tuna at FOBs.

Year	Quarter	Fishing sets
2013	Q1	370
	Q2	351
	Q3	418
	Q4	524
2014	Q1	368
	Q2	286
	Q3	574
	Q4	520
2015	Q1	213
	Q2	424
	Q3	492
	Q4	635
2016	Q1	547
	Q2	389
	Q3	643
	Q4	686
2017	Q1	591
	Q2	541
	Q3	720
	Q4	715
2018	Q1	897
	Q2	610
	Q3	683
	Q4	681

4.2.2.2.2. *Number of floating objects (p)*

The typology of FOBs considered in this study consists of two main categories: (*i*) the DFAD (*ii*) and the other objects. The DFAD category corresponds to man-made FOBs specifically designed to encourage fish aggregation, while the "other" category includes natural drifting objects (VNLOG and ANLOG) and anthropogenic debris (FALOG, and HALOG), as described in Gaertner *et al.* (2016). In terms of data collection, assessing the number of floating objects (*p*) corresponds to one of the main challenges faced by this approach. Indeed, there is still a limited knowledge about the precise number of FOBs at water, especially because the total number of DFADs operated by the tuna purse seine fleets is still considered as a sensitive information. In an attempt to obtain approximated time series of the total number of FOBs in

the study area, we considered the buoy position data available in the Marine Instruments buoys[11] database hosted by the Ob7/IRD. The dataset corresponds to all the position data collected by buoys equipping the DFADs operated by the French purse-seiner fleet. This information constitutes a reliable estimate of the number of DFADs used by the French tuna purse-seiners, since almost all of the DFADs deployed by this fleet were equipped with one of the buoy models from this brand. To provide an estimate of the total number of DFADs, the ratio between the number of buoys used by the Spanish and French vessels (the two main fleets in the study area) provided from 2010 to the end of 2017, by Katara et *al.,* (2018) was considered. The missing ratio for the year 2018 was estimated using the average ratio over the year 2017. This was based on the assumption of a relative stabilization in the exploitation of buoys between the different fleets during this period (namely due to the limitation measures on the number of buoys operated by tuna purse seiners in the Indian Ocean: Resolutions 15/08 and 17/08). The "Other" category was estimated from the proportions of DFAD observed relative to the total number of FOBs reported by observers on board French tuna seiners during the same period. The observer data were collected under the EU Data Collection Framework (DCF) and the French OCUP program (Observateur Commun Unique et Permanent), with an overall average coverage rate of about 50% over the years 2013 to 2017 (Goujon *et al.*, 2017). Finally, the time series of the number of FOBs over the years 2013 – 2018 were derived as the sum of the estimated number of French and Spanish DFADs and the amount of natural and artificial logs.

4.2.2.2.3. *Proportion of inhabited FOBs (f)*

Proportion of inhabited FOBs were derived from data collected by the M3I echosounder buoys from the Marine Instruments database. This buoy model is equipped with an echosounder device (frequency 50 kHz, power 500 W, beam angle of 36°), which provides acoustic information on the underneath biomass associated to DFADs. These data, which represent the largest amount of acoustic data available in the Marine Instruments database over the study period, were processed in presence or absence of tuna aggregation, using a machine learning algorithm (Baidai *et al.*, 2020a). Proportion of inhabited FOBs were then expressed as the number of DFADs classified as inhabited by a tuna aggregation, divided by the total number of

[11] Marine Instruments, Nigrán, Spain, www.marineinstruments.es

DFADs at a daily scale. Quarterly averages were then calculated. Table 4.2 resumes the number of available M3I buoys on a quarterly basis.

Table 4.2: Average number of daily M3I buoys in the study region per quarter.

Year	Quarter	M3I Buoy Count
2013	Q1	494
	Q2	518
	Q3	549
	Q4	505
2014	Q1	459
	Q2	581
	Q3	594
	Q4	840
2015	Q1	850
	Q2	1287
	Q3	1572
	Q4	1764
2016	Q1	2005
	Q2	2236
	Q3	2013
	Q4	2524
2017	Q1	2885
	Q2	2425
	Q3	2494
	Q4	2449
2018	Q1	2456
	Q2	2493
	Q3	2370
	Q4	2545

4.2.2.2.4. *Continuous Residence time of skipjack tuna (CRT)*

Continuous residence times (CRT) of skipjack tuna individuals have been documented in the three oceans, on both anchored and drifting FADs (see Table 4.3). The studies showed that skipjack tuna remained associated with a floating object for an average of 1 to 9 days. In the Indian Ocean, acoustic tagging experiments carried out by Govinden *et al.*, (2010), around drifting FADs revealed that on average, the skipjack CRT around a DFAD is 4.6 days. This average value was considered in this study.

Table 4.3: Summary of main findings from previous studies on skipjack tuna individual CRT assessed under anchored and drifting FADs (FL: Fork length).

FAD type	Studies	Study location	FL (cm)	Findings
Drifting	Dagorn *et al.*, (2007)	Western Indian Ocean	*Not provided*	Average at 0.91 days (maximum: 7.03 days)
	Govinden e*t al.,* (2010)	Mozambique Chanel, (Western Indian Ocean)	47 – 57	Between 0.09 – 18.33 days with median at 4.47days and average at 4.58 days
	Matsumoto *et al.,* (2014)	Equatorial central Pacific Ocean	36 – 65	From 0.0 to 6.4 days (with average value at 2.3 days)
	Matsumoto e*t al,.* (2016)	Equatorial central Pacific Ocean	34 – 65	Less than 7 days
	Scutt *et al.*, (2019)	Western Central Pacific Ocean	46 – 60	Median at 1 day (maximum: 18 days)
	Tolotti *et al.*, (2020)	Eastern Atlantic Ocean	39 – 61	Average of 9.19 days (maximum value to 15 days)
Anchored	Govinden *et al*., (2013)	Maldives Islands (Indian Ocean)	37 – 54	Between 0.20 – 3.75 days
	Rodriguez-Tress *et al*., (2017)	Mauritius Islands (Indian Ocean)	41 - 59	2.5 days (average value)

4.2.2.2.5. *Continuous absence times (CAT)*

At the time of the study, no direct measurement of skipjack CATs has yet been carried out in the study area, mainly due to the complexity of the experimental protocol to be implemented. However, considering that the encounter of a FOB by a tuna is more likely for higher FOB densities, this implies decreasing CATs for increasing numbers of FOBs (Rodriguez-Tress *et al.*, 2017). Based on these arguments, the CAT was related to the number of FOBs according to the following ansatz:

$$CAT = \frac{1}{\phi p} \tag{4.8}$$

Where ϕ is a parameter that relates the number of FOBs in the system to the CAT. A detailed section on the significance and plausible magnitude order of ϕ is provided on Supplementary information S7 of this chapter. Time series of CAT were thus derived from Equation (4.8), considering the number of FOBs (estimated following the procedure described at section 4.2.2.2.2), and different values for ϕ ranging between 2e-6 and 1.

4.2.2.3. Abundance estimates from field data

The associated skipjack population (X_a) was assessed using Equation (4.5), considering, for each quarter, the values of *m, f, p* and *CRT* obtained from field data. By substituting the definition of CAT from Equation (4.8) into the Equation (4.7), the free-swimming population (X_u) can be expressed through the following relationship:

$$X_u = \frac{mf}{\phi CRT} \tag{4.9}$$

The Equation (4.1) was then used to perform assessments of the abundance of the total skipjack tuna population (N). In addition, the sensitivity of N and X_u were tested with respect to the different values of ϕ considered, and the consistency of the quarterly abundances of the total population obtained was analysed with respect to the total nominal catches made in the same time period and area. Finally, the relative trends of the different abundance indices are also presented using the first quarter of year 2013 as a reference.

4.3. Results

4.3.1. *Time series of proportion of inhabited FOBs (f) and FOB-associated biomass (m)*

The proportion of inhabited FOBs exhibits a relative stability over time, with an average around 0.45 (SE 0.01) over the whole study period (Figure 4.2). This stable trend, especially marked from mid-2015 onwards, contrasts with the gradual increase in the skipjack catches at FOBs, here considered as a proxy of the associated skipjack biomass observed during the same period (Figure 4.3).

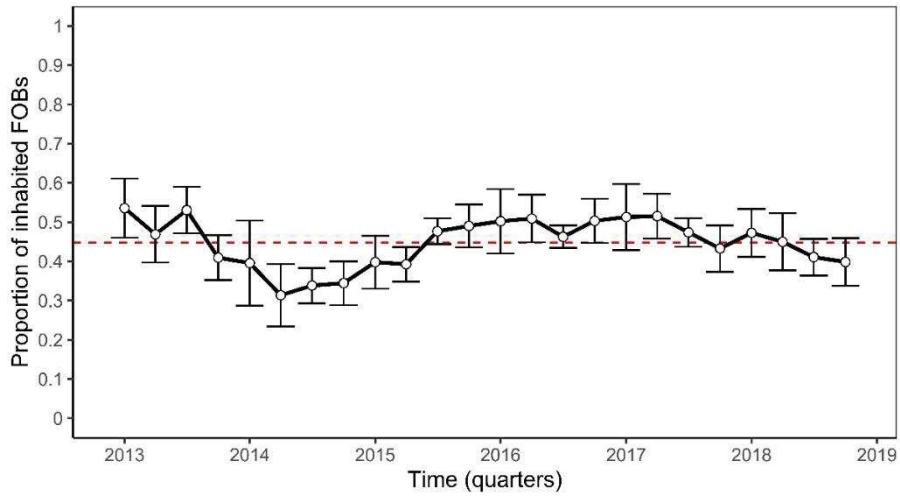

Figure 4.2: Time series of the average daily proportion of FOBs inhabited by tuna aggregations in the study area over 2013-2018. The red dashed line represents the average proportion of inhabited FOBs over 2013-2018.

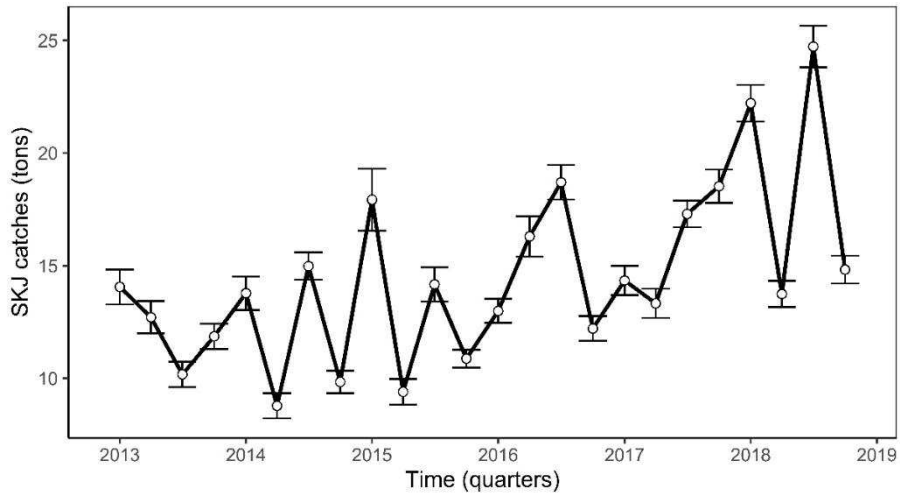

Figure 4.3: Time series of the average skipjack tuna catches at FOBs in the study area over 2013 – 2018.

4.3.2. *Time series of the estimated number of FOBs (p)*

The evolution of the number of FOBs revealed that DFADs constitute the main driver of FOB density in the study area, given the relative low percentage of "other" floating objects over time (Figure 4.4). Two main trends emerge: (*i*) the period before 2015 characterized by a steady increase in the number of FOBs, and (*ii*) the period after 2015 with a plateau about 11,000 FOBs (Figure 4.5).

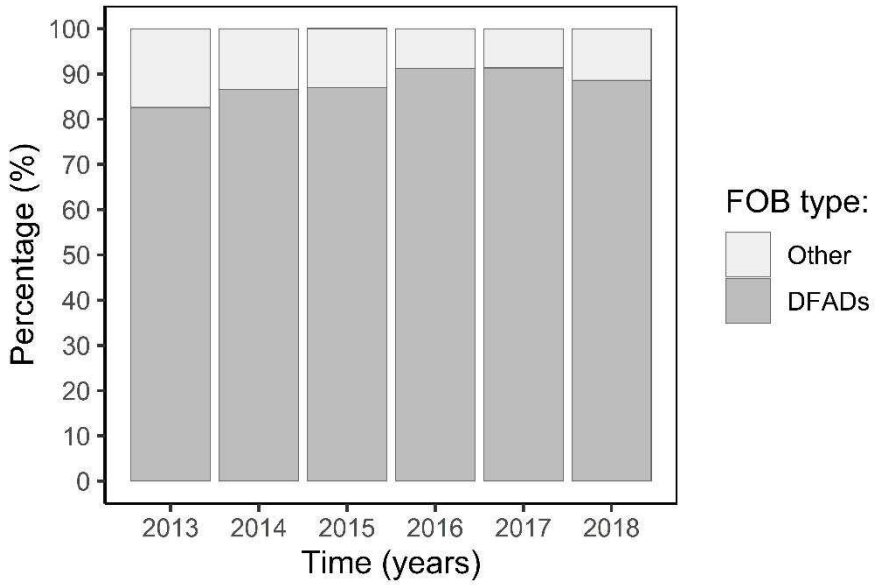

Figure 4.4: Proportions of drifting fish aggregating devices (DFADs) and other types of natural and artificial objects (Other) reported by observers on board French tuna seiners.

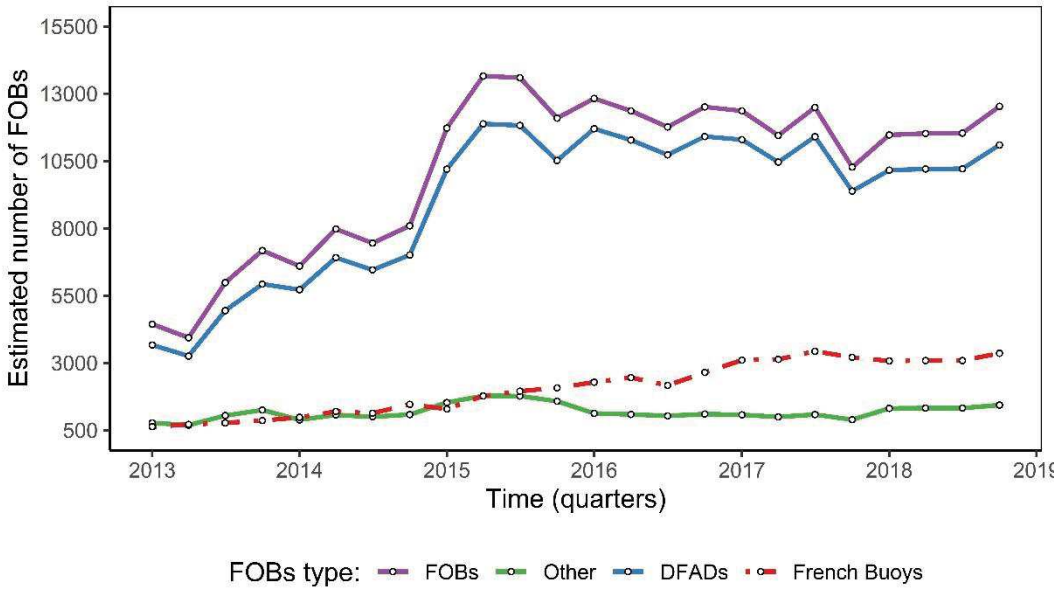

Figure 4.5: Temporal evolution of the number of active French buoys (French FOBs equipped with buoys), the estimated numbers of drifting fish aggregating devices (DFADs) and others objects (Other), and the estimated total number of floating objects (FOBs) in the study area (FOBs = DFADs + Other).

4.3.3. *Time series of continuous absence time (CAT)*

The CAT time series (Figure 4.6) estimated using Equation (4.8) reveal that for higher values of ϕ ($\phi \geq$ 2e-5); skipjack individuals would spend very short durations in the non-associated state during the study period (between 5 days and less than 1 day on average). Lower values of ϕ provide larger values of CAT, characterized by temporal trends that sharply decrease over time as the number of FOBs increases, and stabilize after 2015 at about 17, 28 and 41 days for ϕ values of 5e-6, 3e-6 and 2e-6 respectively.

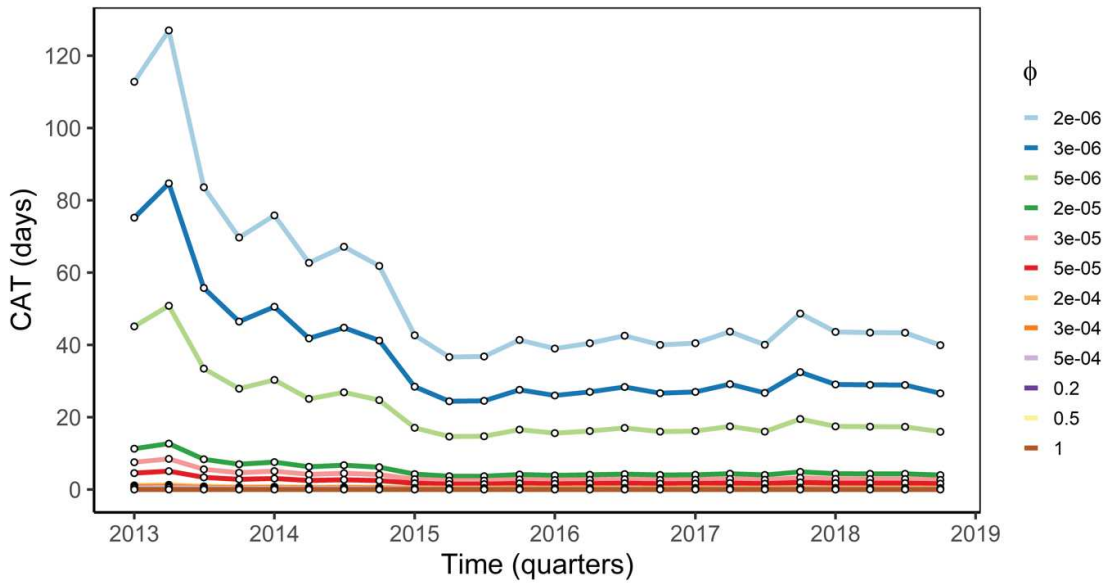

Figure 4.6: Average CATs estimated for different values of ϕ.

4.3.4. *Abundance indices of the skipjack tuna population*

The evolution of the associated population obtained from Equation (4.5) follows a similar trend to that of the number of FOBs, with the typical trends observed before and after 2015 (Figure 4.7A). However, from 2017 onwards, the increase in the associated population tends to be less marked and more irregular, with a relative minimum during the second quarter of 2018.

Although the general trends in the free-swimming population obtained from Equation (4.9) do not really change for the ϕ values comprised between 2e-6 and 5e-6, their order of magnitude is nevertheless highly dependent on this parameter (Figure 4.7B). The unassociated population showed an initial decrease, in line with the fast increase in the number of FOBs and the

associated population at the beginning of the time series, followed by a relative stabilization since 2016.

The sensitivity analysis of the total population abundance with respect to ϕ shows that the values of this parameter comprised between 2e-6 and 5e-6 provide absolute values of the total skipjack tuna population consistent with the total catches of this species reported in the study area (Figure 4.7C). Considering the lowest ϕ value used (2e-6), the total skipjack biomass in the western Indian Ocean ranged from the minimum value of 0.3 million tons in the second quarter of 2014 to 1.3 million tons in early 2018.

The relative indices produced for values of ϕ between 2e-6 and 5e-6 reveal that during 2014 the abundance of the total skipjack population rapidly declined to values more than half those of the reference year. The year 2015 was characterized by a steady increase in the total skipjack population, which appears to be stabilizing around the reference threshold since 2018 (Figure 4.8). In addition, the trends in the relative abundance of the total population appear to be insensitive to the ϕ values considered in the range of ϕ values between 2e-6 and 5e-6.

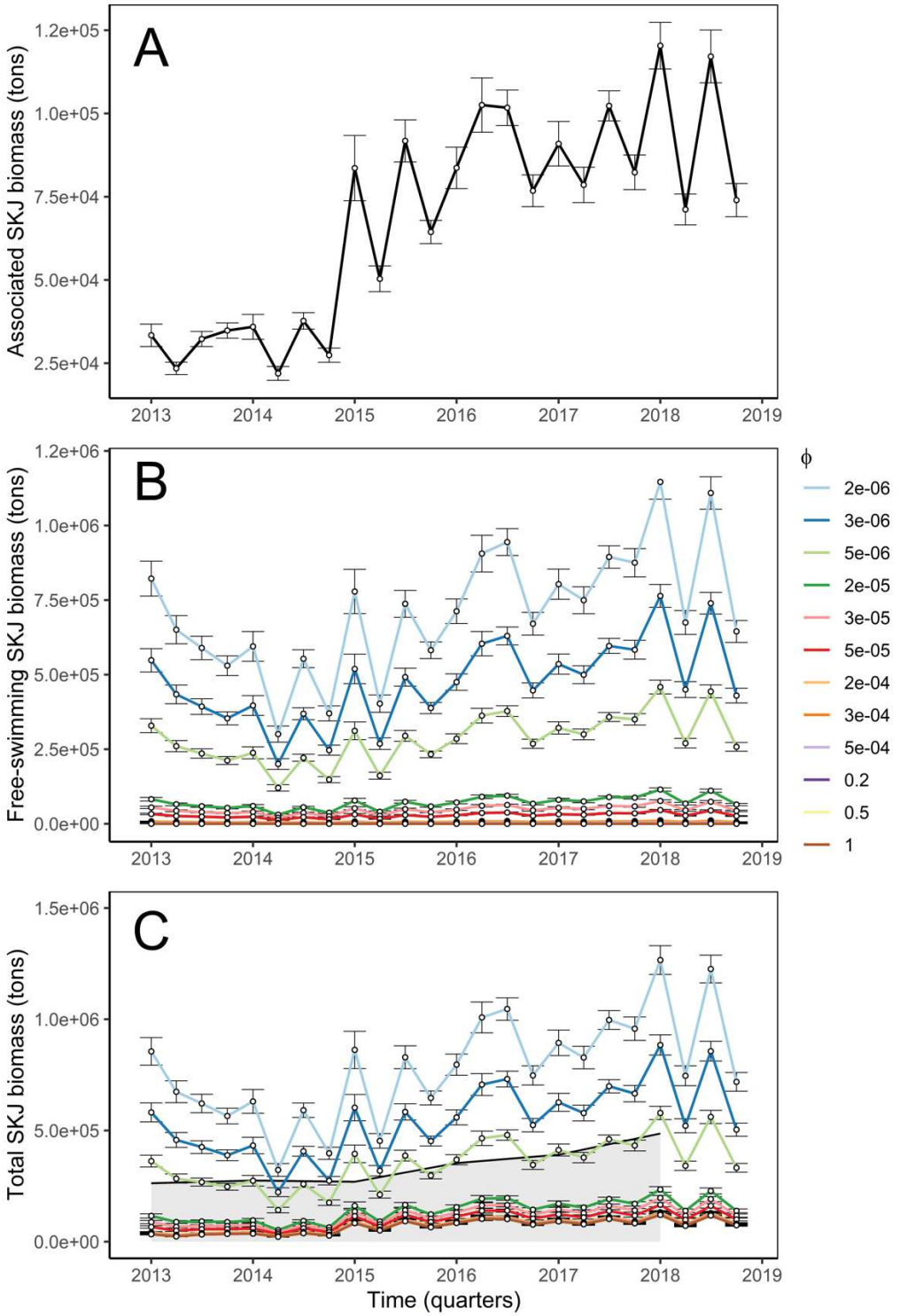

Figure 4.7: Time series of the absolute abundances of associated (panel A), unassociated (panel B) and total skipjack population (panel C) under different values of ϕ. The shaded area corresponds to values below the nominal catch data used for stock assessment of skipjack tuna[12], in the western Indian Ocean (IOTC area delimited by African and Asian shorelines, to the south by latitude 45°, and to the east and west by longitudes 20°E and 80°E, respectively), during 2013-2018.

[12] The IOTC nominal catch datasets used and related details are publicly available at the following address https://www.iotc.org/WPTT/22DP/Data/03-NC

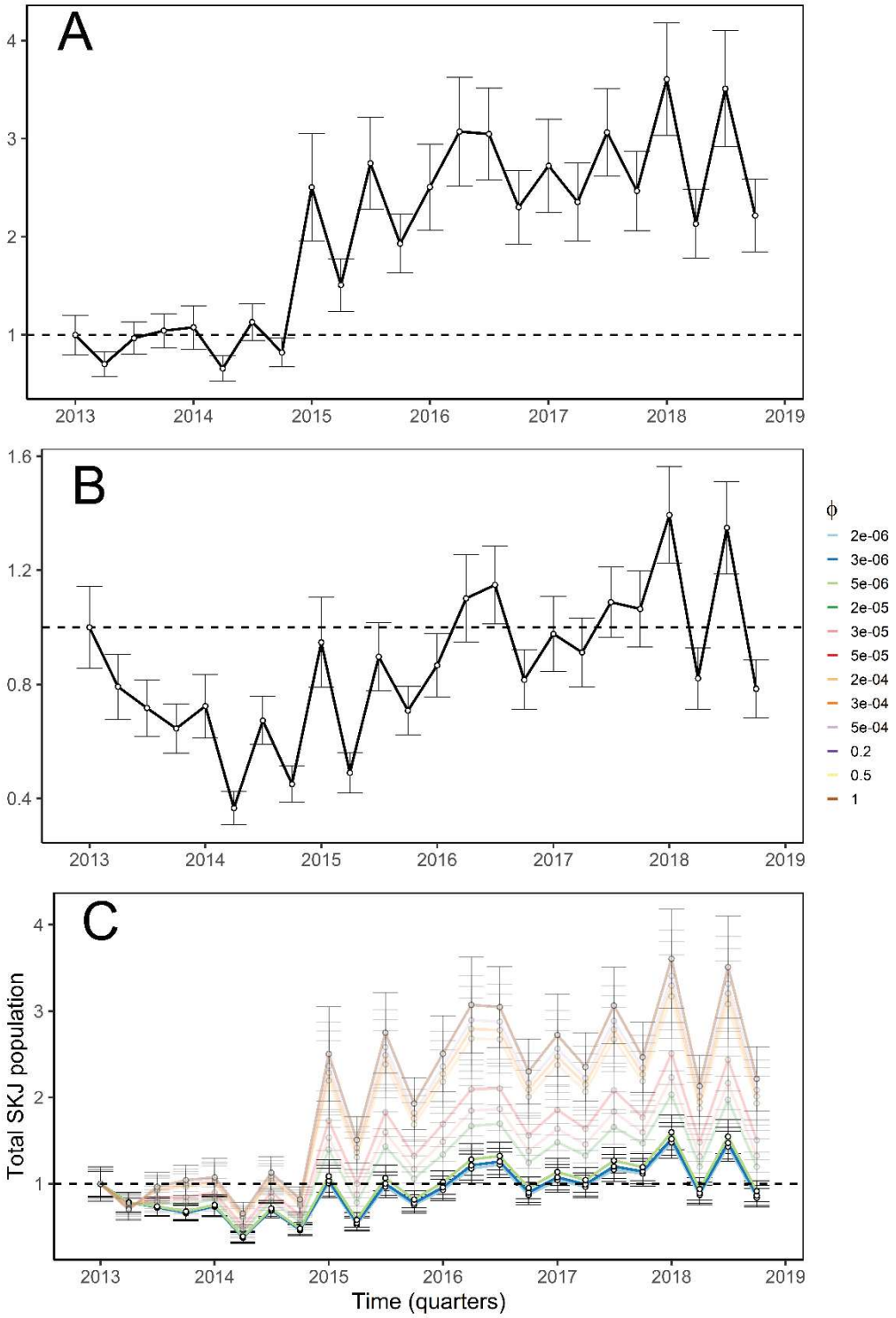

Figure 4.8: Evolution of relative abundance of associated (panel A), unassociated (panel B) and total skipjack population (panel C), compared to the first quarter of 2013, under different values of ϕ. The low opacity curves correspond to the ϕvalues that were found to be inconsistent with the total catches diagnostics.

4.4. Discussion

We propose a new approach, which can provide absolute abundance indices of tropical tuna populations, from a set of descriptive metrics of their associative behaviour around floating objects (namely residence and absence times) and the occupancy rate of these objects by tuna aggregations. Using tuna behavioural data collected through electronic tagging technologies, and the massive amount of DFAD monitoring data flowing from echosounder buoys of tuna purse seine fleets, the approach has the ability to take into account the different components of the tuna population (free-swimming tuna and associated tuna).

Although based on the associative behaviour of species, this method remains relatively independent of the understanding of the causative factors underlying this behaviour (Capello *et al.*, 2016). Indeed, an individual is here assimilated to a "computational unit" integrating different environmental and biological factors, and yielding as outputs the observables used as input data in the approach. The method also relies on the ability of monitoring the occupancy of floating objects by the tuna species. This is achieved by exploiting the acoustic data from echosounder buoys, but currently without the ability to discriminate between tuna species in the multi-species aggregation under the object. Besides this aspect, another major issue associated with the use of acoustic data from buoys to assess the occupancy of floating objects is related to the biomass threshold at which buoys are able to detect the presence of a tuna aggregation. Large detection thresholds are likely to significantly underestimate the abundance estimates derived from the modelling approach. Complementary simulations studies would be useful to properly assess the biases related to this buoy technical limitation on the abundance index. In the case of the buoy model used in this study, this threshold is assumed to be about 1 ton (Baidai *et al.*, 2020a). As fishing operations are very rarely carried out on DFADs with less than 1 ton of associated biomass, the presence of this detection threshold has nevertheless made it possible to ensure consistency between the dataset of FAD occupancy (f) and that of their associated biomass (m) estimated from catch data. Furthermore, since their introduction in the tropical purse seine fishery, buoy technology has constantly been evolving (Lopez *et al.*, 2014). It can therefore be expected that current buoy models, which provide relatively poor estimates of associated biomass (Baidai *et al.*, 2020a), will evolve towards models with better detection and estimation performances.

Using behavioural analyses or site occupancy patterns to predict species abundance is not a new idea. For a wide range of species, several statistical and mathematical models have been used

to relate the presence/absence at occupancy sites to the abundance (He and Gaston, 2000a, 2000b; He *et al.*, 2002; Warren *et al.*, 2003; MacKenzie and Nichols, 2004; Hui *et al.*, 2009). On the other hand, Dell and Hobday, (2008) have developed an approach relying on the use of schooling behaviour metrics to infer the population size of southern bluefin tuna, following the hypothesis that homogeneity in school structure would reflect the status of a tuna population (the more individuals of similar size, the larger are populations). Our approach is nevertheless the first, which melds behavioural ecology data with occupancy rate to provide insights on the population dynamics of tropical tuna species.

The approach is fairly generalizable to all populations of species exhibiting associative behaviour around aggregating points, although some of its unique characteristics may look limiting to some extent. Indeed, the approach requires the fulfilment of a number of key conditions for its application. The most important concerns the equilibrium condition which defines the state of the system where the state variables (namely here the proportions of inhabited points and associated animals) no longer vary over time. In the case of skipjack tuna considered in this study, fulfilment of the equilibrium condition was evaluated by analysing the stationarity of the time series of the proportion of inhabited FOBs on the quarterly time scale considered (see Supplementary information S5). This time scale was chosen in accordance with the usual time strata used for stock assessments in the Indian Ocean. However, for this approach, the correct determination of the time strata should rather have resulted from the analysis of the stationarity of the system, which would have identified the adequate time periods for the application of the model, validating the equilibrium condition. This includes that the length of these periods could vary over time, depending on the dynamics of the system observed. Although, the stock assessment time scale was fortunately found to be relatively suitable for the skipjack population in this case study, it is likely to be problematic for the implementation of this modelling approach to other species.

In addition, the approach needs accurate estimates of the local absolute abundance around the aggregating points. Depending on the cases, these estimates may be potentially biased by the characteristics and sampling strategies used. For skipjack tuna, information on the biomass around the FOBs was collected from FOB-associated purse seine catches, with nevertheless the potential risk that purse seiners only target FOBs with "higher productivity" (FOBs with largest biomasses), which would have led to a biased estimator of the average population around the FOBs. Due to the paucity of information on this aspect of fishing strategy of purse seiners, the likelihood of disparities in the aggregative characteristics of FOBs was assessed by examining

the occupancy rate of FOBs by tuna aggregations (namely the overall proportion of time they are occupied by tunas). The analysis was based on the principle that FOBs with higher aggregative/attractive properties (i.e. those aggregating the highest biomasses), should theoretically host tuna aggregations more often and longer than others. This would result in a multimodal distributions of the FOB occupancy rates by tunas (with different modes for each type of FOBs). The analysis did not provide clear evidences of a significant heterogeneity between FOBs characteristics (see Supplementary information S6). Therefore, it was concluded that the purse seine catch data under FOBs could be considered as an unbiased estimator as it could not be proven that some FOBs would aggregate more fish than others would.

The hypothesis of a single associative behavioural response of individuals raised by the approach is also of concern. In this work, the residence time of skipjack tuna under a FOB (CRT) was assumed constant. However, some authors have evidenced that the CRT may significantly vary depending on the individual size (Ohta and Kakuma, 2005; Robert *et al.*, 2012), or due to variability of the local conditions around FOBs (Robert *et al.*, 2013a). A more recent study has also evidenced that increasing FOB densities could potentially result in an increase of CRTs (Pérez *et al.*, 2020). In addition, the occurrence of a turn-over process of tuna schools under FOBs (Weng *et al.*, 2013; Baidai *et al.*, 2020a), or the meeting point hypothesis (Fréon and Dagorn, 2000) suggest that tuna individuals may switch from one school to another under FOBs. Thus, CRTs may also vary due to social interactions between tunas. This aspect should also be clearly analysed with regard to its impacts on the abundance estimates. However, as demonstrated by Capello *et al.* 2016, the modelling framework supporting our indices shows high robustness for a heterogeneous system with variable CRTs. In addition, from the wide range of studies on CRT of tuna individuals, it appears that this metric has a relatively small range of variation, with values from one to about ten days, the highest average value measured for skipjack tuna (see Table 4.3). The low variability of CRTs is also suggested by the analytical estimates of the average CRTs of individuals under each FOB, from FOB occupancy metrics, presented in Supplementary information S8. In a general way, the development of specific electronic tagging programs would be essential to clearly assess the influence of the various factors (e.g. space, time and individual-size and social interaction) on the variability of this metric.

Data collection represented one of the major challenges of this approach. For example, although the technology exists to allow the measurement of the continuous absence time of tuna (*CAT*), this metric has so far received very little attention and there is currently a critical lack of

information on this essential data to understand the associative behaviour of tuna (Dagorn *et al.*, 2007c; Robert *et al.*, 2012, 2013b; Rodriguez-Tress *et al.*, 2017). This limitation was overcome by a conjecture on an inverse proportionality relationship between the CAT and the number of FOBs through the parameter of ϕ. Although, the plausible order of magnitude of this parameter has been estimated both empirically and analytically (see Supplementary information S7), uncertainties remained on its actual value. On the other hand, the contribution of analytical methods could be of great interest in improving knowledge on CATs. Indeed, previous studies demonstrated that tunas perform a random walk between two FOB associations and show an oriented movement only within an average radius of 10 km from a FOB (Girard *et al.*, 2004). Therefore, the encounter and association of a tuna with a drifting FOB can be roughly modelled as the encounter of two random walkers separated at their initial position by a distance equal to the average distance between FOBs (assuming that a tuna leaves one FOB for another). A precise knowledge of the fine-scale spatial distribution of floating objects at sea could thus make possible to derive the range of values of CAT and association probability.

Unfortunately, the availability of data on FOBs represented a major limitation encountered in this study. DFADs actually constituted the most important category of FOBs, as indicated by the work from Dagorn *et al.*, (2013b), and corroborated by the results from this study (see Figure 4.5). Currently almost all of them are equipped with satellite linked echosounder buoys (Lopez *et al.*, 2014; Moreno *et al.*, 2019a), whose geolocation data could allow to reconstruct densities of floating objects at fine spatial and temporal scales. However, availability of these data still remain problematic, and relatively limited depending on fleets, companies or buoy manufacturers (Moniz and Herrera, 2019; Grande *et al.*, 2020).

Nevertheless, these different issues do not detract from the potential of this new alternative for assessing abundance of tropical tuna species and especially skipjack tuna, whose stocks are notoriously difficult to assess. Due to their high and variable productivity, (i.e. annual recruitment is a large proportion of total biomass), detecting the effect of fishing on the skipjack population with standard fisheries data and stock assessment methods is particularly difficult (Maunder and Deriso, 2007; De Bruyn and Murua, 2011). Moreover, skipjack catches mainly derive from DFAD-based fishing from purse-seiners (ISSF, 2019). This raises several uncertainties concerning abundance indices derived from catch-per-unit of effort (CPUE) of purse seine fisheries, given the inherent complexity in identifying an adequate unit effort for the purse seine fleet (Fonteneau *et al.*, 1999). This work provides an abundance assessment

method independent of effort data, and particularly adapted to skipjack populations, as this species constitutes the predominant tuna species associated with floating objects (Dagorn *et al.*, 2013a). Despite the relatively short length of the available time series, our findings indicate that the massive increase in the use of DFADs by tuna seiners before 2015 (see Figure 4.5 and Maufroy *et al.*, 2017), may have led to a significant shift from the free-swimming state towards the associated one. The resulting increase in catchability is likely to constitute a consistent explanation for the gradual decline in total population size observed over this period. The abundance of skipjack increased after 2015 and then stabilized. This trend coincides with the first management plans for DFADs in the Indian Ocean, especially the limitations of the number of DFADs used per vessel from 2015 (IOTC Resolution 15/08 and 17/08). These limitations could be thought as one one of the factors driving the abundance trend observed from this period onwards. However, it is worth to note that they did not actually contribute to reduce the number of total DFADs in the water. Hence, the main drivers of skipjack abundance should be sought in terms of environmental conditions or biological and fisheries characteristics of skipjack.

Finally, the new abundance indices presented in this work illustrate the important contribution that echosounder buoys and electronic tagging data can make to improving stock assessments of tropical tuna. To date, the collection of these data is mainly carried out either to enhance general knowledge on the ecology of tuna species (behavioural metrics) or for regulatory purposes (number of DFADs). The possibility of deriving from these data, abundance indices independent of catch-per-unit-effort data, could certainly be a powerful driver for tuna RFMOs to gather funds dedicated to the development of electronic data collection programs.

Acknowledgements

This project was co-funded by the ANR project BLUEMED (ANR-14-ACHN-0002) and "Observatoire des Ecosystèmes Pélagiques Tropicaux exploités" (Ob7) from IRD/MARBEC. The authors are grateful to ORTHONGEL and its contracting parties (CFTO, SAPMER, SAUPIQUET) for providing the echosounder buoys data. The authors also thank all the skippers who gave time to share their experience and knowledge on the echosounder buoys. The authors sincerely thank the contribution of the staff of the Ob7 on the fishery data and the databases of the echosounder buoys. We are also deeply grateful to the buoy manufacturers for their useful advice and information on their echosounder buoys.

Supplementary information S5

Validation of the equilibrium condition

1. Context

The system's equilibrium represents the core assumption for estimating abundance of tuna from the dynamics of their associative behaviour. At equilibrium, the amount of populations joining FOBs is assumed equal to the amount that leaves the FOBs (S5.1). For each FOB *i*, this leads:

$$\mu_i X_u(t) - \theta_i X_i(t) = 0 \qquad (S5.1)$$

Similarly, the amount of FOBs that become inhabited by tunas remains equal to the number of FOBs that are emptied as shown in the following equation:

$$\nu(p - p_a(t)) - \eta p_a(t) = 0 \qquad (S5.2)$$

where p_a and p denote the number of inhabited FOBs and the total number of FOBs respectively; ν represents the probability per unit of time (transition rate) for an empty FOB to become occupied by a tuna aggregation, and η is the rate at which an occupied FOB becomes empty. Following a similar reasoning to that of Capello *et al.,* (2016) on the relationship between association and departure probabilities and CATs and CRTs; ν and η can be inferred from the *continuous absence time of aggregation at a floating object* (FOB-aCAT or aCAT), and the continuous time during which a FOB hosts a tuna aggregation or *aggregation's continuous residence time at a floating object* (FOB-aCRT or aCRT). Since, the survival curves of aCATs and aCRTs follows a time-independent process (Baidai et *al.*, 2020b), we can write:

$$\nu = \frac{1}{aCAT} \qquad (S5.3)$$

and

$$\eta = \frac{1}{aCRT} \qquad (S5.4)$$

This implies that at equilibrium, the proportion of FOB inhabited by tunas should remain stationary over time and follow the below relationship:

$$f = \frac{p_a}{p} = \frac{aCRT}{aCAT + aCRT} \qquad (S5.5)$$

2. Methodology

The quarterly averages of aCRTs and aCATs were calculated from time series of presence/absence of tuna obtained along the drifts of FOBs equipped with M3I buoys in the study area. The daily proportion of inhabited FOBs was also calculated and its time evolution was examined on a quarterly basis. Finally, the quarterly averages of these proportions were used to verify the validity of the Equation S5.5.

3. Results

Figure S5.1 shows the strong agreement between the two terms of the Equation S5.5 (Student's t test : $t = 0.646$, $p = 0.521$). In addition, although upward (e.g. Q1-2013 and Q2-2013) and downward trends (e.g. Q3-2013) were observed in some quarters, the proportion of FOBs inhabited by tuna during the observation period can generally be considered stationary (Figure S5.2).

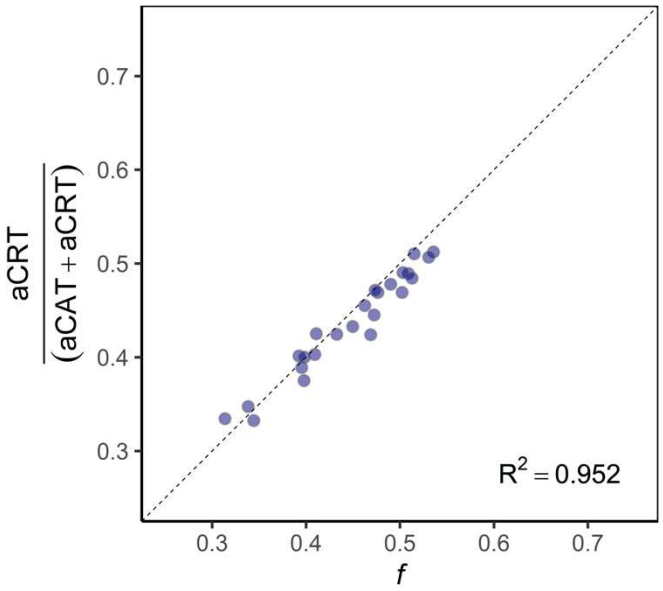

Figure S5.1: Relation between quarterly averages of proportions of inhabited FOBs, aCATs and aCRTs. The black dashed line represents the isoline 1:1.

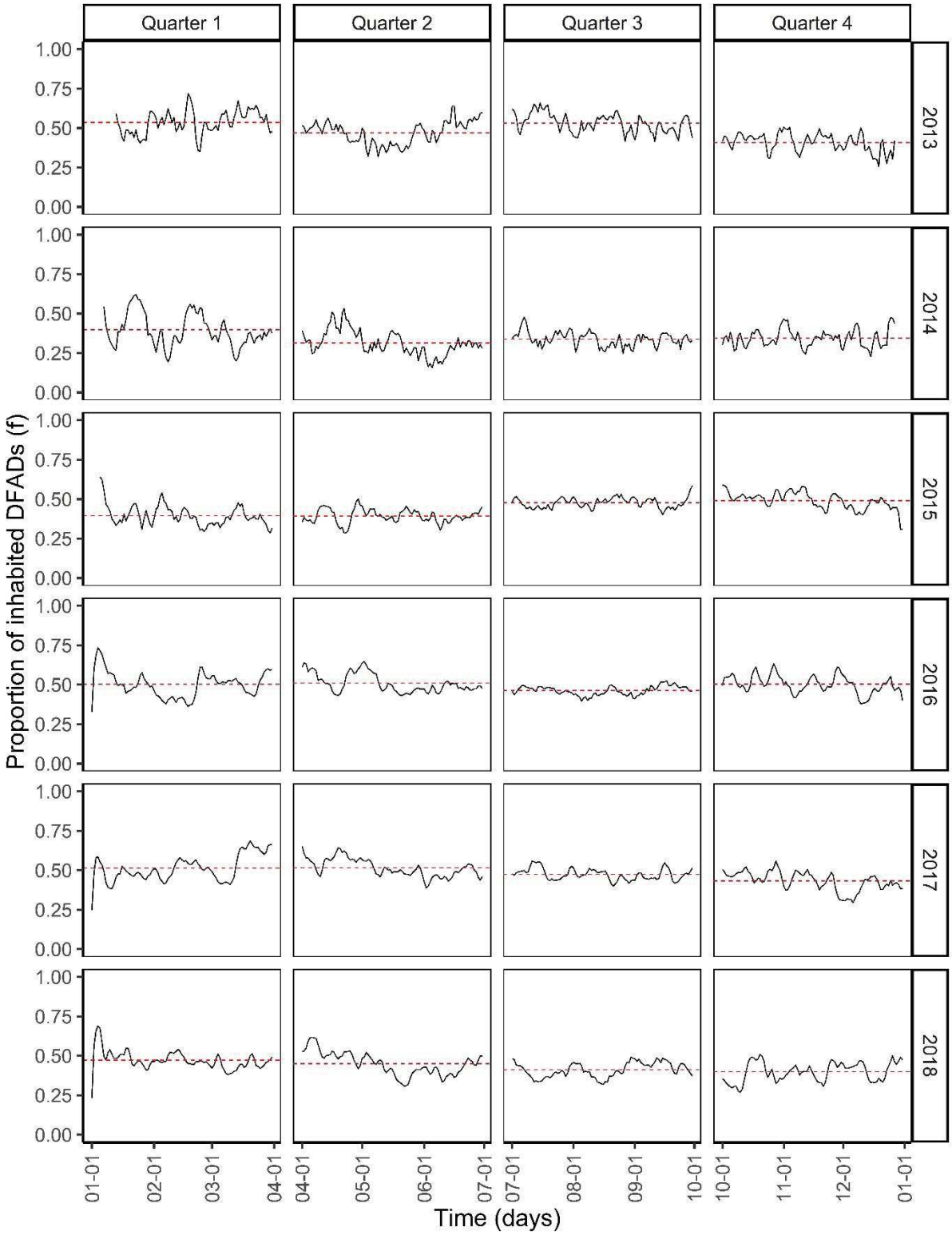

Figure S5.2: Time series of daily proportions of inhabited FOBs in the study area over 2013-2018. The red dashed lines represents the quarterly average values of the daily proportion of inhabited FOBs.

Supplementary information S6

Homogeneity of aggregative characteristics of FOBs

1. Context

The average population associated (*m*) with one FOB is estimated from average catches of tuna seiners under DFADs. This estimator might potentially be biased (overestimated), if tuna seiners only target FOBs with high tuna biomasses. This would also imply the existence of heterogeneity in the aggregative/attractive characteristics between FOBs. Indeed, the most attractive FOBs (i.e. those which aggregate the highest biomasses), should theoretically host tuna aggregations more often and longer than the others. Thus, heterogeneity in attraction or retention characteristics of FOBs should therefore, be reflected by the occurrence of multiple modes in the distributions of FOB occupancy rate in the study area.

2. Methodology

In order to investigate the possibility of such heterogeneity, distributions of FOB occupancy rates (proportion of the total time during which a FOB hosts tuna over its soak time) were examined from time series of tuna presence/absence measured along the drifts of FOBs equipped with a M3I echosounder buoy in the study area. The analysis was done considering, on the one hand, all FOBs in the data set and, on the other hand, only those on which fishing operations were carried out.

3. Results

The results showed that despite a large variability in FOB occupancy rates, affecting FOBs in general (Figure S6.1) but also the subset of FOBs on which fishing operations were reported (Figure S6.2), no characteristic multimodality could be identified. Hence, FOBs properties (attraction and retention characteristics) can be considered relatively homogeneous, and the average DFAD-associated catches of tuna seiners should represent an unbiased estimator of the local tuna abundance under a FOB.

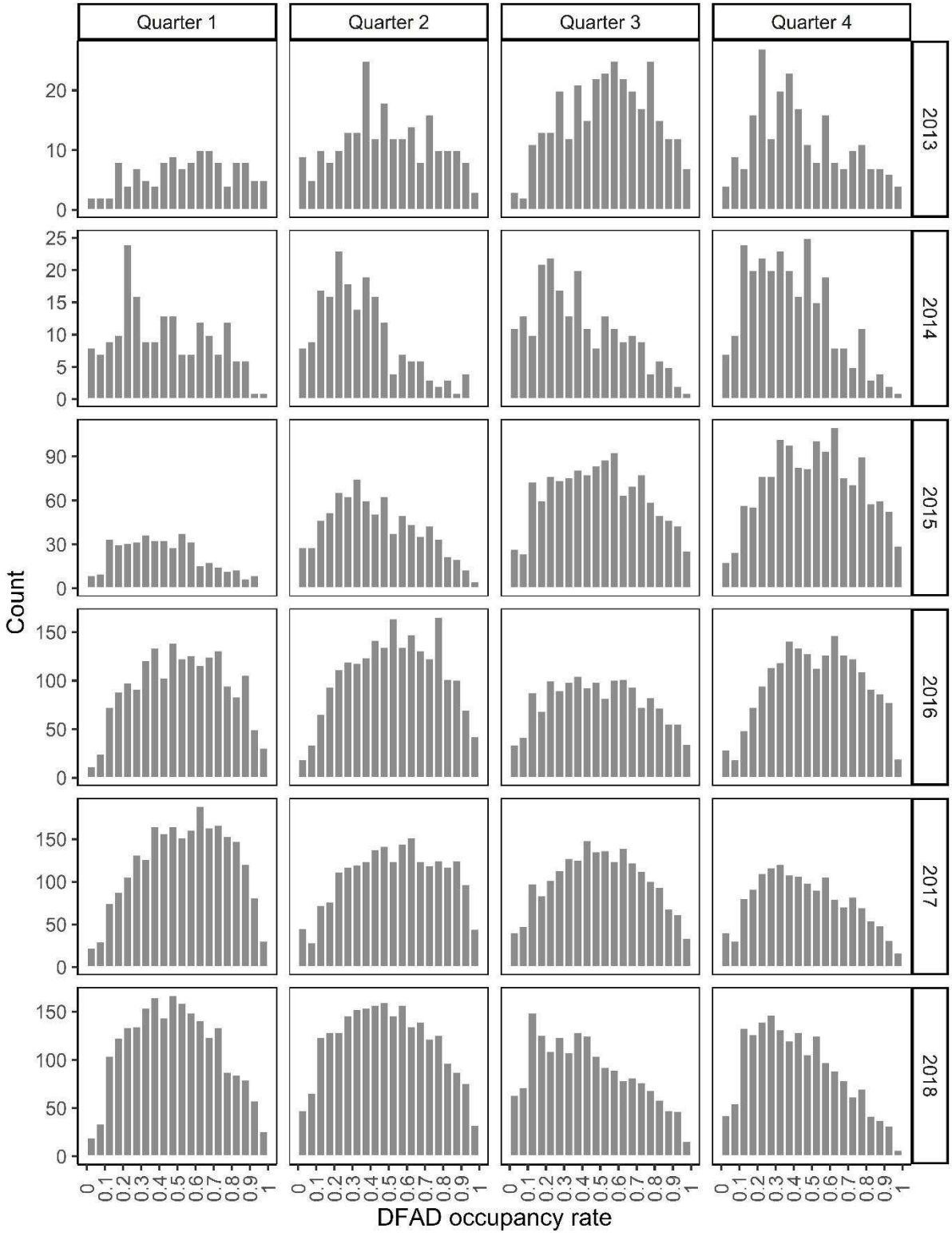

Figure S6.1: Proportion of DFAD occupancy time by tuna aggregations in the study area over 2013-2018.

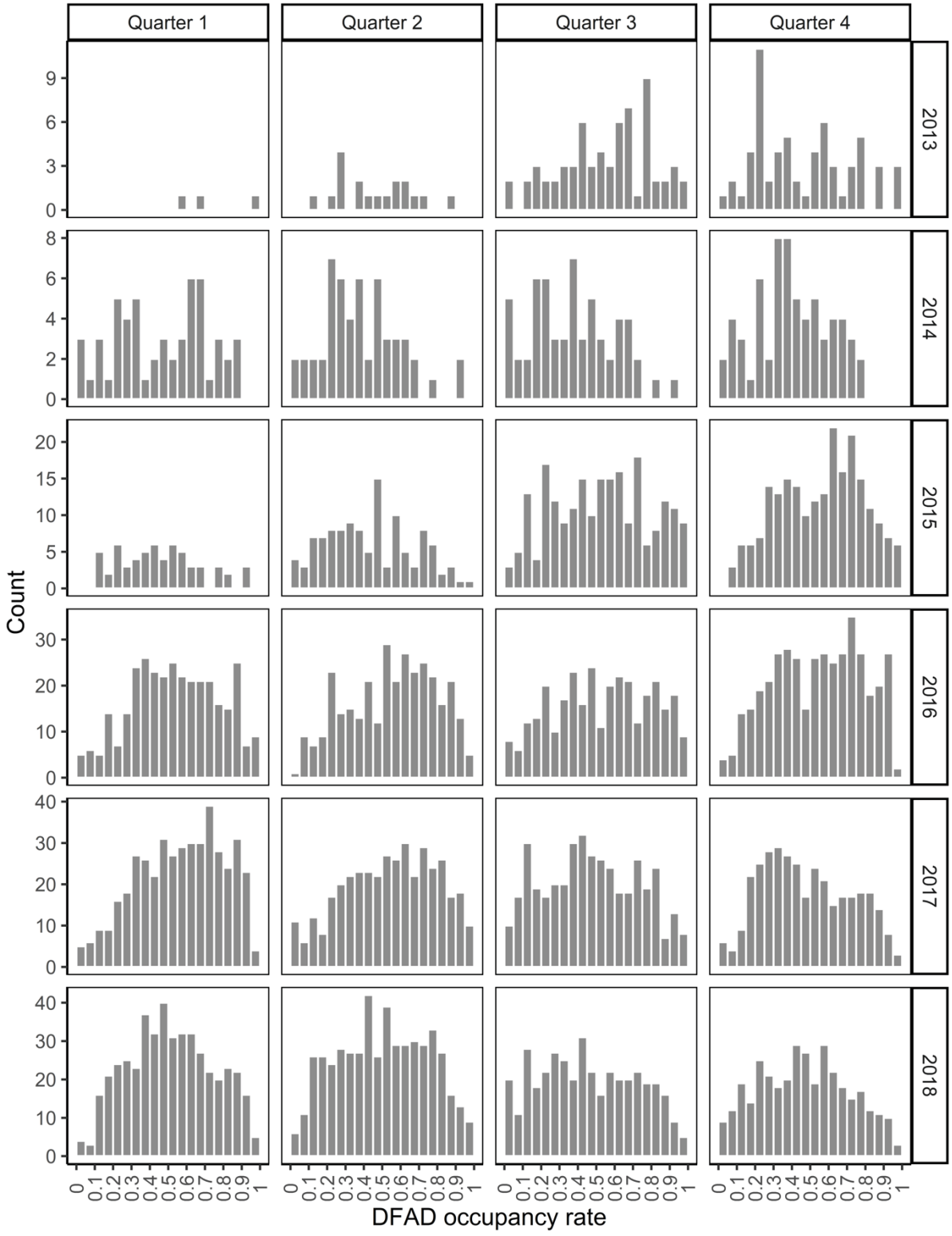

Figure S6.2: Proportion of occupancy time by tuna aggregations on fished DFADs in the study area over 2013-2018.

Supplementary information S7

The ϕ significance

Currently, there are no reliable observational data for CAT of tropical tunas, one of the main variables used in the proposed abundance assessment model. To overcome this limitation, the relation between CAT and the number of FOBs in the system has been estimated based on an *ansatz* introducing the parameter ϕ. This parameter is intended to move from the local scale at which associative processes take place (where the CAT are measured), to the scale of oceanic regions considered for the abundance estimates (where the number of FOBs is estimated). Indeed, following Capello *et al.*, (2016), for a system at equilibrium, the CAT can be related to the number of FOBs in the system (p) and the association probability (μ_i), defined as the probability for a non-associated fish to associate with a FOB i, as follows

$$CAT = \frac{1}{\sum_{i=1}^{p} \mu_i} \qquad (S7.1)$$

However, at oceanic scales considered, the associative processes of a tuna can realistically only concern a limited number of FOBs (p_0), corresponding to those that the tuna may encounter locally following its departure from another FOB. Therefore, p_0 represents the number of FOBs likely to be locally visited by the tuna, and located in the area S_0 that can be explored by the tuna between two consecutive associations. Herein referred to as the "local interaction zone", S_0 thus corresponds to the basic space-time unit within which the associative processes of a tuna take place (Figure S7.1). It is assumed that within it, all FOBs have the same probability of being visited and hosting tuna. The CAT definition can therefore be rewritten according to the following equation:

$$CAT = \frac{1}{p_0 \mu_i} \qquad (S7.2)$$

Considering a homogeneous distribution of FOBs, it is possible to write:

$$\frac{p}{S} = \frac{p_0}{S_0} \qquad (S7.3)$$

where S represents the area of the oceanic scale considered for the abundance assessment. Inserting the above relation into the CAT definition provided at Equation (S7.2) leads to:

$$CAT = \frac{1}{\left(\frac{S_0}{S}\mu_i\right)p} \qquad (S7.4)$$

By considering CAT definition from Equation (4.8) (see Chapter 4: section 4.2.2.2.5), it is therefore possible to express the parameter ϕ as the product of the surface ratio and the association probability:

$$\phi = \frac{S_0}{S}\mu_i \qquad (S7.5)$$

The area S_0 depends on the search dynamics of the tuna (random walk) and is currently unknown. However, it can be assumed that S_0 could be limited to the theoretical area that a tuna could cover during the basic unit of time considered (namely one day the time unit considered in this study). This would correspond to a circle with radius equal to the maximum distance travelled by a tuna in 24 hours (case of a "straight swim" to the FOB). Considering tunas moving at a constant speed of 1 BL/s (body length/s), for tunas of 50 cm, the local interaction area would thus extend to about 6,000 km². Considering the 13 million km² of the study area, the surface ratio S_0/S would therefore correspond approximately to 5e-4. Considering that μ_i in Equation (S7.5) is always < 1 (since μ_i is a probability per unit time), the order of magnitude of S_0/S is consistent with the low values of ϕ, which provided the most plausible estimates of tuna abundances ($\phi \sim$ 1e-6).

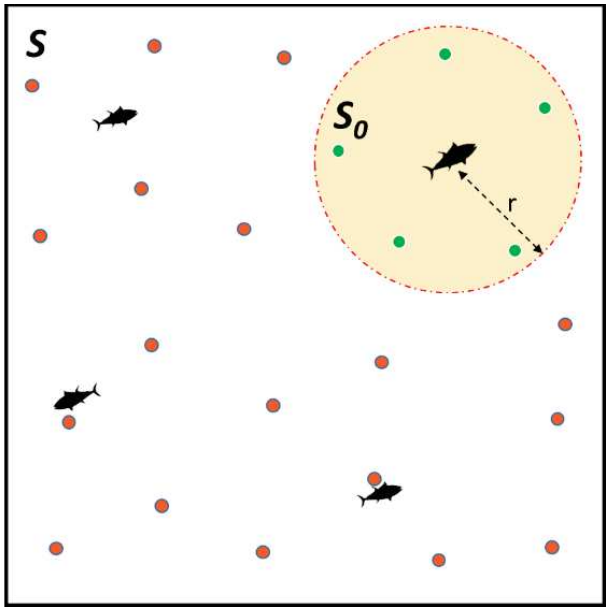

Figure S7.1: Schematic view of the local tuna environment. The green dots represent the FOBs with similar probabilities to be reached by the tuna located at the center of the circle. Conversely, the orange dots are the least likely to be reached by the same tuna. *S* and S_0 denotes respectively for the global zone and the local interaction zone of the tuna, and *r* represent the radius of the local interaction zone.

Supplementary information S8

Stability and empirical assessment of CRTs

1. Context

As an alternative to the proposed modelling approach, the association of tuna schools with FOBs can be modelled as a Bernoulli process and the relation between the total number of schools and their dynamics can be solved analytically. The approach considers a system of tuna schools and FADs located within their local environment (or local zone of interaction, see Supplementary information S7). This section describes the mathematical considerations behind this alternative approach and their implications for the study of tuna population and behaviour.

2. Model definition

We consider *Xi* as a random variable representing the number of tuna schools that associate with a FOB *i* per unit time. Considering the association of tuna with a FOB as a Bernoulli trial, *Xi* can be described through a binomial law of parameters X_{u0} (i.e. the number of free-swimming tuna schools that can locally associate with the FOB *i*), and μ_i (i.e. the association probability with the FOB *i*).

$$X_i \sim B(X_{u0}, \mu_i) \tag{S8.1}$$

The probability for a FOB to have K-associated tuna schools at a given time can then be expressed by the binomial law as follows:

$$P(X_i = K) = \binom{X_{u0}}{K} \mu_i^K (1-\mu_i)^{(X_{u0}-K)} \tag{S8.2}$$

The probability to have at least one inhabited FOB per unit time thus corresponds to:

$$P(X_i \geq 1) = 1 - P(X_i = 0) = 1 - \left[1-\mu_i\right]^{X_{u0}} \tag{S8.3}$$

Considering the ansatz on the CAT, (see Supplementary equation S7.4) we can write:

$$\mu_i = \frac{1}{p_0 CAT} \tag{S8.4}$$

hence:

$$P(X_i \geq 1) = 1 - \left[1 - \left(\frac{1}{p_0 CAT}\right)\right]^{X_{u0}} \quad (S8.5)$$

As a FOB is occupied if at least one fish is associated with it, the probability per unit of time for an empty FOB to become occupied by a tuna (ν, see Supplementary information S5), thus equals to the probability described above (probability to have at least one inhabited FOB per unit time):

$$P(X \geq 1) = \nu = \frac{1}{aCAT} \quad (S8.6)$$

In the limit of a large free population (X_{u0}) and a small association probability (μ_i), the relation (S8.3) can be approximated by a Poisson law:

$$\frac{1}{aCAT} = 1 - e^{\left(\frac{X_{u0}}{p_0 CAT}\right)} \quad (S8.7)$$

From Capello et *al.*, (2016), the free population X_{u0} can be related to the total population N_0 through the following relation (referring here to the number of tuna schools instead of the biomass):

$$X_{u0} = \frac{CRT}{CRT + CAT} N_0 \quad (S8.8)$$

Therefore, the Equation (S8.6) can be rewritten, solving for N_0:

$$N_0 = -p_0(CAT + CRT)\, log\left(1 - \frac{1}{aCAT}\right) \quad (S8.9)$$

The above equation relates the total population present in a given area with observables such as the number of FOBs (p_0), the continuous absence time of aggregation at a floating object (FOB-aCAT or aCAT), and the individual associative dynamics of tunas (CAT and CRT). The equation is valid at a local scale (see Supplementary information S7). In addition, since the equation (S8.8) implies that:

$$\frac{CAT}{CRT} = \frac{X_{u0}}{X_{a0}} \quad (S8.10)$$

with X_{a0} representing the total associated population on the local scale considered, the equation (S8.7) can be rewritten as follows:

$$\frac{1}{aCAT} = 1 - e^{\left(\frac{X_{a0}}{p_0 CRT}\right)} \quad (S8.11)$$

By substituting X_{a0} with its definition from equation (4.5) (see Chapter 4 section 4.2.1):

$$X_{a0} = mfp_0 \qquad (S8.12)$$

It is possible to derive the average continuous residence time (CRT) spent by tuna individuals at FOBs through the following relation:

$$CRT = \frac{log(1-f)}{log\left(1-\frac{1}{aCAT}\right)} \qquad (S8.13)$$

An alternative expression of CRT can also be derived from the Equations (S8.8) and (S8.9), as follows:

$$CRT = \frac{mf}{log\left(1-\frac{1}{aCAT}\right)} \qquad (S8.14)$$

This also allows to express *m* here denoting the average number of schools associated to a FOB according to this relation:

$$m = \frac{f}{log(1-f)} \qquad (S8.15)$$

3. Application to skipjack tuna in Indian Ocean

3.1. *Methodology*

The time series of estimated CRTs and number of schools associated to a FOB (*m*) in the study region were provided on a quarterly basis from Equation (S8.13), using the proportion of inhabited FOBs (*f*) and the aggregation continuous absence time (aCAT), measured from echosounder buoy data. By dividing the average number of schools under a FOB estimated from Equation (S8.15) by the FOB associated catches, we also provided time series of the average size of a school unit associated with a FOB.

Skipjack abundances were then determined over the study period in terms of number of schools from Equation (S8.9) on the one hand, and total biomass (using the average school unit sizes estimated above) on the other hand, considering the CATs calculated from equation (4.8), with a value of 2e-6 for ϕ. The abundances calculated from the analytically estimated CRTs (Equation S8.13), and the experimental CRT value of 4.58 days observed by Govinden *et al*.,

(2010), were compared. Finally, the trends obtained from this alternative approach were also compared with those from Figure 4.7 (chapter 4: section 4.3.4) considering the ϕ value of 2e-6.

3.2. *Results*

3.2.1. Time series of estimated CRT

The estimated average continuous residence time (CRT) obtained through Equation (S8.13), exhibits a stable trend stability over time, with an average around 4.27 days over the whole study period. These values and trends appears very consistent with the observational values from acoustic tagging experiments carried out in the study area (see Chapter 4: Table 4.3).

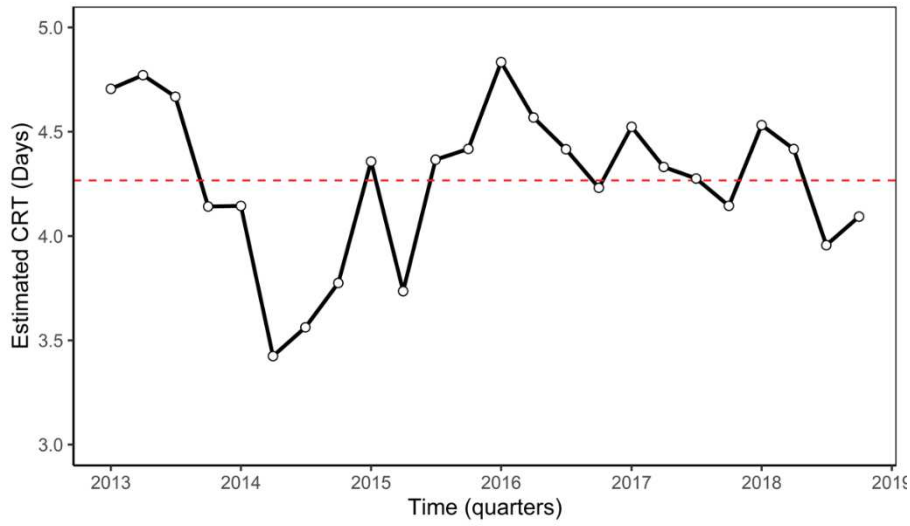

Figure S8.1: Temporal evolution of estimated average continuous residence time (CRT) of tuna individuals around FOBs. The red dashed line represents the estimate average value of CRT over 2013-2018.

3.2.2. *Evolution of the number and the size of skipjack tuna schools associated to a FOB*

The average number of skipjack schools associated obtained through Equation (S8.15) has stabilized since 2016, after a sharp decrease during 2013-2015, probably linked to the increase in the number of FOBs during the same period (Figure S8.2). At the same time, although subject to relative variability, the average size of skipjack school units has been increasing steadily since 2015 (Figure S8.3).

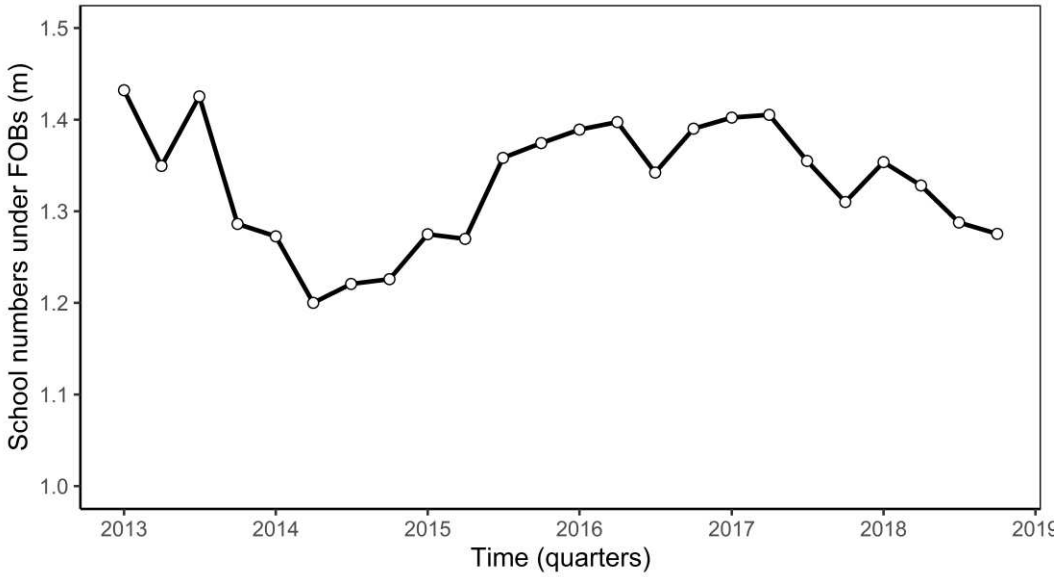

Figure S8.2: Evolution of the average number of skipjack tuna schools associated to a FOB over 2013 – 2018

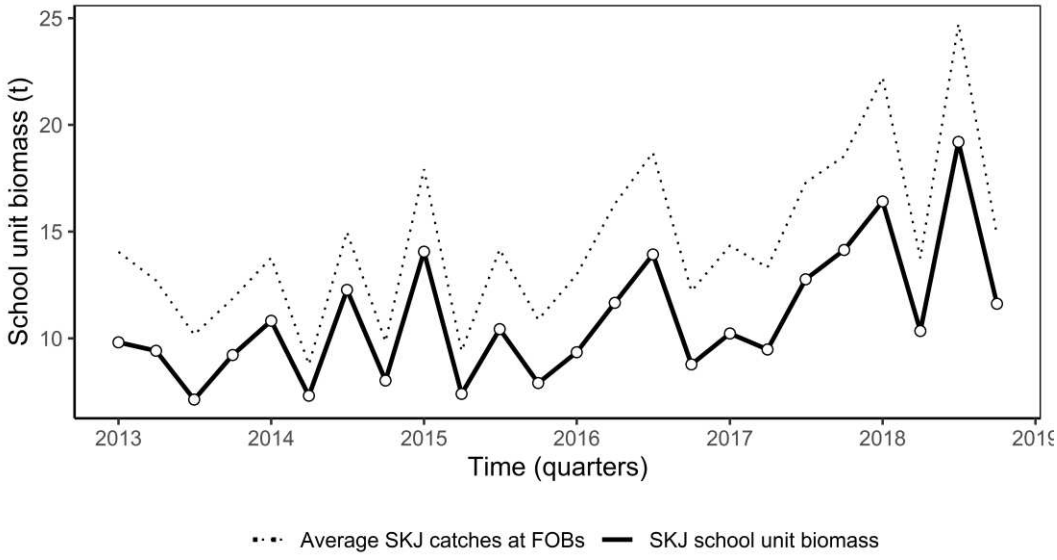

Figure S8.3: Evolution of the average biomass of a skipjack tuna school unit associated to a FOB over 2013 – 2018

3.2.3. *Time series of skipjack tuna school Abundance*

Abundance trends obtained from Equations (4.4) and (S8.9), using both estimated and fixed experimental CRT values, were found to be relatively similar (Figure S8.4). The two models yield broadly similar results in terms of biomass. However, the abundance of skipjack schools has been generally declining since 2017, while their total biomass has been steadily increasing. The hypothesis of a possible attenuation of skipjack schools fragmentation induced by the stabilization in the number of FOBs could be explored to explain these observations.

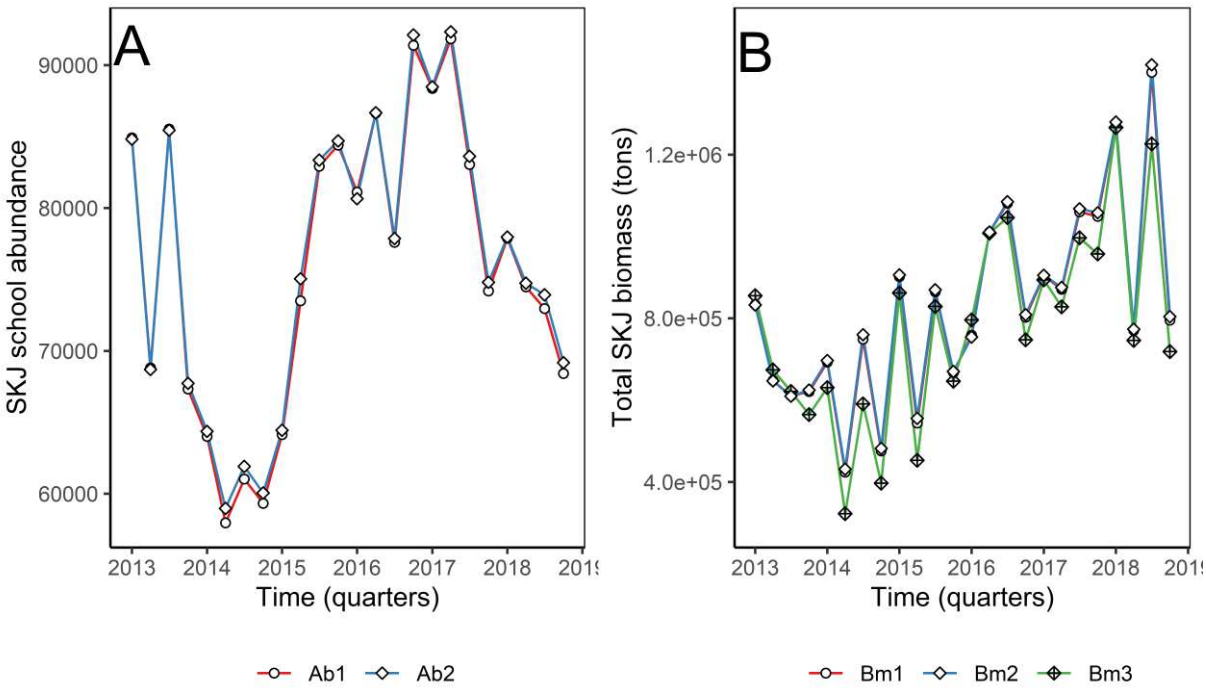

Figure S8.4: Comparisons of (panel A) time series of skipjack schools abundances obtained from Equation (S8.9) with estimated CRTs from Equation (S8.13) and experimental CRT value of 4.58 days observed by Govinden *et al.*, 2010 (respectively *Ab1* and *Ab2*); and (panel B) time series of total skipjack biomass obtained from school size units and Equation (S8.9) for estimated and experimental CRTs (*Bm1* and *Bm2*, respectively). *Bm3* represents the abundance trends obtained from Equation (4.4). CAT were calculated considering a ϕ value of 2e-6.

Supplementary information S9

Abundance indices for tropical tunas based on their associative behaviour around floating objects: Stochastic simulations

1. Algorithm description

We simulated the associative dynamics of a population of N tuna in an array of p FOBs (Capello *et al.,* 2016). The model assumes that each tuna is likely to reach every FOBs of the array (i.e. $S=S_0$, see Supplementary information S7). Tunas can be in two states, either free-swimming (unassociated) or associated to one of the p FOBs of the array. At each time step, each tuna can change its state according to the association and the departure probability (respectively μ_i and θ_i). The stochastic simulations followed a standard Monte Carlo algorithm, in which the acceptance (or rejection) of the state change was implemented through comparisons with a pseudo-random number ξ sampled from a uniform distribution in the interval (0, 1]. An associated tuna changes its state (thus become free) if $\xi \leq \theta_i$. Conversely, if $\xi \leq \mu_i p$ a free-swimming tuna will associate to a randomly sampled FOBs of the array. The model were considered for a homogeneous system, with all FOBs having the same arrival and departure probabilities $\mu_i = \mu$ and $\theta_i = \theta$.

The initial state of all tunas was assigned as unassociated and the system was let to evolve during 1,000 time steps, following the above procedure. The Monte Carlo simulations were run for 100 replica. For each replica, a set of metrics were calculated after the equilibrium was attained (constant numbers of fish unassociated and associated with FOBs, and constant numbers of inhabited and empty FOBs):

- Tuna behavior metrics: *CRT* and *CAT* (respectively Continuous Residence Time and Continuous Absence Time);
- FOB occupancy metrics: f (proportion of FOB occupied by at least one tuna), and m (average number of tuna associated to the FOBs that are occupied.

The abundance index of the total population (N) were then estimated for each of the replicates from Equation (4.6) (see Chapter 4: section 4.2.1), and the mean and standard deviation of the index was estimated.

Sensitivity of the abundance index was also analyzed with respect to the numbers of FOBs (p), and the association probabilities (μ_i). The other parameters were fixed at constant values. The model parameters considered for the different case studies are shown in Table S9.1.

Table S9.1: Model parameters. The cells in bold represent the model parameters that are varied in the sensitivity analysis.

Parameters	Description	Values
N	Total number of tunas	1000
p	Total number of FOBs	**500, 250, 100, 50**
μ_i	Association probability	**4e-4, 8e-4, 4e-5, 2e-5, 8e-5**

2. Results from stochastic simulations

Temporal evolution of the system state variables are presented on Figure S9. ***1***. The convergence of the abundance index shows little sensitivity to the number of FOBs in the system and the tuna association probability (Figure S9.2). The main effects of the increase in the number of FOBs are observed on CAT, with the largest effects observed for the lowest association probabilities (Figure S9.3A). Increases in the number of FOBs or the association probability result in shorter CATs. Indeed, CAT is theoretically inversely proportional to the product between the number of FOBs and the association probability (Equation 4.8). The longest CATs, observed for the lowest association probabilities, correspond to the scenarios of least pronounced associative behaviour, with CATs in simulations around 500 steps, i.e. 100 times longer than the durations in the associated state. In contrast, the fraction of FOBs occupied by fish in the system (f) and the continuous absence time of aggregation at FOBs exhibit much less sensitivity to the increase in the number of FOBs. Rather, fluctuations in these variables appear primarily driven by changes in the fish association probability (Figure S9.3B and Figure S9.3D respectively). Finally, an increase in the total number of FOBs results in a relative decrease in the average fish biomass associated with FOBs (m) and in the average continuous residence time of aggregation at FOBs.

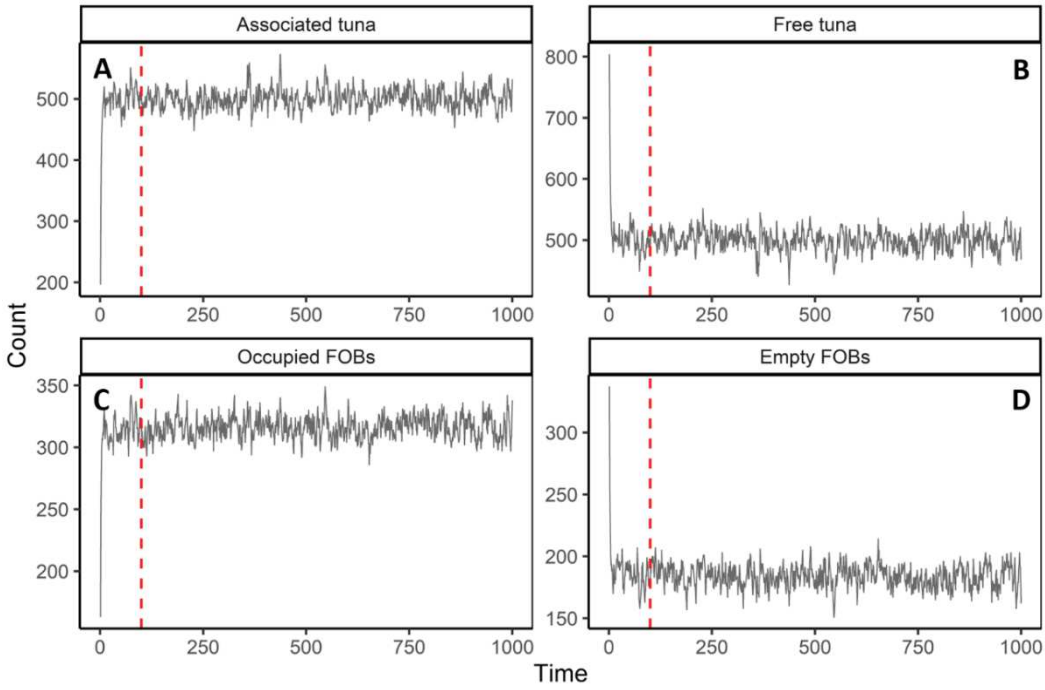

Figure S9. 1: : Example of the evolution of the system's properties as a function of the simulation time: (Panel A) Number of associated tunas, (Panel B) Number of free-swimming tunas, (Panel C) Number of FOBs occupied by at least one tuna; (Panel D) Number of empty FOBs. Red dashed lines indicate the timestep=100 from which equilibrium is considered to be attained. Model parameters: p=500, μ_i =4e-4.

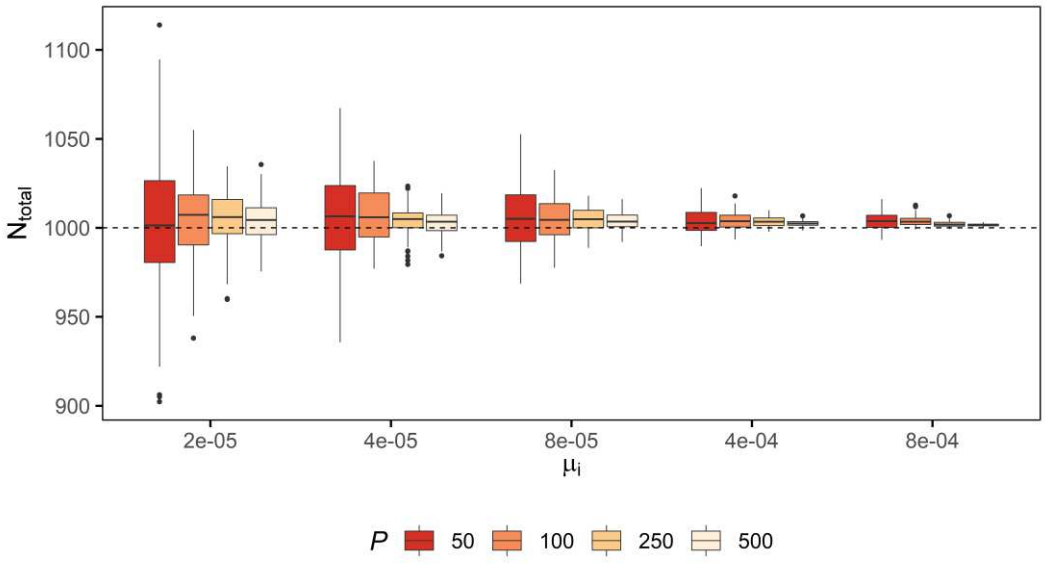

Figure S9.2: Effect of the probability of association (μ_i) and the number of FOBs (p) on the total abundance index (N). The departure probability and the total fish population are kept fixed at 0.2 and 1,000 respectively. The dashed black horizontal line corresponds to the asymptotic limit.

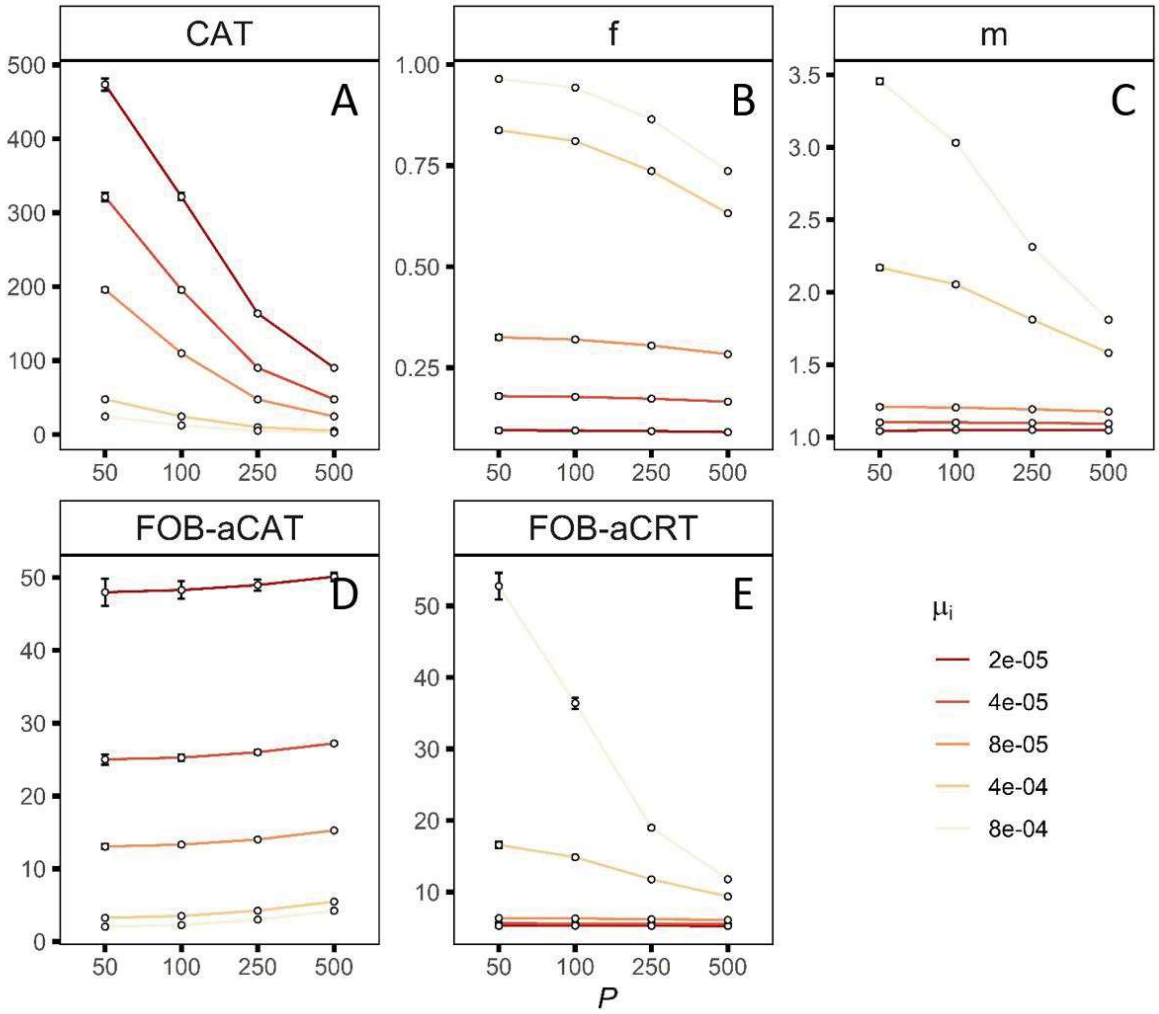

Figure S9.3: Effects of the association probability (μ_i) and the number of FOBs (p) on (panel A) the simulated continuous absence times (*CAT*), (panel B) the proportion of inhabited FOBs (f), (panel C) the average FOB-associated biomass (m), (panel D) the continuous absence time of aggregation at a floating object (FOB-aCAT), and (panel E) the aggregation's continuous residence time at a floating object (FOB-aCRT). The departure probability and the total fish population are kept fixed at 0.2 and 1,000 respectively.

General Discussion

"*Perfection of means and confusion of goals seem – in my opinion – to characterize our age*".

Albert Einstein

5.1. Overview and synthesis of main results

Tropical tunas are globally distributed species that represent a significant part of the global fish and seafood economy (Campling, 2012; Galland *et al.*, 2016), and also play a critical role in the health and functioning of the marine ecosystem (Collette *et al.*, 2011). The availability of reliable tools to estimate the size of their populations is therefore a key priority to ensure their sustainable exploitation. This concern represented the core aim of the present thesis, driven by the idea of exploiting the characteristic associative behaviour of these species with objects floating at sea to directly derive their abundance. As a prerequisite, the idea implied to improve the general knowledge about this behavioural trait, notably through new sources of information for these species. On this aspect, the data from satellite-linked echosounder buoys equipping drifting fish aggregating devices (DFADs) used by tropical tuna purse seiners to increase their catches, has constituted a major asset. Since their introduction in the tropical tuna purse seine fishery in the early 2010's, echosounder buoys represent an unprecedented source of information on fish aggregations associated with DFADs, which so far, were primarily intended for commercial and industrial use as fishing aid.

This thesis provides a standard methodology to process this heterogeneous mass of industry-based data for scientific applications (Chapter 1), including an alternative approach to the classical echo-integration for the processing of acoustic data collected by fisher's echosounder buoys (Chapter 2). Based on machine learning, the approach makes possible to provide reliable information on the presence or absence of tunas within the multi-species aggregation of fish under DFADs. Obtaining accurate biomass estimates from echosounder buoys appeared to be more challenging. This may well be a typical limit of the current buoy models, as previous works based on different brands has also produced poor performance in terms of biomass estimates (Orue *et al.*, 2019a). Currently, the echosounder buoy technology represents a powerful source of qualitative data on DFAD-associated fish aggregations. However, its technical constraints (limited angle, detection range, sampling frequencies, etc.), as well as the characteristics of DFAD aggregations (multi-species with highly variable target strengths), and environmental variability are all factors that seem to significantly hamper the current reliability of its quantitative biomass estimates. Nevertheless, this gap may very soon be closed, given the near-continuous improvement of the hardware and software of new buoy models, with the introduction of various innovative features such as multiple sampling frequencies, digital correction of time varied gain (TVG) and consideration of possible environmental biases (e.g.

built-in inclinometer for some models to ensure vertical sampling and avoid incorrect surface echoes).

Despite the current usage limits, using instrumented DFADs as tools to observe the open-sea through echosounder buoy data has provided new clues for a better understanding of the associative dynamics of tuna aggregations around DFADs (Chapter 3). This thesis has indeed brought answer elements to some key questions for which little information existed to date, including: How long does it take a floating object to be colonized by tuna, and how long does the associated tuna aggregation remain under the object? By introducing the FOB-aCRT (aggregation's continuous residence time at a floating object) and the FOB-aCAT (continuous absence time of aggregation at a floating object), in the study of the behaviour of tunas at floating objects, this work has evidenced that the associative dynamics of tuna aggregations at floating objects were ocean-specific and generally determined by time-independent processes. For instance, DFAD colonization by tuna aggregations has been shown to vary from a couple of weeks in the Atlantic Ocean to more than a month in the Indian Ocean. Moreover, the analysis of tuna occupancy patterns of DFADs revealed that floating objects remained empty much longer in the Indian Ocean than in the Atlantic Ocean and showed a significant difference in the proportion of occupancy times between the oceans. The population abundance, cited as one of the main causative factors of this variability, could thus be estimated through a modelling approach combining the DFAD occupancy by tuna aggregations with metrics describing their behaviour at the individual scale. New absolute abundance indices of the different components of tuna populations (associated and free-swimming) was presented in Chapter 4. Their application in the Indian Ocean since the implementation of echosounder on buoys equipping DFADs, has made it possible to estimate the trends in the abundance of skipjack tuna populations, from almost a decade.

This general discussion is not intended to revisit the different points already covered in the previous chapters of the thesis, but rather to focus on the implications of these results for both current knowledge of tuna ecology and the management of their stocks, and to outline the main conclusions that emerge as well as future and possible directions of research.

5.2. Implications on tuna behaviour: Structure of tuna aggregations under floating objects

To date, the actual ecological and evolutionary determinants underlying the associative behaviour of tropical tuna species with floating objects are still unclear. However, several hypotheses have been proposed (see review in Fréon and Dagorn, 2000; Castro *et al.*, 2002), and an extensive work carried out on this question in recent decades have provided elements for a better understanding of these mechanisms and a rough scenario of the aggregative processes under floating objects (FOBs). Different free-swimming tuna schools distributed within a relatively large area start to aggregate around a drifting object once they have detected it (Girard *et al.*, 2004; Wang *et al.*, 2012). These multiple schools are organized around the FOB, probably by species and size (Josse *et al.*, 2000; Moreno *et al.*, 2007b; Trygonis *et al.*, 2016), and form around it, a single or multi-species aggregation of tunas, whose structure may exhibit significant day-night variations (Forget *et al.*, 2015; Lopez *et al.*, 2017b). The tuna aggregation can remain stable for up to two or three weeks depending on oceans (Baidai *et al.*, 2020b), presumably due to a high turnover process between schools (Weng *et al.*, 2013). However, it generally remains under the FOB for only a few days (about 4 to 5 days in the Atlantic and Indian Oceans). This short duration corresponds approximately to the average residence time of a tuna individual (and hence a single school) measured under a FOB, especially that of skipjack tuna (see Chapter 3: Table 3.3). With around 75% of the overall DFAD-associated catches, skipjack tuna represents the predominant species in tuna aggregations under floating objects (Dagorn *et al.*, 2013a). Although this species does not have a swim bladder (Boyra *et al.*, 2018), its high representativity under FOBs suggests that it is most likely to be the main responsible for the patterns used by the supervised classification approach applied in this study, to discriminate between the presence and absence of tunas under a FOB (Baidai *et al*., 2020a). Therefore, the tuna absence situations as obtained from buoys could be linked either to the departure of all tuna schools or only those of skipjack from the FOB. At this level, the technical limitations of echosounder buoys (sampling cone, impossibility to discriminate between species, poor quantitative estimates, etc.), make them the least appropriate instruments for an accurate observation of the structure of the FOB aggregation and the typical dynamics of each species. Complementary studies combining different observation techniques (e.g. buoys or sonar with passive acoustic telemetry), in order to directly relate the residence times measured simultaneously at the scale of the FOB

aggregation and the different species and sizes of individuals that compose it, could make a considerable contribution to a better understanding of this process.

Nevertheless, a possible explanation for the similarity between the residence times of the FOB aggregation and the individual skipjack could lie in a schooling behavior with a single school associated to the floating object. Although this explanation contrasts with the empirical observations of multiple schools structure made by fishers (Moreno *et al.*, 2007), and more specifically with the findings of Wang *et al.* (2012) regarding the structure of skipjack schools associated with FOBs; it may be supported by the massive increase in the number of drifting fish aggregating devices (DFADs) used over the last decade. Indeed, it should be noted that the two studies are more than a decade old. They actually correspond to a situation when the densities of floating objects were very much lower than currently. According to Maufroy *et al*. (2017), the number of DFADs in the Atlantic and Indian Oceans at least quadrupled between 2007 and 2013; and Figure 4.8 (Chapter 4) indicates that for the Indian Ocean, this increase continued with a multiplication factor of two until 2015, after which it stabilized.

Analyzing the status of skipjack populations in the Indian Ocean from the 1990s to 2016, Fonteneau and Marsac (2016) have proposed the hypothesis of a possible school fragmentation by DFADs, affecting this species. The hypothesis suggests that the growing number of DFADs could have sucked out free schools and partitioned the available biomass into smaller schools (Marsac *et al*., 2017). It was corroborated by the overall decrease of skipjack associated biomass and the dominance of small schools sets at FADs over the period from 2007 to 2016. However, since 2016, there has been a steady increase in average catches of skipjack under FADs, coinciding with the adoption of FAD management plans in 2015 for this ocean. It could therefore be plausible that the current situation is approaching an attenuation of this fragmentation phenomenon, with skipjack schools decreasing in number, but increasing in school size (see Supplementary information S8: Figure S8.4). This could also be consistent with the explanatory hypothesis proposed above, which relates the predominance of short-term residence modes in the FOB aggregation to a schooling behavior, resulting from the concomitant reduction in the number of associated schools under a FOB.

The oceanic differences in the occurrence of short-term residence modes (representing 94% and 62% of the observed modes in the Indian and Atlantic Oceans, respectively) could therefore result from similar causes to those proposed for the interpretation of durations of FOB vacancy (FOB-aCAT) between the two oceans, i.e. a smaller number of unassociated tuna schools and/or higher FOB densities in the Indian Ocean than in the Atlantic Ocean. The higher proportion of

skipjack tuna catches in free-swimming schools in the Atlantic Ocean compared to the Indian Ocean, observed for the French purse seine fleet in Figure 5.1 may be consistent with this hypothesis. However, further studies will be necessary to account in this interpretation for the effect of a possible variability in the fishing strategies of this fleet (e.g. potential effect of the fishing zones, with tuna seiners operating in strata with larger numbers of free skipjack schools in the Atlantic than in the Indian). Comparative assessments of the abundance of tuna populations (including the number of schools) in their associated and free-swimming components between the two oceans should also help validate the hypotheses proposed for the interpretation of the differences in the dynamics of tuna aggregations around floating objects identified in this work. On this aspect, the novel abundance index provided by this thesis should therefore be of great interest.

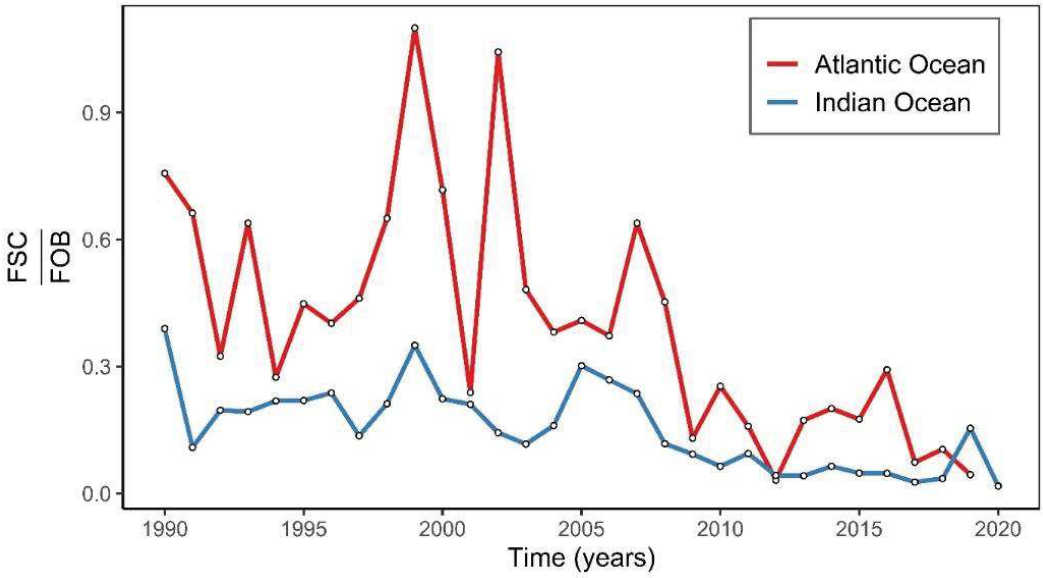

Figure 5.1: Evolution of the ratio between the numbers of skipjack tuna catches on free-swimming schools (FSC) and under floating objects (FOB) by the French fleet of tuna seiners from 1990 to 2019. Catches data were obtained from fishing logbooks of purse seine vessels.

5.3. Associative Behaviour Based abundance Index (ABBI): What next?

In accordance with its overall objective, this thesis provides a new abundance index for tropical tuna populations based on the combination of metrics of the associative dynamics of tunas at the individual and aggregation scales. The Associative Behaviour-Based abundance Index

(ABBI) provides absolute estimates of the abundance of the total population of tuna and its free-swimming and associated components. ABBI is based on a relatively simple modelling framework using five main inputs: (i) the total number of floating objects (natural or artificial logs and DFADs), (ii) the proportion of these objects that are occupied by tunas, (iii) the local abundance of tunas around them, (iv) the continuous residence time of tuna individuals around a floating object (CRT), and (v) their continuous absence time (CAT).

The low number of input data required and the availability of technological means to collect them constitute both major assets offered by this novel index. On the one hand, as shown in Chapter 4, it is possible to derive from echosounder buoys the information related to the number of floating objects, the dynamics and characteristics of associated tuna aggregations, including their biomass if species discrimination and better quantitative estimates could be achieved from the acoustic data they provide. In the current state of echosounder buoy technology, DFAD catches from purse-seiners are nevertheless the only way for obtaining the required information on local tuna abundance around floating objects. Obviously, the actual nature of these data sources (fisher's buoys and tuna catches) implies that ABBI cannot be considered as fully independent of fisheries. Independent surveys aiming at assessing through spatial sampling the proportion of inhabited floating objects as well as their amount of associated biomass could, to a certain extent, turn this index into truly fishery-independent. However, such surveys would have limited relevance with regard to the cost-effectiveness and the wide spatial and temporal coverage offered by the current data sources from the purse seine fishery.

On the other hand, the continuous progress in electronic tagging and tracking technology now make it possible to collect increasingly detailed information on behaviour of marine animals (Nielsen *et al.*, 2009). Recent years have seen the development of an increasing number of electronic tagging studies on the behaviour of tuna around floating objects, which have provided valuable information on the associative dynamics of tuna individuals, especially on their CRTs (e.g. Ohta and Kakuma, 2005; Dagorn *et al.*, 2007b; Robert *et al.*, 2012; Matsumoto *et al.*, 2014, 2016; Rodriguez-Tress *et al.*, 2017; Scutt *et al.*, 2019; Tolotti *et al.*, 2020). Nevertheless, additional efforts for a regular and large-scale collection of these data are highly desirable, since the current collection of CRTs is usually related to short-term projects, and remains rather episodic and generally limited to certain oceanic regions.

On the other hand, Supplementary information S5 from the Chapter 4 indicated that, under a number of assumptions, the CRT could also be derived from the data collected by the echosounder buoys, using an analytical approach. Additional studies would be of great interest

to assess the likelihood of these assumptions and the robustness of this approach in order to reduce the amount of input data required for abundance estimates based on ABBI.

The major concern in terms of data collection is mostly related to the measurement of CAT. Assessing the time between two consecutive associations of a tuna fish is a rather logistically complex task. Given their high mobility, tracking tuna species using passive acoustic telemetry, for CAT measurements, would require relatively large acoustic arrays and a considerable monitoring effort. Moreover, an overestimation of the CAT values measured as a result of the association of tuna with non-instrumented aggregation points in the monitored zone (e.g. floating objects, whales or whale sharks), would remain difficult to exclude. The significant differences in the vertical behaviour of tunas between associated and free-swimming states, highlighted by Schaefer and Fuller, (2005, 2010), could represent a relevant asset to be considered for further experimental studies aiming at measuring CATs.

In Chapter 4, assumptions on the relationship between CAT and the density of floating objects have introduced a proportionality parameter (ϕ), which was shown to result from two key parameters: the association probability and the area of the local interaction zone of the tuna (see Supplementary Information S7). Conceptually, the local interaction zone represents the base observation unit of the tuna associative process. It is assumed that within it, associations of tuna with objects could be considered relatively equally probable. The size of the local interaction zone mainly results from the search dynamics of the tuna individual, but it is also very likely to depend on the density of floating objects. For the purposes of this study, the plausible ranges of these values were determined based on empirical considerations. However, further studies using analytical techniques for modelling movement patterns of tunas in an array of floating objects would greatly help to provide accurate estimates of these parameters. They would also be useful to address the uncertainties on the absolute estimates of the abundance index, to assess its sensitivity to the assumptions about the homogeneity of the floating objects system (i.e. constant association probability), and the possible variability in the size of the local interaction zone.

Considered in relative terms, ABBI is however, very insensitive to the two above-mentioned parameters. Despite its short duration, the time series of the relative abundance of the Indian Ocean skipjack population estimated from ABBI has proven to be relatively consistent with the recent assessments of skipjack abundance carried out by Medley *et al.*, (2020) using the standardised CPUE derived from the Bayesian GLM model for the Maldives pole and line fishery (Figure 5.2). Although derived from the relatively small exclusive economic zone of the

Maldives, the CPUE of the Maldives pole and line (Maldives PL CPUE), is an abundance index traditionally used for the assessment of skipjack tuna in the Indian Ocean (Kolody *et al.*, 2011; Sharma *et al.*, 2012; IOTC, 2014, 2017).

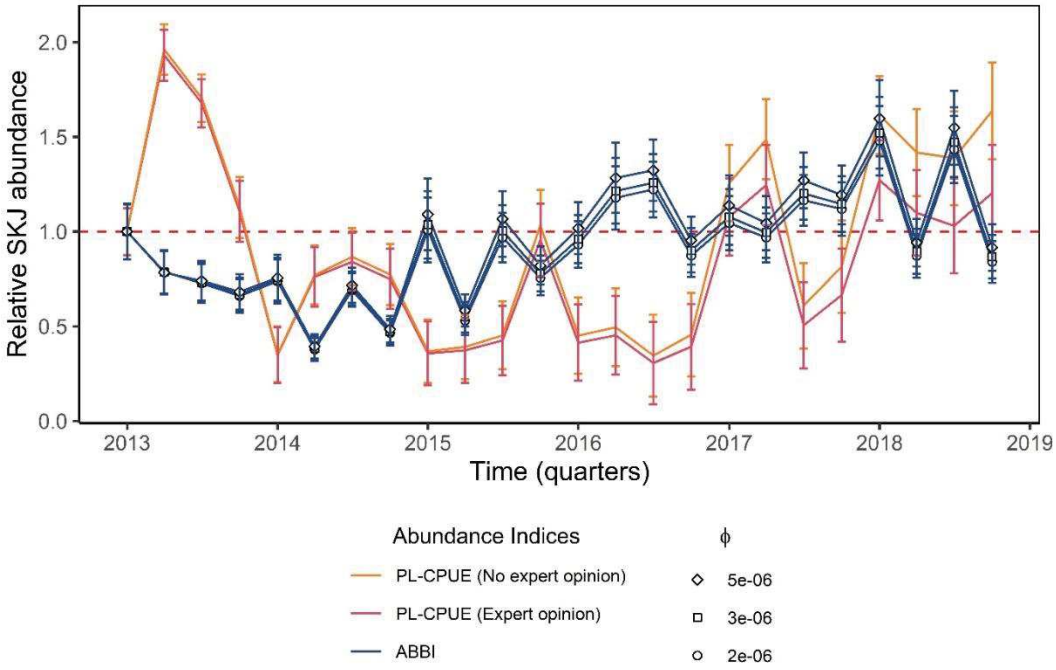

Figure 5.2: Trends in the relative abundance of skipjack tuna in the Indian Ocean derived from the Associative Behaviour Based Index (ABBI) under the most plausible ϕ values, and from standardised catch and effort data from Maldives pole and line fishing (PL-CPUE), corrected or not by expert opinions.

Similarly to the Buoy Abundance Index (BAI) proposed by Santiago et *al.*, (2016, 2019), the concept of ABBI is broadly based on the use of the associated part of the tropical tuna population in order to produce estimates of the total population size. Nevertheless, contrary to the BAI, the ABBI incorporates the associative characteristics of the species in its approach and has the capacity to provide estimates for both the free-swimming and the associated components of the tuna population. The BAI is a relative abundance index also based on data from echosounder buoys, and built on the assumption that trend in the abundance of the associated component of the tuna population, estimated through buoy acoustic data, would reflect that of its total abundance. However, the relationship between the total tuna population and its associated component could be much more complex and vary over time particularly under the influence of the density of floating objects. For example, abundance estimates carried out using ABBI in the Western Indian Ocean have shown a steady increase in the size of the associated

component of the skipjack population, parallel to the increase in the number of floating objects from 2013 to 2015, despite the general decline in the total skipjack population observed over the same period. This example highlights the potential biases that can occur without a good understanding and consideration of the associative dynamics of tropical tuna species in assessments of their total population based on their associated component.

It may also be relevant to assess the consistency of the estimates made for each of the population components with the trends in abundance derived from the standardized CPUE calculated from the different fishing modes of tuna purse seiners, i.e. free schools and FAD fishing (Guery *et al.*, 2020). Similarly, linking absolute abundance estimates from ABBI with those derived from population assessments based on genetic approaches, i.e. Close-Kin Mark Recaptures (Bravington et *al.*, 2016a), could also be of major interest. For instance, this could make it possible to check in an absolute manner the validity of some of the conjectures on which the ABBI modelling approach is based, including the orders of magnitude of the local interaction zone and the CATs, currently empirically estimated.

In addition, this first application of the ABBI was implemented over a relatively large area (i.e. Western Indian Ocean). A better understanding of tuna dynamics, notably skipjack tuna, could eventually be achieved through spatially restricted analyses allowing, on the one hand, to explore the spatial variabilities of its abundance and the various descriptive metrics of its associative behavior and, on the other hand, to clearly identify the nature of the relationships between these variabilities and the environmental conditions. Modelling techniques could then be used for a predictive mapping of tuna abundance, with a direct interest in an operational management of tuna fisheries.

Currently, the relative abundance estimates of the total population derived from the ABBI have been proposed as a complementary abundance index for the 2020 Indian Ocean skipjack stock assessment (IOTC, 2020b). The extension of this first example of application to other oceans (especially the Atlantic Ocean), tuna RFMOs, as well as to other tropical tuna species for which a number of stocks are estimated to be below abundance healthy levels (ISSF, 2019), would be worth considering in the coming years.

5.4. Echosounder buoy data in an operational management of fisheries

On several aspects, the data collected by satellite echosounder buoys on DFADs has proven to be relevant to address some of the key questions raised by the management of tropical tuna fisheries. The very first aspect is related to the new source of information that echosounder buoys may represent for the assessment of the spatio-temporal distribution of tropical tuna species. As shown by Baidai *et al.* (2019, 2020c), echosounder buoys data make possible a near real-time and large-scale mapping of the presence of tunas under floating objects. Such information could be adequately integrated into the management of tuna fisheries, in particular to support decision-making on spatio-temporal conservation measures. For instance, an evaluation of the effects of the FAD moratorium implemented by the ICCAT (International Commission for the Conservation of Atlantic Tunas) since 2013 revealed that, although relatively well applied by the main fisheries, the initial results of this measures have been relatively unsatisfactory with respect to the expected objectives (Fonteneau *et al.*, 2016). The FAD moratorium is part of the ICCAT multi-annual program for the conservation and management of tropical tunas and consists in a time/area closure of operations on floating objects, including fishing, intended to reduce catches of tropical tunas and improve their stock status, especially juvenile yellowfin and bigeye tunas. The limited amount of tuna catches under FADs compared to the total catches in the closure strata considered in the early years of the implementation of the moratorium, along with the great flexibility of modern tuna fleets were identified as the main causes of its poor performance. Currently, the closure area extends to the entire ICCAT convention area (ICCAT, 2020). The information on spatio-temporal distribution of tunas provided by echosounder buoys could provide a valuable and complementary scientific basis to support this type of management measures, by helping to identify or validate the priority areas and periods to be targeted.

At the same time, a better understanding of the influence of the environment on tuna distribution could be obtained through Species Distribution Models (SDMs) linking these new data to oceanic conditions. In recent years, SDMs have emerged as an effective tool to improve ecological and evolutionary knowledge about species as well as to predict their responses to multiple drivers of change, primarily for conservation and management purposes.(Rushton *et al.*, 2004; Elith and Leathwick, 2009; Araújo *et al.*, 2019). The combination of data from echosounder buoys with remote sensing systems through these modelling techniques has the potential to provide new predictive tools relevant to the management of tropical tunas.

Additionally, information from fisher's buoys are likely to provide an interesting support to small scale and artisanal fisheries. Tuna and tuna-like fish usually undertake large migrations that take them into the coastal waters of various countries. However, the access to these tuna resources by small-scale and artisanal fisheries appears to be limited to a large extent by the competition imposed on them by industrial fishing operating close inshore, particularly in West Africa, but also in America and throughout Asia (Pauly, 2006, 2018). In addition, in most of these countries, although they offer advantages such as funding for fisheries-related infrastructure and projects, the mechanisms of fisheries access agreements are relatively considered questionable in terms of their fairness and sustainability (Kaczynski and Fluharty, 2002; Andriamahefazafy and Kull, 2019; Belhabib *et al.*, 2019). Some of their limitations are for example, reflected in the low level of compensation for artisanal and small-scale fisheries, which receive negligible development subsidies from governments (Jacquet and Pauly, 2008; Pauly, 2018). The integration within fisheries agreements of mechanisms for sharing information on fish distribution, notably through data collected by buoys of industrial purse-seiner fleets in the countries' EEZs, could probably play a useful role in structuring the access to pelagic fish resources between these different actors. For instance, echosounder buoy data could be used to carry out a real-time mapping of the tuna occurrence in the countries' EEZs, which could contribute to a better access to coastal tuna resources by local fishermen. The approach could also be extended to species not targeted by industrial fishing. Indeed, FAD aggregations generally consists of a variable level of species considered as bycatch by tuna purse seiners, but which are often critical for food security and the economy of coastal communities (Failler, 2014). Recent work using machine-learning techniques has shown that it is possible to estimate with a relative accuracy, the amount of bycatch associated with each FAD from buoy acoustic data (L. Mannoci, 2020, pers. comm.). The rapid progress in both buoy technology and data processing techniques, together with the increasing volume of data from buoys, make it possible to envisage future improvements in this field of research, with the possibility of identifying and mapping local "bycatch" hotspots which would constitute a significant support to improve catches and reduce fishing effort in artisanal and subsistence fisheries.

At a more global scale, GPS-data from buoys provide information with high spatial and temporal resolution on near-surface currents around the globe (Imzilen *et al.*, 2019). This data collection can be a valuable asset in addressing DFAD beaching and its impacts on sensitive ecosystems (Maufroy *et al.*, 2015; Davies *et al.*, 2017; Escalle *et al.*, 2019b). Through the

continuous monitoring of ocean circulation they provide, data from instrumented DFADs could potentially constitute a privileged survey tool for monitoring marine debris that is currently a major environmental concern (Sheavly and Register, 2007; Cozar *et al.*, 2014), and for identifying pollution hotspots in coastal or marine ecosystems.

On these many aspects, the reliability and availability of the data collected by these instruments are decisive. In recent years, most tuna RFMOs have strengthened the reporting requirements on the number of DFADs used by purse seiners (e.g. IOTC: Res. 19/08; ICCAT: Rec 19-02; IATTC: C-19-01; WCPFC: CMM 2018-01) in response to their increasing use and the uncertainties about their impacts on ecosystems, stocks and ecology of associated species (Dagorn *et al.*, 2013a). However, the availability of data from echosounder buoys remains yet dependent on the good will of the ship-owners and fleets possessing this information. The commercial and high strategic nature of these data for tuna purse seiners remains by far the major limitation to their open-access. For instance, the data used in the present thesis has been acquired after long negotiations, leading to a data exchange agreement with the fishing companies and buoy manufacturers. This may be detrimental, as it is undeniable that under the traditional rules of confidentiality involving anonymization, delayed availability or gridding of data prior to their scientific use, the availability of buoy data to a wider community of scientists or decision-makers (given their transnational nature), could greatly contribute to the overall refinement of knowledge about the marine pelagic environment, and improve the management of fisheries. However, the responsibility for improving the availability of data from fishers' buoys and their integration into an operational management of fisheries and marine ecosystems lies primarily with the tuna RFMOs and their stakeholders. The development of studies highlighting the importance and relevance of greater accessibility to these data is likely to give a decisive impetus to this concern.

5.5. Conclusion and Perspectives

From the stones of ancient shepherds to today's complex mathematical models, assessing animal populations, whether for exploitation, control or conservation purposes, has always been a challenging task. In this context, the present thesis had the goal to provide new and non-conventional abundance index for tropical tuna species, whose management is of high importance for both human communities and marine ecosystems. To achieve this goal, the thesis work has been devoted to the development of a new methodological framework that exploits the continuous stream of data collected by echosounder buoys and the associative behavioural traits of tropical tuna species with floating objects, in order to provide novel abundance index for their populations. In line with its objective, this thesis has produced a number of tools dedicated to the standard processing of the heterogeneous mass of data from commercial echosounder buoys, including a new approach to characterize fish aggregations under floating objects from the acoustic data provided. It also offered results that illustrate the importance of this new data source to improve the understanding of the associative behaviour of tuna with floating objects. Indeed, the analysis of echosounder buoy data has made it possible to introduce additional metrics to characterize the associative dynamics of tuna aggregations, and to infer the size of the populations from which they originate.

The most important result of this work undeniably lies in the new methodology to produce a direct abundance index for tropical tuna species. Based on a modelling approach that combine occupancy of floating objects by tunas, with metrics describing their associative behaviour at individual scale, this index provides direct and absolute estimates of the population size of tropical tunas as well as of its two different components, namely the associated and free-swimming populations. Such index is of major interest for stock estimates as it can help to address the need for complementary approaches beside the CPUE, which currently represents the main abundance index used for tropical tunas. A first concrete application of this new method has made it possible to produce abundance estimates for skipjack in the Western Indian Ocean, which have recently been adopted by the IOTC for the assessment of skipjack stocks for the year 2020.

Although highly desirable, the generalisation of this method (i.e. to other oceans, tuna-RFMOs or species), remains closely linked to the development of dedicated data collection programmes for improving and updating knowledge on individual residence and absence times of tuna species, as well as to a change in the current paradigm regarding availability of buoys data.

However, these aspects are currently more a matter for decision-makers than actual technical or scientific considerations.

Finally, although initially intended for tropical tuna species, the index from this work has conceptually the potential to be extended to any population of animal species that exhibit an associative behaviour around aggregating points, either objects (e.g. non-tuna species associated to floating objects see Fréon and Dagorn, (2000)) or other living animals (e.g. seabird and cetaceans (Evans, 1982); facultative parasites such as mites (Proctor and Owens, 2000); etc.). Further studies assessing this potential could open up new prospects for the application of this abundance index to a wider range of animal species in the future.

References

Albert, J. A., Beare, D., Schwarz, A.-M., Albert, S., Warren, R., Teri, J., Siota, F., Andrew, N.L. 2014. The Contribution of Nearshore Fish Aggregating Devices (FADs) to Food Security and Livelihoods in Solomon Islands. PLoS One, 9: e115386. https://dx.plos.org/10.1371/journal.pone.0115386

Alemany, F., Quintanilla, L., Velez-Belchí, P., García, A., Cortés, D., Rodríguez, J.M., Fernández de Puelles, M.L., González-Pola C., López-Jurado, J.L. 2010. Characterization of the spawning habitat of Atlantic bluefin tuna and related species in the Balearic Sea (Western Mediterranean). Progress in Oceanography, 86: 21–38. http://dx.doi.org/10.1016/j.pocean.2010.04.014

Andriamahefazafy, M., and Kull, C. A. 2019. Materializing the blue economy: Tuna fisheries and the theory of access in the Western Indian Ocean. Journal of Political Ecology, 26: 403–424. https://doi.org/10.2458/v26i1.23040

Ariz, J., Delgado, A., Fonteneau, A., Gonzales Costas, F., and Pallarés, P. 1992. Logs and tunas in the eastern tropical Atlantic: A review of present knowledge and uncertainties. *In* Proceedings of the international workshop on fishing for tunas associated with floating objects, La Jolla, CA, pp. 21–65.

Araújo, M. B., Anderson, R. P., Barbosa, A. M., Beale, C. M., Dormann, C. F., Early, R., Garcia, R. A., et Guisan, A., Maiorano, L., Babak, N., O'Hara, R. B., Zimmermann, N. E., and Rahbek, C. 2019. Standards for distribution models in biodiversity assessments. Science Advances, 5: 1–12. http://dx.doi.org/10.1126/sciadv.aat4858

Armstrong, M.J., Payne, A.I.L., and Cotter, A.J.R. 2008. Contributions of the Fishing Industry to Research through Partnerships. *In* Advances in Fisheries Science, pp. 63–84. Blackwell Publishing Ltd., Oxford, UK. http://doi.wiley.com/10.1002/9781444302653.ch4

Baidai, Y., Capello, M., Billet, N., Floch, L., Simier, M., Sabarros, P., and Dagorn, L. 2017. Towards the derivation of fisheries-independent abundance indices for tropical tunas: Progress in the echosounders buoys data analysis. IOTC-2017-WPTT19-22. https://www.iotc.org/sites/default/files/documents/2017/10/IOTC-2017-WPTT19-22_Rev1.pdf (last accessed: October 6, 2020).

Baidai, Y., Dagorn, L., Amande, M. J., Gaertner, D., and Capello, M. 2019. Mapping Tuna Occurrence Under Drifting Fish Aggregating Devices From fisher's echosounder buoys in Indian Ocean. IOTC-2019-WPTT21-56_Rev1. https://www.iotc.org/sites/default/files/documents/2019/10/IOTC-2019-WPTT21-56_Rev1.pdf (last accessed: October 6, 2020).

Baidai, Y., Dagorn, L., Amande, M. J., Gaertner, D., and Capello, M. 2020a. Machine learning for characterizing tropical tuna aggregations under Drifting Fish Aggregating Devices (DFADs) from commercial echosounder buoys data. Fisheries Research, 229: 105613. https://doi.org/10.1016/j.fishres.2020.105613

Baidai, Y., Dagorn, L., Amande, M. J., Gaertner, D., and Capello, M. 2020b. Tuna aggregation dynamics at Drifting Fish Aggregating Devices: A view through the eyes of commercial echosounder buoys. ICES Journal of Marine Science. *In press* http://dx.doi.org/10.1093/icesjms/fsaa178

Baidai, Y., Dagorn, L., Amande, M. J., Gaertner, D., and Capello, M. 2020c. Mapping tuna occurrence under Drifting Fish Aggregating Devices from fisher's echosounder buoys in Atlantic Ocean. Collective Volume of Scientific Papers ICCAT, 76: 777–784.

Bamber, J. C., and Hill, C. R. 1979. Ultrasonic attenuation and propagation speed in mammalian tissues as a function of temperature. Ultrasound in Medicine & Biology, 5: 149–157. https://linkinghub.elsevier.com/retrieve/pii/0301562979900838

Bard, F.-X., Stretta, J.-M., and Slepoukha, M. 1985. Les épaves artificielles comme auxiliaires de la pêche thonière en océan Atlantique : quel avenir ? Pêche Maritime, 1291: 655–659. https://horizon.documentation.ird.fr/exl-doc/pleins_textes/pleins_textes_7/b_fdi_55-56/010022579.pdf (last accessed: October 6, 2020).

Barlow, J., and Taylor, B. L. 2005. Estimates of sperm whale abundance in the northeastern temperate pacific from a combined acoustic and visual survey. Marine Mammal Science, 21: 429–445. https://doi.org/10.1111/j.1748-7692.2005.tb01242.x.

Baske, A., Gibbon, J., Benn, J., and Nickson, A. 2012. Estimating the use of drifting Fish Aggregation Devices (FADs) around the globe. Discussion paper, Washington, D.C. 8 pp. https://www.pewtrusts.org/-/media/assets/2015/11/global_fad_report.pdf (last accessed: October 6, 2020).

Basson, M., and Farley, J. H. 2014. A standardised abundance index from commercial spotting data of southern bluefin tuna (*Thunnus maccoyii*): random effects to the rescue. PLoS One, 9: e116245. https://dx.plos.org/10.1371/journal.pone.0116245

Bauer, R. K., Bonhommeau, S., Brisset, B., and Fromentin, J. M. 2015. Aerial surveys to monitor bluefin tuna abundance and track efficiency of management measures. Marine Ecology Progress Series, 534: 221–234. https://doi.org/10.3354/meps11392.

Bauer, R. K., Forget, F., Fromentin, J.-M., and Capello, M. 2020. Surfacing and vertical behaviour of Atlantic bluefin tuna (*Thunnus thynnus*) in the Mediterranean Sea: implications for aerial surveys. ICES Journal of Marine Science, 77: 1979–1991. https://academic.oup.com/icesjms/article/77/5/1979/5862935.

Baum, J. K., and Worm, B. 2009. Cascading top-down effects of changing oceanic predator abundances. Journal of Animal Ecology, 78: 699–714. https://doi.org/10.1111/j.1365-2656.2009.01531.x.

Belhabib, D., Sumaila, U. R., and Le Billon, P. 2019. The fisheries of Africa: Exploitation, policy, and maritime security trends. Marine Policy, 101: 80–92. https://doi.org/10.1016/j.marpol.2018.12.021

Bell, J. D., Kronen, M., Vunisea, A., Nash, W. J., Keeble, G., Demmke, A., Pontifex, S., and

Andréfouët S. 2009. Planning the use of fish for food security in the Pacific. Marine Policy, 33: 64–76. https://linkinghub.elsevier.com/retrieve/pii/S0308597X08000778

Bell, J. D., Allain, V., Allison, E. H., Andréfouët, S., Andrew, N. L., Batty, M. J., Blanc, M., Dambacher, J. M., Hampton, J., Hanich, Q., Harley, S., Lorrain, A., McCoy, M., McTurk, N., Nicol, S., Pilling, G., Point, D., Sharp, M. K., Vivili, P., and Williams, P. 2015. Diversifying the use of tuna to improve food security and public health in Pacific Island countries and territories. Marine Policy, 51: 584–591. http://dx.doi.org/10.1016/j.marpol.2014.10.005

Bertrand, A. 2000. Acoustic estimation of longline tuna abundance. ICES Journal of Marine Science, 57: 919–926. https://academic.oup.com/icesjms/article-lookup/doi/10.1006/jmsc.2000.0579

Bishop, J. 2006. Standardizing fishery-dependent catch and effort data in complex fisheries with technology change. Reviews in Fish Biology and Fisheries, 16: 21–38. https://doi.org/10.1007/s11160-006-0004-9.

Bosch, P., López, J., Ramírez, H., and Robotham, H. 2013. Support vector machine under uncertainty: An application for hydroacoustic classification of fish-schools in Chile. Expert Systems with Applications, 40: 4029–4034. https://doi.org/10.1016/j.eswa.2013.01.006.

Boyce, D., Tittensor, D., and Worm, B. 2008. Effects of temperature on global patterns of tuna and billfish richness. Marine Ecology Progress Series, 355: 267–276. http://www.int-res.com/abstracts/meps/v355/p267-276

Boyra, G., Moreno, G., Sobradillo, B., Pérez-Arjona, I., Sancristobal, I., and Demer, D. A. 2018. Target strength of skipjack tuna (*Katsuwonus pelamis*) associated with fish aggregating devices (FADs). ICES Journal of Marine Science, 75: 1790–1802. https://doi.org/10.1093/icesjms/fsy041.

Brandt, S. B. 1991. Acoustic measures of the abundance and size of pelagic planktivores in Lake Michigan. Canadian Journal of Fisheries and Aquatic Sciences, 48: 894–908. https://doi.org/10.1139/f91-106

Bravington, M. V., Grewe, P. M., and Davies, C. R. 2016a. Absolute abundance of southern bluefin tuna estimated by close-kin mark-recapture. Nature Communications, 7: 1–8. http://dx.doi.org/10.1038/ncomms13162

Bravington, M. V., Skaug, H. J., and Anderson, E. C. 2016b. Close-Kin Mark-Recapture. Statistical Science, 31: 259–274. http://projecteuclid.org/euclid.ss/1464105042 (last accessed: October 6, 2020)

Brehmer, P., Sancho, G., Trygonis, V., Itano, D., Dalen, J., Fuchs, A., Faraj, A., and Taquet M. 2019. Towards an Autonomous Pelagic Observatory: Experiences from Monitoring Fish Communities around Drifting FADs. Thalassas, 35: 177–189. https://doi.org/10.1007/s41208-018-0107-9.

Breiman, L. 2001. Random forests. Machine Learning, 45: 5–32. https://link.springer.com/content/pdf/10.1023/A:1010933404324.pdf (last accessed: October 6, 2020).

Buckland, S. T., Rexstad, E. A., Marques, T. A., and Oedekoven, C. S. 2015. Distance Sampling: Methods and Applications. Methods in Statistical Ecology. Springer International Publishing, Cham. http://link.springer.com/10.1007/978-3-319-19219-2.

Capello, M., Robert, M., Soria, M., Potin, G., Itano, D., Holland, K., Deneubourg, J. L., and Dagorn, L. 2015. A methodological framework to estimate the site fidelity of tagged animals using passive acoustic telemetry. PLoS One, 10: e0134002. https://dx.plos.org/10.1371/journal.pone.0134002

Campling, L. 2012. The Tuna 'Commodity Frontier': Business Strategies and Environment in the Industrial Tuna Fisheries of the Western Indian Ocean. Journal of Agrarian Change, 12: 252–278. http://doi.wiley.com/10.1111/j.1471-0366.2011.00354.x

Capello, M., Deneubourg, J. L., Robert, M., Holland, K. N., Schaefer, K. M., and Dagorn, L. 2016. Population assessment of tropical tuna based on their associative behavior around floating objects. Scientific Reports, 6: 1–14.http://dx.doi.org/10.1038/srep36415

Castro, J. J., Santiago, J. A., and Santana-Ortega, A. T. 2002. A general theory on fish aggregation to floating objects: An alternative to the meeting point hypothesis. Reviews in Fish Biology and Fisheries, 11: 255–277.

Churnside, J. H., Wilson, J. J., Oliver, C. W., and Environmental Technology Laboratory (Environmental Research Laboratories). 1998. Evaluation of the capability of the experimental oceanographic fisheries Lidar (FLOE) for tuna detection in the Eastern Tropical Pacific. NOAA technical memorandum ERL ETL ; 287. 74 pp. https://repository.library.noaa.gov/view/noaa/17394 (last accessed: October 6, 2020).

Cohen, J. 1968. Weighted kappa: Nominal scale agreement provision for scaled disagreement or partial credit. Psychological Bulletin, 70: 213–220.

Colefax, A. P., Butcher, P. A., and Kelaher, B. P. 2018. The potential for unmanned aerial vehicles (UAVs) to conduct marine fauna surveys in place of manned aircraft. ICES Journal of Marine Science, 75: 1–8. https://doi.org/10.1093/icesjms/fsx100.

Collette, B. B., Carpenter, K. E., Polidoro, B. A., Juan-Jordá, M. J., Boustany, A., Die, D. J., Elfes, C., and Fox, W., Graves, J., Harrison, L. R., Mc Manus, R., Minte-Vera, C. V., Nelson, R., Restrepo, V., Schratwieser, J., Sun, C.-L., Amorim, A., Brick Peres, M., Canales, C., Cardenas, G., Chang, S.-K., Chiang, W.-C., de Oliveira Leite, N., Harwell, H., Lessa, R., Fredou, F. L., Oxenford, H. A., Serra, R., Shao, K.-T., Sumaila, R., Wang, S.-P., Watson, R. and Yáñez, E. 2011. High Value and Long Life—Double Jeopardy for Tunas and Billfishes. Science, 333: 291–292. https://www.sciencemag.org/lookup/doi/10.1126/science.1208730

Cowling, A., and O'Reilly, J. 1999. Data analysis of the aerial surveys (1993-1999) for juvenile Southern Bluefin Tuna in the Great Australian Bight. RMWS/99/xx.

Cozar, A., Echevarria, F., Gonzalez-Gordillo, J. I., Irigoien, X., Ubeda, B., Hernandez-Leon, S., Palma, A. T., Navarro, S., Garcia-de-Lomas, J., Ruiz, A., Fernandez-de-Puelles, M. L., and Duarte, C. M. 2014. Plastic debris in the open ocean. Proceedings of the National Academy of Sciences, 111: 10239–10244. http://www.pnas.org/cgi/doi/10.1073/pnas.1314705111

Dagorn, L., Holland, K. N., and Itano, D. G. 2007a. Behavior of yellowfin (*Thunnus albacares*) and bigeye (T. obesus) tuna in a network of fish aggregating devices (FADs). Marine Biology, 151: 595–606. http://link.springer.com/10.1007/s00227-006-0511-1.

Dagorn, L., Pincock, D., Girard, C., Holland, K., Taquet, M., Sancho, G., Itano, D., and Aumeeruddy, R. 2007b. Satellite-linked acoustic receivers to observe behavior of fish in remote areas. Aquatic Living Resources, 20: 307–312. http://www.alr-journal.org/10.1051/alr:2008001

Dagorn, L., Holland, K. N., Restrepo, V., and Moreno, G. 2013a. Is it good or bad to fish with FADs? What are the real impacts of the use of drifting FADs on pelagic marine ecosystems? Fish and Fisheries, 14: 391–415. http://dx.doi.org/10.1111/j.1467-2979.2012.00478.x

Dagorn, L., Bez, N., Fauvel, T., and Walker, E. 2013b. How much do fish aggregating devices (FADs) modify the floating object environment in the ocean? Fisheries Oceanography, 22: 147–153. http://dx.doi.org/10.1111/fog.12014

Dai, L., Wang, X., Staples, K. W., Zhou, C., Tang, H., and Xu, L. 2020. Factors influencing successful fishing of tuna free-swimming schools in the equatorial western Pacific Ocean. Turkish Journal of Fisheries and Aquatic Sciences, 20: 341–350. http://dx.doi.org/10.4194/1303-2712-v20_5_02

Davies, T., Curnick, D., Barde, J., and Chassot, E. 2017. Potential environmental impacts caused by beaching of drifting fish aggregating devices and identification of management solutions and uncertainties. IOTC-2017-WGFAD01-08 Rev_1. https://www.iotc.org/sites/default/files/documents/2017/04/IOTC-2017-WGFAD01-08_Rev_1.pdf (last accessed: October 6, 2020).

Davies, T. K., Mees, C. C., and Milner-Gulland, E. J. 2014. The past, present and future use of drifting fish aggregating devices (FADs) in the Indian Ocean. Marine Policy, 45: 163–170. http://dx.doi.org/10.1016/j.marpol.2013.12.014

De Bruyn, P., and Murua, H. 2011. Indicators of stock status for skipjack tuna in the Indian Ocean. IOTC-2011-WPTT13-28. 17 pp. https://www.iotc.org/sites/default/files/documents/proceedings/2011/wptt/IOTC-2011-WPTT13-28.pdf (last accessed: October 6, 2020).

Dell, J. T., and Hobday, A. J. 2008. School-based indicators of tuna population status. ICES Journal of Marine Science, 65: 612–622. http://dx.doi.org/10.1093/icesjms/fsn032

Deudero, S., Merella, P., Massutí, E., and Alemany, F. 1999. Fish communities associated with FADs. Scientia Marina, 63: 199–207.

Diouf, P. S., Sane, K., and Lankester, K. 2001. Pour une pêche durable en Afrique de l'Ouest. *In* Rapport de l'atelier sur les conditions régionales minimales d'accès aux zones de pêche. Nouakchott, Mauritanie. 5pp. http://www.ntiposoft.com/domaine_200/pdf/uicn_peche_durable.pdf (last accessed: October 6, 2020).

Doray, M., Josse, E., Gervain, P., Reynal, L., and Chantrel, J. 2006. Acoustic characterisation of pelagic fish aggregations around moored fish aggregating devices in Martinique (Lesser Antilles). Fisheries Research, 82: 162–175. https://doi.org/10.1016/j.fishres.2006.06.025.

Duffy, L. M., Kuhnert, P. M., Pethybridge, H. R., Young, J. W., Olson, R. J., Logan, J. M., Goñi, N., Romanov, E, Allain, V., Staudinger, M. D., Abecassis, M., Choy, C. A., Hobday, A. J., Simier, M., Galván-Magaña, F.; Potier, M. and Ménard, F. 2017. Global trophic ecology of yellowfin, bigeye, and albacore tunas: Understanding predation on micronekton communities at ocean-basin scales. Deep-Sea Research Part II: Topical Studies in Oceanography, 140: 55–73. http://dx.doi.org/10.1016/j.dsr2.2017.03.003

Duparc, A., P. Cauquil, M. Depestris, P. Dewals, D. Gaertner, A. Hervé, J. Lebranchu, F.Marsac, and P. Bach. 2018. Assessment of accuracy in processing purse seine tropical tuna catches with the T3 methodology using French fleet data.19pp.

Elith, J., and Leathwick, J. R. 2009. Species distribution models: Ecological explanation and prediction across space and time. Annual Review of Ecology, Evolution, and Systematics, 40: 677–697. https://doi.org/10.1146/annurev.ecolsys.110308.120159.

Escalle, L., Scutt, P. J., and Pilling, G. 2019a. Beaching of drifting FADs in the WCPO : Recent science, management advice and in-country data collection programmes. SPC Fisheries Newsletter, 160: 9–14. https://www.spc.int/DigitalLibrary/Doc/FAME/InfoBull/FishNews/160/FishNews160_09_Escalle.pdf (last accessed: October 6, 2020).

Escalle, L., Scutt P., J., Brownjohn, M., Brouwer, S., Sen Gupta, A., Van Sebille, E., Hampton, J., and Pilling, G. 2019b. Environmental versus operational drivers of drifting FAD beaching in the Western and Central Pacific Ocean. Scientific Reports, 9: 14005. http://www.nature.com/articles/s41598-019-50364-0

Evans, P. G. H. 1982. Associations between seabirds and cetaceans: a review. Mammal Review, 12: 187–206. http://doi.wiley.com/10.1111/j.1365-2907.1982.tb00015.x

Eveson, J. P., Patterson, T. A., Hartog, J. R., and Evans, K. 2018a. Modelling surfacing behaviour of southern bluefin tuna in the Great Australian Bight. Deep Sea Research Part II: Topical Studies in Oceanography, 157–158: 179–189. https://doi.org/10.1016/j.dsr2.2018.03.007

Eveson, J. P., Bravington, M. V., and Farley, J. H. 2018b. Accounting for environmental and observer effects in estimating abundance of southern bluefin tuna from aerial survey data. Plos One, 13: e0207790. https://dx.plos.org/10.1371/journal.pone.0207790

Eveson, P., Farley, J., and Bravington, M. 2016. The aerial survey index of abundance: 2016 updated results. CCSBT-ESC/1609/09. 32 pp. https://www.ccsbt.org/en/system/files/ESC21_09_CCSBT_Aerial%20survey.pdf (last accessed: October 6, 2020).

Failler, P. 2014. Climate Variability and Food Security in Africa: The Case of Small Pelagic Fish in West Africa. Journal of Fisheries & Livestock Production, 02. https://doi.org/10.4172/2332-2608.1000122.

Fernandes, P., Gerlotto, F., Holliday, D., Nakken, O., and Simmonds, E. 2002. Acoustic applications in fisheries science: The ICES contribution. ICES Marine Science Symposia, 215: 483–492. https://imr.brage.unit.no/imrmlui/bitstream/handle/11250/107495/sym_2002_215b.pdf?sequence=11 (last accessed: October 6, 2020).

Fernandes, P. G. 2009. Classification trees for species identification of fish-school echotraces. ICES Journal of Marine Science, 66: 1073–1080. https://dx.doi.org/10.1093/icesjms/fsp060.

Filmalter, J. D., Dagorn, L., Cowley, P. D., and Taquet, M. 2011. First Descriptions of the Behavior of Silky Sharks, Carcharhinus Falciformis, Around Drifting Fish Aggregating Devices in the Indian Ocean. Bulletin of Marine Science, 87: 325–337. http://www.ingentaconnect.com/content/10.5343/bms.2010.1057

Fonteneau, A., Gascuel, D., and Pallarés, P. 1998. Vingt-cinq ans d'évaluation des ressources thonières de l'Atlantique : Quelques réflexions methodologiques. Collective Volume of Scientific Papers ICCAT, 50: 523–561.

Fonteneau, A., Gaertner, D., and Nordstrom, V. 1999. An overview of problems in the CPUE-abundance relationship for the tropical purse seine fisheries. Collective Volume of Scientific Papers ICCAT, 49: 259–276.

Fonteneau, A., Pallarés, P., and Pianet, R. 2000. A worldwide review of purse seine fisheries on FADs. *In* Pêche thonière et dispositifs de concentration de poissons, Caribbean-Martinique, 15-19 Oct 1999, pp. 15–35. https://archimer.ifremer.fr/doc/00042/15278/12664.pdf (last accessed: October 6, 2020).

Fonteneau, A., Chassot, E., and Bodin, N. 2013. Global spatio-temporal patterns in tropical tuna purse seine fisheries on drifting fish aggregating devices (DFADs): Taking a historical perspective to inform current challenges. Aquatic Living Resources, 26: 37–48. http://www.alr-journal.org/10.1051/alr/2013046

Fonteneau, A., Chassot, E., and Gaertner, D. 2015. Managing tropical tuna purse seine fisheries through limiting the number of drifting fish aggregating devices in the Atlantic: food for thought. Collective Volume of Scientific Papers ICCAT, 71: 460–475.

Fonteneau, A., Gaertner, D., Maufroy, A., and Amandè, M. J. 2016. Effects of the ICCAT FAD Moratorium on the tuna Fisheries and tuna stocks. Collected Volume of Scientific Papers ICCAT, 72: 520–533.

Fonteneau, A., Marsac, F. 2016. Fishery indicators suggest symptoms of overfishing for the Indian Ocean skipjack stock. IOTC-2016-WPTT18-INF02. 15p. https://www.iotc.org/sites/default/files/documents/2016/11/IOTC-2016-WPTT18-INFO2_Rev1_Fishery_indicators_SKJ.pdf (last accessed: October 6, 2020).

Foote, K. G. 1983. Linearity of fisheries acoustics, with addition theorems. Journal of the Acoustical Society of America, 73: 1932–1940.

Forget, F. G., Capello, M., Filmalter, J. D., Govinden, R., Soria, M., Cowley, P. D., and Dagorn, L. 2015. Behaviour and vulnerability of target and non-target species at drifting fish aggregating devices (FADs) in the tropical tuna purse seine fishery determined by acoustic telemetry. Canadian Journal of Fisheries and Aquatic Sciences, 72: 1398–1405. http://www.nrcresearchpress.com/doi/10.1139/cjfas-2014-0458

Fréon, P., and Dagorn, L. 2000. Review of fish associative behaviour toward a generalisation of the meeting point hypothesis. Reviews in Fish Biology and Fisheries, 10: 183–207.

Fromentin, J.-M., Farrugio, H., Deflorio, M., and De Metrio, G. 2003. Preliminary results of aerial surveys of bluefin tuna in the western Mediterranean Sea. Collective Volume of Scientific Papers ICCAT, 55: 1019–1027.

Fromentin, J. 2010. Tagging bluefin tuna in the Mediterranean Sea: challenge or mission: impossible? Collective Volume of Scientific Papers ICCAT, 65: 812–821.

Gaertner, D., Pallarés, P., 2002. The European Union Research Project, Efficiency of Tuna Purse-Seiners and Effective Effort (ESTHER): Scientific report of project. Doc. SCTB15-FTWG-3. 13pp. https://www.spc.int/digitallibrary/doc/fame/meetings/sctb/15/ftwg_3.pdf (last accessed: October 6, 2020).

Gaertner, D., Hallier, J.-P., and Maunder, M. N. 2004. A tag-attrition model as a means to estimate the efficiency of two types of tags used in tropical tuna fisheries. Fisheries Research, 69: 171–180. https://linkinghub.elsevier.com/retrieve/pii/S0165783604001353

Galland, G. G., Rogers, A., and Nickson, A. 2016. Netting billions: a global valuation of tuna. 1–22 pp. http://www.pewtrusts.org/en/research-and-analysis/reports/2016/05/netting-billions-a-global-valuation-of-tuna (last accessed: October 6, 2020).

García, A., Alemany, F., De la Serna, J. M., Oray, I., Karakulak, S., Rollandi, L., Arigo, A., *et al.* 2005. Preliminary results of the 2004 bluefin tuna larval surveys off different Mediterranean sites (Balearic Archipelago, Levantine Sea and the Sicilian Channel). Collective Volume of Scientific Papers ICCAT, 58: 1420–1428.

Gershman, D., Nickson, A., and O'Toole, M. 2015. Estimating The Use of FADS Around the World. 20 pp. https://www.pewtrusts.org/-/media/assets/2015/11/global_fad_report.pdf (last accessed: October 6, 2020).

Gilman, E., Passfield, K., and Nakamura, K. 2014. Performance of regional fisheries management organizations: Ecosystem-based governance of bycatch and discards. Fish and Fisheries, 15: 327–351. https://doi.org/10.1111/faf.12021.

Girard, C., Benhamou, S., and Dagorn, L. 2004. FAD: Fish Aggregating Device or Fish Attracting Device? A new analysis of yellowfin tuna movements around floating objects. Animal Behaviour, 67: 319–326. https://doi.org/10.1016/j.anbehav.2003.07.007

Gjøsæter, H., Dommasnes, A., and Røttingen, B. 1998. The Barents sea capelin stock 1972–1997. A synthesis of results from acoustic surveys. Sarsia, 83: 497–510. https://doi.org/10.1080/00364827.1998.10420446

Goujon, M., Maufroy, A., Relot-Stirnemann, A., Moëc, E., Bach, P., Cauquil, P., and Sabarros, P. 2017. Collecting data on board french tropical tuna purse seiners with common observers: results of orthongel's voluntary observer program OCUP in the Atlantic Ocean (2013-2017). IOTC-2017-WPDCS13-22_Rev1. 22pp. https://www.iotc.org/sites/default/files/documents/2017/11/IOTC-2017-WPDCS13-22_Rev1_-_OBS_PS_FRA.pdf (last accessed: October 6, 2020)

Goujon, M., Maufroy, A., Relot-Stirnemann, A., Moëc, E., Amand, Cauquil, P., Sabarros, P., and Bach P. 2018. Collecting data on board french tropical tuna purse seiners with common observers: results of ORTHONGEL's voluntary observer program OCUP in the Atlantic Ocean (2013-2017). Collective Volume of Scientific Papers ICCAT, 74: 3784–3805.

Govinden, R., Dagorn, L., Soria, M., and Filmalter, J. 2010. Behaviour of Tuna associated with Drifting Fish Aggregating Devices (FADs) in the Mozambique Channel. IOTC-2010-WPTT-25. 22 pp. https://www.iotc.org/sites/default/files/documents/proceedings/2010/wptt/IOTC-2010-WPTT-25.pdf (last accessed: October 6, 2020).

Govinden, R., Jauhary, R., Filmalter, J., Forget, F., Soria, M., Adam, S., and Dagorn, L. 2013. Movement behaviour of skipjack (*Katsuwonus pelamis*) and yellowfin (*Thunnus albacares*) tuna at anchored fish aggregating devices (FADs) in the Maldives, investigated by acoustic telemetry. Aquatic Living Resources, 26: 69–77. http://www.alr-journal.org/10.1051/alr/2012022

Grande, M., Capello, M., Baidai, Y., Uranga, J., Boyra, G., Quincoces, I., Orue, B., Ruiz, J., Zudaire, I., Murua, H. 2020. From fishermen to scientific tools: progress on the recovery and standardized processing of instrumented buoys data. Collected Volume of Scientific Papers ICCAT, 76: 881–891.

Gregory, R. D., Gibbons, D. W., and Donald, P. F. 2000. Bird census and survey techniques. *In* Bird census techniques, pp.17–56. Elsevier. https://doi.org/10.1016/C2009-0-03531-4

Guery, L., Aragno, V., Kaplan, D., Grande, M., Baez, J. C., Abascal, F., Uranga, J., et al. 2020. Skipjack CPUE series standardization by fishing mode for the European purse seiners operating in the Indian Ocean. IOTC-2020-WPTT22(DP)-12. https://iotc.org/sites/default/files/documents/2020/06/IOTC-2020-WPTT22DP-12.pdf (last accessed: October 6, 2020).

Hallier J.P., Parajua J.I. 1992. Review of tuna fisheries on floating objects in the Indian Ocean. *In*: Fishing for tunas associated with floating objects. La Jolla : IATTC, 25 p. International Workshop on Fishing for Tunas Associated with Floating Objects, La Jolla (USA), 1992/02/11-14. https://horizon.documentation.ird.fr/exl-doc/pleins_textes/pleins_textes_6/b_fdi_37-38/42871.pdf (last accessed: October 6, 2020)

Hampton, I. 1992. The role of acoustic surveys in the assessment of pelagic fish resources on the South African continental shelf. South African Journal of Marine Science, 12: 1031–1050. https://doi.org/10.2989/02577619209504760

Hampton, I. 1996. Acoustic and egg-production estimates of South African anchovy biomass over a decade: comparisons, accuracy, and utility. ICES Journal of Marine Science, 53: 493–500. https://doi.org/10.1006/jmsc.1996.0071

Harley, S. J., Myers, R. A., and Dunn, A. 2001. Is catch-per-unit-effort proportional to abundance? Canadian Journal of Fisheries and Aquatic Sciences, 58: 1760–1772. http://www.nrcresearchpress.com/doi/abs/10.1139/f01-112

He, F., and Gaston, K. J. 2000a. Estimating species abundance from occurrence. American Naturalist, 156: 553–559. https://doi.org/10.1086/303403

He, F., and Gaston, K. J. 2000b. Occupancy-abundance relationships and sampling scales. Ecography, 23: 503–511. https://www.jstor.org/stable/3683080

He, F., Gaston, K., and Wu, J. 2002. On species occupancy-abundance models. Écoscience, 9: 119–126. https://www.jstor.org/stable/42901393

Hearn, W. S., and Polacheck, T. 2003. Estimating long-term growth-rate changes of southern bluefin tuna (*Thunnus maccoyii*) from two periods of tag-return data. Fishery Bulletin, 101: 58–74. https://spo.nmfs.noaa.gov/sites/default/files/pdf-content/2003/1011/hearnf.pdf (last accessed: October 6, 2020).

Hilborn, R., and Walters, C. J. 1992. Quantitative Fisheries Stock Assessment: Choice, Dynamics and Uncertainty. Springer US, Boston, MA. XV, 570 pp. http://link.springer.com/10.1007/978-1-4615-3598-0

Hilborn, R. 2003. The state of the art in stock assessment: where we are and where we are going. Scientia Marina, 67: 15–20. http://doi.org/10.3989/SCIMAR.2003.67S115.

Hilborn, R. 2012. The evolution of quantitative marine fisheries management 1985-2010. Natural Resource Modeling, 25: 122–144. http://doi.wiley.com/10.1111/j.1939-7445.2011.00100.x.

Holland, K. N., Brill, R. W., and Chang, R. K. C. 1990. Horizontal and vertical movements of yellowfin and bigeye tuna associated with fish aggregating devices. Fishery Bulletin, 88: 493–507. https://www.st.nmfs.noaa.gov/spo/FishBull/883/holland.pdf (last accessed: October 6, 2020).

Hoyle, S. D., Leroy, B. M., Nicol, S. J., and Hampton, W. J. 2015. Covariates of release mortality and tag loss in large-scale tuna tagging experiments. Fisheries Research, 168: 47–48. https://linkinghub.elsevier.com/retrieve/pii/S016578361500096X

Hui, C., McGeoch, M. A., Reyers, B., Roux, P. C., Greve, M., and Chown, S. L. 2009. Extrapolating population size from the occupancy–abundance relationship and the scaling pattern of occupancy. Ecological Applications, 19: 2038–2048. http://doi.wiley.com/10.1890/08-2236.1.

ICCAT. 2014. Report of the 2014 ICCAT East and West Atlantic Skipjack stock assessment meeting. Dakar. 98 pp. https://www.iccat.int/Documents/SCRS/DetRep/SKJ_SA_ENG.pdf (last accessed: October 6, 2020).

ICCAT. 2018. Report of the 2018 ICCAT bigeye tuna stock assessment meeting. Pasaia. 92 pp. Available at : https://www.iotc.org/sites/default/files/documents/2020/06/IOTC-2020-WPTT22DP-10.pdf (last accessed: October 6, 2020).

ICCAT. 2019. Report of the 2019 ICCAT yellowfin tuna stock assessment meeting. Grnad-Bassam. 117 pp. Available at: https://www.iccat.int/Documents/SCRS/DetRep/YFT_SA_ENG.pdf (last accessed: October 6, 2020).

ICCAT. 2020. Compendium management recommendations and resolutions adopted by ICCAT for the conservation of Atlantic tunas and tuna-like species. 447pp. https://www.iccat.int/Documents/Recs/COMPENDIUM_ACTIVE_ENG.pdf (last accessed: October 6, 2020)

Ichinokawa, M., Coan, A. L., and Takeuchi, Y. 2008. Transoceanic migration rates of young North Pacific albacore, *Thunnus alalunga*, from conventional tagging data. Canadian Journal of Fisheries and Aquatic Sciences, 65: 1681–1691. https://doi.org/10.1139/F08-095.

Imzilen, T., Chassot, E., Barde, J., Demarcq, H., Maufroy, A., Roa-Pascuali, L., Ternon, J.-F. and Lett, C. 2019. Fish aggregating devices drift like oceanographic drifters in the near-surface currents of the Atlantic and Indian Oceans. Progress in Oceanography, 171: 108–127. https://doi.org/10.1016/j.pocean.2018.11.007.

Ingram, G. W., Richards, W. J., Lamkin, J. T., and Muhling, B. 2010. Annual indices of Atlantic bluefin tuna (*Thunnus thynnus*) larvae in the Gulf of Mexico developed using delta-lognormal and multivariate models. Aquatic Living Resources, 23: 35–47. https://doi.org/10.1051/alr/2009053.

Ingram, G. W. J., Richards, W. J., Scott, G. P., and Turner, S. C. 2007. Development of indices of bluefin tuna (*Thunnus thynnus*) spawning biomass in the Gulf of Mexico using delta-lognormal models. Collective Volume of Scientific Papers ICCAT, 60: 1057–1069.

Ingram, G. W. J. 2013. Annual indices of bluefin tuna (*Thunnus thynnus*) spawning biomass in the Gulf of Mexico developed using delta-lognormal and multivariate models. Collective Volume of Scientific Papers ICCAT, 69: 1-980–991.

Ingram, G. W. J., Alvarez-Berastegui, D., García, A., Pollack, A. G., Lopez-Jurado, J. L., and Alemany, F. 2015. Development of Indices of Larval Bluefin Tuna (*Thunnus Thynnus*) in the Western Mediterranean Sea. Collective Volume of Scientific Papers ICCAT, 71: 1279–1296.

IOTC. 2014. Indian Ocean Skipjack Tuna Stock Assessment 1950- 2013 (Stock Synthesis). IOTC–2014–WPTT16–43-Rev3. http://iotc.org/sites/default/files/documents/2015/01/IOTC-2014-WPTT16-43_Rev_3_-_SKJ_SS3_SA.pdf (last accessed: October 6, 2020).

IOTC. 2017. Indian Ocean Skipjack Tuna Stock Assessment 1950-2011 (Stock Synthesis). IOTC–2017–WPTT19–47-Rev1. https://www.iotc.org/sites/default/files/documents/2017/10/IOTC-2017-WPTT19-47_Rev1_SKJ_SS3.pdf (last accessed: October 6, 2020).

IOTC. 2020a. Tag data processing for IOTC tropical tuna assessments. IOTC–2020–WPTT22(DP)–10. https://iotc.org/sites/default/files/documents/2020/06/IOTC-2020-WPTT22DP-10.pdf (last accessed: October 6, 2020).

IOTC. 2020b. Report of the 22nd Session of the IOTC Working Party on Tropical Tunas, Data Preparatory Meeting. IOTC–2020–WPTT22(DP)–R[E]. 35 pp. https://www.iotc.org/sites/default/files/documents/2020/07/IOTC-2020-WPTT22DP-RE.pdf (last accessed: October 6, 2020).

ISSF. 2019. Status Of The World Fisheries For Tuna: October 2019. Washington, D.C., USA. 113 pp. http://iss-foundation.org/resources/downloads/?did=512 (last accessed: October 6, 2020).

Jachmann, H. 2002. Comparison of aerial counts with ground counts for large African herbivores. Journal of Applied Ecology, 39: 841–852. https://doi.org/10.1046/j.1365-2664.2002.00752.x.

Jacquet, J., and Pauly, D. 2008. Funding priorities: Big barriers to small-scale fisheries. Conservation Biology, 22: 832–835. https://doi.org/10.1111/j.1523-1739.2008.00978.x.

Jech, J. M., Johnson, J. J., Lutcavage, M., Vanderlaan, A. S. M., Rzhanov, Y., and LeRoi, D. 2020. Measurements of juvenile Atlantic bluefin tuna (Thunnus thynnus) size using an unmanned aerial system. Journal of Unmanned Vehicle Systems, 8: 140–160. http://www.nrcresearchpress.com/doi/10.1139/juvs-2018-0039

Josse, E., and Bertrand, A. 2000. In situ acoustic target strength measurements of tuna associated with a fish aggregating device. ICES Journal of Marine Science, 57: 911–918. https://academic.oup.com/icesjms/article-lookup/doi/10.1006/jmsc.2000.0578

Kaczynski, V. M., and Fluharty, D. L. 2002. European policies in West Africa: Who benefits from fisheries agreements? Marine Policy, 26: 75–93. https://doi.org/10.1016/S0308-597X(01)00039-2.

Kakuma, S. 2001. Synthesis on moored FADs in the North West Pacific region. Actes de Colloques IFREMER: 63–77. http://archimer.ifremer.fr/doc/00042/15281 (last accessed: October 6, 2020).

Katara, I., Gaertner, D., Maufroy, A., and Chassot, E. 2016. Standardization of catch rates for the eastern tropical atlantic bigeye tuna caught by the French purse seine DfAD fishery. Collective Volume of Scientific Papers ICCAT, 72: 406–414.

Katara, I., Gaertner, D., Billet, N., Lopez, J., Fonteneau, A., Murua, H., and Baez, J. C. 2017. Standardisation of skipjack tuna CPUE for the EU purse seine fleet operating in the Indian Ocean. IOTC-2017-WPTT19-38. https://www.iotc.org/sites/default/files/documents/2017/10/IOTC-2017-WPTT19-38_SKJ_EU_PS_CPUE.pdf (last accessed: October 6, 2020).

Katara, I., Gaertner, D., Marsac, F., Grande, M., Kaplan, D., Agurtzane, U., Loreleï, G., and Mathieu, D., Antoine, D., Laurent, F., Jon, L., and Francisco, A. 2018. Standardisation of yellowfin tuna CPUE for the EU purse seine fleet operating in the Indian Ocean. IOTC–2018–WPTT20–36_Rev1. https://www.iotc.org/sites/default/files/documents/2018/10/IOTC-2018-WPTT20-36_Rev1.pdf (last accessed: October 6, 2020).

Katsanevakis, S., Weber, A., Pipitone, C., Leopold, M., Cronin, M., Scheidat, M., Doyle, T. K., Buhl-Mortensen, L., Buhl-Mortensen, P., D'Anna, G., de Boois, I., Dalpadado, P., Damalas, D., Fiorentino, F., Garofalo, G., Giacalone, V. M., Hawley, K. L., Issaris, Y., Jansen, J., Knight, C. M., Knittweis, L., Kröncke, I., Mirto, S., Muxika, I., Reiss, H., Skjoldal, H. R. and Vöge, S. 2012. Monitoring marine populations and communities:

Methods dealing with imperfect detectability. Aquatic Biology, 16: 31–52. https://doi.org/10.3354/ab00426.

Kolody, D., Herrera, M., and Million, J. 2011. Indian Ocean Skipjack Tuna Stock Assessment 1950-2009 (Stock Synthesis). IOTC-2011-WPTT13-31_Rev1. https://www.iotc.org/sites/default/files/documents/proceedings/2011/wptt/IOTC-2011-WPTT13-31_Rev1.pdf (last accessed: October 6, 2020).

Kolody, D., and Hoyle, S. 2015. Evaluation of tag mixing assumptions in western Pacific Ocean skipjack tuna stock assessment models. Fisheries Research, 163: 127–140. http://dx.doi.org/10.1016/j.fishres.2014.05.008

Kolody, D., and Bravington, M. 2019. Is Close-Kin Mark Recapture feasible for IOTC Yellowfin Tuna Stock Assessment. IOTC–2019–WPM10–25-rev.1. https://www.iotc.org/sites/default/files/documents/2019/10/IOTC-2019-WPM10-25_Rev1.pdf (last accessed: October 6, 2020).

Krebs, C. J. 1999. Ecological Methodology. Welsey Educational Publishers, Inc., Menlo Park, CA, Menlo Park, CA. 620p

Kuhn, M. 2008. Building Predictive Models in R Using the caret Package. Journal Of Statistical Software, 28: 1–26. http://www.jstatsoft.org/v28/i05/paper

Kuhn, M., and Johnson, K. 2013. Applied Predictive Modeling. Springer New York, New York, NY. 600 pp.

Lamkin, J., Muhling, B., Lyczkowski-Shultz, J., Ingram, W., Malca, E., Zapfe, G., Gerard, T., Millett, A., Privoznik, S. 2015. Developing new early life history-based fishery independent indices for western Atlantic bluefin tuna. Collective Volume of Scientific Papers ICCAT, 71: 1238–1246.

Langley, A., and Million, J. 2012. Determining an appropriate tag mixing period for the Indian Ocean yellowfin tuna stock assessment. IOTC–2012–WPTT14–31. https://www.iotc.org/sites/default/files/documents/proceedings/2012/wptt/IOTC-2012-WPTT14-31.pdf (last accessed: October 6, 2020).

Larese, J. P. 2005. Using LIDAR to detect tuna schools unassociated with dolphins in the Eastern tropicam Pacific, a review and current status. NOAA-TM-NMFS-SWFSC-378. https://repository.library.noaa.gov/view/noaa/3417 (last accessed: October 6, 2020).

Lehodey, P., Hampton, J., and Leroy, B. 1999. Preliminary Results on Age and Growth of Bigeye Tuna (*Thunnus Obesus*) From the Western and Central Pacific Ocean As Indicated By Daily Growth Increments and Tagging Data. YFT-2. Tahiti. 1–18 pp. https://www.spc.int/DigitalLibrary/Doc/FAME/Meetings/SCTB/12/BET_2.pdf (last accessed: October 6, 2020).

Lennert-Cody, C. E., and Hall, M. A. 2001. The development of the purse seine fishery on drifting Fish Aggregating Devices in the Eastern Pacific Ocean: 1992-1998. Actes de Colloques IFREMER: 78–107. https://archimer.ifremer.fr/doc/00042/15282/12668.pdf (last accessed: October 6, 2020).

Leroy, B., Nicol, S., Lewis, A., Hampton, J., Kolody, D., Caillot, S., and Hoyle, S. 2015. Lessons learned from implementing three, large-scale tuna tagging programmes in the western and central Pacific Ocean. Fisheries Research, 163: 23–33. http://dx.doi.org/10.1016/j.fishres.2013.09.00

Lewis, J. C. 1970. Wildlife census methods: a resume. Journal of wildlife diseases, 6: 356–364. https://www.jwildlifedis.org/doi/pdf/10.7589/0090-3558-6.4.356

Lewis, T., Gillespie, D., Lacey, C., Matthews, J., Danbolt, M., Leaper, R., McLanaghan, R. and Moscrop, A. 2007. Sperm whale abundance estimates from acoustic surveys of the Ionian Sea and Straits of Sicily in 2003. Journal of the Marine Biological Association of the United Kingdom, 87: 353–357. https://doi.org/10.1017/S0025315407054896

Liaw, A., and Wiener, M. 2002. Classification and regression by randomForest. R news, 2: 18–22.

Lopez, J., Moreno, G., Sancristobal, I., and Murua, J. 2014. Evolution and current state of the technology of echo-sounder buoys used by Spanish tropical tuna purse seiners in the Atlantic, Indian and Pacific Oceans. Fisheries Research, 155: 127–137. http://dx.doi.org/10.1016/j.fishres.2014.02.033

Lopez, J., Moreno, G., Boyra, G., and Dagorn, L. 2016. A model based on data from echosounder buoys to estimate biomass of fish species associated with fish aggregating devices. Fishery Bulletin, 114: 166–178. http://dx.doi.org/10.7755/FB.114.2.4

Lopez, J., Moreno, G., Lennert-Cody, C., Maunder, M., Sancristobal, I., Caballero, A., and Dagorn, L. 2017a. Environmental preferences of tuna and non-tuna species associated with drifting fish aggregating devices (DFADs) in the Atlantic Ocean, ascertained through fishers' echo-sounder buoys. Deep-Sea Research Part II: Topical Studies in Oceanography, 140: 127–138. http://dx.doi.org/10.1016/j.dsr2.2017.02.007

Lopez, J., Moreno, G., Ibaibarriaga, L., and Dagorn, L. 2017b. Diel behaviour of tuna and non-tuna species at drifting fish aggregating devices (DFADs) in the Western Indian Ocean, determined by fishers' echo-sounder buoys. Marine Biology, 164: 44. http://link.springer.com/10.1007/s00227-017-3075-3

Lutcavage, M. 1995. The feasibility of direct photographic aerial assessment of giant bluefin tuna in New England waters. Fishery Bulletin, 93: 495–503.

Lutcavage, M., Kraus, S., and Hoggard, W. 1997. Aerial survey of giant bluefin tuna, *Thunnus thynnus*, in the Great Bahama Bank, Straits of Florida, 1995. Fishery Bulletin, 95: 300–310.

MacKenzie, D. I., and Nichols, J. D. 2004. Occupancy as a surrogate for abundance estimation. Animal Biodiversity and Conservation, 27: 461–467. https://doi.org/57325.

Maclennan, D. N. 1990. Acoustical measurement of fish abundance. The Journal of the Acoustical Society of America, 87: 1–15. https://doi.org/10.1121/1.399285.

Macusi, E. D., Abreo, N. A. S., and Babaran, R. P. 2017. Local Ecological Knowledge (LEK) on Fish Behavior Around Anchored FADs: the Case of Tuna Purse Seine and Ringnet Fishers from Southern Philippines. Frontiers in Marine Science, 4: 1–13. http://journal.frontiersin.org/article/10.3389/fmars.2017.00188

Majkowski, J. 2007. Global fishery resources of tuna and tuna-like species. FAO. Fisheries Technical Paper, 483: 66. http://www.fao.org/3/a-a1291e.pdf (last accessed: October 6, 2020).

Malfante, M., Mars, J. I., Dalla Mura, M., and Gervaise, C. 2018. Automatic fish sounds classification. The Journal of the Acoustical Society of America, 143: 2834–2846. https://doi.org/10.1121/1.5036628

Marsac, F., Fonteneau, A., Lucas, J., Baez, J. C., and Floch, L. 2017. Data-derived fishery and stocks status indicators for skipjack tuna in the Indian Ocean. IOTC-2017-WPTT19-43. 21 pp. https://www.iotc.org/documents/data-derived-fishery-and-stocks-status-indicators-skipjack-tuna-indian-ocean (last accessed: October 6, 2020).

Matsumoto, T., Satoh, K., and Toyonaga, M. 2014. Behavior of skipjack tuna (*Katsuwonus pelamis*) associated with a drifting FAD monitored with ultrasonic transmitters in the equatorial central Pacific Ocean. Fisheries Research, 157: 78–85. http://dx.doi.org/10.1016/j.fishres.2014.03.023.

Matsumoto, T., Satoh, K., Semba, Y., and Toyonaga, M. 2016. Comparison of the behavior of skipjack (*Katsuwonus pelamis*), yellowfin (*Thunnus albacares*) and bigeye (*T. obesus*) tuna associated with drifting FADs in the equatorial central Pacific Ocean. Fisheries Oceanography, 25: 565–581. http://doi.wiley.com/10.1111/fog.12173

Maufroy, A., Chassot, E., Joo, R., and Kaplan, D. M. 2015. Large-scale examination of spatio-temporal patterns of drifting Fish Aggregating Devices (dFADs) from tropical tuna fisheries of the Indian and Atlantic Oceans. PLoS One, 10: 1–21. https://doi.org/10.1371/journal.pone.0128023

Maufroy, A., Kaplan, D. M., Bez, N., De Molina, A. D., Murua, H., Floch, L., and Chassot, E. 2017. Massive increase in the use of drifting Fish Aggregating Devices (dFADs) by tropical tuna purse seine fisheries in the Atlantic and Indian oceans. ICES Journal of Marine Science, 74: 215–225. https://doi.org/10.1093/icesjms/fsw175

Maunder, M. N., and Punt, A. E. 2004. Standardizing catch and effort data: A review of recent approaches. Fisheries Research, 70: 141–159. https://linkinghub.elsevier.com/retrieve/pii/S0165783604001638

Maunder, M. N., Sibert, J. R., Fonteneau, A., Hampton, J., Kleiber, P., and Harley, S. J. 2006. Interpreting catch per unit effort data to assess the status of individual stocks and communities. ICES Journal of Marine Science, 63: 1373–1385. https://doi.org/10.1016/j.icesjms.2006.05.008.

Maunder, M. N., and Deriso, R. B. 2007. Using Indicators of stock status when traditional reference points are not available: Evaluation and application to skipjack tuna in the Eastern Pacific Ocean. La Jolla, California. 229–248 pp.

McGowan, M. F., and Richards, W. J. 1986. Distribution and abundance of bluefin tuna (*Thunnus thynnus*) larvae in the Gulf of Mexico in 1982 and 1983 with estimates of the biomass and population size of the spawning stock for 1977, 1978, and 1981-1983. Collective Volume of Scientific Papers ICCAT, 24: 182–195.

Medley, P., Ahusan, M., and Shiham, A. M. 2020. Bayesian Skipjack and Yellowfin Tuna CPUE Standardisation Model for Maldives Pole and Line 1970-2019. IOTC-2020-WPTT22(DP)-11. https://www.iotc.org/sites/default/files/documents/2020/06/IOTC-2020-WPTT22DP-11.pdf (last accessed: October 6, 2020).

Melvin, G. D., Munden, J., and Finley, M. 2018. Development of Fishery Independent Index of Abundance for Atlantic Bluefin Tuna in the Gulf of St Lawrence. Collective Volume of Scientific Papers ICCAT, 74: 2570–2585.

Minch, T. 2020. Update To the Gulf of Saint Lawrence Acoustic Index of Abundance for Atlantic Bluefin Tuna. Collective Volume of Scientific Papers ICCAT, 76: 117–122.

Mitsunaga, Y., Endo, C., Anraku, K., Selorio, C. M., and Babaran, R. P. 2012. Association of early juvenile yellowfin tuna Thunnus albacares with a network of payaos in the Philippines. Fisheries Science, 78: 15–22. http://link.springer.com/10.1007/s12562-011-0431-y

Moniz, I., and Herrera, M. 2019. Using FADs to develop better abundance indices for tropical tuna. Collective Volume of Scientific Papers ICCAT, 75: 2196–2201.

Moreno, G., Josse, E., Brehmer, P., and Nøttestad, L. 2007a. Echotrace classification and spatial distribution of pelagic fish aggregations around drifting fish aggregating devices (DFAD). Aquatic Living Resources, 20: 343–356. https://doi.org/10.1051/alr:2008015

Moreno, G., Dagorn, L., Sancho, G., García, D., and Itano, D. 2007b. Using local ecological knowledge (LEK) to provide insight on the tuna purse seine fleets of the Indian Ocean useful for management. Aquatic Living Resources, 20: 367–376. http://www.alr-journal.org/10.1051/alr:2008014

Moreno, G., Dagorn, L., Sancho, G., and Itano, D. 2007c. Fish behaviour from fishers' knowledge: the case study of tropical tuna around drifting fish aggregating devices (DFADs). Canadian Journal of Fisheries and Aquatic Sciences, 64: 1517–1528. http://www.nrcresearchpress.com/doi/abs/10.1139/f07-113

Moreno, G., Dagorn, L., Capello, M., Lopez, J., Filmalter, J., Forget, F., Sancristobal, I., . and Holland, K. 2016. Fish aggregating devices (FADs) as scientific platforms. Fisheries Research, 178: 122–129. http://dx.doi.org/10.1016/j.fishres.2015.09.021

Moreno, G., Boyra, G., Sancristobal, I., Itano, D., and Restrepo, V. 2019. Towards acoustic discrimination of tropical tuna associated with Fish Aggregating Devices. Plos One, 14: e0216353. http://dx.plos.org/10.1371/journal.pone.0216353

Muhling, B. A., Lamkin, J. T., and Roffer, M. A. 2010. Predicting the occurrence of Atlantic bluefin tuna (*Thunnus thynnus*) larvae in the northern Gulf of Mexico: Building a classification model from archival data. Fisheries Oceanography, 19: 526–539. https://doi.org/10.1111/j.1365-2419.2010.00562.x.

Muhling, B. A., Lamkin, J. T., Alemany, F., García, A., Farley, J., Ingram, G. W., Berastegui, D. A., *et al.* 2017. Reproduction and larval biology in tunas, and the importance of restricted area spawning grounds. Reviews in Fish Biology and Fisheries, 27: 697–732. http://link.springer.com/10.1007/s11160-017-9471-4

Muir, J., Itano, D., Hutchinson, M., Leroy, B., and Holland, K. 2012. Behavior of target and non-target species on drifting FADs and when encircled by purse seine gear. Western and Central Pacific Fisheries Commision - Scientific Committee 8: 8 pp. https://www.wcpfc.int/file/3494/download?token=qeH2a6tL (last accessed: October 6, 2020).

Murtagh, F., and Legendre, P. 2014. Ward's Hierarchical Agglomerative Clustering Method: Which Algorithms Implement Ward's Criterion? Journal of Classification, 31: 274–295. https://doi.org/10.1007/s00357-014-9161-z

National Research Council. 2000. Improving the Collection, Management, and Use of Marine Fisheries Data. The National Academies Press, Washington, D.C. 236pp. http://www.nap.edu/catalog/9969 (last accessed: October 6, 2020).

Nelson, P. A. 2003. Marine fish assemblages associated with fish aggregating devices (FADs):

Effects of fish removal, FAD size, fouling communities, and prior recruits. Fishery Bulletin, 101: 835–850. http://fishbull.noaa.gov/1014/12nelson.pdf (last accessed: October 6, 2020).

Nielsen, J. L., Arrizabalaga, H., Fragoso, N., Hobday, A. J., Lutcavage, M. E., and Sibert, J. R. 2009. Tagging and Tracking of Marine Animals with Electronic Devices. Reviews: Methods and Technologies in Fish Biology and Fisheries. Springer Netherlands, Dordrecht. 458pp. http://link.springer.com/10.1007/978-1-4020-9640-2.

Noda, J. J., Travieso, M. C., Sánchez-Rodríguez, D., Travieso, C. M., and Sánchez-Rodríguez, D. 2016. Automatic Taxonomic Classification of Fish Based on Their Acoustic Signals. Applied Sciences , 6: 443. https://doi.org/10.3390/app6120443

Ohta, I., and Kakuma, S. 2005. Periodic behavior and residence time of yellowfin and bigeye tuna associated with fish aggregating devices around Okinawa Islands, as identified with automated listening stations. Marine Biology, 146: 581–594. http://link.springer.com/10.1007/s00227-004-1456-x

Oliver, C. W., Armstrong, W. A., and Young, J. A. 1994. Development of an airborne LIDAR system to detect tunas in the eastern tropical Pacific purse-seine fishery. NOAA Technical Memorandum: NOAA-TM-NMFS-SWFSC-204. ftp://ftp.library.noaa.gov/noaa_documents.lib/NMFS/SWFSC/TM_NMFS_SWFSC/NOAA-TM-NMFS-SWFSC-204.pdf (last accessed: October 6, 2020).

Orue, B., Lopez, J., Moreno, G., Santiago, J., Boyra, G., Soto, M., and Murua, H. 2019a. Using fishers' echo-sounder buoys to estimate biomass of fish species associated with drifting fish aggregating devices in the Indian Ocean. Revista de Investigación Marina, AZTI, 26: 1–13.

Orue, B., Lopez, J., Moreno, G., Santiago, J., Soto, M., and Murua, H. 2019b. Aggregation process of drifting fish aggregating devices (DFADs) in the Western Indian Ocean: Who arrives first, tuna or non-tuna species? Plos One, 14: e0210435. https://doi.org/10.1371/journal.pone.0210435

Orue, B., Lopez, J., Moreno, G., Santiago, J., Boyra, G., Uranga, J., and Murua, H. 2019c. From fisheries to scientific data: A protocol to process information from fishers' echo-sounder buoys. Fisheries Research, 215: 38–43. https://linkinghub.elsevier.com/retrieve/pii/S0165783619300633

Orue, B., Pennino, M. G., Lopez, J., Moreno, G., Santiago, J., Ramos, L., and Murua, H. 2020. Seasonal Distribution of Tuna and Non-tuna Species Associated With Drifting Fish Aggregating Devices (DFADs) in the Western Indian Ocean Using Fishery-Independent Data. Frontiers in Marine Science, 7: 1–17. https://doi.org/10.3389/fmars.2020.00441.

Pauly, D. 2006. Major Trends in Small-Scale Marine Fisheries, with Emphasis on Developing Countries, and Some Implication fro Social Sciences. Maritime Studies, 4: 7–22. http://www.marecentre.nl/mast/documents/Pauly_Mast2006vol_4no_2_new.pdf (last accessed: October 6, 2020).

Pauly, D. 2018. A vision for marine fisheries in a global blue economy. Marine Policy, 87: 371–374. https://doi.org/10.1016/j.marpol.2017.11.010.

Pérez, G., Dagorn, L., Deneubourg, J. L., Forget, F., Filmalter, J. D., Holland, K., Itano, D., Adam, S., Jauharee, R., Beeharry, P.S., and Capello, M.. 2020. Effects of habitat

modifications on the movement behavior of animals: the case study of Fish Aggregating Devices (FADs) and tropical tunas. Movement Ecology, 8: 1–11. https://doi.org/10.1186/s40462-020-00230-w

Petit, M. 1991. Aerospatial remote sensing as catalyst of an operational marine fishery (Halieutic) science. International Journal of Remote Sensing, 12: 713–724. https://doi.org/10.1080/01431169108929688

Pope, K. L., Lochmann, S. E., and Young, M. K. 2010. Methods for assessing fish populations. *In* In: Hubert, Wayne A; Quist, Michael C., eds. Inland Fisheries Management in North America, 3rd edition. Bethesda, MD: American Fisheries Society: 325-351.

Porteiro, C., Carrera, P., and Miquel, J. 1996. Analysis of Spanish acoustic surveys for sardine, 1991-1993: Abundance estimates and inter-annual variability. ICES Journal of Marine Science, 53: 429–433. https://doi.org/10.1006/jmsc.1996.0060

Probst, P., Wright, M. N., and Boulesteix, A. L. 2019. Hyperparameters and tuning strategies for random forest. Wiley Interdisciplinary Reviews: Data Mining and Knowledge Discovery, 9: 1–15. https://doi.org/10.1002/widm.1301.

Proctor, H., and Owens, I. 2000. Mites and birds: diversity, parasitism and coevolution. Trends in Ecology & Evolution, 15: 358–364. https://linkinghub.elsevier.com/retrieve/pii/S0169534700019248

R Core Team. 2019. R: A language and environment for statistical computing. R Foundation for Statistical Computing, Vienna, Austria. http://www.r-project.org/

Richards, W. J. 1976. Spawning of bluefin tuna (*Thunnus thynnus*) in the Atlantic Ocean and adjacent seas. Collective Volume of Scientific Papers ICCAT, 5: 267–278.

Richards, W. J., and Potthoff, T. 1980. Distribution and abundance of bluefin tuna larvae in the Gulf of Mexico in 1977 and 1978. I Collective Volume of Scientific Papers ICCAT, 9: 433–441.

Robert, M., Dagorn, L., Deneubourg, J. L., Itano, D., and Holland, K. 2012. Size-dependent behavior of tuna in an array of fish aggregating devices (FADs). Marine Biology, 159: 907–914. https://doi.org/10.1007/s00227-011-1868-3.

Robert, M., Dagorn, L., Filmalter, J. D., Deneubourg, J. L., Itano, D., and Holland, K. 2013a. Intra-individual behavioral variability displayed by tuna at fish aggregating devices (FADs). Marine Ecology Progress Series, 484: 239–247. https://doi.org/10.3354/meps10303

Robert, M., Dagorn, L., Lopez, J., Moreno, G., and Deneubourg, J. L. 2013b. Does social behavior influence the dynamics of aggregations formed by tropical tunas around floating objects? An experimental approach. Journal of Experimental Marine Biology and Ecology, 440: 238–243. https://doi.org/10.1016/j.jembe.2013.01.005.

Robinson, C. J., and Goómez-Gutieérrez, J. 1998. Daily vertical migration of dense deep scattering layers related to the shelf-break area along the northwest coast of Baja California, Mexico. Journal of Plankton Research, 20: 1679–1697. http://dx.doi.org/10.1093/plankt/20.9.1679

Robotham, H., Bosch, P., Gutiérrez-Estrada, J. C., Castillo, J., and Pulido-Calvo, I. 2010. Acoustic identification of small pelagic fish species in Chile using support vector

machines and neural networks. Fisheries Research, 102: 115–122. http://www.sciencedirect.com/science/article/pii/S0165783609002793.

Roch, M. A., Soldevilla, M. S., Hoenigman, R., Wiggins, S. M., and Hildebrand, J. A. 2008. Comparison of machine learning techniques for the classification of echolocation clicks from three species of odontocetes. Canadian Acoustics, 36: 41–47. https://jcaa.caa-aca.ca/index.php/jcaa/article/view/1989/1736

Rodriguez-Tress, P., Capello, M., Forget, F., Soria, M., Beeharry, S., Dussooa, N., and Dagorn, L. 2017. Associative behavior of yellowfin *Thunnus albacares*, skipjack *Katsuwonus pelamis*, and bigeye tuna *T. obesus* at anchored fish aggregating devices (FADs) off the coast of Mauritius. Marine Ecology Progress Series, 570: 213–222. http://www.int-res.com/abstracts/meps/v570/p213-222

Rouyer, T., Brisset, B., Bonhommeau, S., and Fromentin, J. M. 2018. Update of the Abundance Index for Juvenile Fish Derived From Aerial Surveys of Bluefin Tuna in the Western Mediterranean Sea. Collective Volume of Scientific Papers ICCAT, 74: 2887–2902.

Rouyer, T., Brisset, B., Tremblay, Y., and Fromentin, J. 2020. Update of the French Aerial Survey Index of Abundance and First Attempt. Collective Volume of Scientific Papers ICCAT, 76: 1–15.

Royer, F., Fromentin, J. M., and Gaspar, P. 2004. Association between bluefin tuna schools and oceanic features in the Western Mediterranean. Marine Ecology Progress Series, 269: 249–263. http://dx.doi.org/10.3354/meps269249.

Rushton, S. P., Ormerod, S. J., and Kerby, G. 2004. New paradigms for modelling species distributions? Journal of Applied Ecology, 41: 193–200. http://doi.wiley.com/10.1111/j.0021-8901.2004.00903.x.

Santiago, J., Lopez, J., Moreno, G., Quincoces, I., Soto, M., and Murua, H. 2016. Towards a Tropical Tuna Buoy-derived Abundance Index (TT-BAI). Collective Volume of Scientific Papers ICCAT, 72: 714–724.

Santiago, J., Uranga, J., Quincoces, I., Orue, B., Merino, G., Murua, H., and Boyra, G. 2019. A novel index of abundance of juvenile yellowfin tuna in the Atlantic Ocean derived from echosounder buoys. 2nd Joint t-RFMO FAD Working Group meeting: 24. https://www.iccat.int/Documents/CVSP/CV076_2019/n_6/CV076060321.pdf (last accessed: October 6, 2020).

Schaefer, K. M., and Fuller, D. W. 2005. Behavior of bigeye (*Thunnus obesus*) and skipjack (*Katsuwonus pelamis*) tunas within aggregations associated with floating objects in the equatorial eastern Pacific. Marine Biology, 146: 781–792. http://link.springer.com/10.1007/s00227-004-1480-x.

Schaefer, K. M., and Fuller, D. W. 2010. Vertical movements, behavior, and habitat of bigeye tuna (*Thunnus obesus*) in the equatorial eastern Pacific Ocean, ascertained from archival tag data. Marine Biology, 157: 2625–2642. https://doi.org/10.1007/s00227-010-1524-3.

Schaefer, K. M., and Fuller, D. W. 2013. Simultaneous behavior of skipjack (*Katsuwonus pelamis*), bigeye (*Thunnus obsesus*), and yellowfin (*T. albacares*) tunas, within large multi-species aggregations associated with drifting fish aggregating devices (FADs) in the equatorial eastern Pacific Ocean. Marine Biology, 160: 3005–3014. https://doi.org/10.1007/s00227-013-2290-9.

Schwarz, C. J., and Seber, G. A. F. 1999. Estimating animal abundance: Review III. Statistical Science, 14: 427–456. https://www.jstor.org/stable/2676809.

Scott, G. P., Turner, S. C., Grimes, C. B., Richards, W. J., and Brothers, E. B. 1993. Indices of larval bluefin tuna, *Thunnus thynnus*, abundance in the Gulf of Mexico; modelling variability in growth, mortality, and gear selectivity. Bulletin of Marine Science, 53: 912–929. https://www.ingentaconnect.com/content/umrsmas/bullmar/1993/00000053/00000002/art00023# (last accessed: October 6, 2020).

Scott, G. P., and Lopez, J. 2014. The use of FADs in Tuna Fisheries. 71 pp. Available at : http://www.europarl.europa.eu/RegData/etudes/note/join/2014/514002/IPOL-PECH_NT(2014)514002_EN.pdf (last accessed: October 6, 2020).

Scutt, P., Leroy, B., Peatman, T., Escalle, L., and Smith, N. 2019. Electronic tagging for the mitigation of bigeye and yellowfin tuna juveniles by purse seine fisheries. WCPFC-SC15-2019/EB-WP-08. https://www.wcpfc.int/file/302866/download?token=5nmVHVYt (last accessed: October 6, 2020).

Seber, G. A. F. 1986. A Review of Estimating Animal Abundance. Biometrics, 42: 267. http://dx.doi.org/10.2307/2531049

Seber, G. A. F. 1992. A Review of Estimating Animal Abundance II. International Statistical Review, 60: 129–166. https://www.jstor.org/stable/1403646

Seber, G. A. F., and Schwarz, C. J. 2002. Capture-recapture: Before and after EURING 2000. Journal of Applied Statistics, 29: 5–18. https://www.tandfonline.com/doi/full/10.1080/02664760120108700

Sempo, G., Dagorn, L., Robert, M., and Deneubourg, J. L. 2013. Impact of increasing deployment of artificial floating objects on the spatial distribution of social fish species. Journal of Applied Ecology, 50: 1081–1092. https://doi.org/10.1111/1365-2664.12140.

Sharma, R., Herrera, M., and Million, J. 2012. Indian Ocean Skipjack Tuna Stock Assessment 1950 - 2011 (Stock Synthesis). IOTC–2012–WPTT14–29 Rev–1. http://iotc.org/sites/default/files/documents/proceedings/2012/wptt/IOTC-2012-WPTT14-29%20Rev_1.pdf (last accessed: October 6, 2020).

Sheavly, S. B., and Register, K. M. 2007. Marine Debris & Plastics: Environmental Concerns, Sources, Impacts and Solutions. Journal of Polymers and the Environment, 15: 301–305. http://link.springer.com/10.1007/s10924-007-0074-3

Shiham, A. M., and Sibert, J. R. 2002. Population dynamics and movements of skipjack tuna (*Katsuwonus pelamis*) in the Maldivian fishery: analysis of tagging data from an advection-diffusion-reaction model. Aquatic Living Resources, 15: 13–23. https://linkinghub.elsevier.com/retrieve/pii/S0990744002011555

Sibert, J. R., Hampton, J., Fournier, D. A., and Bills, P. J. 1999. An advection-diffusion-reaction model for the estimation of fish movement parameters from tagging data, with application to skipjack tuna (*Katsuwonus pelamis*). Canadian Journal of Fisheries and Aquatic Sciences, 56: 925–938. http://dx.doi.org/10.1139/cjfas-56-6-925

Simmonds, E. J., and MacLennan, D. N. 2005. Fisheries acoustics second edition. 437 pp.

Skalski, J. R., Ryding, K. E., and Millspaugh, J. J. 2005. Estimating Population Abundance. *In* Wildlife Demography, pp. 435–539. https://linkinghub.elsevier.com/retrieve/pii/B9780120887736500109

Sokal, R. R. 1958. A statistical method for evaluating systematic relationships. Univ. Kansas, Science Bulletin., 38: 1409–1438.

Southwood, T. R. E., and Henderson, P. A. 2009. Ecological methods. John Wiley & Sons. http://doi.wiley.com/10.1038/npg.els.0003271

Sparre, P., and Venema, S. C. 1998. Introduction to tropical fish stock assessment. Part 1. Manual. FAO Fisheries Technical Paper No. 306.1, rev. 2, Rome, Italy. 407pp.

Stéquert, B., and Marsac, F. 1989. Tropical tuna surface fisheries in the Indian Ocean. FAO Fisheries Technical Paper 282, Rome. 282pp.

Straube, W. L., and Arthur, R. M. 1994. Theoretical estimation of the temperature dependence of backscattered ultrasonic power for noninvasive thermometry. Ultrasound in Medicine & Biology, 20: 915–922. http://linkinghub.elsevier.com/retrieve/pii/0301562994900515

Sund, P. N., Blackburn, M., and Williams, F. 1981. Tunas and their environment in the Pacific Ocean: A review. Oceanography and Marine Biology: An Annual Review, 19: 443–512.

Taquet, M., Dagorn, L., Gaertner, J.-C., Girard, C., Aumerruddy, R., Sancho, G., and Itano, D. 2007. Behavior of dolphinfish (*Coryphaena hippurus*) around drifting FADs as observed from automated acoustic receivers. Aquatic Living Resources, 20: 323–330. http://www.alr-journal.org/10.1051/alr:2008008

Tolotti, M. T., Forget, F., Capello, M., Filmalter, J. D., Hutchinson, M., Itano, D., Holland, K., and Dagorn, L. 2020. Association dynamics of tuna and purse seine bycatch species with drifting fish aggregating devices (FADs) in the tropical eastern Atlantic Ocean. Fisheries Research, 226: 105521. https://doi.org/10.1016/j.fishres.2020.105521

Toresen, R., Gjøsæter, H., and De Barros, P. 1998. The acoustic method as used in the abundance estimation of capelin (*Mallotus villosus* Muller) and herring (*Clupea harengus* Linne) in the Barents Sea. Fisheries Research, 34: 27–37. https://doi.org/10.1016/S0165-7836(97)00077-5

Torres-Irineo, E., Gaertner, D., Chassot, E., and Dreyfus-León, M. 2014a. Changes in fishing power and fishing strategies driven by new technologies: The case of tropical tuna purse seiners in the eastern Atlantic Ocean. Fisheries Research, 155: 10–19. http://dx.doi.org/10.1016/j.fishres.2014.02.017

Torres-Irineo, E., Amandè, M. J., Gaertner, D., de Molina, A. D., Murua, H., Chavance, P., Ariz, J., *et al.* 2014b. Bycatch species composition over time by tuna purse-seine fishery in the eastern tropical Atlantic Ocean. Biodiversity and Conservation, 23: 1157–1173. https://doi.org/10.1007/s10531-014-0655-0.

Trygonis, V., Georgakarakos, S., Dagorn, L., and Brehmer, P. 2016. Spatiotemporal distribution of fish schools around drifting fish aggregating devices. Fisheries Research, 177: 39–49. http://dx.doi.org/10.1016/j.fishres.2016.01.013

Uranga, J., Arrizabalaga, H., Boyra, G., Hernandez, M. C., Goñi, N., Arregui, I., Fernandes, J. A., *et al.* 2017. Detecting the presence-Absence of bluefin tuna by automated analysis of medium-range sonars on fishing vessels. PLoS One, 12: 1–18. https://doi.org/10.1371/journal.pone.0171382.

Uranga, J., Arregui, I., Martinez, U., Boyra, G., Gary, D., Godard, I., and Arrizabalaga, H. 2020. Acoustic-Based fishery-independent abundance index of juvenile bluefin tunas in the Bay of Biscay : Results From the First Three Surveys and Challenges. Collective Volume of

Scientific Papers ICCAT, 76: 455–470.

Varman, K. S., and Sukumar, R. 1995. The line transect method for estimating densities of large mammals in a tropical deciduous forest: An evaluation of models and field experiments. Journal of Biosciences, 20: 273–287. https://doi.org/10.1007/BF02703274.

Viñas, J., and Tudela, S. 2009. A Validated Methodology for Genetic Identification of Tuna Species (Genus *Thunnus*). PLoS One, 4: e7606. https://dx.plos.org/10.1371/journal.pone.0007606.

Wang, X., Xu, L., Chen, Y., Zhu, G., Tian, S., and Zhu, J. 2012. Impacts of fish aggregation devices on size structures of skipjack tuna Katsuwonus pelamis. Aquatic Ecology, 46: 343–352. http://dx.doi.org/10.1007/s10452-012-9405-0

.Warren, M., McGeoch, M. A., and Chown, S. L. 2003. Predicting abundance from occupancy: A test for an aggregated insect assemblage. Journal of Animal Ecology, 72: 468–477. http://dx.doi.org/10.1046/j.1365-2656.2003.00716.x.

Weber, T. C., Lutcavage, M. E., and Schroth-Miller, M. L. 2013. Near resonance acoustic scattering from organized schools of juvenile Atlantic bluefin tuna (*Thunnus thynnus*) . The Journal of the Acoustical Society of America, 133: 3802–3812. https://doi.org/10.1121/1.4802646

Weng, J.-S., Hung, M.-K., Lai, C.-C., Wu, L.-J., Lee, M.-A., and Liu, K.-M. 2013. Fine-scale vertical and horizontal movements of juvenile yellowfin tuna (*Thunnus albacares*) associated with a subsurface fish aggregating device (FAD) off southwestern Taiwan. Journal of Applied Ichthyology, 29: 990–1000. http://doi.wiley.com/10.1111/jai.12265

Wessel, P., and Smith, W. H. F. 1996. A global, self-consistent, hierarchical, high-resolution shoreline database. Journal of Geophysical Research: Solid Earth, 101: 8741–8743. https://doi.org/10.1029/96JB00104.

Wilson, G. J., and Delahay, R. J. 2001. A review of methods to estimate the abundance of terrestrial carnivores using field signs and observation. Wildlife Research, 28: 151. https://doi.org/10.1071/WR00033.

Ye, Y., and Dennis, D. 2009. How reliable are the abundance indices derived from commercial catch–effort standardization? Canadian Journal of Fisheries and Aquatic Sciences, 66: 1169–1178. http://www.nrcresearchpress.com/doi/10.1139/F09-070

Yoo, H. J. S., Stewart-Oaten, A., and Murdoch, W. W. 2003. Converting visual census data into absolute abundance estimates: A method for calibrating timed counts of a sedentary insect population. Ecological Entomology, 28: 490–499. https://doi.org/10.1046/j.1365-2311.2003.00523.x.

Young, J. W., Lansdell, M. J., Campbell, R. A., Cooper, S. P., Juanes, F., and Guest, M. A. 2010. Feeding ecology and niche segregation in oceanic top predators off eastern Australia. Marine Biology, 157: 2347–2368. https://doi.org/10.1007/s00227-010-1500-y.

Zaugg, S., van der Schaar, M., Houégnigan, L., Gervaise, C., and André, M. 2010. Real-time acoustic classification of sperm whale clicks and shipping impulses from deep-sea observatories. Applied Acoustics, 71: 1011–1019. http://www.sciencedirect.com/science/article/pii/S0003682X1000112X

Žydelis, R., Dorsch, M., Heinänen, S., Nehls, G., and Weiss, F. 2019. Comparison of digital video surveys with visual aerial surveys for bird monitoring at sea. Journal of

Ornithology, 160: 567–580. Springer Berlin Heidelberg.
https://doi.org/10.1007/s10336-018-1622-4

Abstract

Representing the majority of the world's tuna catches, tropical tuna species are of critical importance due to their essential role as food and economic resource. The sustainable management of this valuable resource depends on an accurate estimate of the abundance of the exploited populations and the impact of fishing pressure on them. The present thesis provides a new direct abundance index for tropical tuna populations that account for their free-swimming and associated components. Indeed, tropical tuna species are characterized by a singular behavioral trait that causes them to associate with floating objects drifting at sea. This characteristic has led to the development of a specific fishing mode widely used in tuna purse seine fishery, consisting in the capture of schools associated to floating objects. Recent decades have thus seen the massive deployment of thousands of floating objects known as fish aggregating devices (FADs), specifically designed to attract and concentrate tuna schools. The drifting FADs are equipped with satellite-linked echosounder buoys, which ensure their continuous monitoring, providing fishers with near-real time information on their location and associated tuna biomasses. This thesis presents a standard methodological framework for processing the information from echosounder buoys for scientific use, including a new approach based on supervised learning for processing the acoustic data they provide. The analysis of these data has allowed improving the general knowledge on the associative dynamics of tuna aggregations. Ocean-specific differences were evidenced, with notably longer periods of absence of tuna under FADs in the Indian Ocean than in the Atlantic Ocean. The novel index for estimating tuna abundances proposed by this thesis also exploit this associative behavior. It relies on a modelling approach combining data on the dynamics of the occupancy of floating objects from echosounder buoys with data on the associative dynamics of tuna individuals from electronic tagging. An initial application to the western Indian skipjack tuna population has made it possible to provide time series of absolute and relative abundances, used for stock assessments of this species. This new index addresses the current critical need for complementary methods for estimating tropical tuna abundances, expressed by all regional fisheries management organizations.

Keywords: Direct Abundance index; Tropical Tunas; Associative behaviour; Fish Aggregating Devices; Echosounder buoys.

Résumé

Représentant la majorité des captures mondiales de thon, les thons tropicaux sont des espèces d'une importance capitale du fait de leur rôle essentiel en tant que ressource alimentaire et économique. La gestion durable de cette précieuse ressource est tributaire d'une estimation correcte de l'abondance des populations exploitées ainsi que de l'impact de la pression de pêche sur celles-ci. La présente thèse fournit un nouvel indice direct d'abondance capable d'évaluer de manière absolue les tailles des populations de thons tropicaux ainsi que de leurs composantes en nage libre et associée. Les espèces tropicales thonières se caractérisent en effet par un trait comportemental singulier, les amenant à s'associer en masse autour d'objets flottants dérivant en mer. Cette caractéristique est à la base du développement d'un mode de pêche pratiquée par les thoniers senneurs, consistant en la capture des bancs associés aux objets flottants. Ces dernières décennies ont ainsi vu le déploiement massif de milliers de dispositifs de concentration de poissons (DCP) qui sont des objets flottants spécifiquement conçus pour attirer et concentrer les bancs de thons, et généralement équipées de bouées échosondeurs. Ces bouées fournissent en continu aux pêcheurs des informations sur la localisation des DCP et les biomasses de thons associées. Cette thèse propose un cadre méthodologique standard pour le traitement des informations issues de ces dispositifs à des fins d'utilisation scientifique, incluant une nouvelle approche basée sur l'apprentissage supervisé pour l'exploitation des données acoustiques qu'ils fournissent. L'analyse de ces données a permis d'élargir le champ de connaissances sur les dynamiques associatives des agrégations de thons. Il a ainsi été montré que ces dernières différaient significativement entre océans, avec notamment des périodes d'absence de thons sous DCP plus longues dans l'océan Indien que dans l'Atlantique. Le nouvel indice d'abondance proposé par cette thèse exploite également le comportement associatif de ces espèces. Il s'appuie sur une approche de modélisation combinant les données sur les dynamiques d'occupation des objets flottants issues des bouées échosondeurs, aux données de dynamiques associatives individuelles des thons, collectées par marquage électronique. Une première application aux populations de listao de l'océan Indien occidental a permis de fournir des séries temporelles d'abondance absolues et relatives, méthode adoptée pour les évaluations de stocks de cette espèce par la CTOI (Commission des Thons de l'Océan Indien). Ce nouvel indice vient répondre aux besoins critiques actuels de méthodologies complémentaires pour les estimations d'abondance des thons tropicaux (estimations directes), exprimés par l'ensemble des organisations régionales de gestion des pêcheries.

Keywords: Indice direct d'abondance ; Thons tropicaux ; Comportement associatif ; Dispositifs de concentration de poissons ; Bouées échosondeurs.